ECOLE POLYTECHNIQUE DE BRUXELLES

ULB

UNIVERSITÉ LIBRE DE BRUXELLES, UNIVERSITÉ D'EUROPE

DEVELOPMENT AND PHYSICOCHEMICAL CHARACTERIZATION OF CALIX[6]ARENE-BASED CHEMICAL RECOGNITION SYSTEMS

Thèse présentée en vue de l'obtention du diplôme de

Docteur en Sciences de l'Ingénieur et Technologies

EMILIO BRUNETTI

Promotors

KRISTIN BARTIK

IVAN JABIN

Laboratories

Engineering of Molecular NanoSystems

Laboratoire de Chimie Organique

Academic Year

2016-2017

ABSTRACT

Synthetic molecular receptors find applications in the selective extraction, transport and detection of neutral or charged species and the study of these systems is an important facet of supramolecular chemistry. In this thesis, we focused our attention on a specific family of molecular receptors called calix[6]arenes. These receptors possess a hydrophobic cavity formed by 6 aromatic rings that can accommodate small organic molecules. They can furthermore be easily functionalized and give rise to for example ditopic receptors or sensing systems. We worked with two families of calix[6]arenes but also looked at the complexation properties of some related compounds: a homooxacalix[3]arene and a resorcin[4]arene derivatives.

The first part of this thesis is devoted to the study of the complexation properties of a fluorescent calix[6]tris-pyrenylurea. The binding of anions, ion pairs, ion triads and phospholipids was monitored by ^{1}H Nuclear Magnetic Resonance (NMR) and Emission Spectroscopy. Our results showed that the receptor exhibits a remarkable selectivity for the sulfate anion in DMSO for which a binding constant of the order of 10^3 M^{-1} was found. In chloroform the affinity for sulfate is of the order of 10^5 M^{-1} and the selective recognition of ammonium-$TBASO_4$ triads was observed (TBA = tetra-*n*-butylammonium; ammonium = $PrNH_3^+$, $HexNH_3^+$ or $DodNH_3^+$). This work has been reported in the paper "Fluorescent Chemosensors for Anions and Contact Ion Pairs with a Cavity-Based Selectivity" Emilio Brunetti, Jean-François Picron, Karolina Flidrova, Gilles Bruylants, Kristin Bartik and Ivan Jabin *J. Org. Chem.* **2014**, *79*, 6179–6188.

We also showed that calix[6]tris-pyrenylurea displays a remarkable selectivity in chloroform for phospholipids bearing a phosphatidylcholine head (PCs) over those bearing a phosphoethanolamine head (PEs). We were able to show that this fluorescent receptor is able to extract PCs from a water solution enabling their quantification. This work has been reported in the paper "A Selective Calix[6]arene-based Fluorescent Chemosensor for Phosphatidylcholine Type Lipids" Emilio Brunetti, Steven Moerkerke, Johan Wouters, Kristin Bartik and Ivan Jabin *Org. Biomol. Chem.* **2016**. Accepted Manuscript. DOI: 10.1039/C6OB01880G.

The second part of this thesis is devoted to the evaluation of the binding properties of different receptors incorporated into dodecylphosphocholine (DPC) micelles. This strategy was used to make the hydrophobic molecular receptors "water-compatible" without having to undertake

synthetic modifications. Our results showed that a calix[6]azacryptand-based receptor can be incorporated into DPC micelles, either as a zinc complex or as a polyammonium at low pH. We observed that the zinc complex incorporated in the micelles is able to bind small and long linear primary amines in its cavity and we were able to highlight that complexation is driven by the hydrophobic effect. This work has been reported in the paper "Primary Amine Recognition in Water by a Calix[6]aza-cryptand Incorporated in Dodecylphosphocholine Micelles" Emilio Brunetti, Alex Inthasot, Flore Keymeulen, Olivia Reinaud, Ivan Jabin and Kristin Bartik *Org. Biomol. Chem.* **2015**, *13*, 2931-2938.

We also validated the micellar incorporation strategy with a homooxacalix[3]tris-acid and with a resorcin[4]arene zinc complex bearing four methyl-imidazole moieties. Once incorporated into DPC micelles, we showed that the two receptors can bind small organic guests: the homooxacalix[3]arene derivative can bind *tert*-butylammonium or adamantylammonium, albeit with low affinity and the resorcin[4]arene-based zinc complex can bind acetate and acetylacetone.

The final part of this thesis is devoted to the work undertaken in order to try and elucidate the guest exchange mechanism of calix[6]arene-zinc complexes where the zinc is tri-coordinated to the calixarene-based ligand and coordinates a guest molecule inside the calixarene cavity. The hypothesis that we put forward is that when the zinc is only tri-coordinated to the calixarene ligand, the guest exchange mechanism involves a zinc penta-coordinated intermediate where the zinc atom is simultaneous coordinated to an *endo*-complexed guest (inside the cavity) and an *exo*-complexed molecule (outside the cavity). 1D EXchange SpectroscopY experiments (EXSY) were undertaken with two calix[6]arene-zinc complexes where the zinc is tri-coordinated to the calixarene ligand and with a calix[6]arene-zinc complex where the zinc is tetra-coordinated to the calixarene ligand. The exchange of different guests (ethanol, dimethylformamide and acetonitrile) was monitored in deuterated dichloromethane. We observed that in all cases water accelerates guest exchange but that the guest residence times are highly dependent on the acidity of the metal center and on the nature of the guest buried inside the cavity.

Keywords: supramolecular chemistry, molecular receptors, calix[6]arenes, Nuclear Magnetic Resonance (NMR), Emission Spectroscopy, chemosensors, micelle, 1D EXchange SpectroscopY (EXSY).

“A chemist who does not know mathematics is seriously handicapped”

Irving Langmuir

ACKNOWLEDGMENTS

I wish to express my sincere gratitude to my supervisors, Professor Kristin Bartik and Professor Ivan Jabin for the continuous support during my PhD. I want particularly to thank them for following-up my research, for their patience, motivation and immense knowledge. Their guidance helped me throughout all the time of the research and

writing of this thesis. I could not have imagined better advisors and mentors. I am also truly grateful to them for having allowed me to travel and participate in conferences throughout my thesis. The drafting of my thesis was really intense but their corrections were extremely helpful in all circumstances.

Besides my advisor, I would like to thank the other members of my thesis committee, Prof.

Olivia Reinaud, Prof. Michel Luhmer and Prof. Gilles Bruylants for their insightful comments and

encouragement: without whose knowledge and expertise this study would not have been possible.

I want also to thank very warmly Dr. Picron, my Master's Thesis supervisor, for his encouragement and support throughout the first years of my thesis.

Special thanks also to all the members of the Engineering of Molecular NanoSystems and Laboratoire de Chimie Organique groups for their invaluable assistance and for the perfect atmosphere.

Je vais désormais passer au français :

En premier lieu, je tiens à remercier Mélanie, qui m'a ''baby-sitté'' pendant toutes ces années, en m'aidant plus particulièrement pour toutes les questions administratives liées à ma thèse.

Un grand merci aussi à Simon pour l'ambiance au sein du laboratoire. Nous n'avons pas souvent travaillé ensemble mais cela a été toujours fort sympathique. Merci pour les petits coups d'eau

le matin (parfois fort utiles), pour m'avoir fait découvrir IMDB, pour tes films coréens (au passage Old Boy ne mérite que 3). Merci pour tous les souvenirs liés aux tartes de chez Françoise, aux quiches (lardonnées, bien sûr), au café ''nutromé'', au maître *durumiste*, à la fougère, au maître saucier, au labos foireux.

Je remercie également mes collègues de longue date Flore et Mathieu (oui un *t* est suffisant !), avec qui j'ai eu de discussions stimulantes mais surtout pour les moments géniaux que nous avons passés ensemble pendant ces trois années de thèse commune. Merci pour vos conseils, que ce soit pour

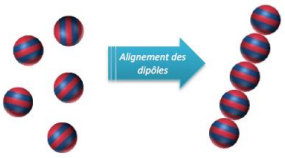

le FRIA, pour l'aide dans les différents rapports à rendre, pour la thèse et les présentations à remettre, pour tout le temps passé en conférence ou en école doctorale. Ça a été vraiment génial. Je n'oublierai jamais les moments passés aux YBMRS (désolé pour ta nuit Mathieu) et dans les différentes écoles doctorales et congrès (t'as réussi à la fermer finalement ta valise ?). Vous m'avez manqué cette dernière année.

Merci à Ana (Anita) pour les bons moments passés au labo et ailleurs. Merci à Maurice (Raptout) pour toutes tes vidéos foireuses, pour ta déclamation de la

Bible et pour les vidéos de *japanese bug fight*. Merci également à Hennie, la dernière arrivée, pour les bons conseils, que ce soit d'un point de vue scientifique ou culinaire. Merci à Glenn, partenaire fidèle de cookies blancs et de Kafkaf.

Merci également à mon équipe de football avec laquelle on a rejoint la deuxième

place au tournoi interpersonnel 2014-2015. Un grand merci tout particulièrement à Lionel, Kevin, Ludo, Jérôme (et Mathieu). Merci à l'équipe de badminton : Steven, Damien, Alex, Roy et Gaël.

Un grand merci aussi aux autres membres du LCO avec qui de près ou de loin j'ai pu collaborer :Sara, Alice, Pascale, Angélique, Alexandra, Steven, Damien, Gaël, Roy et Alex :

Je tiens aussi à remercier les occupants du troisième étage avec qui j'ai pu partager des moments très sympas pendant ces quatre années de thèse. Un grand merci à Sofia, Gaétan et Dounia,

Ludo, Lio, Jérôme et Kevin. Merci également à Rita, Lidija et Luca pour leur disponibilité tout au long de ces années et merci également à Arnaud de Paris.

Je tiens aussi à remercier les mémorants qui sont passés au laboratoire et avec qui j'ai pu travailler : Anne-Isabelle et Olga, mais aussi ceux avec qui j'ai plutôt collaboré en dehors du cadre universitaire (Sylvain et Max).

Merci à mes amis (surtout les *Laux*) qui me chambrent depuis des années en me disant que je ne fais pas un vrai travail. Merci à mon père pour l'ultime correction qui a dû être pénible à lire pour un non-scientifique. Un grand merci à ma mère pour m'avoir enduré ces dernières années et pendant les derniers moments stressant.

Enfin et surtout Géraldine qui, bien que trop souvent à l'étranger, m'a aidé pour la mise en page et bien d'autres choses.

TABLE OF CONTENT

LIST OF ABBREVIATIONS

⊃	Included
AcO$^-$	Acetate
Ar*H*	Aromatic protons
CIS	Complex Induced Shift
δ	Chemical shift
DCM-d$_2$	Deuterated dichloromethane
DMF	Dimethylformamide
DOSY	Diffusion-Ordered SpectroscopY
D$_2$O	Deuterium oxide
DPC	Dodecylphosphocholine
DPC-d$_{38}$	Deuterated dodecylphosphocholine
DOPC	1,2-Dioleoyl-sn-glycero-3-phosphocholine
Equiv. (eq.)	Equivalent
EtOH	Ethanol
EXSY	EXchange SpectroscopY
F	Fluorescence intensity
G	Guest
H	Host
Hepes	4-(2-hydroxyethyl)-1-piperazineethanesulfonic acid
HG	Host-Guest complex
H-bond	Hydrogen bond
IMI	Imidazolidin-2-one
k	Kinetic constant
***K* (*K*$_a$)**	Binding constant
λ	Wavelength
OMe	Methoxy group
NMR	Nuclear Magnetic Resonance
T$_1$	Longitudinal relaxation time
TBA	Tetra-*n*-butylammonium
***t*Bu**	*Tert*-butyle
τ$_m$	Mixing time
TREN	Tris(2-aminoethyl)amine
UV-vis	Ultra-Violet visible
XRD	X-Ray Diffraction

LIST OF FIGURES

CHAPTER 1. GENERAL INTRODUCTION

CHAPTER 2. STUDY OF A FLUORESCENT CALIX[6]ARENE FOR THE RECOGNITION OF ANIONS, CONTACT ION-PAIRS AND PHOSPHOLIPID

CHAPTER 3. INCORPORATION AND STUDY OF CAVITANDS IN MICELLES

CHAPTER 4. FUNNEL COMPLEXES: STUDY OF EXCHANGE DYNAMICS

CHAPTER 5. CONCLUSIONS

CHAPTER 6. MATERIALS AND METHODS

CHAPTER 7. APPENDICES

LIST OF TABLES

CHAPTER 1. GENERAL INTRODUCTION

CHAPTER 4. FUNNEL COMPLEXES: STUDY OF EXCHANGE DYNAMICS

Chapter 1.
General Introduction

The work presented in this thesis falls in the field of supramolecular chemistry, the area of chemistry that focuses on chemical systems made up of a discrete number of assembled molecular subunits or components. In this thesis, we focused more particularly on calix[6]arenes receptors. In this chapter, we will first introduce the context of supramolecular chemistry and present calix[6]arenes and their binding properties. We will then introduce in more detail the two main families of calixarenes we worked with.

1.1. SUPRAMOLECULAR CHEMISTRY

Supramolecular chemistry focuses essentially on the weaker and reversible non-covalent interactions between molecules. In 1894, Emil Fischer proposed the "Lock and Key" model to visualize the interaction between an enzyme and its substrate. Even though successive studies have shown that not all enzymatic reactions can be explained with this model, it laid the foundations for the concept of molecular complementarity in biochemistry, further taken up in supramolecular chemistry. The importance of supramolecular chemistry was recognized by the 1987 Nobel Prize for Chemistry, which was awarded to Donald J. Cram, Jean-Marie Lehn, and Charles J. Pedersen for their "development and use of molecules with structure-specific interactions of high selectivity". The development of selective "host-guest" complexes in which a host molecule (receptor) recognizes and selectively binds a guest was cited as an important part of their work (Figure 1-1).

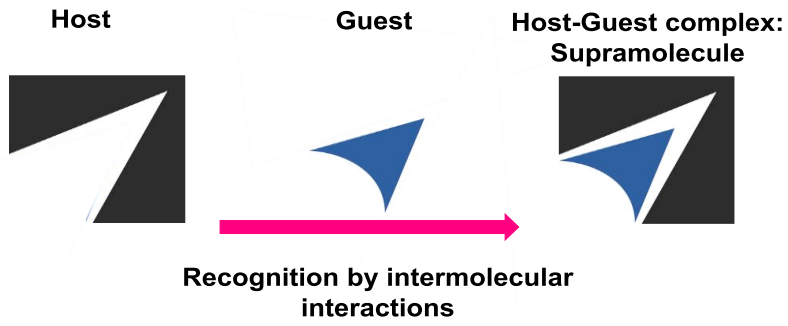

Figure 1-1. Schematic representation of the interactive between a host and a guest molecule.

The definition of supramolecular chemistry given by Jean-Marie Lehn is: "*Au-delà de la chimie moléculaire fondée sur la liaison covalente, s'étend ainsi un domaine qu'on peut nommer supramoléculaire: la chimie des interactions moléculaires, des associations de deux ou*

plusieurs espèces chimiques, les complexes, et de la liaison intermoléculaire".[1] More recently, supramolecular chemistry has been once again put forward by the 2016 Nobel Prize for Chemistry awarded to Jean-Pierre Sauvage, J. Fraser Stoddart and Ben Feringa for their "design and production of molecular machines with controllable movements".

In a supramolecule, the different entities interact through low energy (compared to covalent interactions) "non-covalent interactions", such as coordination bonds, H-bonds, ionic, or Van der Waals interactions (Table 1-1).[2] We can also cite more unconventional non-covalent interactions, such as anion-π or halogen-bonds.[3] The supramolecule is characterized by the spatial arrangement of its different components and by its stability.[4] The individual molecular entities are not modified in their chemical structure, but the new system acquires new properties in comparison to the molecules composing it.

Table 1-1. Examples of non-covalent interactions.

Type of interaction	**Energy (KJ/mol)**
Van der Waals	< 5
H-bond	1 to 120
CH-π, cation-π, π-π	1 to 80
Ion-Ion	200 to 300
Ion-Dipole	50 to 200
Dipole-Dipole	5 to 50
Coordination (metal-ligand)	200 to 350

Non-covalent interactions are of prime-importance in biological systems,[5] such as for the forming of the DNA double helix or the maintenance of the phospholipids bilayer in cellular membranes.[6] Inspired by nature, chemists have been interested in developing synthetic supramolecular systems able to recognize different chemical species. Such systems, called molecular receptors, find applications in many different fields such as catalysis, environmental monitoring or medical diagnostics. Many different types of receptors, which can complex

[1] Lehn, J.-M. *Leçon inaugurale au Collège de France*, **1980**.
[2] Steed, J.W.; Turner, D.R.; Wallace, K.J. *Core Concepts In Supramolecular Chemistry And Nanochemistry*, John Wiley & Sons, Chichester, **2007**.
[3] Ma, J. C.; Dougherty, D. A. *Chem. Rev.* **1997**, *97*, 1303-1324.
[4] Lehn, J.-M. *Supramolecular Chemistry*, VCH, Weinheim, **1995**.
[5] Berg, J.M.; Stryer, L.; Tymoczko, J.L. *Biochemistry*, 5th ed.; Freeman, New York **2002**. Kovbasyuk, L.; Kramer, R. *Chem. Rev.* **2004**, *104*, 3161-3187.
[6] Lawrence, D.S.; Jiang, T.J.; Levett, M. *Chem. Rev*. **1995**, *95*, 2229-2260.

cations, anions or neutral species, have been developed over the past thirty years. Much work has focused on the development of systems, which are selective and even more importantly stable in water. A class of macrocyclic synthetic receptors is the one composed by those bearing a cavity (thus also called cavitands). Examples of these are cucurbit[n]uriles, cyclodextrines, cyclotriveratrilenes, cryptophanes, homoxacalix[n]arenes, pillar[n]arenes, resorcin[n]arenes (the list is not exhaustive,

Figure 1-2). In the context of this thesis, we are interested in a particular class of macrocyclic receptors called calix[6]arenes, which possess a cavity that can accommodate small organic molecules.

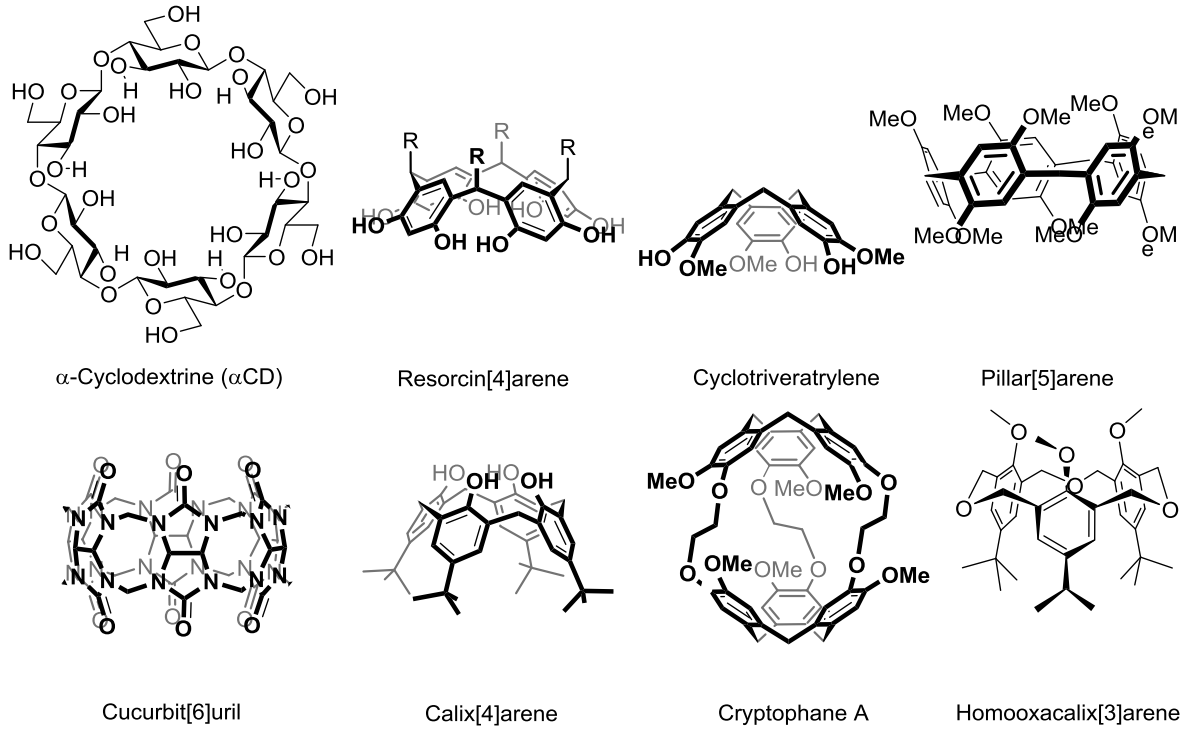

Figure 1-2. Examples of macrocyclic molecular receptors bearing a cavity.

1.2. CALIX[6]ARENES

Calix[n]arenes are macrocyclic organic molecules composed of *n* para-substituted phenolic units (4 to 16) linked by methylene bridges. Their name comes from the Greek *calix* (flask) as the structure of a calixarene molecule in its cone conformation resembles a flask, and *arene* for the aromatic units. These molecules were discovered in the early 40's by Zinke[7] but calixarene

[7] Zinke, A.; Ziegler, E. *Ber.* **1941**, *B74*, 1729-1736.

chemistry really developed with the work of Gutsche in the 80's who managed to describe a simple procedure for the synthesis of the *p*-*t*Bu-calix[n]arene (good yields were obtained for n=4, 6 and 8).[8] The calixarenes are obtained via a macrocyclisation reaction of *p*-*t*Bu-phenol with formaldehyde in the presence of a base (Figure 1-3).

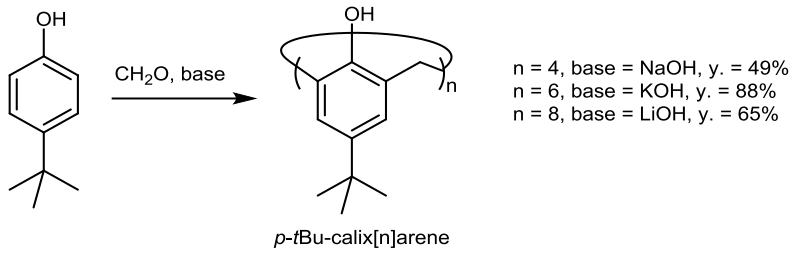

Figure 1-3. Synthesis of the *p*-*t*Bu-calix[n]arene.

Calix[6]arenes exhibit conformational flexibility as the inversion of the phenolic units is possible. This inversion involves a rotation around the methylene bridges where either the hydroxyl group (OH group) or the tertio-butyl group can toggle into the calix cavity (Figure 1-4).

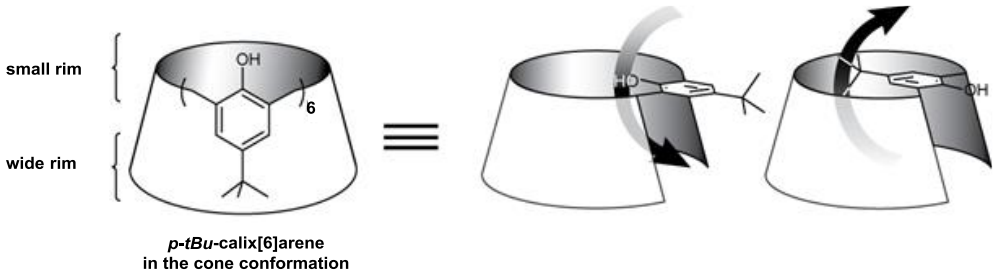

Figure 1-4. Inversion modes of the phenolic units of calix[6]arenes.

A consequence of the conformational flexibility is that 8 different specific conformations are possible for calix[6]arenes (Figure 1-5).

[8] Gutsche, C.D. **1998**. Calixarenes Revisited, Monographs in Supramolecular Chemistry.

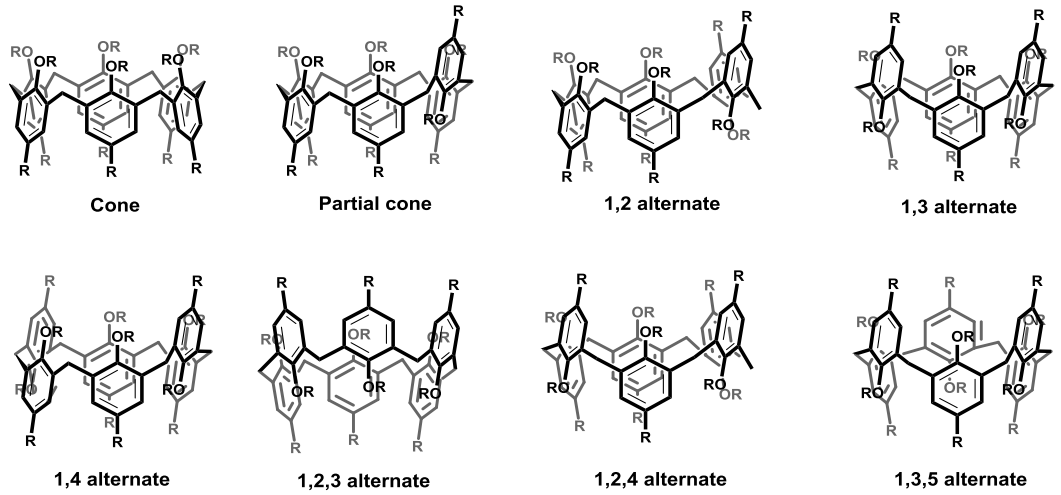

Figure 1-5. Eight specific conformations of calix[6]arenes.

When all the phenolic units point in the same direction, the calixarene is said to be in its cone conformation and a *wide rim* (composed of the *t*Bu groups) and a *small rim* (composed of the OH groups) can be distinguished. In their cone conformation, calix[6]arenes have a cavity, which can accommodate small organic molecules. Thus, they can be envisaged for the inclusion of different guests. Different strategies have been developed so as to prevent the conformational flexibility of calix[6]arenes and ensure that they adopt their cone conformation and have thus a well-defined cavity. Three strategies are described below.

Coordination chemistry

A first possibility is to use coordination interactions involving metal cations (e.g. Zn^{2+}, Cu^{n+}) that can bind to nitrogen containing groups grafted onto the narrow rim. These types of systems are called "funnel complexes" because the free coordination site of the metal cation is within a hydrophobic cavity, which can act as a molecular funnel for neutral organic guest molecules (Figure 1-6). The guest molecules bind to the metal by coordination interactions.[9]

[9] For example: Blanchard, S.; Le Clainche, L.; Rager M.-N.; Chansou, B.; Tuchagues, J.-P.; Duprat, A.F.; Le Mest, Y.; Reinaud, O. *Angew. Chem. Int. Ed. Engl.* **1998**, *37*, 2732-2735. Rondelez, Y.; Bertho, G.; Reinaud O.; *Angew. Chem. Int. Ed. Engl.* **2002**, *41*, 1044-1046.

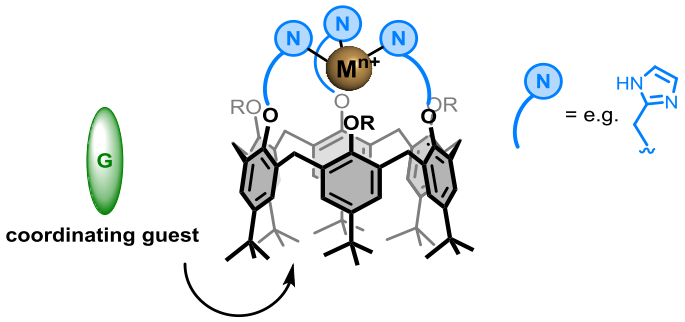

Figure 1-6. Rigidification strategy of calix[6]arenes via the coordination of a metallic cation.[10]

In the same context, another strategy reported is the introduction of groups on the small rim of the calixarene that allows the coordination to an anion (Figure 1-7).

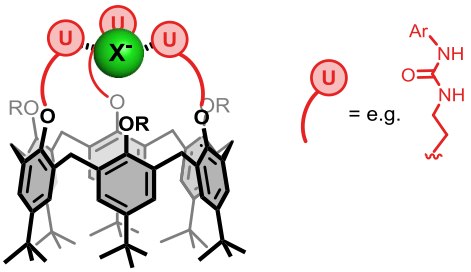

Figure 1-7. Rigidification strategy of calix[6]arenes via the coordination to an anion.[11]

Self-assembling[12]

A second possibility is to exploit the self-assembly of complementary organic functions. For example, an ion-paired cap can close the cavity efficiently and restricts the calixarene in its cone conformation. Examples of such self-assembled systems with calix[6]arenes have been

[10] Sénèque, O.; Rager, M.-N.; Giorgi, M.; Reinaud, O. *J. Am. Chem. Soc.* **2000**, *122*, 6183-6189. Sénèque, O.; Rondelez, Y.; Le Clainche, L. ; Inisan, C. ; Rager, M.-N. ; Giorgi, M.; Reinaud, O. *Eur. J. Inorg. Chem*. **2001**, 2597-2604.

[11] Hamon, M.; Ménand, M.; Le Gac, S. p.; Luhmer, M.; Dalla, V.; Jabin, I. *J. Org. Chem.* **2008**, *73*, 7067-7071;

[12] Lehn, J.-M.; Rigault, A.; Siegel, J.; Harrowfield, J.; Chevrier, B.; Moras, D. *Proc. Natl. Acad. Sci.* **1987**, *84*, 2565-2569. Pfeil, A.; Lehn, J.-M. *J. Chem. Soc., Chem. Commun.* **1992**, 838-840. Tecila, P.; Dixon, R. P.; Slobodkin, G.; Alavi, D.H.; Waldeck, D.H.; Hamilton, A.D. *J. Am. Chem. Soc.* **1990**, *112*, 9408-9410. Whitesides, G.M.; Mathias, J. P.; Seto, C. T. *Science* **1991**, *254*, 1312-1319.

reported in order to form capsules[13] and rotaxanes[14] in solution. Such strategy, based on a calix[6]tris-amine, has been developed in our laboratory in the past years (Figure 1-8).[15]

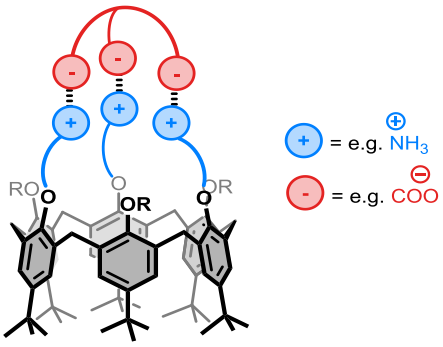

Figure 1-8. Calix[6]arenic receptor obtained by rigidification via self-assembly.

Grafting of covalent bonds

A third possibility is to close the narrow rim with covalent bridges between the phenolic units. Examples are calix[6]arenes bearing an aza-cryptand cap (Figure 1-9).

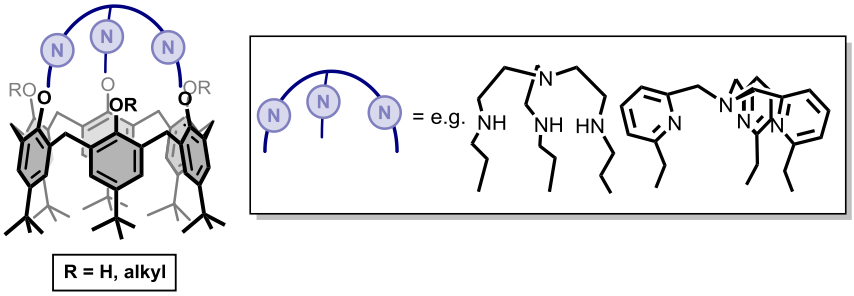

Figure 1-9. Rigidification of calix[6]arenes by covalent grafting of an aza-cryptand cap.[16]

In the next two sections, we will focus on the two main families of calixarene we have worked with: (i) calix[6]arenes-zinc complexes, known as "*funnel complexes*" and (ii) calix[6]arenes functionalized with urea moieties.

[13] For example: Arduini, A.; Ferdani, R.; Pochini, A.; Secchi, A.; Ugozzoli, F.; Sheldrick, G. M.; Prados, P.;Gonzalez, J.J.; de Mendoza, J. J. *Sup. Chem.* **2001**, *1*, 1-4 ; Rincon, A. M.; Prados, P.; De Mendoza, J. *Eur. J. Org. Chem.* **2002**, 640-644.

[14] For example : Credi, A.; Dumas, S.; Silvi,S.;Venturi, M.; Arduini, A.; Pochini, A.; Secchi, A. *J. Org. Chem.* **2004**, *69*, 5881-5887. Arduini, A.; Ciesa, F.;Fragassi, M.; Pochini, A.; Secchi, A. *Angew. Chem. Int. Ed.* **2005**, *44*, 278-281.

[15] For example: Darbost, U.; Giorgi, M.; Hucher, N.; Jabin, I.; Reinaud, O. *Supramol. Chem.* **2005**, *17*, 243-250. Le Gac, S.; Marrot, J.; Reinaud, O.; Jabin, I. *Angew. Chem., Int. Ed. Engl.* **2006**, *45*, 3123-3126. Le Gac, S.; Picron, J.-F.; Reinaud, O.; Jabin, I. *Org. Biomol. Chem.* **2011**, *9*, 2387-2396.

[16] For example: Darbost, U.; Giorgi, M.; Reinaud, O.; Jabin, I. *J. Org. Chem.* **2004**, *69*, 4879-4884; Zeng, X.; Hucher, N.; Reinaud, O.; Jabin, I. *J. Org. Chem.* **2004**, *69*, 6886-6889; Jabin, I.; Reinaud, O. *J. Org. Chem.* **2003**,

1.3. FUNNEL COMPLEXES

Calix[6]arenes that are functionalized on alternate phenolic positions (positions 1,3,5) by three amino arms that can complex a metallic cation are known as "funnel complexes". The binding of the metal ion constrains the calix[6]arene into its cone conformation, leaving a single metal coordination site accessible for guest binding inside the cavity (Figure 1-6).

One of the reasons for the interest in calix[6]arene funnel complexes, is that they can be seen as models for the active site of metallo-enzymes. Indeed, many enzymes contain a metallic cation, which can have a structural role, be involved in the recognition process, or be active in the catalytic process. The analysis of the mechanisms of these enzymes is not straightforward as they are very unstable when out of their biological environment. Over the years, chemists have therefore been interested in the design of synthetic model systems that can be used to elucidate the functioning of metallo-enzymes.

Zinc is the second most abundant transition metal cation found in biological systems and zinc metallo-enzymes play many important roles in the human body.[17] The most commonly observed binding geometry at the level of the coordination sphere of the zinc cation is tetrahedral. The zinc cation present in the active site of carbonic anhydrase is for example coordinated to three histidine moieties and to a water molecule.[18] There are also many enzymes, such as astacins or β-lactamase, where a penta-coordinated trigonal bipyramidal coordination geometry is observed.[18] Accurate models for the active site of metallo-enzymes must present the following characteristics:

- coordinating arms, which reproduce the direct environment near the metal (first coordination sphere);
- groups that reproduce aminoacids residues which are in proximity with the metallic center that stabilize the substrate (second coordination sphere). The selectivity for the substrate is also given by the arranging of these residues in the active site;
- an access funnel (hydrophobic cavity that plays the role of the enzymatic pocket) that controls the arrival of the substrate. This funnel allows the protection of the active site

68, 3416-3419; Zeng, X.; Coquière, D.; Alenda, A.; Garrier, E.; Prangé, T.; Li, Y.; Reinaud, O.; Jabin, I. *Chem. Eur. J.* **2006**, *12*, 6393-6402.

[17] McCall, K.A.; Huang, C.; Fierke, C.A. *The Journal of nutrition* **2000**, *130*, 1437S–1446S. Silva, J.J.R.F.D; Williams, R.J.P. *The Biological Chemistry of the Elements*; The Inorganic Chemistry of Life, 2nd ed.; Oxford University press: New York, **2001**.

[18] Lipscomb, W.N.; Sträter, S. *Chem. Rev.* **1996**, *96*, 2375-2434.

from the external media permitting the approach of the substrate and the expulsion of the product after the catalysis (third coordination sphere).

Calix[6]arenes, such as those being developed in the laboratories of Prof. Reinaud and Prof. Jabin, are good models as they present a cavity, which can host organic molecules, and a binding site for metallic cations. They do not only imitate the "first coordination sphere" thanks to the ligands present on the narrow rim but also the "second and third coordination sphere" thanks to the hydrophobic cavity. Three families of calix[6]arenes have been developed: calix[6]N_3, calix[6]N_3Z and the calix[6]aza-cryptands (Figure 1-10). In this thesis, we are mainly interested in the calix[6]N_3 and calix[6]aza-cryptands that are described in more detail in the next sections.

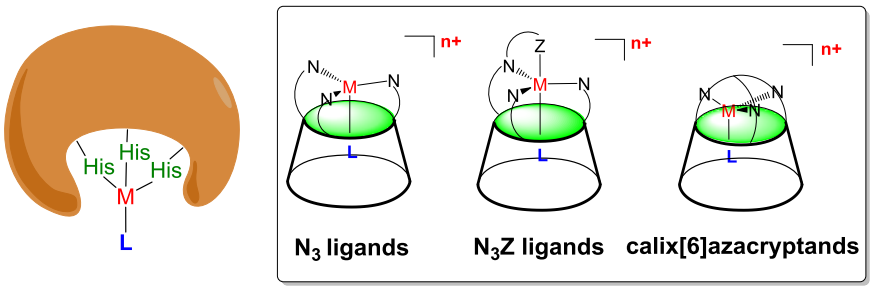

Figure 1-10. Supramolecular approach for the mimic of the active site metallo-enzymes.

1.3.1. CALIX[6]N_3

The first generation of models developed bear three nitrogen arms in position 1-3-5 at the level of the small rim of the calixarene. Different ligands have been developed (Figure 1-11).

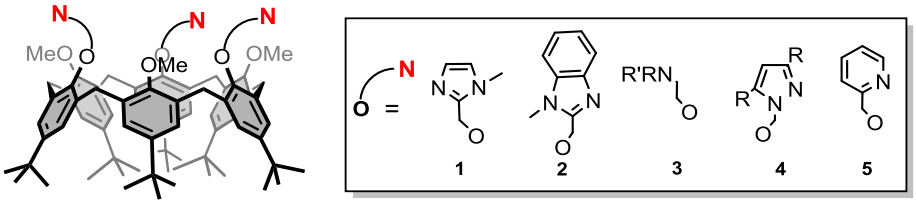

Figure 1-11. Schematic representation of the family of receptors calix[6]N_3.[10]

The most studied receptor for copper (II) and zinc complexation is the one with 3 methtyl-imidazole moieties grafted on the small rim that for the sake of convenience we will call calix[6]tris-imidazole or host **1**. In the **1.Zn**$^{2+}$ complex, the cation coordinated to the imidazole moieties acquires a tetrahedral geometry. XRD and ^{1}H NMR spectroscopy studies in organic

solvents have shown that, in the absence of any coordinating guest, two water molecules are included in the calixarene cavity: the first molecule is linked to the metal, whereas the second one is linked to the first water molecule and to a phenolic oxygen by H-bonding interactions (Figure 1-12).[19,20]

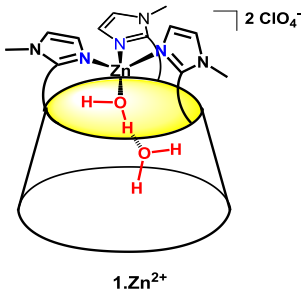

Figure 1-12. Host **1.Zn**$^{2+}$ with two water molecules buried in the cavity.[19]

Host **1.Zn**$^{2+}$ is known to bind neutral guest molecules at the level of the metal center. The affinity for some neutral guest was determined against water and DMF, and the relative affinity constants are given in Table 1-2.[21] Results showed that:

- the guest is exchangeable;
- a selectivity is observed in terms of the affinity of the guest for the metal and of its size and shape;
- the system formed is stabilized by H-bonds and CH-π interactions;
- anionic guests are not recognized inside the cavity due to the electrostatic repulsion generated by the second coordination sphere (oxygen atoms present at the small rim).

[19] Sénèque, O.; Rondelez, Y.; Le Clainche, L. ; Inisan, C. ; Rager, M.-N. ; Giorgi, M.; Reinaud, O. *J. Am. Chem. Soc*. **2001**, *123*, 8442-8443.
[20] Sénèque, O. **2002**. PhD thesis: Nouveaux ligands biomimétiques dérivés de calix[6]arenes. Etude de la complexation du zinc et du cuivre et comparaison avec les systemes naturels protéiques. U.F.R. Biomedicale, Université Paris Descartes.
[21] Sénèque, O.; Giorgi, M. ; Reinaud, O. *Supramol. Chem.* **2003**, *15*, 573–580.

Table 1-2. Relative affinity constants $K_{L/water}$ and $K_{L/DMF}$ at 298 K for guest exchange for **1.Zn^{2+}** in $CDCl_3$.[19]

Guest (G)	$K_{L/water}$ (M)	$K_{L/DMF}$ (M^{-1})
Heptylamine	>2	>25
2-Methylbutylamine	>2	>25
2-Butylylamine	0.78	9
DMF	0.082	1
Ethanol	0.39	4,7
Propan-1-ol	0.013	0.16
Propan-2-ol	0.0004	0.005
Acetonitrile	0.031	0.38
Propionitrile	0.011	0.13

The selectivity for the different *endo*-complexed guests is conditioned by steric hindrance at the level of the coordinating atom (O or N) and at its α-position which explains why primary amines and primary alcohols are preferred guest molecules.[20] Another important property of **1.Zn^{2+}**, highlighted by XRD, is that the imidazole arms twist around the metal center forming a helix. This induces chirality in the complex. The helix can twist in two opposite directions, giving rise to two enantiomeric conformers, which are at equilibrium. Passing from one conformer to another is called the "helical inversion" (Figure 1-13).[22]

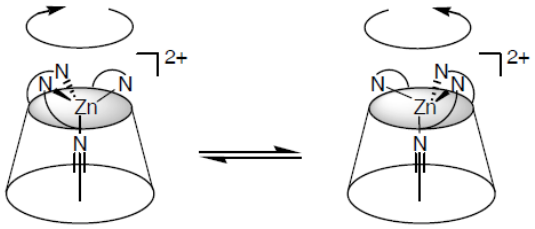

Figure 1-13. Equilibrium between the two enantiomeric conformers with an acetonitrile molecule buried inside the cavity.

1.3.2. CALIX[6]AZA-CRYPTANDS

The calix[6]aza-cryptand family (Figure 1-14), with its covalently linked nitrogen arms, presents advantages compared to the systems with three independent nitrogen arms.[22]

[22] For the synthesis of **6** see: Jabin, I.; Reinaud, O. *J. Org. Chem.* **2003**, *68*, 3416-3419; of **7** see: Zeng, X.; Coquière, D.; Alenda, A.; Garrier, E.; Prangé, T.; Li, Y.; Reinaud, O.; Jabin, I. *Chem. Eur. J.* **2006**, *12*, 6393-6402; of **8** see: Zeng, X.; Hucher, N.; Reinaud, O.; Jabin, I. *J. Org. Chem.* **2004**, *69*, 6886-6889; of **9** see: Garrier, E.; Le Gac, S.; Jabin, I. *Asymm.* **2005**, *16*, 3676-3771.

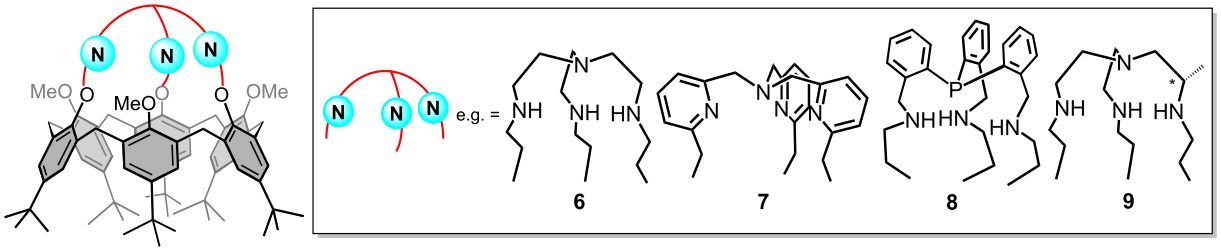

Figure 1-14. Schematic representation of the calix[6]aza-cryptands ligand family.[22]

The systems with three independent arms generally exhibit a low affinity for the metal and the metallic complexes have been shown to exhibit a lack of stability in the presence of coordinating species such as hydroxyl group or DMSO.[20] Moreover, the metal is exposed giving rise to an *exo*-coordination site accessible in the apical position for an exogenous molecule (Figure 1-15).

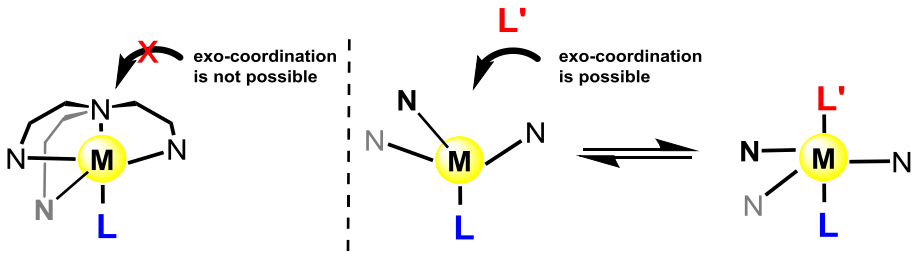

Figure 1-15. Schematic representation of metallic site of the calix[6]aza-cryptand family (left) and the calix[6]N_3 family (right).

A grafted cap gives rise to the following advantages:

- a higher stability of the metal complexes formed thanks the chelate effect;
- the metal center is protected from the bulk and no *exo*-coordination is possible.

The most studied aza-cryptand complex is the calix[6]tren **6** (Figure 1-16). This macrocycle is functionalized by a *tris*(2-aminoethyl)*amine* cap called *tren*. Its host-guest properties have been intensively studied in organic solvents.[23,24] Results show that this host can accommodate neutral guests in chloroform (Figure 1-16A). Recognition is possible thanks to the multiple H-bond interactions between the ammonium head and the calixarene, but also thanks to CH-π

[23] Izzet, G.; Douziech, B.; Prangé, T.; Tomas, A.; Jabin, I.; Le Mest, Y.; Reinaud, O. *Proc. Natl. Acad. Sci. USA* **2005**, *102*, 6831-6836; Darbost, U.; Zeng, X.; Rager, M.-N.; Giorgi, M.; Jabin, I.; Reinaud, O. *Eur. J. Inorg. Chem.* **2004**, 4371-4374.
[24] Darbost, U.; Rager, M.-N.; Petit, S.; Jabin, I.; Reinaud, O. *J. Am. Chem. Soc.* **2005**, *127*, 8517-8525.

interactions between the organic part of the ammonium and the aromatic unities of the cavity of the calixarene.

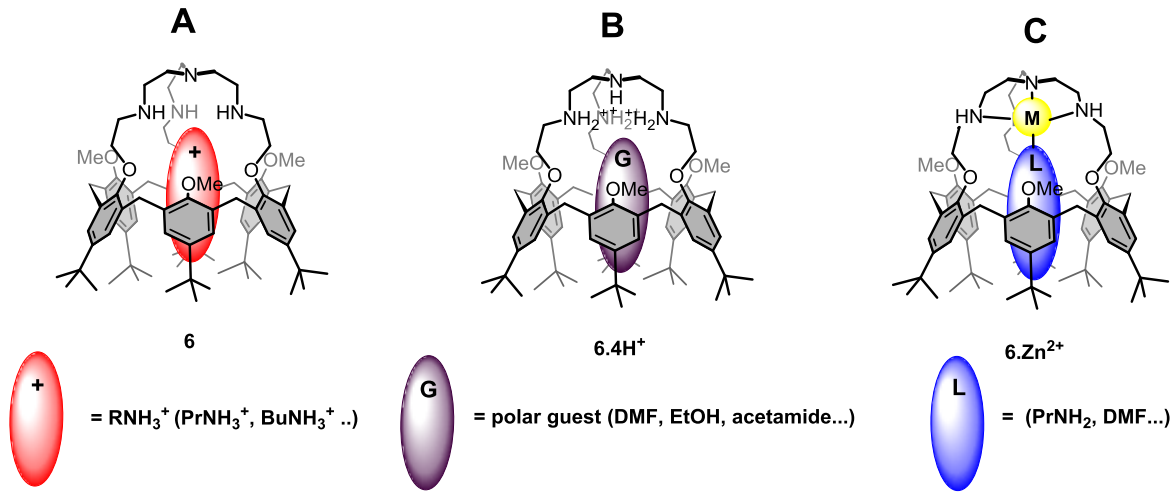

Figure 1-16. (A) the neutral ligand can accommodate a primary ammonium; (B) the tetra-protonated ligand can accommodate neutral polar molecules such as an amide or an alcohol; (C) the metallic complex (Zn^{2+}, Cu^{2+} etc.) can complex a molecule with a coordinating group.

Affinities of host **6** for different guests relative to ethylammonium ($EtNH_3^+$) have been measured by NMR.[24] Results (in $CDCl_3$ at 298 K) showed that the affinity is dependent on the length of the ammonium chain and its degree of substitution: propylammonium ($K_{PrNH3+/EtNH3+}$ = 3) and butylammonium ($K_{BuNH3+/EtNH3+}$ = 0.1). For $(CH_3)_2NH_2^+$ the relative affinity constant determined was 0.05 and no interaction was observed for hindered quaternary ammoniums ($(CH_3)_4N^+$).

The tetra-protonated system **6.4H**$^+$ exhibits good recognition properties for neutral polar guests, such as alcohols, nitriles, aldehydes amides and DMSO, in $CDCl_3$ (Figure 1-16B).[24] The complexes are stabilized by dipole-charge interactions between the polar guest and the protonated cap of the receptor but also thanks to H-bond and CH-π interactions.

When a metal cation such as (Zn^{2+} or Cu^{2+}) is coordinated to **6**, the system can *endo*-complex different types of guests (Figure 1-16C). The affinities relative to DMF of **6.Zn**$^{2+}$ for different guests have been determined by NMR (in $CDCl_3$ at 298 K) and have showed that amines are preferred over alcohols and amides and that the affinity is dependent on the length of the amine chain: $K_{PrNH2/DMF}$ = 1600, $K_{OctylNH2/DMF}$ = 0.9, $K_{MeCONH2/DMF}$ = 0.4 and $K_{EtOH/DMF}$ = 0.4.[24] It has also been shown that when **6.Zn**$^{2+}$ is in the presence of $PrNH_2$ and DMF only **6.Zn**$^{2+}$**⊂PrNH**$_2$

is observed but that, upon addition of TFA, a de-metalation occurs and the formation of **6.4H$^+$⊂DMF** is observed. The addition of NEt_3 reestablishes **6.Zn^{2+}⊂PrNH$_2$**.

1.4. CALIX[6]UREAS-BASED RECEPTORS

The complexation of a cation or an anion by a neutral receptor is always in competition with the association of the guest with its counter-ion. In the context of host-guest chemistry this is problematic as it can lead to the precipitation of the ion-pair or it can even inhibit the complexation of the charged guest. In order to override this problem, the classical strategy is the use of non-coordinating counter-ions (TBA^+, Pic^-, BF_4^-, PF_6^-, ClO_4^- etc.). Another strategy, which has come under considerable spotlight in the last years,[25] is the development of systems that can simultaneously complex the two partners of the ion-pair. This strategy can indeed lead to a minimization of the competition due to the formation of the free ion-pair but can also find interesting applications in the recognition of zwitterionic types of guest such as phospholipids.

1.4.1. COMPLEXATION OF ION-PAIRS: THE STRATEGY

A considerable amount of work has been devoted to the design of ditopic molecular receptors capable of complexing ion-pairs. Three strategies are reported for the recognition of ion-pairs as described below (Figure 1-17).

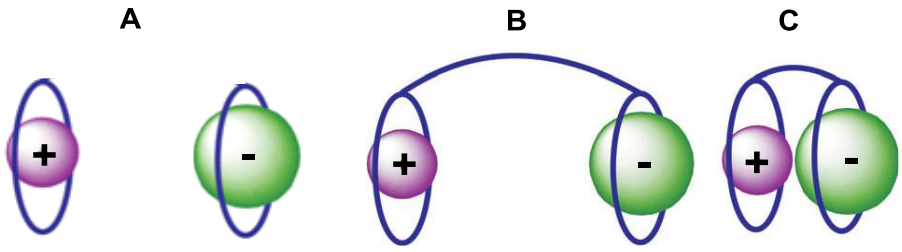

Figure 1-17. The three strategies used for ion-pair recognition: A "Dual Host" strategy, B ditopic receptors for dissociated ion-pairs; C ditopic receptors for contact ion-pairs.[26]

The Dual-Host strategy

This strategy involves two different receptors: one for each partner of the ion-pair. As it requires two receptors this strategy cannot give rise to cooperative processes (Figure 1-17A).

[25] Kim, S.K.; Sessler, J.L. *Chem. Soc. Rev.* **2010**, *39*, 3784-3809.
[26] McConnell, A.J.; Beer, P. D. *Angew. Chem Int. Ed.* **2012**, *5*, 2-12.

Ditopic receptors for dissociated ion-pair

This approach allows the complexation of the two partners of the ion-pair within the same receptor, at the level of two recognition sites that are spatially distinct. The complexation of the first partner can lead to a modification of the receptor conformation that can favor or disfavor the complexation of the second partner. Thus this strategy can lead to allosteric processes (Figure 1-17B).

Ditopic receptors for contact ion-pairs

This third strategy permits the complexation of the two partners of the ion-pair in close proximity within the receptor. This close proximity can allow the establishment of an ionic interaction between the two partners. This is energetically favorable as it avoids the dissociation of the ion-pair and can possibly lead to a cooperative process (Figure 1-17C). As calix[6]arenes can be designed as molecular receptors for ditopic guests, in this thesis we are particularly interested in this strategy since we want to exploit them for the recognition of different types of analytes.

1.4.2 CALIX[6]UREAS FOR CONTACT ION-PAIR RECOGNITION

Calix[6]arenes can be easily functionalized at the small rim with moieties capable of recognizing an anion. The cavity, for its part, can host a cationic molecule. These systems are undoubtedly suitable candidates for recognizing ion-pairs.

Neutral anions receptors typically contain H-bond donor groups such as sulfonamides,[27] amides,[28] (thio)ureas,[29] pyrroles,[30] carbazoles[31] or indoles[32]. The grafting of arms bearing such moieties on the small rim of calix[6]arenes make the systems suitable candidates for the recognition of ion-pairs as the calixarene cavity can potentially accommodate a cationic species. The calix[6]arenes bearing two (thio)ureas arms developed by Yang et al. and those bearing

[27] Davis, A.P.; Perry, J.J.; Williams, R.P. *J. Am. Chem. Soc*. **1997**, *119*, 1793.
[28] Bondy, C. R.; Loeb, S. J. *Coord. Chem. Rev.* **2003**, *240*, 77-99.
[29] Gomez, D. E.; Fabrizzi, L.; Licchelli, M.; Monzani, E. *Org. Biomol. Chem.* **2005**, *3*, 1495-1500.
[30] Cafeo, G.; Kohnke, F.H.; La Torre, G.L.; Parisi, M.F.; Nascone, R.P.; White, A.J.P.; Williams, D.J. *Chem. Eur. J*. **2002**, *8*, 3148-3149. Cafeo, G.; Kohnke, F.H.; White, A.J.P.; Garozzo, D.; Messina A. *Chem. Eur. J*. **2007**, *13*, 649-656.
[31] Chmielewski, M.J.; Charon, M.; Jurczak, *J. Org. Lett.* **2004**, *6*, 3501-3504. Piatek, P.; Lynch, V.M.; Sessler, J.L. *J. Am. Chem. Soc.* **2004**, *126*, 16073-16076.
[32] Curiel, D.; Cowley, A.; Beer, P.D. *Chem. Commun*. **2005**, 236-238. Sessler, J.L.; Cho, D.-G.; Lynch, V. *J. Am. Chem. Soc*. **2006**, *128*, 16518-16519.

three urea arms developed by Reinhoudt et al. (Figure 1-18) have been shown to efficiently complex, in organic solvents, anions at the level of the urea groups.[33,34] The recognition of ion-pairs was however not evaluated by these groups with these systems.

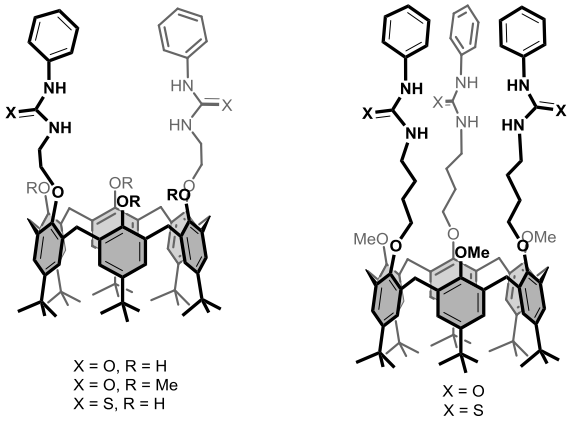

Figure 1-18. Left: Yang's receptors; Right: Reinhoudt's receptors.

A calixarene-based receptor, similar to the ones of Yang and Reinhoudt, has been synthetized in the Jabin laboratory (calix[6]tris-phenylurea, host **10**).[11] The NMR study of the complexation capabilities of host **10** has shown that this is an excellent heteroditopic[35] receptor for contact in pairs such as ammonium halides like $PrNH_3^+Cl^-$ (Figure 1-19).

[33] Nam, K.; Kim, D.S.; Yang, Y.S. *Bull. Korean Chem. Soc*. **1998**, *19*, 1133-1136.
[34] Scheerder, J.; Engbersen, J.F.J.; Casnati, A.; Ungaro, R.; Reinhoudt, D.N. *J. Org. Chem.* **1995**, *60*, 6448-6454.
[35] Which possess two distinct sites of recognition.

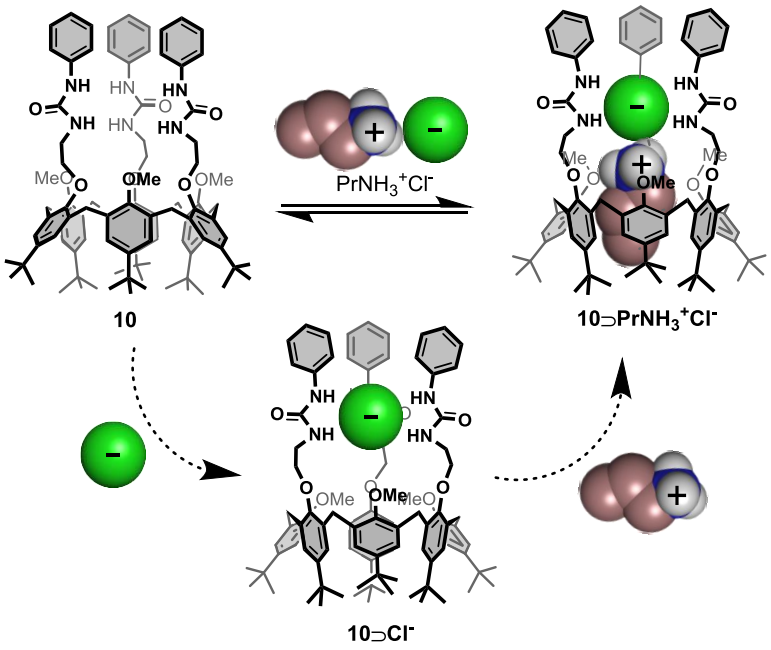

Figure 1-19. Recognition mode for contact ion-pairs with receptor **10**.[11]

Recognition of the anion via H-bonding interactions at the level of the urea moieties polarizes the receptor promoting the *endo*-complexation of the ammonium inside the cavity. The ammonium is stabilized by an ionic interaction with the anion and by non-covalent interactions (CH-π and H-bonding interactions) with the calix structure. A cooperative effect is observed in the sense that the complexation of an ammonium ion is possible only if the anion is simultaneously bound at the level of the urea groups. It was furthermore observed that the anions with the higher binding affinity are not those that best promote the inclusion of the ammonium. This was rationalized as a consequence of the size of the anion and by the fact that the stronger the interaction with the urea moieties, the more the charge density will be weakened at the level of the anion and consequently the ionic interaction with the ammonium. The remarkable properties of this receptor are the consequence of the close proximity of the two binding sites that enables the complexation of contact ion-pairs.

Calix[6]arenes with a cryptamide or cryturea cap have also been developed in the Jabin's laboratory for ion-pair recognition. Receptor **11**, shown in Figure 1-20, has for example been shown to complex various ammonium fluorides with good affinity.[36] The chelate effect is of course beneficial. Calixcrypturea **12** shows similar characteristics to its cryptamide

[36] Lascaux, A.; Le Gac, S.; Wouters, J.; Luhmer, M.; Jabin, I. *Org. Biomol. Chem.* **2010**, *8*, 4607-4616 ; Lascaux, A.; Delahousse, G.; Ghostin, J.; Bouillon, J.-P.; Jabin, I. *Eur. J. Org. Chem.* **2011**, 5272-5278.

analog (Figure 1-20). [37,38]. It complexes not only linear ammonium halides but also biological ammoniums.

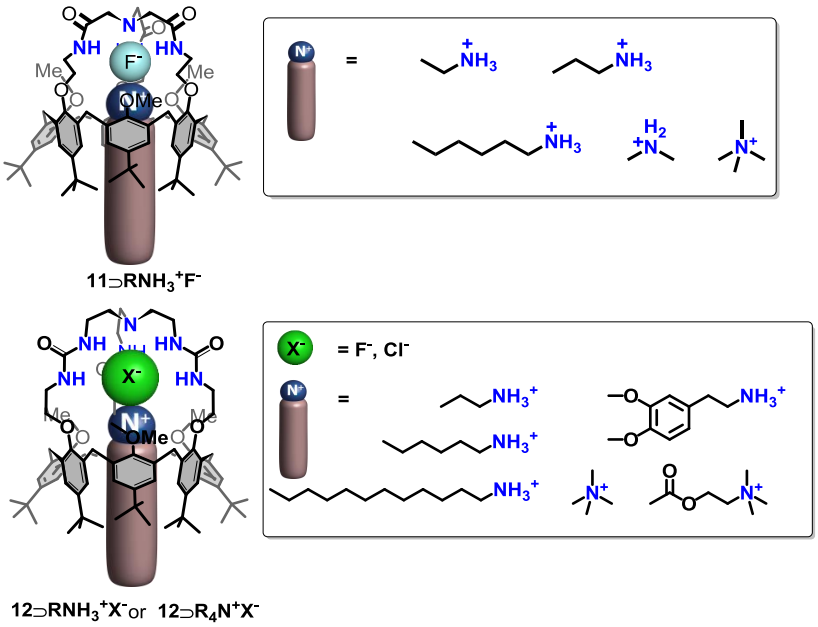

Figure 1-20. Complexation of a contact ion-pair with receptors **11** and **12**.

Other systems synthesized and studied in the Jabin's group, in this case for the binding of ion triads, are the calix[6]tube-(thio)ureas **13a-b,** which display two divergent cavities linked by three (thio)urea arms.[39] It was shown that **13a-b** exhibit efficient binding properties for contact ion triads and a selectivity for primary or secondary ammoniums associated to a divalent anion (ex. : SO_4^{2-}) (Figure 1-21). **13b** was also shown to be able to bind larger ammoniums in protic solvents. XRD results showed that the cascade complexes are stabilized through a solid arrangement of hydrogen-bonding interactions. It was also observed that ammonium nitrate salts can be selectively extracted from water to chloroform as the nitrate anion combines weak hydration with good geometrical complementarity with the tris-thiourea binding site.

[37] Ménand, M.; Jabin, I. *Org. Lett.* **2009**, *11*, 673-676.
[38] Ménand, M.; Jabin, I. *Chem. Eur. J.* **2010**, *16*, 2159-2169.
[39] Moerkerke, S.; Ménand, M.; Jabin, I. *Chem. Eur. J.* **2010**, *16*, 11712-11719; Moerkerke, S.; Le Gac, S.; Topic´, F.; Rissanen, K.; Jabin, I. *Eur. J. Org. Chem.* **2013**, 5315–5322.

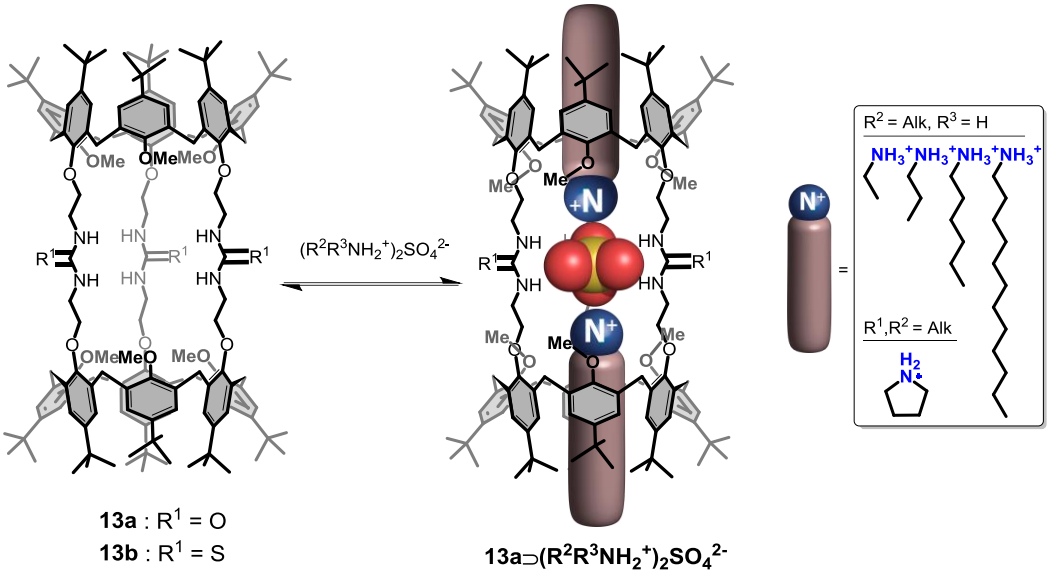

Figure 1-21. Complexation of a contact ion with a calix[6]tube-(thio)ureas **13a-b**.

Very recently, it has been reported that the thio(urea) derivative **13b**, is able to selectively bind phosphatidylcholines (PCs) over phosphatidylethanolamines (PEs).[40] The binding of the PCs is made possible thanks to multiple H-bonding interactions between their anionic moiety and the tris-thiourea groups of the host, as well as through cation-π and CH-π interactions between their cationic $(CH_3)N^+$ group and one of the two polyaromatic calixarene cavities. Moreover, results showed that the fatty acid chains of the bound lipids do not protrude from the second calixarene cavity but from one of the three macrocycles formed by the thio-urea arms.

[40] Moerkerke, S.; Wouters, J.; Jabin, I. *J. Org. Chem.* **2015**, *80*, 8720-8726.

1.5. AIM OF THE THESIS

As we have seen in this introduction, calix[6]arenes are versatile scaffolds to build molecular hosts that can be exploited in molecular recognition processes. Their interesting and polyvalent complexation properties depend on their functionalization. Different calix[6]arene based systems have been studied in this thesis, using mainly Nuclear Magnetic Resonance (NMR), UV-visible and emission spectroscopies.

The calixarene cavity offers recognition selectivity, via form and size complementarity, and a first goal of our work is to see if **systems with grafted chromophores could be used for the selective sensing of different guests**. We report in **chapter 2** our studies undertaken with **fluorescent receptors** calix[6]tris-pyrenylurea **14a-b** (Figure 1-22).

We first completed the work that Dr. Picron initiated in the framework of its PhD thesis under the supervision of Prof. Jabin[41], devoted to the recognition of ions and ammonium salts. We also studied the receptors for the sensing of phospholipids.

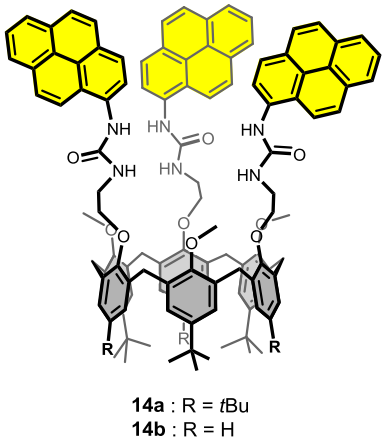

14a : R = *t*Bu
14b : R = H

Figure 1-22. Structure of receptors **14a-b**.

Another goal of the thesis is to evaluate the possibility to **transfer calixarenes and related hydrophobic receptors into aqueous media using micelles**. Hydrophobic receptors incorporated into micelles can indeed be exploited for the recognition of analytes in an aqueous environment. The studies undertaken on the binding capacities of the calix[6]tren zinc complex (**6.Zn**$^{2+}$) incorporated in doceylphosphocholine (DPC) micelles are reported in **chapter 3**. The

[41] Picron, J.-F. **2012**. PhD thesis: Synthèse et étude de récepteurs calix[6]aréniques porteurs de fluorophores. Laboratoire de Chimie Organique, Université Libre de Bruxelles.

binding potential of a homooxacalix[3]arene derivative (**15**) and a resorcin[4]arene-based zinc complex (**16.Zn^{2+}**) incorporated in DPC micelles is also evaluated and the results are also described in **chapter 3** (Figure 1-23).

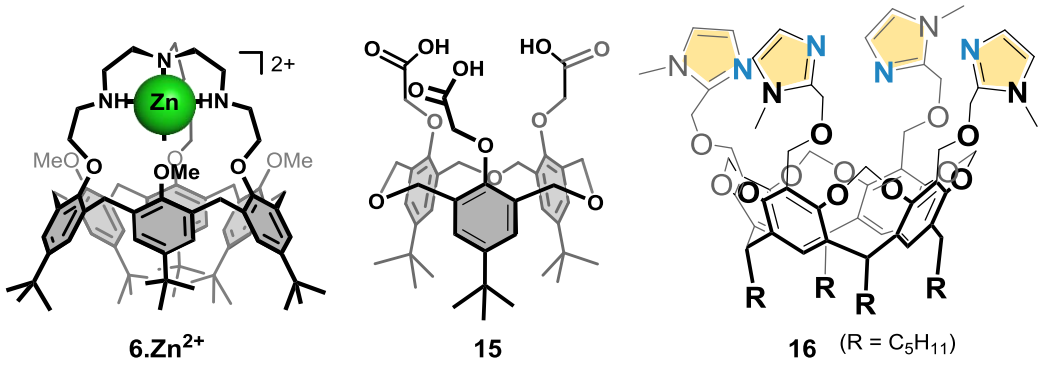

Figure 1-23. Structure of **6.Zn^{2+}**, **15** and **16**.

The last goal of the thesis is to try and **elucidate the mechanism of guest exchange of the funnel complex** (**1.Zn^{2+}**). The hypothesis put forward is that the *exo*-coordination of a ligand (solvent or another coordinating molecule) at the level of the zinc cation is required for exchange to occur. In other words, guest exchange requires an intermediate step. The model behind this hypothesis is described in detail in **chapter 4**. In order to validate it, we measure the residence time of various guests in the cavity of **1.Zn^{2+}** as a function of the concentration of different possible *exo*-ligands. Similar receptors calix[6]tris-benzimidazole zinc (**2.Zn^{2+}**) and calix[6]tren zinc (**6.Zn^{2+}**) are also studied in this context.

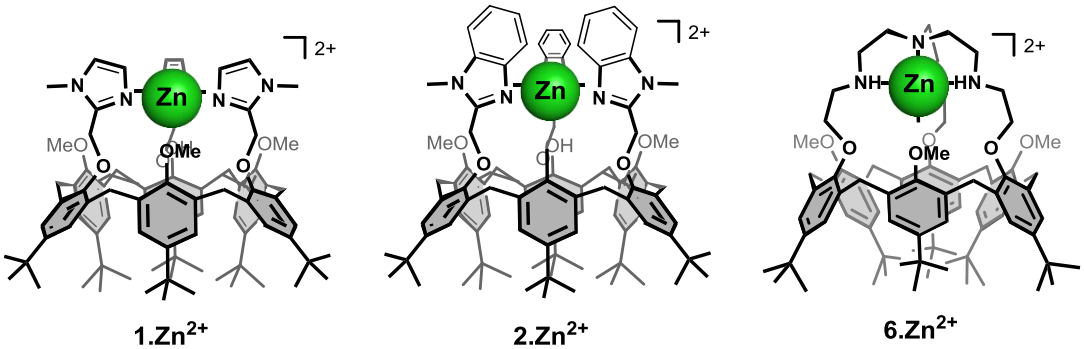

Figure 1-24. Structures of **1.Zn^{2+}**, **2.Zn^{2+}** and **6.Zn^{2+}**.

CHAPTER 2.
STUDY OF A FLUORESCENT CALIX[6]ARENE FOR THE RECOGNITION OF ANIONS, CONTACT ION-PAIRS AND PHOSPHOLIPIDS

In this chapter we discuss the work that we have undertaken with a fluorescent calix[6]arene receptor bearing urea moieties. The binding of anions, contact ion-pairs and phospholipids was monitored by NMR and emission spectroscopies.

2.1. COMPLEXATION OF ANIONS AND CONTACT ION-PAIRS

2.1.1. CONTEXT OF THE RESEARCH

As presented in the Introduction (section 1.4.2), calix[6]tris-phenylurea (host **10**) (Figure 2-1) is an excellent heteroditopic receptor for contact ion-pairs such as ammonium halides.[1] It indeed combines:

- a site composed of three urea moieties which can bind anions;
- a cavity adapted to the *endo*-complexation of small organic molecules.

A remarkable positive cooperativity has been reported as the complexation of the ammonium is only observed if the anion is complexed at its recognition site. The recognition process is *induced fit* driven, involving a conformational reorganization of the calixarene structure.

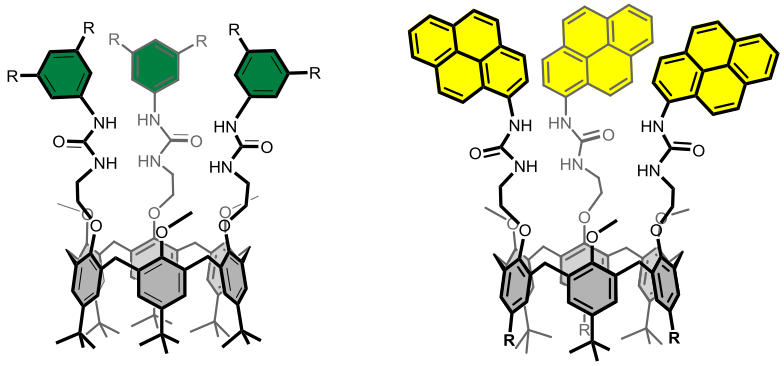

Figure 2-1. Structures of calix[6]tris-phenylurea **10a-b** and calix[6]tris-pyrenylurea **14a-b**.

In order to monitor the complexation process by UV-visible absorption and emission spectroscopies, Dr. Jean-François Picron synthesized and studied, in the framework of his PhD thesis, the calix[6]tris-pyrenylurea **14a**, which bears three pyrenyl chromophores (Figure 2-1).[2] He studied the complexation of different anions and monovalent ion-pairs in different organic

[1] Hamon, M.; Ménand, M.; Le Gac, S.; Luhmer. M.; Dalla, V.; Jabin, I. *J. Org. Chem.* **2008**, *73*, 7067-7071.
[2] Picron, J.-F. **2012**. PhD thesis: Synthèse et étude de récepteurs calix[6]aréniques porteurs de fluorophores. Laboratoire de Chimie Organique, Université libre de Bruxelles.

solvents (DMSO, $CHCl_3$, $CHCl_3/CH_3CN$ 1:1) by NMR and emission spectroscopies. He also undertook preliminary studies with ion triads.

In the framework of this thesis we have undertaken complementary studies with **14a** and have also looked at the binding properties of **14b**, which was synthetized by Dr. Karolina Flidrova in the Jabin's laboratory. We rationalized all the acquired data and it is all reported in the paper "*Fluorescent Chemosensors for Anions and Contact Ion Pairs with a Cavity-Based Selectivity*" which was published in the *Journal of Organic Chemistry* (**2014**, *79*, 6179–6188).

2.1.2. SUMMARY OF PUBLISHED RESULTS

In the paper "*Fluorescent Chemosensors for Anions and Contact Ion Pairs with a Cavity-Based Selectivity*", the synthesis of the fluorescent calix[6]tris-pyrenlyurea hosts **14a** and **14b** is reported. The complexation properties of both systems are also described in detail.

Host **14a** exhibits a remarkable selectivity for the sulfate anion in DMSO. An important drop of the fluorescence intensity is indeed observed only upon addition of SO_4^{2-}. A significantly weaker drop is observed with AcO^- and none with the other anions tested (halides, HSO_4^-, nitrate). In $CDCl_3$, the host forms complexes of different stoichiometry with the tested monovalent anions (e.g. Cl^-, AcO^-) but forms a 1:1 complex with sulfate, as confirmed by Job Plot experiments. This contrasts with the results obtained with parent receptor **10,** where 1:1 complexes were observed for all monovalent anions in $CDCl_3$. The presence of pyrenes at the level of the urea moieties clearly creates steric hindrance preventing the receptor to adapt to smaller anions.

Host **14a** is also able to bind ammonium ions efficiently in $CDCl_3$ when a sulfate anion is present at the level of the urea moieties. This cooperative binding has already been observed for host **10**. The studies undertaken with SO_4^{2-}-$PrNH_3^+$ (with TBA^+ as a counter-ion) show that guest exchange is slow on the NMR chemical shift timescale. Signals for the NH protons of the receptors appear downfield upon titration attesting of the interaction of the sulfate anion with the urea moieties via H-bonding interactions. The inclusion of the $PrNH_3^+$ inside the cavity is attested by the presence of high field signals in the NMR spectrum, due to the anisotropy cones of the aromatic cycles. Binding constants were too high to be determined by ^{1}H NMR ($\log K > 4$ for SO_4^{2-}-$PrNH_3^+$), but were determined by UV-vis absorption and emission spectroscopies. Upon addition of the guest to a solution of **14a**, a new absorption band, signature of the emergence of a new complex, is observed. An increase in the monomer emission and a decrease

in the excimer emission is also observed, suggestive of the separation of the urea groups upon anion coordination. Affinity for SO_4^{2-}-$PrNH_3^+$ of the order of log K ~ 5 was determined.

The interaction of the TBA^+ counter-ion with the receptor at the level of the pyrene units was also highlighted. The complexation of this quaternary ammonium, which is in fast exchange on the chemical shift timescale, was evidenced through ^{1}H DOSY NMR and a log K ~ 2 was determined. CH-π interactions between the TBA^+ and the pyrenes are probably at the origin of this favorable interaction.

The binding of bigger ammonium salts (e.g. TBA^+-SO_4^{2-}-$HexNH_3^+$ or TBA^+-SO_4^{2-}-$DodNH_3^+$) was evaluated with **14a** and also receptor **14b** (Figure 2-1). The latter receptor only presents three *t*Bu groups at the level of the large rim of the calix[6]arene. The *t*Bu groups bound to the phenyl rings that bear the urea moieties have been removed as it was observed with **14a** that they point inside the cavity upon anion coordination disturbing the potential complexation of guests that protrudes out of the cavity. Upon addition of TBA^+-SO_4^{2-}-$HexNH_3^+$or TBA^+-SO_4^{2-}-$DodNH_3^+$, the formation of the corresponding inclusion complexes was observed with **14b.** With **14a** we observe a competition between the inclusion complex (long chain ammonium in the cavity) and the complex with only the sulfate. Furthermore, only host **14b** was able to bind 3,4-O-dimethyldopammonium sulfate salt.

In conclusion calix[6]arene-based receptors have been synthetized and have shown to bind ion-pairs via urea moieties grafted on their small rim and their cavity. Moreover, a third recognition site was observed at the level of the pyrenyl groups, which are able to weakly bind the counter-ion TBA^+. The complexes formed are stabilized by H-bonding interactions, ionic interactions and CH-π interactions (Figure 2-2 for **14⊃TBAPrNH$_3$SO$_4$**).

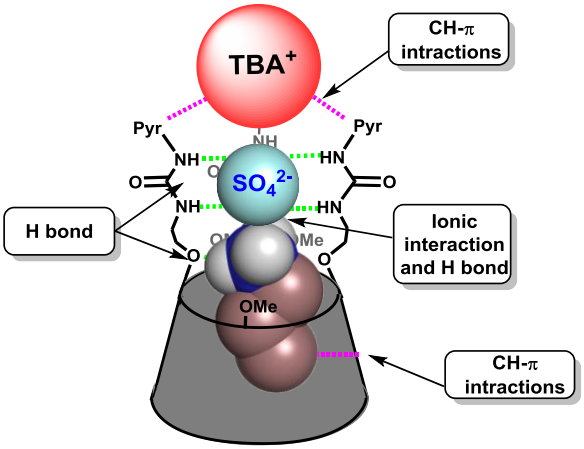

Figure 2-2. Representation of the recognition mode for the complexation of TBA^+-$PrNH_3^+$-SO_4^{2-} by **14**.

In this context, the present work opens interesting perspectives for the elaboration of unique fluorescent cavity-based systems for the selective sensing of anions or biologically relevant ammonium salts such as neurotransmitters.

JOC The Journal of Organic Chemistry

Article

pubs.acs.org/joc

Fluorescent Chemosensors for Anions and Contact Ion Pairs with a Cavity-Based Selectivity

Emilio Brunetti,[†,‡] Jean-François Picron,[†] Karolina Flidrova,[§] Gilles Bruylants,[‡] Kristin Bartik,*[,‡] and Ivan Jabin*[,†]

[†]Laboratoire de Chimie Organique, Université Libre de Bruxelles (ULB), Avenue F.D. Roosevelt 50, CP160/06, B-1050 Brussels, Belgium

[‡]Engineering of Molecular NanoSystems, Ecole Polytechnique de Bruxelles, Université Libre de Bruxelles (ULB), Avenue F.D. Roosevelt 50, CP165/64, B-1050 Brussels, Belgium

[§]Department of Organic Chemistry, Prague Institute of Chemical Technology (PICT), Technicka 6, 166 28 Prague 6, Czech Republic

Supporting Information

ABSTRACT: The association of a concave macrocyclic compound to one or multiple fluorophores is an appealing strategy for the design of chemosensors. Indeed, as with biological systems, a cavity-based selectivity can be expected with such fluorescent receptors. Examples of calix[6]arene-based systems using this strategy are rare in the literature, and to our knowledge, no examples of fluorescent receptors that can bind organic contact ion pairs have been reported. This report describes the straightforward synthesis of fluorescent calix[6]arene-based receptors **4a** and **4b** bearing three pyrenyl subunits and the study of their binding properties toward anions and ammonium salts using different spectroscopies. It was found that receptor **4a** exhibits a remarkable selectivity for the sulfate anion in DMSO, enabling its selective sensing by fluorescence spectroscopy. In $CDCl_3$, the receptor is able to bind ammonium ions efficiently only in association with the sulfate anion. Interestingly, this cooperative binding of ammonium sulfate salts was also evidenced in a protic environment. Finally, a cavity-based selectivity in terms of size and shape of the guest was observed with both receptors **4a** and **4b**, opening interesting perspectives on the elaboration of fluorescent cavity-based systems for the selective sensing of biologically relevant ammonium salts such as neurotransmitters.

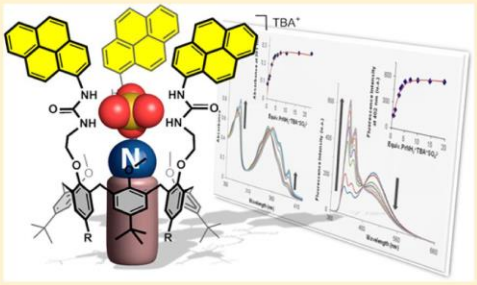

INTRODUCTION

The design of artificial receptors that can selectively bind charged or neutral species with high affinity is a major objective in supramolecular chemistry.[1] Indeed, such receptors could find many applications in various areas and can for example be envisaged for the sensing of chemical species in the fields of biological and environmental analyses.[2] A classical strategy for the design of such chemosensors consists of grafting one or multiple fluorophores onto a molecular receptor that displays a high selectivity for a given guest.[3] Indeed, fluorescence spectroscopy is particularly sensitive and allows the detection of chemical species at nanomolar concentrations.[4] For the elaboration of the molecular receptor, the use of cavity-based macrocyclic compounds[5] is particularly attractive because, in strong relation to natural systems, it can be expected that the cavity will ensure very high selectivity.[6] Calixarenes[7] are well-known concave macrocyclic compounds that have been widely used for the development of fluorescent chemosensors.[8] However, these fluorescent systems have been obtained quasi-exclusively using calix[4]arenes, whose cavities are too small for the recognition of organic guests, and therefore, they have been mostly used as a platform for the preorganization of a recognition site outside of the cavity.[9] Surprisingly, only a few papers have described the use of fluorescent calix[6]arenes,[10] despite the fact that these larger oligomers can accommodate organic guests in their cavities.[11] Moreover, to our knowledge, there are no examples of fluorescent receptors that can bind organic contact ion pairs,[12] as most of the systems are devoted to the recognition of cations,[13] anions,[14] or neutral guests.[15]

As part of our continuous interest in the synthesis and study of calix[6]arene-based receptors for neutral[16] or charged[17] species, we wanted to exploit the cavity-based selectivity of these receptors for the design of highly selective fluorescent systems. In this regard, we were interested in the elaboration of fluorescent derivatives of calix[6]tris(urea) compounds **1a** and **1b** (Figure 1). Indeed, it was reported that these receptors can efficiently bind either anions or, in a cooperative way, organic contact ion pairs.[18] The three converging urea groups allow strong binding to anions, which in turn can lead to the strong

Received: April 25, 2014
Published: June 16, 2014

dx.doi.org/10.1021/jo5009146 | J. Org. Chem. 2014, 79, 6179−6188

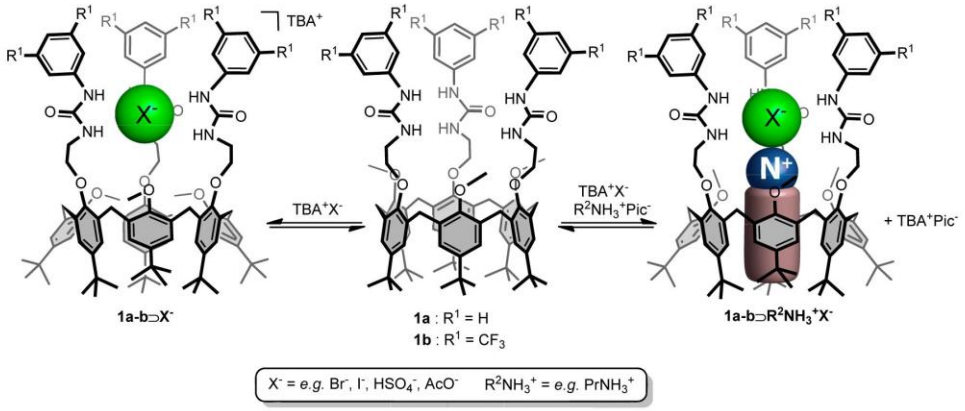

Figure 1. Host–guest properties of calix[6]tris(phenylurea) receptors **1a** and **1b** toward anions and contact ion pairs.

Scheme 1. Synthesis of Calix[6]tris(pyrenylurea) Receptors 4a and 4b[a]

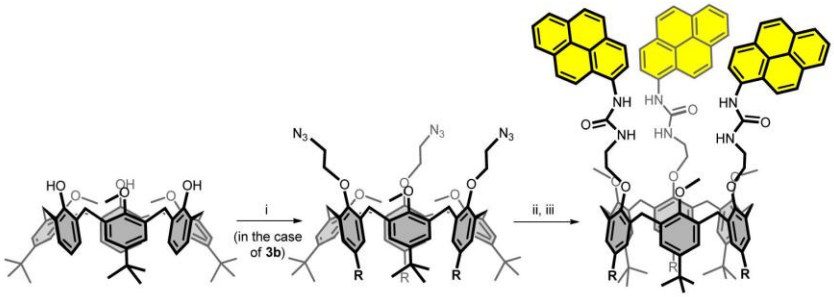

[a]Reagents and conditions: (i) 2-azidoethyl-4-methylbenzenesulfonate, NaH, THF, reflux, 77%; (ii) PPh_3, CO_2, THF, rt; (iii) pyren-1-amine, THF, 50 °C, 70% and 35% overall yields from **3a** and **3b**, respectively.

binding of an ion paired ammonium accommodated in the calixarene cavity. The proximity of the two binding sites is crucial in the recognition process as it circumvents the highly energetically unfavorable separation of the cobound ions.[19] It is noteworthy to mention that calix[6]tris(urea) receptors **1a** and **1b** constitute one of the rare examples of molecular receptors able to bind organic contact ion pairs.[20]

With the aim of studying the potential of transforming system **1a** into a sensor, we have grafted fluorophores in close proximity to the tris(urea) binding site. The pyrenyl group was chosen as the fluorophore[21] as the variation of the excimer to monomer emission intensity ratio can yield information on conformational changes of the receptor upon binding.[22] Besides the synthesis of new fluorescent calix[6]arene-based receptors, the aims of this study were to see (i) whether the binding properties of the receptors were preserved despite the introduction of bulky fluorophores in close proximity to the urea groups, (ii) whether it was possible to give rise to an effective anion or ion-pair sensor in terms of detection by fluorescence spectroscopy, and (iii) whether cavity-based selectivity, notably in terms of size and shape complementarities, could be associated with the sensing process. Herein we describe the synthesis of these new fluorescent calix[6]arene-based receptors and the study of their binding properties toward anions and ammonium salts using NMR, UV–vis absorption, and fluorescence spectroscopy.

RESULTS AND DISCUSSION

Synthesis and Characterization of Calix[6]tris(pyrenylurea) Receptors 4a and 4b. The synthesis of two receptors that offer cavities of different size and shape, **4a** and **4b**, was undertaken. Calix[6]tris(azido) **3b** was first obtained in 77% yield through alkylation of the partially de-*tert*-butylated 1,3,5-tris(methoxy)calix[6]arene **2**[23] with an excess of 2-azidoethyl-4-methylbenzenesulfonate.[24] A one-pot, two-step procedure consisting of a domino Staudinger/aza-Wittig reaction (PPh_3/CO_2) and a subsequent addition of pyren-1-amine afforded the desired calix[6]tris(pyrenylurea) compounds **4a** and **4b** in 70% and 35% overall yields from calix[6]tris(azido) precursors **3a**[25] and **3b**, respectively (Scheme 1).

The ^{1}H NMR spectra of calix[6]tris(pyrenylurea) compounds **4a** and **4b** in $CDCl_3$ show broad signals characteristic of C_{3v}-symmetric species (for **4a**, see Figure 2a). When the spectra were recorded in a competing solvent (DMSO-d_6), sharp NMR signals characteristic of a major C_{3v}-symmetric flattened cone conformation were observed for both systems ($\Delta\delta_{ArH} = 0.70$ and 0.72 ppm for **4a** and **4b**, respectively) with the methoxy groups pointing inside the cavity ($\delta_{OMe} = 2.12$ and 2.60 ppm for **4a** and **4b**, respectively; for **4a**, see Figure 2b). In strong analogy with the parent receptors **1a** and **1b**, this solvent-dependent conformational behavior indicates intramolecular self-association of the urea groups through hydrogen-bonding interactions in apolar

dx.doi.org/10.1021/jo5009146 | J. Org. Chem. 2014, 79, 6179–6188

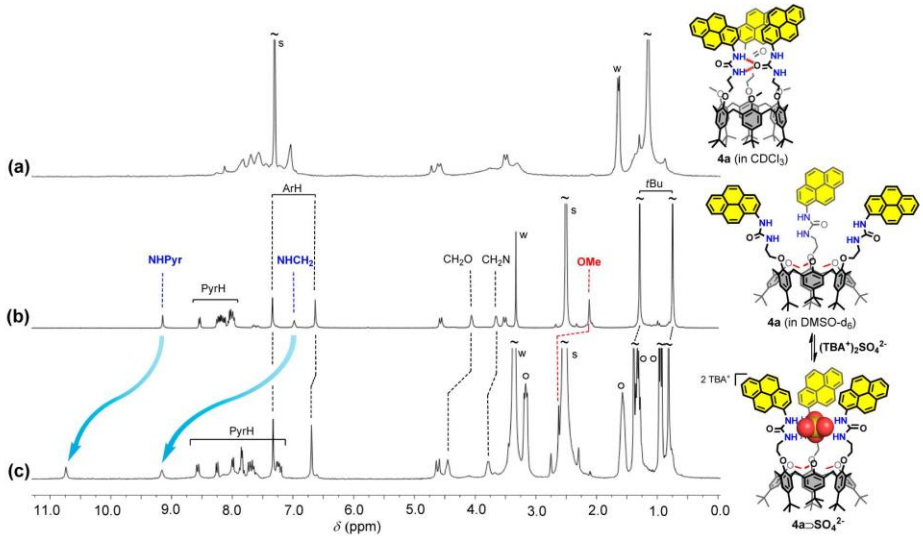

Figure 2. ^{1}H NMR spectra of **4a** at 298 K: (a) in $CDCl_3$ (300 MHz); (b) in DMSO-d_6 (400 MHz); (c) in the presence of 2.5 equiv of $(TBA^+)_2SO_4^{2-}$ in DMSO-d_6 (300 MHz). Labels: O, TBA^+; s, solvent; w, residual water.

Table 1. Affinities of Hosts 4a and 4b toward Different Charged Species at 298 K

complex formed[a]	solvent	log K_{NMR}[b]	log K_{UV-vis}[b]	log K_{fluo}[b]
4a⊃SO_4^{2-}	DMSO-d_6	3.4 ± 0.3	3.6 ± 0.4	3.9 ± 0.4
4a⊃SO_4^{2-}	$CDCl_3$	>4	5.1 ± 0.5	5.4 ± 0.4
4a⊃$PrNH_3^+SO_4^{2-}$	$CDCl_3$	>4	5.3 ± 0.6	5.4 ± 0.1
4a⊃$PrNH_3^+SO_4^{2-}$	$CD_3OD/CDCl_3$ (1:11)	3.9 ± 0.1	4.0 ± 0.3	–
4a⊃$PyrroNH_2^+SO_4^{2-}$	$CDCl_3$	>4	4.1 ± 0.5	4.5 ± 0.2
4b⊃$PrNH_3^+SO_4^{2-}$	$CDCl_3$	>4	5.0 ± 0.2	4.8 ± 0.2

[a] TBA^+ was used as the counterion in all cases. [b] K = [complex]/([host][guest]). K_{NMR}, K_{UV-vis}, and K_{fluo} refer to binding constants determined by NMR, UV–vis absorption, and fluorescence spectroscopy, respectively.

solvents such as $CDCl_3$ (see the structure displayed in Figure 2a, the exchange process between the three nonequivalent urea groups being fast on the NMR chemical shift time scale) and, on the contrary, separation of the bulky pyrenylurea groups in competing solvents (see the structure displayed in Figure 2b).[26] It should be noted that in the particular case of **4a** and **4b**, the self-association of the urea arms could also be due in part to π-stacking interactions between the pyrenyl moieties. Calix[6]-tris(pyrenylurea) receptors **4a** and **4b** exhibit UV–vis absorption bands at 280, 346, and 389 nm in chloroform and at 279, 348, and 390 nm (**4a**) or 285, 354, and 390 nm (**4b**) in DMSO.[27]

Anion Complexation Properties of 4a. The ability of calix[6]tris(pyrenylurea) **4a** to bind anions of various geometries (i.e., Cl^-, AcO^-, HSO_4^-, and SO_4^{2-}) was first investigated in DMSO-d_6 by NMR spectroscopy through the progressive addition of the corresponding tetra-*n*-butylammonium salts ($TBA_n^+X^{n-}$). Except for a weak downfield shift of the urea NH signals, the NMR spectrum of **4a** remained quasi-unchanged upon the addition of a large excess (up to 20 equiv) of either Cl^-, AcO^-, or HSO_4^-. The absence of a conformational reorganization of the calixarene core suggests an extremely weak binding of these anions by only one of the three ureido groups. In strong contrast, upon the progressive addition of $(TBA^+)_2SO_4^{2-}$, downfield shifts of the CH_2O, CH_2N, and OCH_3 signals and upfield shifts of some of the pyrenyl signals were observed (Figure 2c). Significant downfield shifts of the urea NH signals ($\Delta\delta_{NH}$ = 1.60 and 2.18 ppm) were also observed, which clearly indicates strong hydrogen-bonding interactions between the urea groups and the anion. All of these NMR data are compatible with strong binding of the sulfate anion by the convergent NH groups of the pyrenylurea arms, which are thus projected above the small rim upon anion complexation. The resulting host–guest complex **4a⊃SO_4^{2-}** displays a major flattened cone conformation ($\Delta\delta_{ArH}$ = 0.63 ppm and $\Delta\delta_{tBu}$ = 0.57 ppm) with the methoxy groups pointing inside the cavity (δ_{OMe} = 2.55 ppm), as illustrated in Figure 2c. It is noteworthy to mention that only one set of signals is apparent over the course of the titration, evidencing fast host–guest exchange on the NMR chemical shift time scale. Job's plot experiments[28] by UV–vis spectroscopy indicate a 1:1 binding stoichiometry.[27] An association constant of log K = 3.4 ± 0.3 (Table 1) was determined for the binding of the sulfate anion by monitoring the complexation-induced shifts (CISs) of appropriate signals of host **4a** (i.e., signals displaying significant shifts upon complexation and no overlap).[27] UV–vis and fluorescence titrations in DMSO afforded K values on the same order of magnitude (log K = 3.6 ± 0.4 and 3.9 ± 0.4, respectively).[27] The fluorescence spectra show that the monomer emission (402 and 420 nm) decreases and slightly shifts to higher wavelengths while the excimer emission (506 nm) increases slightly upon successive addition of $(TBA^+)_2SO_4^{2-}$ (Figure 3 left). These spectral changes are highly compatible with the anion

dx.doi.org/10.1021/jo5009146 | J. Org. Chem. 2014, 79, 6179–6188

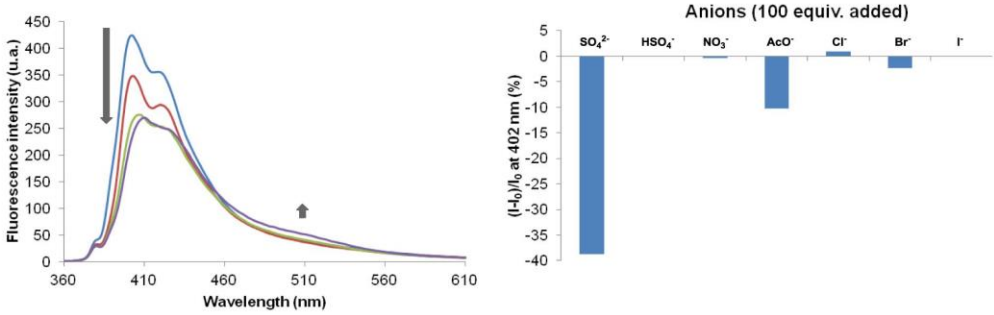

Figure 3. Left: fluorescence spectra of **4a** (~10 μM) upon the addition of TBA_2SO_4 (0, 20, 100, and 500 equiv) in DMSO (excitation at 348 nm). Right: fluorescence intensity changes $[100\% \times (I - I_0)/I_0]$ for **4a** (~10 μM) in DMSO upon the addition of various anions (100 equiv) (excitation at 348 nm). I_0 is the fluorescence emission intensity at 402 nm for free host **4a**, and I is the fluorescence emission intensity after the addition of the anion.

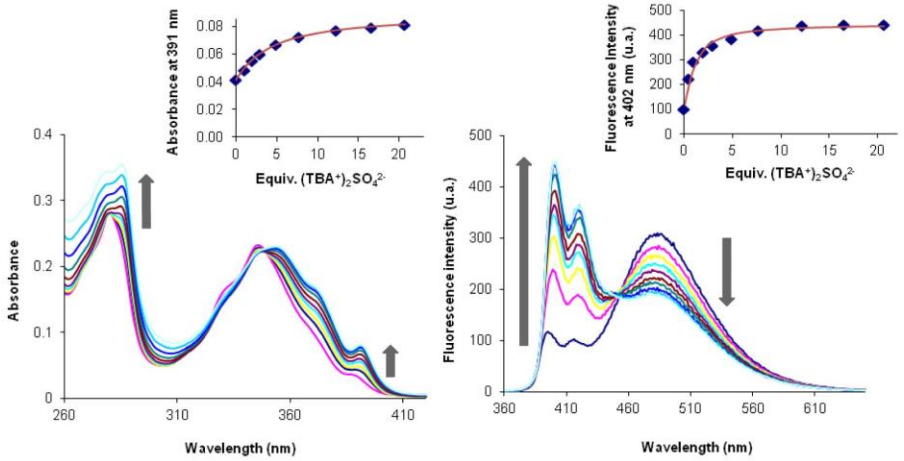

Figure 4. Left: UV−vis spectra of **4a** upon the addition of $(TBA^+)_2SO_4^{2-}$ (0 to 21 equiv) in chloroform. $[\mathbf{4a}]_0 = 4.8 \times 10^{-6}$ M. The inset shows the variation of the absorbance at 391 nm upon the addition of $(TBA^+)_2SO_4^{2-}$. Right: fluorescence spectra of **4a** upon the addition of $(TBA^+)_2SO_4^{2-}$ (0 to 21 equiv) in chloroform. $[\mathbf{4a}]_0 = 4.8 \times 10^{-6}$ M. $\lambda_{ex} = 350$ nm. The inset shows the variation of the fluorescence intensity at 402 nm upon the addition of $(TBA^+)_2SO_4^{2-}$.

coordination at the level of the urea groups resulting in a greater proximity between the pyrene moieties.

To verify that receptor **4a** is indeed a selective sensor for the sulfate anion in DMSO,[29] the binding of common anions of various geometries (i.e., SO_4^{2-}, HSO_4^-, NO_3^-, AcO^-, Cl^-, Br^-, I^-) was investigated by fluorescence spectroscopy. To our delight, only the sulfate anion caused a significant quenching in the emission spectrum of **4a**, confirming the high selectivity for this anion (Figure 3 right).

In a second set of experiments, the binding behavior of **4a** toward anions was evaluated in $CDCl_3$. Again, NMR-monitored titration experiments and Job's plot experiments confirmed the 1:1 complexation of the sulfate anion. The association constant for the host−guest complex $\mathbf{4a}\supset\mathbf{SO_4^{2-}}$ ($\log K > 4$) was too high to be determined accurately by NMR spectroscopy but could however be determined by absorbance and fluorescence titrations (Figure 4), which afforded $\log K$ values of 5.1 ± 0.5 and 5.4 ± 0.4, respectively (Table 1). The fluorescence spectra clearly showed that in this solvent the monomer emission (395 and 415 nm) increases while the excimer emission (484 nm) decreases upon successive additions of $(TBA^+)_2SO_4^{2-}$. These spectral changes are in accordance with a separation of the intramolecularly self-associated urea groups bearing the pyrene moieties upon anion coordination.

In comparison with the results obtained in DMSO, the host−guest properties of **4a** in chloroform are slightly different. The NMR signals of the calixarene, and in particular those of the urea N*H*, are significantly affected upon the successive addition of anions other than sulfate (i.e., Cl^-, Br^-, AcO^-, HSO_4^-, $H_2PO_4^-$), indicating that these anions also bind at the level of the urea groups. However, for these anions the CISs as well as the Job's plot experiments undertaken by NMR spectroscopy were not compatible with a 1:1 binding stoichiometry but more likely corresponded to the formation of mixtures of complexes with different binding ratios.[30] Another surprising difference observed was that the chemical shifts of the protons of the TBA^+ counterion were strongly affected during the titrations with all of the tested anions. In the case of $(TBA^+)_2SO_4^{2-}$, a binding constant with $\log K = 2.6 \pm 0.2$ was determined by monitoring the upfield shift of the N^+CH_2 signal of TBA^+ (Table 2).[27] From this titration, it was possible to evaluate the chemical shift for these protons when the TBA^+ cation is complexed, and the obtained value ($\delta_{N^+CH_2} = 1.62 \pm 0.05$ ppm) suggests that this

dx.doi.org/10.1021/jo5009146 | J. Org. Chem. 2014, 79, 6179−6188

Table 2. Affinities of 4a, 4a⊃SO_4^{2-}, and 4a⊃$PrNH_3^+SO_4^{2-}$ toward TBA^+ ($CDCl_3$, 298 K) and Estimated Chemical Shifts of the N^+CH_2 Protons of the Bound TBA^+ Ion

host	log K^a	$\delta_{N^+CH_2}$ (ppm)^b
4a^c	1.9 ± 0.1	3.11 ± 0.01
4a⊃SO_4^{2-}	2.6 ± 0.2	1.62 ± 0.05
4a⊃$PrNH_3^+SO_4^{2-}$	2.4 ± 0.2	1.74 ± 0.16

^{a}K was determined by following the variation of the chemical shift of the N^+CH_2 protons of TBA^+. ^{b}Estimated by parametric adjustment of the experimental data to the equation $\delta = \delta_{free}y + \delta_{bound}(1 - y)$. ^{c}The NMR titration was performed with $TBA^+BF_4^-$.

cation is located at the level of the pyrenyl units, where it is stabilized through CH−π interactions. It is noteworthy to mention that a similar interaction of TBA^+ with pyrenyl moieties has been reported previously in the literature.[31] In order to better characterize this interaction, host **4a** was also titrated with TBA^+ associated with a low-coordinating anion (i.e., BF_4^-). As with $(TBA^+)_2SO_4^{2-}$, an upfield shift was observed for the TBA^+ protons, and a binding constant of log K = 1.9 ± 0.1 and a chemical shift of 3.11 ± 0.01 ppm for the N^+CH_2 protons of the bound TBA^+ were determined (Table 2).[27] The value of log K was confirmed through DOSY experiments.[27] The higher binding constant observed for the system in the presence of sulfate can be explained by the favorable electrostatic interaction between the ammonium ion and the cobound sulfate but also by the fact that sulfate complexation at the level of the urea units induces a collapse of the pyrenyl units, which form a "π-electron donor cavity" favorable for cation binding. This hypothesis is confirmed by the fact that the chemical shift for the N^+CH_2 protons of the bound TBA^+ ion is significantly more upfield in the presence of sulfate (1.62 ± 0.05 vs 3.11 ± 0.01 ppm). In other words, the complexation of the anion preorganizes the binding site for the TBA^+ cation, leading to a positive cooperativity. It is important to point out that in the absence of the receptor, no significant chemical shift changes were observed for the TBA^+ signals in $CDCl_3$ as a function of $(TBA^+)_2SO_4^{2-}$ or $TBA^+BF_4^-$ concentration (up to 50 mM), confirming that the observed change in chemical shift is indeed due to the interaction with the receptor.

Altogether, the results obtained with receptor **4a** stand in contrast to those obtained with the parent receptors **1a** and **1b**, which exhibit a much lower selectivity for the sulfate anion. Indeed, **1a** and **1b** strongly recognize a large variety of anions with a 1:1 binding stoichiometry (e.g., log K = 2.2 for Br^- and log K > 3.9 for AcO^-, HSO_4^-, and SO_4^{2-} in the case of **1a** in $CDCl_3$[18]). This difference in the behaviors of the two families of receptors may be rationalized by the presence of steric interactions between the bulky pyrenylurea subunits when the three urea arms have to come in close proximity upon anion complexation. In the case of **4a**, the high selectivity for SO_4^{2-} could be due to the fact that this anion is large and doubly charged and displays good complementarity with the tris(urea) binding site.

Ammonium Salt Complexation. The simultaneous complexation of an ammonium ion in the calixarene cavity and an anion at the level of the tris(urea) binding site was investigated by NMR, UV−vis, and fluorescence spectroscopy in chloroform. In a first set of experiments, $PrNH_3^+$ was chosen as the cationic partner as it is known to display a high affinity for the calix[6]arene cavity.[32] The addition of $PrNH_3^+$ associated with a low-coordinating anion (i.e., picrate, Pic^-) did not have an effect on the NMR spectrum of **4a** in $CDCl_3$, which highlights the poor ability of **4a** to bind ammonium ions independently of a coordinating anion. In contrast, upon the addition of ca. 3 equiv of $PrNH_3^+X^-$ (X^- = Cl^-, AcO^-, HSO_4^-), the intracavity binding of the ammonium ion was evidenced by the presence of high-field signals in the NMR spectra (<0 ppm). However, in addition to the NMR signals for the complex **4a⊃PrNH$_3^+$X$^-$**, broad signals corresponding to another calixarene species were observed. Even with a larger excess of the ammonium salt (ca. 10 equiv), it was not possible to obtain only the **4a⊃PrNH$_3^+$X$^-$** complex. The second species could correspond to binding of the ion pair $PrNH_3^+X^-$ with exocomplexation of the ammonium ion (i.e., with the ammonium ion outside of the calixarene cavity at the level of the pyrenyl units). It is noteworthy to mention that the simultaneous addition of ca. 3 equiv of $PrNH_3^+Pic^-$ and $TBA^+HSO_4^-$ did not yield the same NMR spectrum as obtained upon the addition of ca. 3 equiv of $PrNH_3^+HSO_4^-$, as the proportion of complex **4a⊃PrNH$_3^+$HSO$_4^-$** was even lower in this case. This is probably the result of the concomitant complexation of $TBA^+HSO_4^-$ by the calixarene (vide supra) and highlights the importance of the counterion in the case of receptor **4a**. In other words, all of these data indicate a lack of selectivity for the binding process of ammonium salts $PrNH_3^+X^-$.

In view of the high selectivity of **4a** for the sulfate anion, the ability of the receptor to bind this anion when it is associated with an ammonium ion that can be endocomplexed was evaluated in chloroform. Receptor **4a** was unable to extract $(PrNH_3^+)_2SO_4^{2-}$ in $CDCl_3$, but to our delight, the progressive addition of $PrNH_3^+TBA^+SO_4^{2-}$ led to a new and unique NMR pattern displaying sharp signals characteristic of a C_{3v}-symmetric calixarene species (Figure 5a).

After the addition of 1 equiv of the salt $PrNH_3^+TBA^+SO_4^{2-}$, only the signals of this new species were observed, and the spectrum was not influenced by the further addition of a large excess of the salt (ca. 20 equiv), indicating strong and selective 1:1 binding. All of the signals of this new species were assigned by 2D NMR spectroscopy (i.e., COSY and HMBC),[27] and it was thus possible to make the following observations:

(i) The calixarene core adopts a flattened cone conformation ($\Delta\delta_{ArH}$ = 0.57 ppm and $\Delta\delta_{tBu}$ = 0.58 ppm), and the significant downfield shift of the OMe protons (δ_{OMe} = 4.13 ppm) shows that these groups have been expelled from the cavity.

(ii) The N*H* protons of the ureido groups experience a significant downfield shift (δ_{NHPyr} = 10.48 ppm and δ_{NHCH_2} = 8.88 ppm), highlighting the binding of the sulfate anion through hydrogen-bonding interactions.

(iii) High-field signals belonging to the alkyl chain of $PrNH_3^+$ (i.e., δ = −1.26 and −1.92 ppm) attest to the inclusion of the ammonium ion into the cavity with a 1:1 binding ratio. This host−guest exchange process is slow on the NMR chemical shift time scale. The CIS of the NCH_2 protons of the ammonium ion is quite moderate (i.e., −0.47 ppm) in comparison with those of the rest of the alkyl chain (i.e., −3.03 and −2.84 ppm). This result is highly compatible with the presence of the sulfate anion in close proximity to the ammonium ion and thus with the binding of the two ionic partners as a contact ion pair.

(iv) The HMBC spectrum clearly indicates that the *t*Bu groups of the anisole moieties are directed toward the outside of the cavity (see the structure displayed in Figure 5a).

dx.doi.org/10.1021/jo5009146 | J. Org. Chem. 2014, 79, 6179−6188

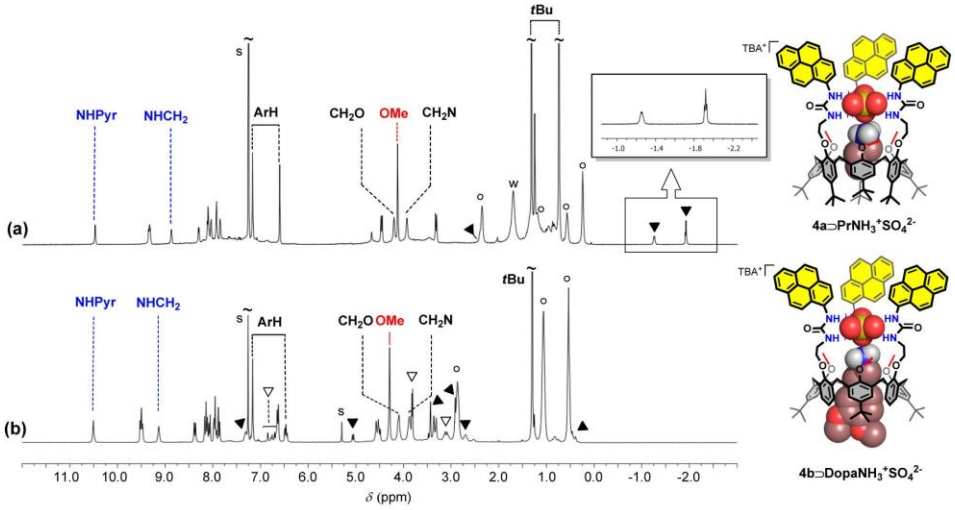

Figure 5. (a) ^{1}H NMR spectrum (600 MHz, 298 K) of **4a** in $CDCl_3$ in the presence of 1 equiv of $PrNH_3^+TBA^+SO_4^{2-}$. (b) ^{1}H NMR spectrum (300 MHz, 298 K) of **4b** in $CDCl_3$ in the presence of ca. 2 equiv of $DopaNH_3^+TBA^+SO_4^{2-}$. Labels: ○, TBA^+; ▼, RNH_3^+ in; ▽, RNH_3^+ out; s, residual solvent; w, residual water.

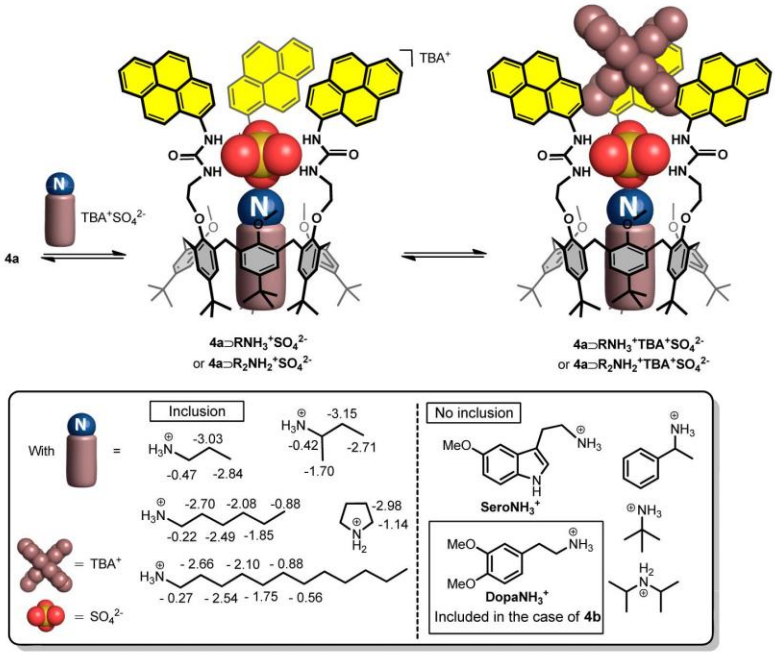

Figure 6. Host–guest properties of calix[6]tris(pyrenylurea) **4a** toward ammonium sulfate salts. Inset: CISs determined by ^{1}H NMR spectroscopy in $CDCl_3$.

(v) The chemical shifts of the TBA^+ protons are strongly affected during the course of the titration as a result of complexation of the TBA^+ cation at the level of the pyrenyl units. The exchange is fast on the NMR chemical shift time scale, and monitoring of the upfield shift of the N^+CH_2 signal yielded a binding constant of $\log K = 2.4 \pm 0.2$ and an estimated chemical shift of 1.74 ± 0.16 ppm for the N^+CH_2 protons of the bound TBA^+ ion. These values are comparable to those observed in the presence of the sole sulfate ion (Table 2).

Altogether, these observations show the formation of the ternary host–guest complex **4a**⊃$PrNH_3^+SO_4^{2-}$ with a weak interaction of the TBA^+ counterion at the level of the pyrenyl units that leads ultimately to the complex **4a**⊃$PrNH_3^+TBA^+SO_4^{2-}$ (Figure 6). In other words, **4a** behaves as a heterotopic receptor

dx.doi.org/10.1021/jo5009146 | J. Org. Chem. 2014, 79, 6179–6188

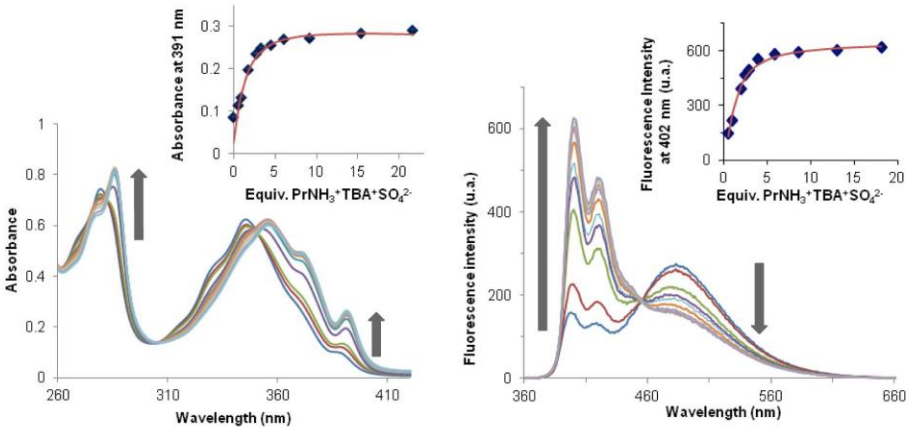

Figure 7. Left: UV−vis spectra of **4a** upon the addition of $PrNH_3^+TBA^+SO_4^{2-}$ (0 to 22 equiv) in chloroform. $[\mathbf{4a}]_0 = 10.0 \times 10^{-6}$ M. The inset shows the variation of the absorbance at 391 nm. Right: fluorescence spectra of **4a** upon the addition of $PrNH_3^+TBA^+SO_4^{2-}$ (0 to 19 equiv) in chloroform. $[\mathbf{4a}]_0 = 4.8 \times 10^{-6}$ M. $\lambda_{ex} = 346$ nm. The inset shows the variation of the fluorescence intensity at 402 nm.

for sulfate ammonium salts, with binding of the anion by the urea groups being a prerequisite for the inclusion of the ammonium ion into the calixarene cavity. This positive cooperativity is clearly due to the fact that these two ions can be bound as a contact ion pair, thus avoiding the highly energetically unfavorable dissociation of the ion pair. The association constant for $PrNH_3^+SO_4^{2-}$ was estimated to be log $K > 4$ by NMR spectroscopy (Table 1). Absorbance and fluorescence titrations in chloroform afforded association constants of log $K = 5.3 \pm 0.6$ and 5.4 ± 0.1, respectively (Figure 7). Again, the spectral changes observed in the fluorescence spectra, namely, an increase of the monomer emission and a decrease of the excimer one, are suggestive of the separation of the self-associated urea groups upon anion coordination.

The affinities of receptors **1a** and **4b** for $PrNH_3^+TBA^+SO_4^{2-}$ were also evaluated in $CDCl_3$ in order to make a comparison with host **4a**.[27] Similarly to **4a**, a high affinity constant for the formation of the complexes **1a**⊃$\mathbf{PrNH_3^+SO_4^{2-}}$ and **4b**⊃$\mathbf{PrNH_3^+SO_4^{2-}}$ was determined by ^{1}H NMR spectroscopy (log $K > 4$). In the case of **4b**, absorbance and fluorescence titrations afforded association constants of log $K = 5.0 \pm 0.2$ and 4.8 ± 0.2, respectively, suggesting that **4a** and **4b** display similar recognition properties toward this ammonium salt. Surprisingly, a weak interaction of the TBA^+ counterion at the level of the phenyl units was also observed in the case of **1a** (log $K = 2.3 \pm 0.2$),[27] but a much higher chemical shift for the N^+CH_2 protons of the bound TBA^+ (2.94 ± 0.02 vs 1.74 ± 0.16 for **1a** vs **4a**, respectively) was estimated and no binding of the TBA^+ was observed when this cation was associated with a low-coordinating anion (i.e., BF_4^-). Again, this positive cooperativity shows that the binding of the ion pair $PrNH_3^+SO_4^{2-}$ preorganizes the binding site for the TBA^+ cation by forming an electron-rich tris(phenyl) cavity.

All of these findings prompted us to investigate the ability of the fluorescent receptor **4a** to bind larger ammonium ions associated with $TBA^+SO_4^{2-}$. To this end, additions of hexyl-, dodecyl-, and (±)-*sec*-butylammonium salts as well as the pyrrolidinium salt to $CDCl_3$ solutions of **4a** were performed. In all cases, the formation of the inclusion complex was clearly evidenced by NMR spectroscopy, and the CISs of these ammonium ions were compatible with their inclusion into the calixarene cavity (Figure 6). In particular, all of the methylene protons of the included alkyl chain of $HexNH_3^+$ appeared as well-separated resonances and, in the case of $DodNH_3^+$, the CISs decreased dramatically from the middle of the alkyl chain, indicating that the dodecyl chain protrudes out of the cavity. For the pyrrolidinium cation ($PyrroNH_2^+$), accurate determinations of the association constants by absorbance and fluorescence titrations afforded log K values of 4.1 ± 0.5 and 4.5 ± 0.2, respectively (Table 1). In the case of the $HexNH_3^+$ and $DodNH_3^+$ salts, accurate determinations of the associations constant were not possible because of the competitive formation of $\mathbf{4a⊃SO_4^{2-}}$.[27] This poor selectivity is likely due to a lower affinity of the calixarene for $HexNH_3^+$ and $DodNH_3^+$ that can be rationalized by the fact that guests with an alkyl chain longer than propyl lead to a steric clash with the introverted *t*Bu groups that close the cavity of the host, forcing the calix[6]arene skeleton to adopt a energetically unfavorable straight conformation.[33] This induced-fit process is clearly evidenced in the NMR spectra of the $\mathbf{4a⊃HexNH_3^+SO_4^{2-}}$ and $\mathbf{4a⊃DodNH_3^+SO_4^{2-}}$complexes. Indeed, the calixarene aromatic units bearing the urea groups adopt a conformation more parallel to the C_3 axis with their *t*Bu groups expelled from the cavity by the alkyl chain of the included ammonium ion ($\Delta\delta_{ArH} = 0.41$ and 0.40 ppm, respectively. Moreover, the inclusion of the bulkier and nonlinear 3,4-*O*-dimethyldopammonium ($DopaNH_3^+$), (±)-α-methylbenzylammonium, and *O*-methylserotonin ($SeroNH_3^+$) ions was not observed, again certainly because of the conformational energy penalty resulting from the steric clash with the *t*Bu groups (Figure 6). Steric hindrance at the level of the ammonium group and its α-position also appeared to be a major selectivity factor because of a steric clash with the small rim of the calixarene. Indeed, the inclusion of *tert*-butylammonium and diisopropylammonium ions was not detected (Figure 6), and the complexation of the (±)-*sec*-butylammonium salt was found to be at least 20 times weaker than that of $PrNH_3^+SO_4^{2-}$. Interestingly, the selective formation of $\mathbf{4a⊃PrNH_3^+SO_4^{2-}}$ was obtained in the presence of a large excess of these ammonium sulfate salts.[27] All of these results clearly show that the calixarene cavity controls the recognition of the cationic guest on the basis of its size and geometry. It was thus of particular interest to investigate the binding of the bulky salts by receptor **4b**, which

dx.doi.org/10.1021/jo5009146 | J. Org. Chem. 2014, 79, 6179−6188

displays an enlarged and more open cavity (Scheme 1). With this receptor, additions of the $SeroNH_3^+$, (±)-α-methylbenzylammonium, $tBuNH_3^+$, and $(iPr)_2NH_2^+$ ions associated with $TBA^+SO_4^{2-}$ did not yield any inclusion complexes, certainly because of poor shape complementarity between the cationic guest and the cavity. However, to our delight, the addition of $DodNH_3^+TBA^+SO_4^{2-}$ and $DopaNH_3^+TBA^+SO_4^{2-}$ in $CDCl_3$ led to the exclusive formation of the corresponding complexes **4b⊃DodNH$_3^+$SO$_4^{2-}$** and **4b⊃DopaNH$_3^+$SO$_4^{2-}$** (Figure 5b). All in all, these results show that both fluorescent receptors **4a** and **4b** can ensure a cavity-based selectivity at the level of the recognition of the ammonium ion and also that fine-tuning of the recognition process can be obtained through modification of the large-rim substituents.

Studies in a Protic Environment. The next challenge was to evaluate the ability of **4a** to bind ammonium salts in a protic environment. The ^1H NMR spectrum of receptor **4a** in a 1:11 $CD_3OD/CDCl_3$ mixture remained unchanged upon the addition of either $(TBA^+)_2SO_4^{2-}$ or $PrNH_3^+Pic^-$. This highlights the extremely weak anion or ammonium ion recognition properties of **4a** in a protic and thus highly competitive environment. Furthermore, the ^1H NMR spectrum of receptor **4a** in a 1:11 $CD_3OD/CDCl_3$ mixture remained unaffected upon the addition of a large excess of $(PrNH_3^+)_2SO_4^{2-}$ (8 equiv), but the subsequent addition of $(TBA^+)_2SO_4^{2-}$ (ca. 1.5 equiv) led to the quantitative formation of the complex **4a⊃PrNH$_3^+$SO$_4^{2-}$**.[27] It is noteworthy to mention that an identical NMR pattern was obtained upon the addition of $PrNH_3^+TBA^+SO_4^{2-}$ to **4a**. This remarkable result highlights once again the importance of the counterion and shows that the presence of a dissociated cation such as TBA^+ is required for the complexation of ammonium sulfate salts by host **4a**. The association constant for $PrNH_3^+SO_4^{2-}$ ($\log K = 3.9 \pm 0.1$) was determined by integration of the ^1H NMR spectrum recorded after the addition of 1 equiv of $PrNH_3^+TBA^+SO_4^{2-}$ (Table 1). A similar $\log K$ value of 4.0 ± 0.3 was obtained by UV−vis titration.[27] It should be noted that in this solvent the binding constant for the complexation of the TBA^+ was too small to be determined accurately. Considering the inertness of the receptor toward $(TBA^+)_2SO_4^{2-}$ and $PrNH_3^+Pic^-$ in a 1:11 $CD_3OD/CDCl_3$ mixture, the strong and simultaneous binding of both partners (i.e., $PrNH_3^+$ and SO_4^{2-}) in this protic environment highlights a remarkable mutual cooperativity. Indeed, the complexation of the sulfate anion can only proceed when an ammonium ion is present in the calixarene cavity, and conversely, without SO_4^{2-} the receptor **4a** is inefficient at binding the ammonium ion. Finally, a certain affinity of receptor **4b** for **DopaNH$_3^+$TBA$^+$SO$_4^{2-}$** in 1:10 $CD_3OD/CDCl_3$ was also observed ($\log K \sim 1.5$ obtained by NMR spectroscopy), showing a remarkable behavior of this receptor for the recognition of biological ammonium salts in a protic environment.

■ CONCLUSION

The straightforward syntheses of the first fluorescent calix[6]-tris(urea) hosts **4a** and **4b** was achieved efficiently. In comparison to the parent receptors **1a** and **1b**, the introduction of bulky pyrenyl groups in close proximity to the anion binding site did not inhibit the binding properties of the receptors toward anions and contact ion pairs. In contrast to **1a** and **1b**, it was observed that receptor **4a** exhibits a remarkable selectivity for the sulfate anion in DMSO, enabling its selective sensing by fluorescence spectroscopy. In $CDCl_3$, **4a** was able to bind ammonium ions efficiently only in association with the sulfate anion. To our delight, this cooperative binding of ammonium sulfate salts was also observed in a protic environment. The binding constants determined by UV−vis absorbance, fluorescence, and NMR titrations were found to be in agreement in all cases. Corroborating conformational changes of the receptor upon binding were evidenced by fluorescence and NMR spectroscopies. Interestingly, cavity-based selectivity in terms of the size and shape of the guest was observed with both receptors **4a** and **4b**. While **4a** displays a strong affinity for small or linear ammonium salts, **4b** was found to have the ability to recognize the 3,4-*O*-dimethyldopammonium sulfate salt and not the corresponding serotonin derivative. In other words, this work opens interesting perspectives on the elaboration of unique fluorescent cavity-based systems for the selective sensing of anions or biologically relevant ammonium salts such as neurotransmitters. Current efforts are now being directed toward the design of water-soluble fluorescent calix[6]arene-based receptors.

■ EXPERIMENTAL SECTION

General Experimental Methods. All of the reactions were performed under an inert atmosphere. Anhydrous THF was obtained through distillation over Na/benzophenone. Silica gel (230−400 mesh) was used for flash chromatography purifications. Chloroform (both deuterated and nondeuterated) was filtered prior to use over a short column of basic alumina to remove traces of HCl/DCl. ^1H NMR spectra were recorded on a 600, 400, or 300 MHz spectrometer, and ^{13}C NMR spectra were recorded on the 300 or 400 MHz spectrometer at 75 or 100 MHz, respectively. 2D NMR spectra (COSY, HSQC, HMBC) were recorded to complete signal assignments. DOSY experiments were recorded on the 600 MHz spectrometer. NMR parameters (acquisition time, recycling times, and signal accumulation) were chosen to ensure that quantitative data could be obtained from signal integration in the 1D ^1H spectra. Traces of residual solvent were used as an internal chemical shift reference. Chemical shifts are quoted on the δ scale. The NMR, UV, and fluorescence spectra were recorded at 298 K, unless otherwise stated. De-*tert*-butylated 1,3,5-tris(methoxy)calix[6]arene **2**,[23] calix[6]tris(azido) **3a**,[25] and 2-azidoethyl-4-methylbenzenesulfonate[24] were prepared as previously described.

Calix[6]tris(azido) 3b. De-*tert*-butylated 1,3,5-tris(methoxy)-calix[6]arene **2** (1.81 g, 2.14 mmol) was dissolved in freshly distilled THF (100 mL), and NaH (60 wt % in oil, 0.510 g, 12.82 mmol) was added. The mixture was heated to reflux for 30 min. Then 2-azidoethyl-4-methylbenzenesulfonate (2.060 g, 8.54 mmol) was added, and the heating was maintained for 48 h. After the mixture was cooled to room temperature, methanol (15 mL) was added, and the solution was stirred for 30 min. Then the solvents were evaporated, and the residue was dissolved in a mixture of CH_2Cl_2 (80 mL) and HCl (80 mL, 1 M). The organic layer was separated, and the aqueous layer was extracted twice with CH_2Cl_2. The combined organic layers were washed twice with brine, filtered through a WA filter, and evaporated under vacuum. The crude product was then purified by flash chromatography on silica gel (CH_2Cl_2/CH_3OH, 100:0 then 95:5) to give calix[6]tris(azido) **3b** (1.730 g, 77% yield). Mp: 125−130 °C (dec.). IR (KBr): ν 2956, 2105, 1455 cm^{-1}. ^1H NMR ($CDCl_3$, 300 MHz, 298 K): δ (ppm) 1.28 (s, 27H, *t*Bu), 2.80 (s, 9H, OCH_3), 3.46 (m, 6H, CH_2N_3), 3.75 (m, 6H, OCH_2), 4.02 (s, 12H, $ArCH_2$), 6.33 (s, 9H, ArH), 7.21 (s, 6H, ArH). ^{13}C NMR ($CDCl_3$, 75 MHz, 298 K): δ (ppm) 30.6, 31.5, 34.2, 51.2, 59.8, 70.9, 123.9, 126.8, 128.2, 133.2, 134.5, 146.1, 153.9, 154.2. ESI-HRMS (CH_2Cl_2/CH_3OH): calcd for $C_{63}H_{79}N_{10}O_6$ $[M + NH_4]^+$ 1071.6184, found 1071.6162.

Calix[6]tris(pyrenylurea) 4a. Calix[6]tris(azido) **3a** (0.350 g, 0.29 mmol) was dissolved in anhydrous THF (10 mL), and triphenylphosphine (0.450 g, 1.72 mmol) was added. Then CO_2 was bubbled through the solution for 5 min. The solution was stirred for 19 h at room temperature and kept under a CO_2 atmosphere. The medium was then purged with argon for 5 min, and 1-aminopyrene (0.273 g, 1.26 mmol) was added. The mixture was then stirred under argon for 48 h at 50 °C. The solvent was evaporated under vacuum, and acetonitrile

dx.doi.org/10.1021/jo5009146 | J. Org. Chem. 2014, 79, 6179−6188

(1 mL) was added. The suspension was sonicated for 15 min and then centrifuged for 15 min, and the supernatant was removed. This operation was repeated six times. The crude product was then purified by flash chromatography on silica gel (CH_2Cl_2/CH_3OH, 100:0 then 99:1 then 95:5) to afford calix[6]tris(pyrenylurea) **4a** (0.370 g, 70% yield). Mp: 208−212 °C (dec.). IR (KBr): ν 3375, 2962, 1655, 1524, 1482 cm^{-1}. ^1H NMR (DMSO-d_6, 298 K, 400 MHz): δ (ppm) 0.75 (s, 27H, *t*Bu), 1.29 (s, 27H, *t*Bu), 2.12 (s, 9H, OMe), 3.50 (d, 6H, $ArCH_2^{eq}$, ^2J = 15.4 Hz), 3.65 (br s, 6H, CH_2N), 4.05 (br s, 6H, CH_2O), 4.56 (d, 6H, $ArCH_2^{ax}$, ^2J = 15.0 Hz), 6.61 (s, 6H, ArH^{Urea}), 6.96 (s, 3H, $NHCH_2$), 7.31 (s, 6H, ArH^{OMe}), 7.92−8.05 (m, 12H, PyrH), 8.07−8.24 (m, 12H, PyrH), 8.51 (d, 3H, PyrH, ^3J = 8.4 Hz), 9.11 (s, 3H, *NH*Pyr). ^{13}C NMR (DMSO-d_6, 298 K, 100 MHz): δ (ppm) 29.0, 30.7, 31.3, 33.5, 33.9, 59.4, 71.9, 120.2, 121.0, 121.2, 123.0, 124.2, 124.5, 124.7, 125.2, 125.3, 126.2, 126.4, 127.3, 128.1, 130.5, 131.1, 132.5, 133.2, 133.7, 144.8, 145.2, 151.4, 153.8, 155.8. ESI-HRMS (CH_2Cl_2/CH_3OH): calcd for $C_{126}H_{132}N_6O_9Na$ $[M + Na]^+$ 1895.9954, found 1895.9949.

Calix[6]tris(pyrenylurea) 4b. Calixarene **4b** was prepared using the same procedure as for **4a** starting from calix[6]tris(azido) **3b** (0.500 g, 0.47 mmol), which gave calix[6]tris(pyrenylurea) **4b** (0.280 g, 35% yield). Mp: 225−230 °C (dec.). IR (KBr): ν 3319, 2961, 1651, 1557, 1485 cm^{-1}. ^1H NMR (DMSO-d_6, 298 K, 300 MHz): δ (ppm) 1.19 (s, 27H, *t*Bu), 2.60 (s, 9H, OMe), 3.61 (br s, 6H, CH_2N), 3.77−4.26 (m, 18H, $CH_2O/ArCH_2^{eq}/ArCH_2^{ax}$), 6.51 (d, 6H, ArH^{Urea}, ^3J = 7.5 Hz), 6.67 (t, 3H, ArH^{Urea}, ^3J = 8.0 Hz), 6.91 (t, 3H, $NHCH_2$, ^3J = 5.0 Hz), 7.23 (s, 6H, ArH^{OMe}), 7.80−8.06 (m, 12H, PyrH), 8.07−8.28 (m, 12H, PyrH), 8.51 (d, 3H, PyrH, ^3J = 8.4 Hz), 9.09 (s, 3H, *NH*Pyr). ^{13}C NMR (DMSO-d_6, 298 K, 75 MHz): δ (ppm) 30.9, 32.1, 34.7, 60.4, 110.0, 120.9, 121.7, 122.0, 124.2, 125.0, 125.3, 125.4, 125.4, 126.1, 126.2, 127.0, 127.3, 127.6, 128.1, 128.2, 131.4, 131.9, 133.6, 134.6, 135.2, 146.4, 154.7, 155.0, 156.7. ESI-HRMS (CH_2Cl_2/CH_3OH): calcd for $C_{114}H_{109}N_6O_9$ $[M + H]^+$ 1706.8290, found 1706.8256.

^1H NMR Characterization of Various Host−Guest Complexes. **4a⊃SO_4^{2-}**: ^1H NMR (DMSO-d_6, 298 K, 300 MHz): δ (ppm) 0.79 (s, 27H, *t*Bu), 1.36 (s, 27H, *t*Bu), 2.55 (s, 9H, OMe), 3.31−3.41 (m, 6H, $ArCH_2^{eq}$)*, 3.75 (br s, 6H, CH_2N), 4.43 (br s, 6H, CH_2O), 4.59 (d, 6H, $ArCH_2^{ax}$, ^2J = 15.0 Hz), 6.67 (s, 6H, ArH^{Urea}), 7.14−7.26 (m, 3H, PyrH), 7.30 (s, 6H, ArH^{OMe}), 7.51−8.18 (m, 18H, PyrH), 8.23 (d, 3H, PyrH, ^3J = 9.0 Hz), 8.55 (d, 3H, PyrH, ^3J = 9.0 Hz), 9.14 (s, 3H, $NHCH_2$), 10.71 (s, 3H, *NH*Pyr). **4a⊃$PrNH_3^+SO_4^{2-}$**: ^1H NMR ($CDCl_3$, 298 K, 600 MHz: δ (ppm) −1.92 (t, 3H, $CH_3^{PrNH_3^+_{in}}$, ^2J = 7.4 Hz), −1.26 (m, 2H, $CH_2^{PrNH_3^+_{in}}$), 0.74 (s, 27H, *t*Bu), 1.32 (s, 27H, *t*Bu), 2.40 (s, 2H, $CH_2NH_3^{+PrNH_3^+_{in}}$)*, 3.32 (d, 6H, $ArCH_2^{eq}$, ^2J = 14.4 Hz), 3.93 (br s, 6H, CH_2N), 4.13 (s, 9H, OMe), 4.20 (br s, 6H, CH_2O), 4.46 (d, 6H, $ArCH_2^{ax}$, ^2J = 14.4 Hz), 6.60 (s, 6H, ArH^{urea}), 7.17 (s, 6H, ArH^{OMe}), 7.80−8.25 (m, 18H, PyrH), 8.30 (d, 3H, PyrH, ^3J = 9 Hz), 9.30−9.40 (m, 6H, PyrH), 8.88 (s, 3H, $NHCH_2$), 10.48 (s, 3H, *NH*Pyr). **4b⊃$DopaNH_3^+SO_4^{2-}$**: ^1H NMR ($CDCl_3$, 298 K, 300 MHz): δ (ppm) 0.46 (m, 2H, $CH_2NH_3^{+DopaNH_3^+_{in}}$)*, 1.30 (s, 27H, *t*Bu), 2.70 (br s, 2H, $CH_2^{DopaNH_3^+_{in}}$), 2.91 (s, 3H, $OMe^{DopaNH_3^+_{in}}$)*, 3.34 (d, 6H, $ArCH_2^{eq}$, ^2J = 14.4 Hz), 3.43 (s, 3H, $OMe^{DopaNH_3^+_{in}}$), 3.87 (m, 1H, $ArH^{DopaNH_3^+_{in}}$ and br s, 6H, CH_2N)*, 4.09 (br s, 6H, CH_2O), 4.11 (m, 1H, $ArH^{DopaNH_3^+_{in}}$)*, 4.29 (s, 9H, OMe), 4.55 (d, 6H, $ArCH_2^{ax}$, ^2J = 14.4 Hz), 5.06 (d, 1H, $ArH^{DopaNH_3^+_{in}}$, ^3J = 8.4 Hz), 6.47 (t, 3H, ArH^{urea}, ^3J = 9.0 Hz), 6.64 (d, 6H, ArH^{urea}, ^3J = 9.0 Hz), 7.16 (s, 6H, ArH^{OMe}), 7.31 (m, 3H, $NH_3^{+DopaNH_3^+_{in}}$)*, 7.82−8.20 (m, 18H, PyrH), 8.38 (d, 3H, PyrH, ^3J = 9.0 Hz), 9.13 (t, 3H, $NHCH_2$, ^3J = 5.1 Hz), 9.43−9.55 (m, 6H, PyrH), 10.51 (s, 3H, *NH*Pyr). Asterisks (*) denote signals assigned thanks to the COSY spectrum.

NMR Titration Experiments. All of these experiments were undertaken following a similar protocol. A known volume (~600 μL) of a solution of known concentration of the host (~2 mM) was placed in an NMR tube, and the ^1H NMR spectrum was recorded. Aliquots of a stock solution of the guest (~5 μL, corresponding to 0.25 equiv of host) were successively added, and the ^1H NMR spectrum was recorded after each addition. Aliquots were added until no changes in the host signals were observed.

UV−Vis and Fluorescence Titration Experiments. All of these experiments were undertaken following a similar protocol. A known volume (~2 mL) of a solution of known concentration of the host (~10^{-5} M) was placed in a cell, and the absorbance or emission spectrum was recorded. Aliquots of a stock solution of the guest (~5 μL, corresponding to 0.5 equiv of host) were successively added, and the spectrum was recorded after each addition. Aliquots were added until no changes in the spectrum were observed. The values obtained for the absorbance/emission were corrected for dilution.

■ ASSOCIATED CONTENT

Supporting Information

^1H NMR, UV−vis, and fluorescence studies of the complexing properties of **4a** and **4b** in $CHCl_3$ and DMSO; Job's plot analysis of the association between host **4a** and SO_4^{2-}; ^1H NMR study of the complexing properties of **1a**; and 1D and 2D NMR spectra of **3b**, **4a**, and **4b**. This material is available free of charge via the Internet at http://pubs.acs.org.

■ AUTHOR INFORMATION

Corresponding Authors

*E-mail: ijabin@ulb.ac.be.

*E-mail: kbartik@ulb.ac.be.

Notes

The authors declare no competing financial interest.

■ ACKNOWLEDGMENTS

J.-F.P. and E.B. received Ph.D. grants from the Fonds pour la Formation à la Recherche dans l'Industrie et dans l'Agriculture (FRIA-FRS, Belgium). This research was supported by the Fonds de la Recherche Scientifique-FNRS (FRFC 2.4.617.10.F Project) and the Agence Nationale de la Recherche (ANR10-BLAN-714 Cavity-zyme(Cu) Project) and was undertaken within the framework of the COST Action CM-1005 "Supramolecular Chemistry in Water".

■ REFERENCES

(1) (a) Lehn, J.-M. *Supramolecular Chemistry: Concepts and Perspectives*; Wiley-VCH: Weinheim, Germany, 1995. (b) Steed, J. W.; Turner, D. R.; Wallace, K. J. *Core Concepts in Supramolecular Chemistry and Nanochemistry*; Wiley, Chichester, U.K., 2007. (c) Hartley, J. H.; James, T. D.; Ward, C. J. *J. Chem. Soc., Perkin Trans. 1* **2000**, 3155−3184.

(2) (a) *New Trends in Fluorescence Spectroscopy: Applications to Chemical and Life Sciences*; Valeur, B., Brochon, J.-C., Eds.; Springer: Berlin, 2001. (b) Nguyen, B. T.; Anslyn, E. V. *Coord. Chem. Rev.* **2006**, *250*, 3118−3127.

(3) (a) de Silva, A. P.; Gunaratne, H. Q. N.; Gunnlaugsson, T.; Huxley, A. J. M.; McCoy, C. P.; Rademacher, J. T.; Rice, T. E. *Chem. Rev.* **1997**, *97*, 1515−1566. (b) Rurack, K.; Resch-Genger, U. *Chem. Soc. Rev.* **2002**, *31*, 116−127.

(4) Valeur, B. *Molecular Fluorescence: Principles and Applications*; Wiley-VCH: Weinheim, Germany, 2002.

(5) For examples of concave macrocyclic chemosensors, see: (a) Sindelar, V.; Cejas, M. A.; Raymo, F. M.; Chen, W.; Parker, S. E.; Kaifer, A. E. *Chem.—Eur. J.* **2005**, *11*, 7054−7059. (b) Bracamonte, A. G.; Veglia, A. V. *Talanta* **2011**, *83*, 1006−1013. (c) Korbakov, N.; Timmerman, P.; Lidich, N.; Urbach, B.; Sa'ar, A.; Yitzchaik, S. *Langmuir* **2008**, *24*, 2580−2587. (d) Freeman, R.; Finder, T.; Bahshi, L.; Willner, I. *Nano Lett.* **2009**, *9*, 2073−2076. (e) Bailey, D. M.; Hennig, A.; Uzunova, V. D.; Nau, W. M. *Chem.—Eur. J.* **2008**, *14*, 6069−6077.

(6) Coquière, D.; Le Gac, S.; Darbost, U.; Sénèque, O.; Jabin, I.; Reinaud, O. *Org. Biomol. Chem.* **2009**, *7*, 2485−2500.

(7) (a) Gutsche, C. D. *Calixarenes Revisited*; Monographs in Supramolecular Chemistry; Stoddart, J. F., Series Ed.; Royal Society of Chemistry: Cambridge, U.K., 1998. (b) *Calixarenes 2001*; Asfari, Z., Böhmer, V., Harrowfield, J., Vicens, J., Eds.; Kluwer Academic Publishers: Dordrecht, The Netherlands, 2001.

(8) (a) Kim, J. S.; Quang, D. T. *Chem. Rev.* **2007**, *107*, 3780−3799. (b) Kim, S. H.; Kim, H. J.; Yoon, J.; Kim, J. S. In *Calixarenes in the*

Nanoworld; Vicens, J., Harrowfield, J., Eds.; Springer: Dordrecht, The Netherlands, 2007; pp 311−333.
(9) (a) Quinlan, E.; Matthews, S. E.; Gunnlaugsson, T. *J. Org. Chem.* **2007**, *72*, 7497−7503. (b) Bu, J.-H.; Zheng, Q.-Y.; Chen, C.-F; Huang, Z.-T. *Org. Lett.* **2004**, *6*, 3301−3303.
(10) (a) Zhang, W.-C.; Zhu, Y.; Li, E.-C.; Liu, T.-J.; Huang, Z.-T. *Tetrahedron* **2000**, *56*, 3365−3371. (b) Zhang, S.; Palkar, A.; Echegoyen, L. *Langmuir* **2006**, *22*, 10732−10738. (c) Mai, J. H.; Liu, J. M.; Li, S. Y.; Jiang, H. F. *Chin. Chem. Lett.* **2009**, *20*, 1191−1194. (d) Jeon, N. J.; Ryu, B. J.; Park, K. D.; Lee, Y. J.; Nam, K. C. *Bull. Korean Chem. Soc.* **2010**, *31*, 3809−3812. (e) Takeshita, M.; Shinkai, S. *Chem. Lett.* **1994**, 1349−1352. (f) Schönefeld, K.; Ludwig, R.; Feller, K.-H. *J. Fluoresc.* **2006**, *16*, 449−454. (g) He, S.; Lu, Y.; Li, Y.-Y.; Lu, Y.; Zeng, X.-S. *Chem. J. Chin. Univ.* **2011**, *9*, 2139−2144. (h) Sreenivasu Mummidivarapu, V. V.; Nehra, A.; Kumar Hinge, V.; Chebrolu, P. R. *Org. Lett.* **2012**, *14*, 2968−2971.
(11) (a) Redshaw, K. *Coord. Chem. Rev.* **2003**, *244*, 45−70. (b) Ikeda, A.; Shinkai, S. *Chem. Rev.* **1997**, *97*, 1713−1734.
(12) For recent reviews of ion-pair receptors, see: (a) Kim, S. K.; Sessler, J. L. *Chem. Soc. Rev.* **2010**, *39*, 3784−3809. (b) McConnell, A. J.; Beer, P. D. *Angew. Chem., Int. Ed.* **2012**, *51*, 5052−5061.
(13) (a) Valeur, B.; Leray, I. *Coord. Chem. Rev.* **2000**, *205*, 3−40. (b) Pradhan, T.; Jung, H. S.; Jang, J. H.; Kim, T. W.; Kang, C.; Kim, J. S. *Chem. Soc. Rev.* **2014**, *43*, 4684−4713. (c) Ho, I.-T.; Haung, K.-C.; Chung, W.-S. *Chem.—Asian J.* **2011**, *6*, 2738−2746.
(14) (a) Gunnlaugsson, T.; Glynn, M.; Tocci (née Hussey), G. M.; Kruger, P. E.; Pfeffer, F. M. *Coord. Chem. Rev.* **2006**, *250*, 3094−3117. (b) Beer, P. D. *Acc. Chem. Res.* **1998**, *31*, 71−80. For a themed issue on anions, see: (c) *Chem. Soc. Rev.* **2010**, *39*, 3597−4003.
(15) (a) *Fluorescent Chemosensors for Ions and Molecule Recognition*; Czarnik, A. W., Ed.; ACS Symposium Series, Vol. *538*; American Chemical Society: Washington, DC, 1993. For a recent example, see: (b) Lee, Y. H.; Liu, H.; Lee, J. Y.; Kim, S. H.; Kim, S. K.; Sessler, J. L.; Kim, Y.; Kim, J. S. *Chem.—Eur. J.* **2010**, *16*, 5895−5901.
(16) Ménand, M.; Leroy, A.; Marrot, J.; Luhmer, M.; Jabin, I. *Angew. Chem., Int. Ed.* **2009**, *48*, 5509−5512.
(17) Izzet, G.; Zeng, X.; Over, D.; Giorgi, M.; Jabin, I.; Le Mest, Y.; Reinaud, O. *Inorg. Chem.* **2007**, *46*, 375−377.
(18) Hamon, M.; Ménand, M.; Le Gac, S.; Luhmer, M.; Dalla, V.; Jabin, I. *J. Org. Chem.* **2008**, *73*, 7067−7071.
(19) Mahoney, J. M.; Beatty, A. M.; Smith, B. D. *J. Am. Chem. Soc.* **2001**, *123*, 5847−5848.
(20) (a) Kubik, S. *J. Am. Chem. Soc.* **1999**, *121*, 5846−5855. (b) Mahoney, J. M.; Davis, J. P.; Beatty, A. M.; Smith, B. D. *J. Org. Chem.* **2003**, *68*, 9819−9820. (c) Lankshear, M. D.; Dudley, I. M.; Chan, K.-M.; Cowley, A. R.; Santos, S. M.; Felix, V.; Beer, P. D. *Chem.—Eur. J.* **2008**, *14*, 2248−2263. (d) Atwood, J. L.; Szumna, A. *Chem. Commun.* **2003**, 940−941. (e) Ménand, M.; Jabin, I. *Chem.—Eur. J.* **2010**, *16*, 2159−2169. (f) Lascaux, A.; Le Gac, S.; Wouters, J.; Luhmer, M.; Jabin, I. *Org. Biomol. Chem.* **2010**, *8*, 4607−4616. (g) Moerkerke, S.; Ménand, M.; Jabin, I. *Chem.—Eur. J.* **2010**, *16*, 11712−11719. (h) Moerkerke, S.; Le Gac, S.; Topić, F.; Rissanen, K.; Jabin, I. *Eur. J. Org. Chem.* **2013**, 5315−5322. (i) Ni, X.-L.; Rahman, S.; Zeng, X.; Hughes, D. L.; Redshaw, C.; Takehiko, Y. *Org. Biomol. Chem.* **2011**, *9*, 6535−6541. (j) Perraud, O.; Robert, V.; Martinez, A.; Dutasta, J.-P. *Chem.—Eur. J.* **2011**, *17*, 4177−4182.
(21) For leading examples of fluorescent calixarene derivatives bearing pyrenyl groups, see: (a) Ni, X.-L.; Wang, S.; Zeng, X.; Tao, Z.; Yamato, T. *Org. Lett.* **2011**, *13*, 552−555. (b) Schazmann, B.; Alhashimy, N.; Diamond, D. *J. Am. Chem. Soc.* **2006**, *128*, 8607−8614. (c) Kim, J. S.; Shon, O. J.; Rim, J. A.; Kim, S. K.; Yoon, J. *J. Org. Chem.* **2002**, *67*, 2348−2351. (d) Kim, S. K.; Lee, S. H.; Lee, J. Y.; Lee, J. Y.; Bartsch, R. A.; Kim, J. S. *J. Am. Chem. Soc.* **2004**, *126*, 16499−16506. (e) Kim, S. K.; Bok, J. H.; Bartsch, R. A.; Lee, J. Y.; Kim, J. S. *Org. Lett.* **2005**, *7*, 4839−4842. (f) Ni, X.-l.; Zeng, X.; Redshaw, C.; Yamato, T. *J. Org. Chem.* **2011**, *76*, 5696−5702.
(22) Winnik, F. M. *Chem. Rev.* **1993**, *93*, 587−614.
(23) van Duynhoven, J. P. M.; Janssen, R. G.; Verboom, W.; Franken, S. M.; Casnati, A.; Pochini, A.; Ungaro, R.; de Mendoza, J.; Nieto, P.; Prados, P.; Reinhoudt, D. N. *J. Am. Chem. Soc.* **1994**, *116*, 5814−5822.
(24) Demko, Z. P.; Sharpless, K. B. *Org. Lett.* **2001**, *3*, 4091−4094.
(25) Ménand, M.; Jabin, I. *Org. Lett.* **2009**, *11*, 673−676.
(26) It should be noted that the NMR spectra remained unchanged upon dilution in $CDCl_3$ (from 7.4 to 0.2 mM), indicating an intramolecular self-association of the urea groups rather than an intermolecular one.
(27) See the Supporting Information.
(28) (a) Job, P. *Ann. Chim. Appl.* **1928**, *9*, 113−203. (b) Blanda, M. T.; Horner, J. H.; Newcomb, M. *J. Org. Chem.* **1989**, *54*, 4626−4636.
(29) For recent examples of receptors that can selectively bind the sulfate anion, see: (a) Hiscock, J. R.; Gale, P. A.; Hynes, M. J. *Supramol. Chem.* **2012**, *24*, 355−360. (b) Cranwell, P. B.; Hiscock, J. R.; Haynes, C. J. E.; Light, M. E.; Wells, N. J.; Gale, P. A. *Chem. Commun.* **2013**, *49*, 874−876. (c) Schaly, A.; Belda, R.; García-España, E.; Kubik, S. *Org. Lett.* **2013**, *15*, 6238−6241. (d) Jin, C.; Zhang, M.; Wu, Li; Guan, Y.; Pan, Y.; Jiang, J.; Lin, C.; Wang, L. *Chem. Commun.* **2013**, *49*, 2025−2027.
(30) (a) Lakshminarayanan, P. S.; Ravikumar, I.; Suresh, E.; Ghosh, P. *Chem. Commun.* **2007**, 5214−5216. (b) Ravikumar, I.; Ghosh, P. *Chem. Commun.* **2010**, *46*, 1082−1084.
(31) (a) Ballistreri, F. P.; Pappalardo, A.; Tomaselli, G. A.; Toscano, R. M.; Sfrazzetto, G. T. *Eur. J. Org. Chem.* **2010**, 3806−3810. Also see: (b) Valderrey, V.; Escudero-Adán, E. C.; Ballester, P. *Angew. Chem., Int. Ed.* **2013**, *52*, 6898−6902.
(32) Darbost, U.; Giorgi, M.; Reinaud, O.; Jabin, I. *J. Org. Chem.* **2004**, *69*, 4879−4884.
(33) Sénèque, O.; Rager, M. N.; Giorgi, M.; Reinaud, O. *J. Am. Chem. Soc.* **2000**, *122*, 6183−6189.

Fluorescent Chemosensors for Anions and Contact Ion Pairs with a Cavity-Based Selectivity

Emilio Brunetti, Jean-François Picron, Karolina Flidrova, Gilles Bruylants, Kristin Bartik* and Ivan Jabin*

Supporting information

List of contents

I. UV-visible and fluorescence studies of **4a** and **4b**

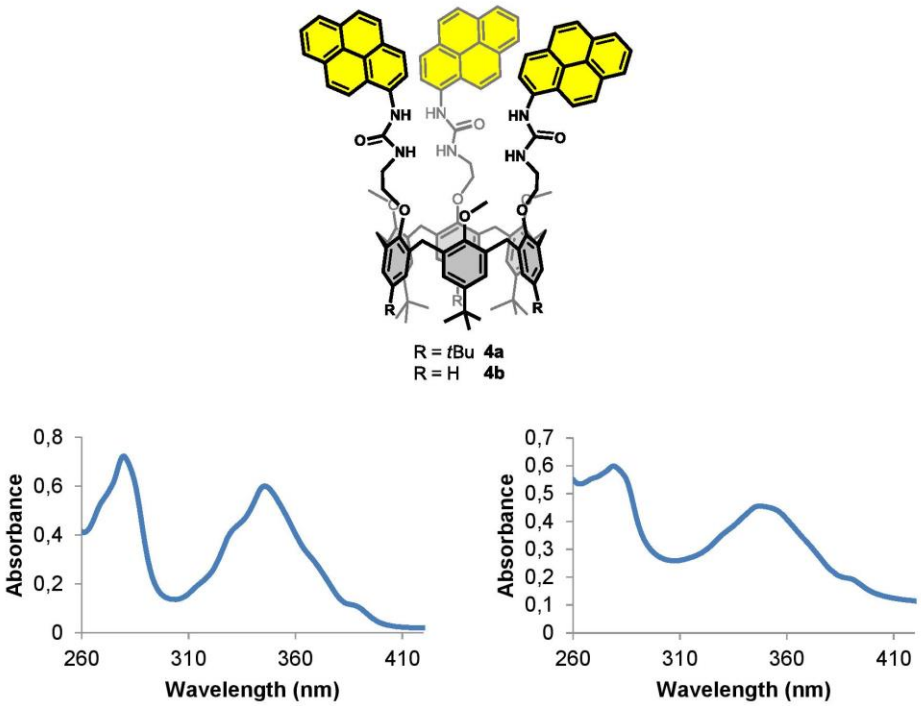

Figure S1. Left: UV-vis spectrum of **4a** in chloroform; $[\mathbf{4a}]_0 = 1.1\times 10^{-5}$ M. Right: UV-vis spectrum of **4a** in DMSO; $[\mathbf{4a}]_0 = 1.1\times 10^{-5}$ M.

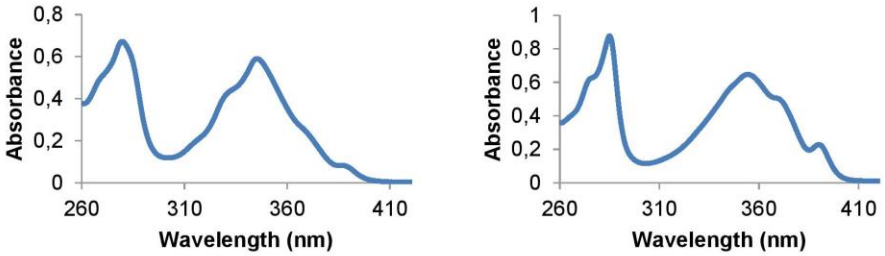

Figure S2. Left: UV-vis spectrum of **4b** in chloroform; $[\mathbf{4b}]_0 = 1.0\times 10^{-5}$ M. Right: UV-vis spectrum of **4b** in DMSO; $[\mathbf{4b}]_0 = 9.7\times 10^{-6}$ M.

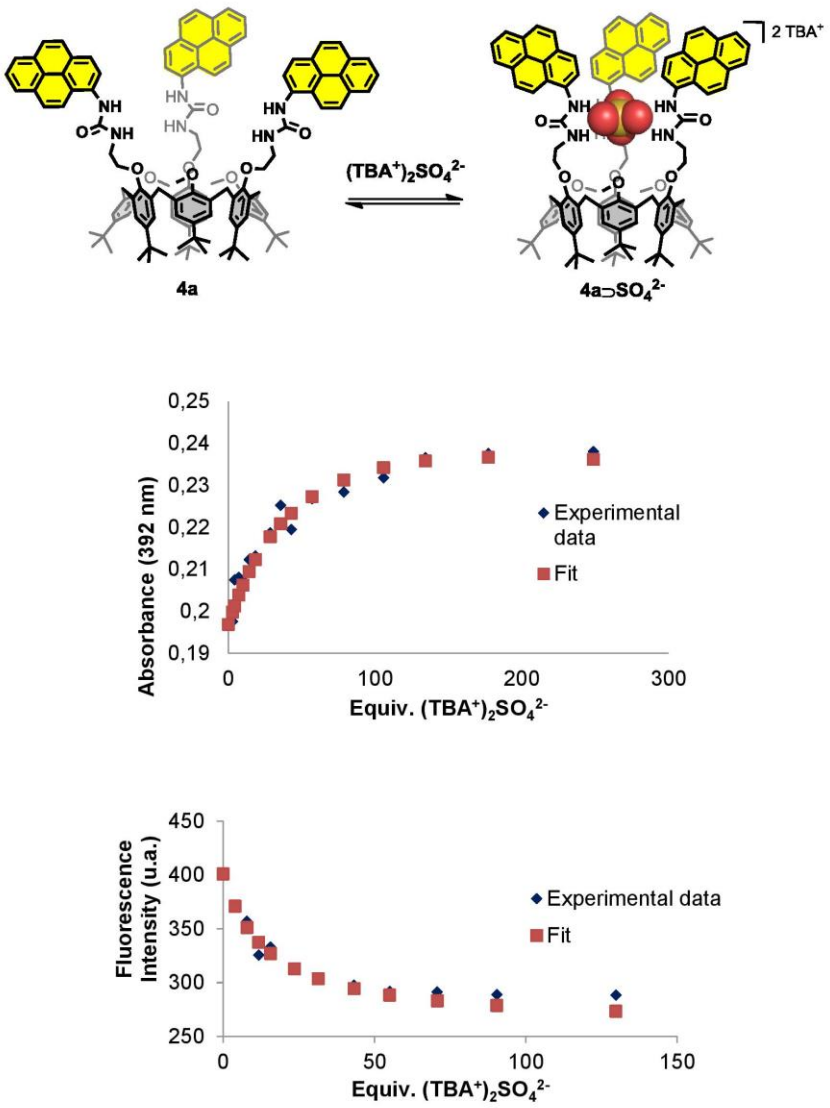

Figure S3. Top: variation of absorbance at 392 nm upon the addition of $(TBA^+)_2SO_4^{2-}$ in DMSO; $[\mathbf{4a}]_0 = 1.0 \times 10^{-5}$ M. Bottom: variation of fluorescence intensity at 402 nm upon the addition of $(TBA^+)_2SO_4^{2-}$; $[\mathbf{4a}]_0 = 1.0 \times 10^{-5}$ M. $\lambda_{ex} = 348$ nm. Parametric adjustment performed with a 1:1 binding model.

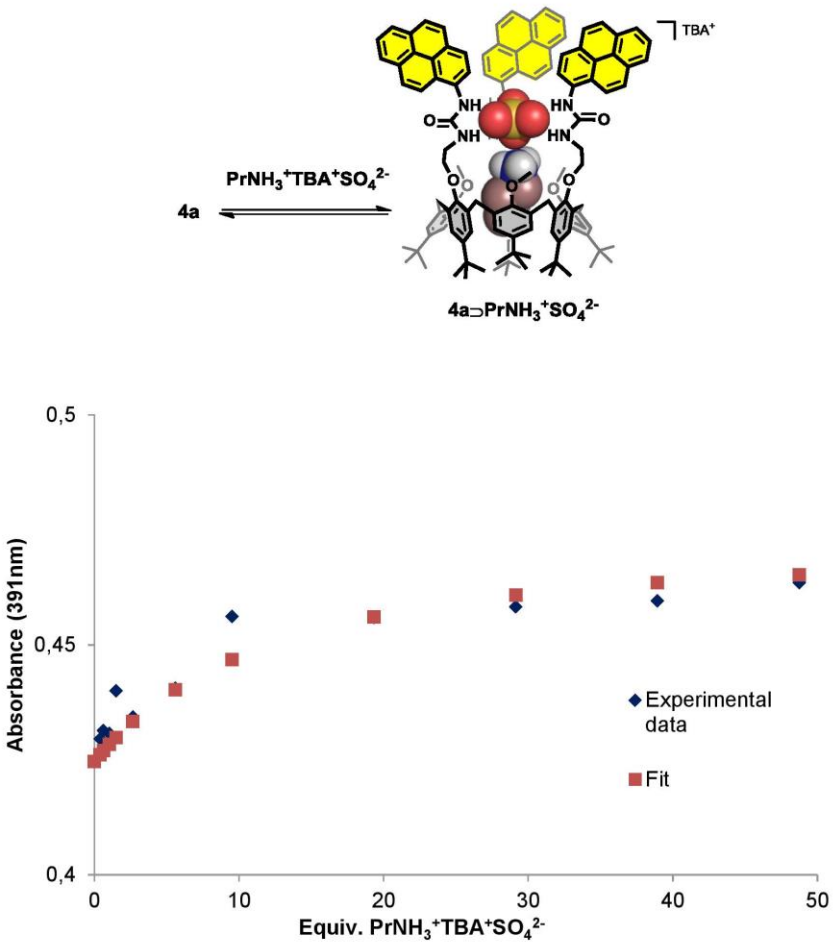

Figure S4. Variation of absorbance at 391 nm of **4a** upon the addition of $PrNH_3^+TBA^+SO_4^{2-}$ (0 to 50 equiv.) in CH_3OH /$CHCl_3$ 1:11; $[\mathbf{4a}]_0 = 0.7 \times 10^{-5}$ M. Parametric adjustment performed with a 1:1 binding model.

II. Job's plot analysis of the association between **4a** and $(TBA^+)_2SO_4^{2-}$

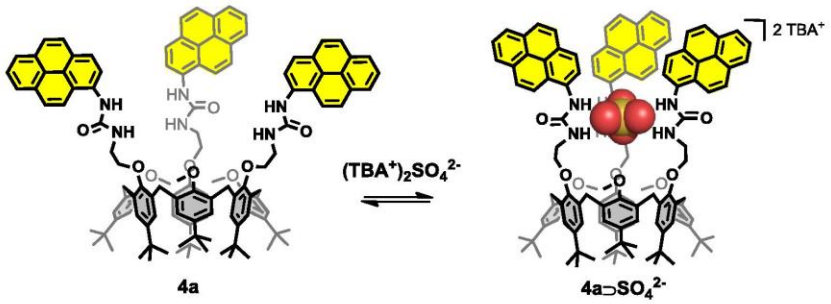

X(host)	V_{host} (µL)	V_{guest} (µL)	A (350nm)	ΔA	ΔA*X
1	2000	0	0.38736	0	0
0.9	1800	200	0.34048	0.038736	0.042192
0.8	1600	400	0.30241	0.077472	0.06796
0.7	1400	600	0.25947	0.116208	0.089523
0.6	1200	800	0.22199	0.154944	0.099222
0.5	1000	1000	0.17781	0.19368	0.104775
0.4	800	1200	0.13744	0.232416	0.099968
0.3	600	1400	0.10225	0.271152	0.085533
0.2	400	1600	0.069779	0.309888	0.0635162
0.1	200	1800	0.02811	0.348624	0.035925
0	0	2000	0	0.38736	0

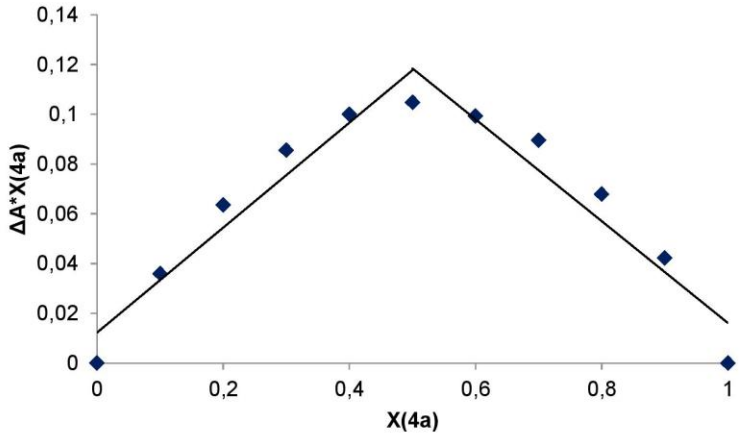

Figure S5. A Job Plot carried out between **4a** and $(TBA^+)_2SO_4^{2-}$ in DMSO. The observed maximum around 0.5 is consistent with the proposed 1:1 complex between **4a** and SO_4^{2-}; [**4a**] + $[(TBA^+)_2SO_4^{2-}]$ = 1.0×10^{-5} M.

III. ^{1}H NMR study of the complexing properties of **4a** and **4b**

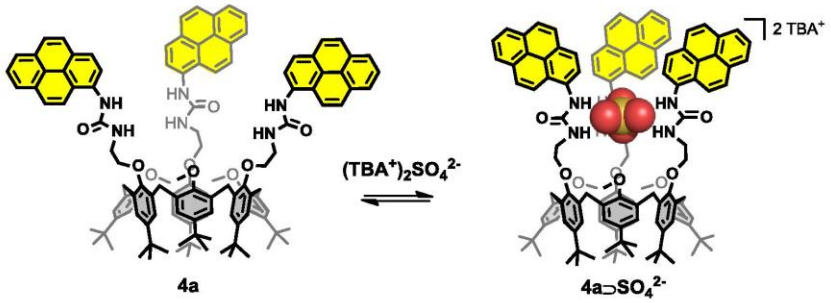

	ArH $_{out}$	ArH $_{in}$	ArCH$_2$ ^{ax}	CH$_2$O	CH$_2$N	OMe	*t*Bu $_{out}$	*t*Bu $_{in}$
Δδ (ppm)	0,013	0,058	0,034	0,370	0,116	0,442	0,064	0,034
Log *K*	-	3,3	3,6	3,4	3,5	-	3,3	3,3

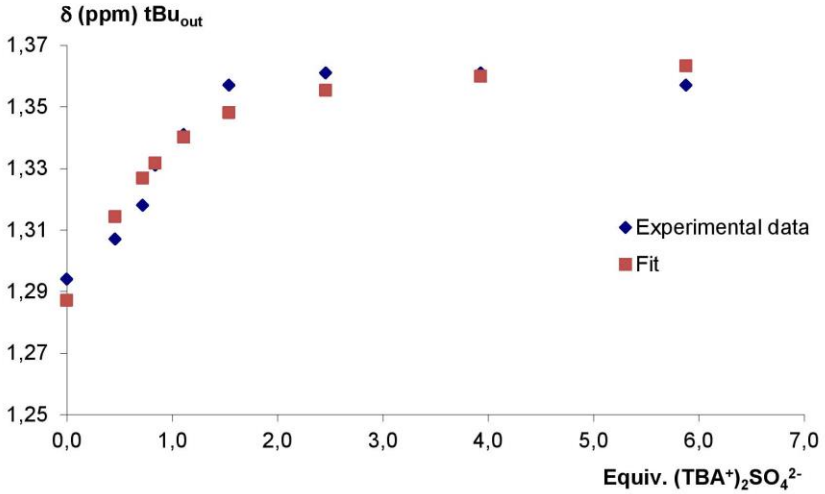

Figure S6. Variation of the chemical shift of the tBu_{out} of **4a** upon the addition of $(TBA^+)_2SO_4^{2-}$ (0 to 6 equiv.) in DMSO-d6 (300 MHz); $[\mathbf{4a}]_0 = 2.53 \times 10^{-3}$ M. Parametric adjustment performed with a 1:1 binding model.

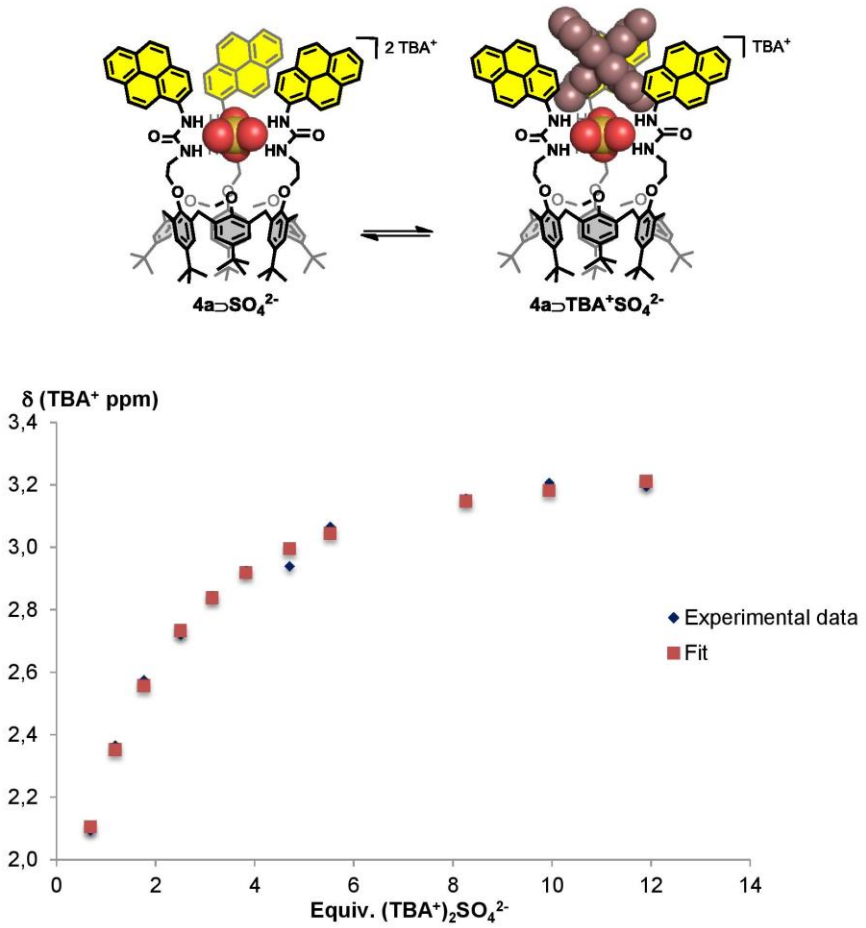

Figure S7. Variation of the chemical shift of TBA^+ (CH_2N^+) upon the addition of $(TBA^+)_2SO_4^{2-}$ (0 to 12 equiv.) to **4a** in $CDCl_3$ (600 MHz); $[\mathbf{4a}]_0 = 2.39 \times 10^{-3}$ M. Parametric adjustment performed with a 1:1 binding model.

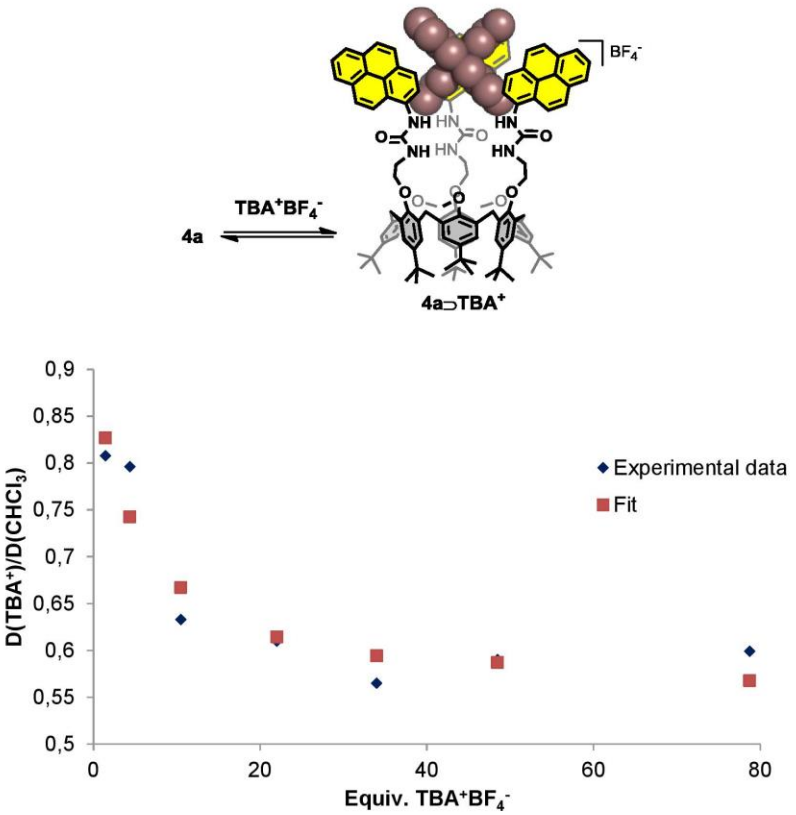

Figure S8. Variation of the diffusion coefficient of TBA^+ normalized by the diffusion coefficient of $CHCl_3$ upon the addition of $TBA^+BF_4^-$ (0 to 80 equiv.) to **4a** in $CDCl_3$ (600 MHz); $[\mathbf{4a}]_0 = 2.82 \times 10^{-3}$ M. Parametric adjustment performed with a 1:1 binding model.

Parameters of the DOSY experiment: 15 values of the magnitude of the gradient pulses ranging between approximately 2 G/cm to 50 G/cm, diffusion delay 100 ms, time-length of the gradient 5 ms, acquisition time 3 s, relaxation delay 10 s, 16 transients.

SI8

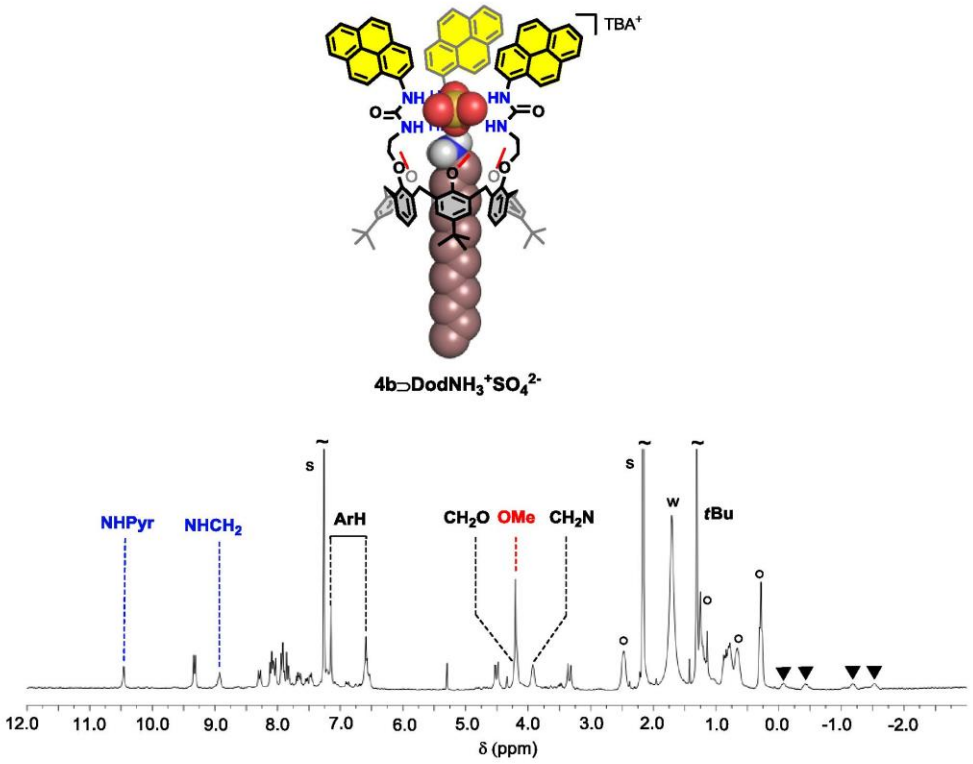

Figure S11. ^{1}H NMR spectrum (300MHz) of **4b** in $CDCl_3$ in the presence of ~1 equiv. of $DodNH_3^+TBA^+SO_4^{2-}$; o = TBA^+; ▼= $DodNH_3^+$ in; s: residual solvent; w: residual water.

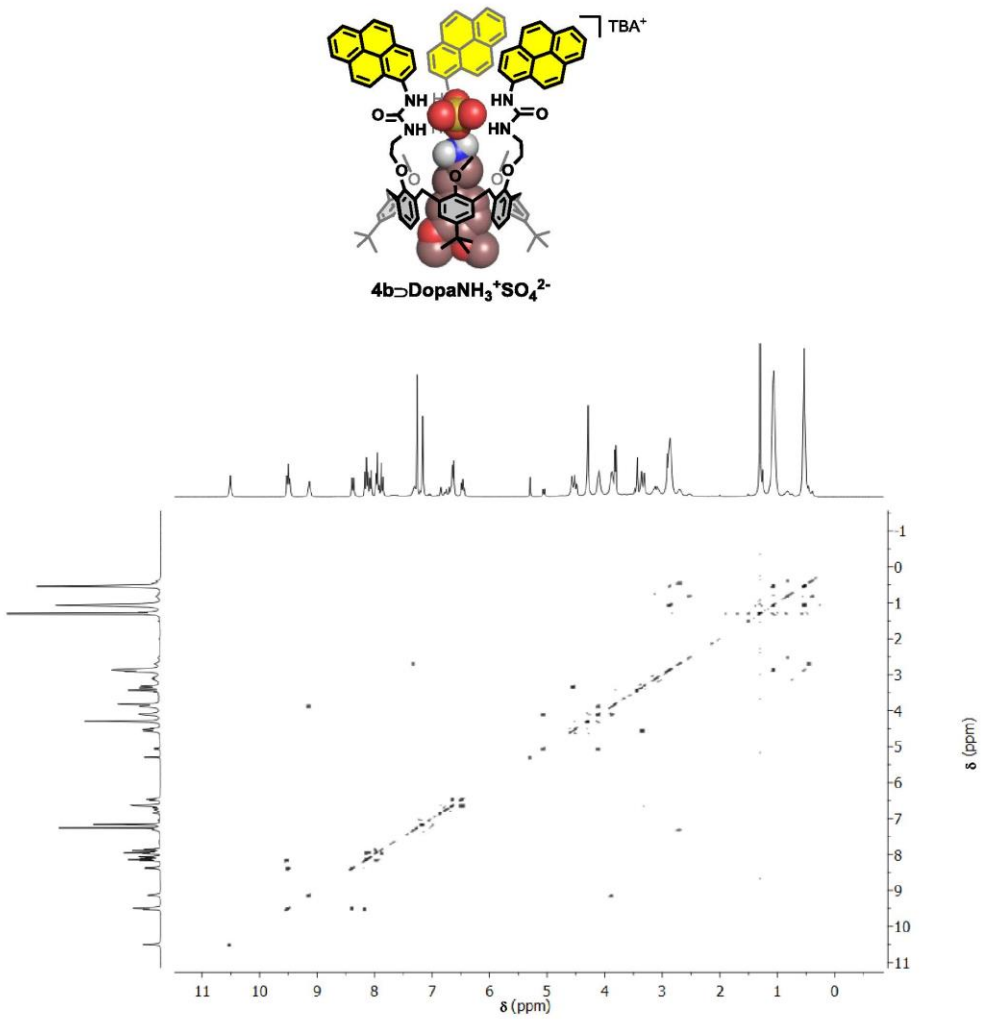

Figure S12. COSY spectrum (300MHz) of **4b** in $CDCl_3$ in the presence of ~2 equiv. of $DopaNH_3^+TBA^+SO_4^{2-}$.

SI12

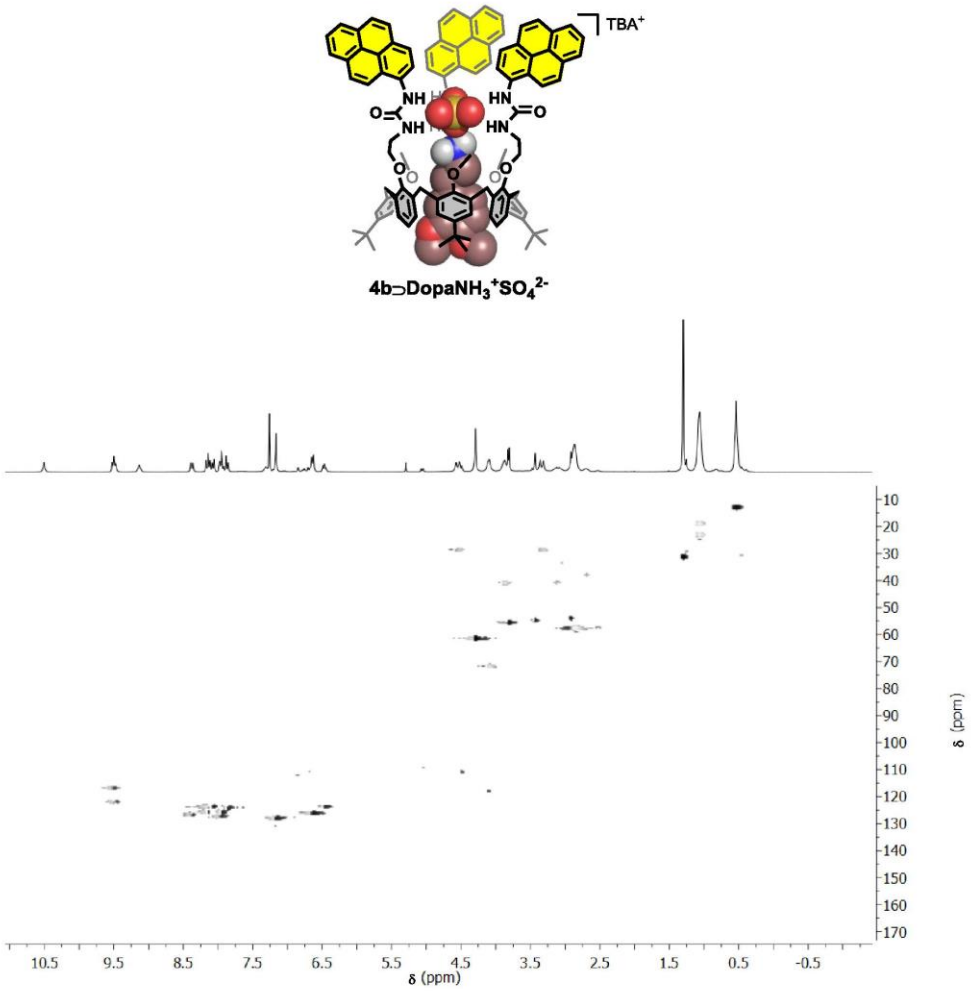

Figure S13. HSQC spectrum of **4b** in $CDCl_3$ in the presence of ~2 equiv. of $DopaNH_3^+TBA^+SO_4^{2-}$.

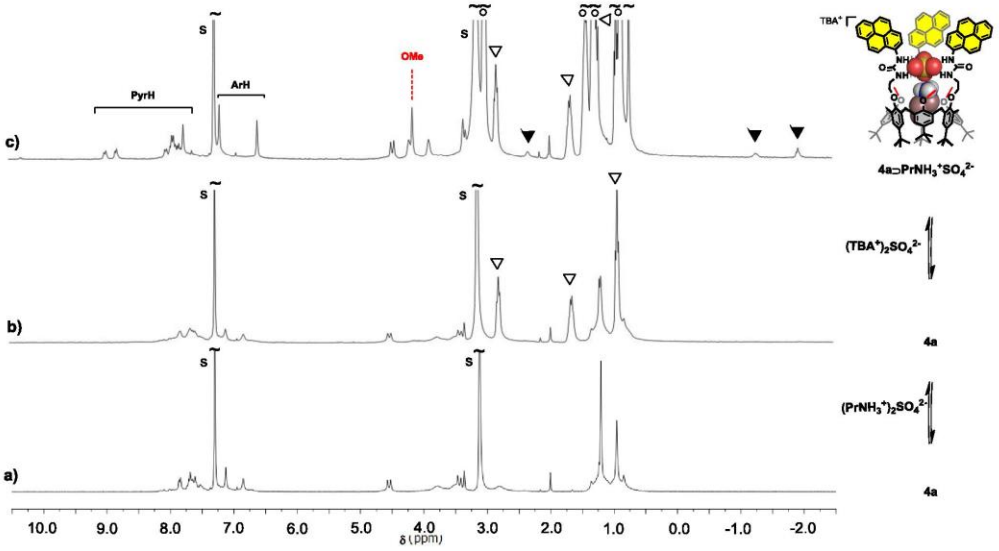

Figure S14. ^{1}H NMR spectrum (300MHz) of a) **4a** in $CD_3OD/CDCl_3$ 1:11; b) after the subsequent addition of ~8 equiv. of $(PrNH_3)_2^+SO_4^{2-}$; c) after the subsequent addition of ~1.5 equiv. of $(TBA)_2^+SO_4^{2-}$ o = TBA^+; ▽= $PrNH_3^+$ out; ▼= $PrNH_3^+$ in; s: residual solvent.

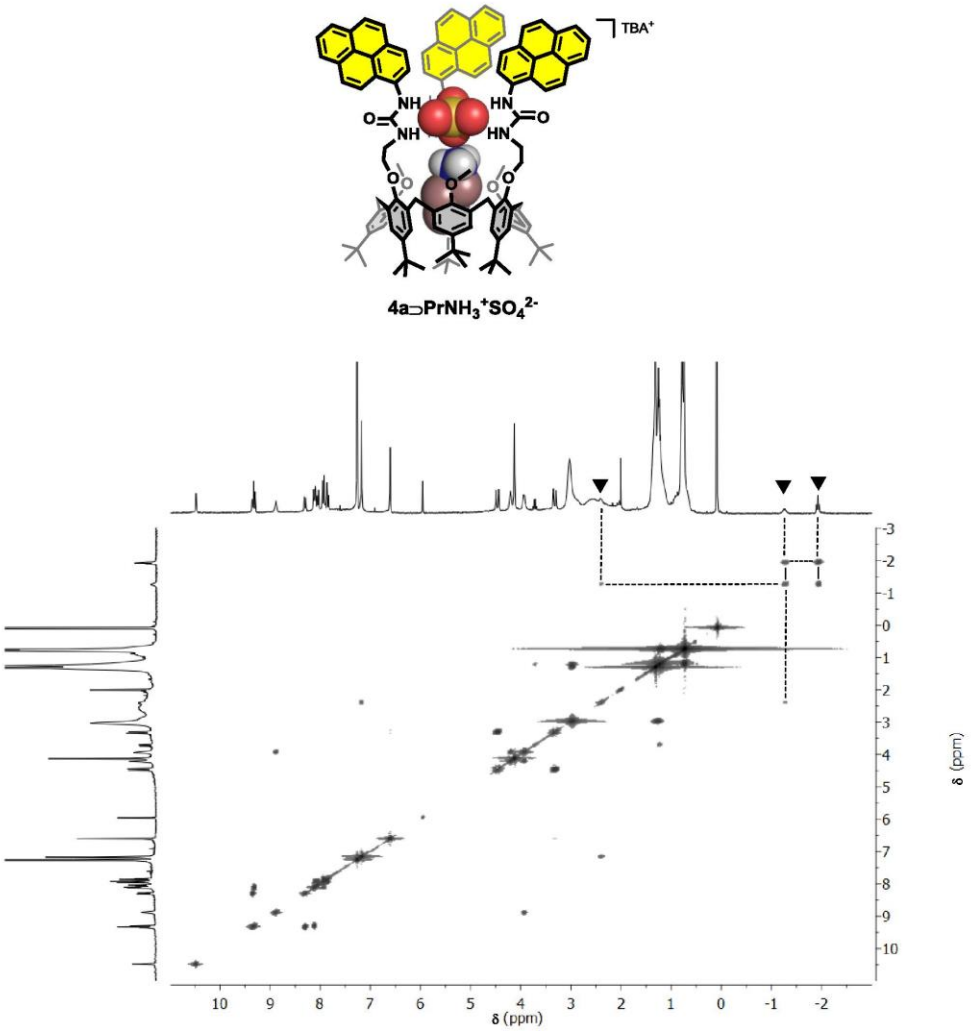

Figure S15. COSY spectrum (300 MHz) of receptor **4a** in the presence of ~4 equiv. of $PrNH_3^+TBA^+SO_4^{2-}$ in $CDCl_3$; ▼= $PrNH_3^+$ in.

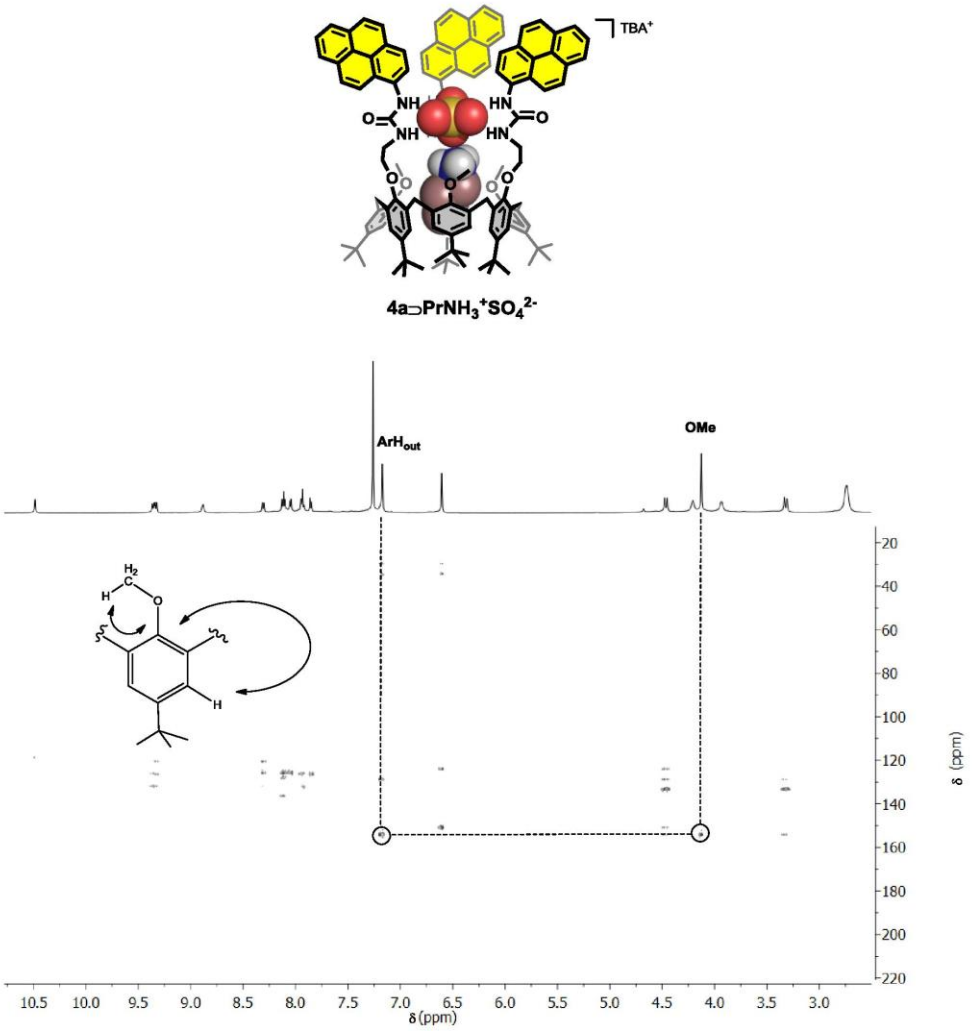

Figure S16. HMBC spectrum of receptor **4a** in the presence of ~4 equiv. of $PrNH_3^+TBA^+SO_4^{2-}$ in $CDCl_3$.

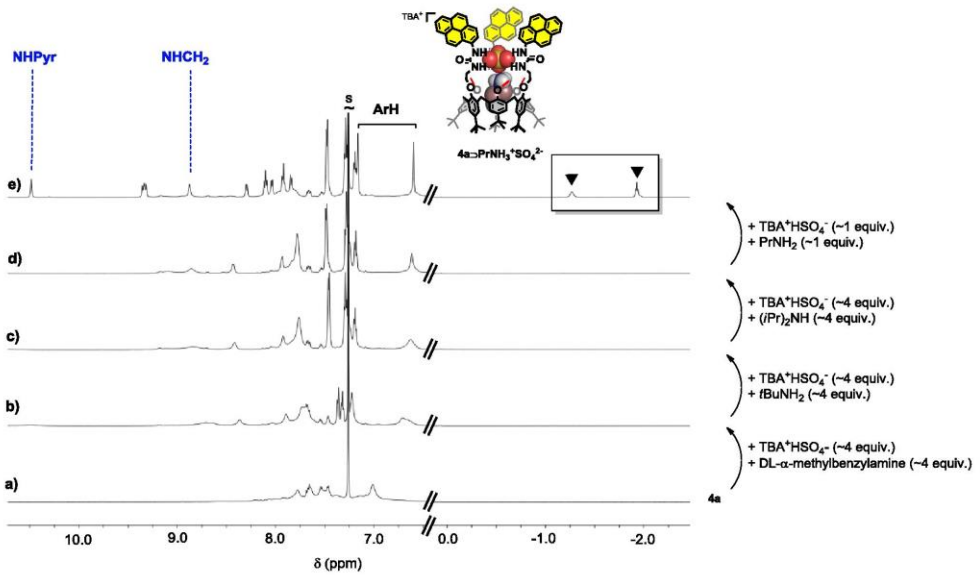

Figure S17. ^{1}H NMR spectrum (600MHz) of a) **4a** in $CDCl_3$; b) after the subsequent addition of ~4 equiv. of $TBA^+HSO_4^-$ and ~4 equiv. of (±)-α-methylbenzylamine; c) after the subsequent addition of ~4 equiv. of $TBA^+HSO_4^-$ and ~4 equiv. of *t*$BuNH_2$; d) after the subsequent addition of ~4 equiv. of $TBA^+HSO_4^-$ and ~4 equiv. of $(iPr)_2NH$; e) after the subsequent addition of ~1 equiv. of $TBA^+HSO_4^-$ and ~1 equiv. of $PrNH_2$; ▼= $PrNH_3^+$ in; s: residual solvent.

Note that the changes observed from a) to d) are due to an interaction between the sole sulfate anion and the urea groups.

IV. ^{1}H NMR study of the complexing properties of **1a**

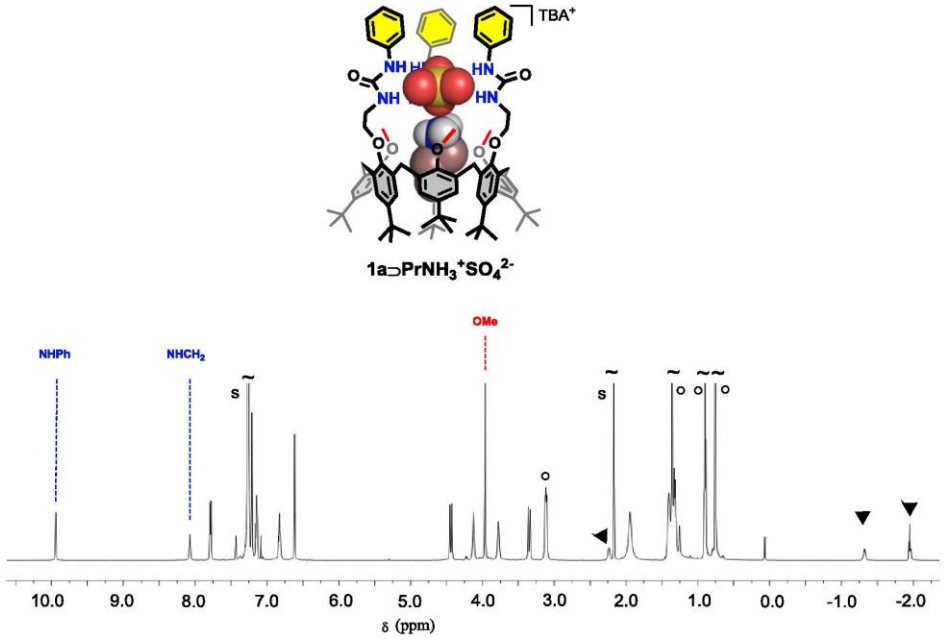

Figure S18. ^{1}H NMR spectrum (600MHz) of **1a** in $CDCl_3$ in the presence of ~1 equiv. of $PrNH_3^+TBA^+SO_4^{2-}$; o= TBA^+; ▼= $PrNH_3^+$ in; s: residual solvent.

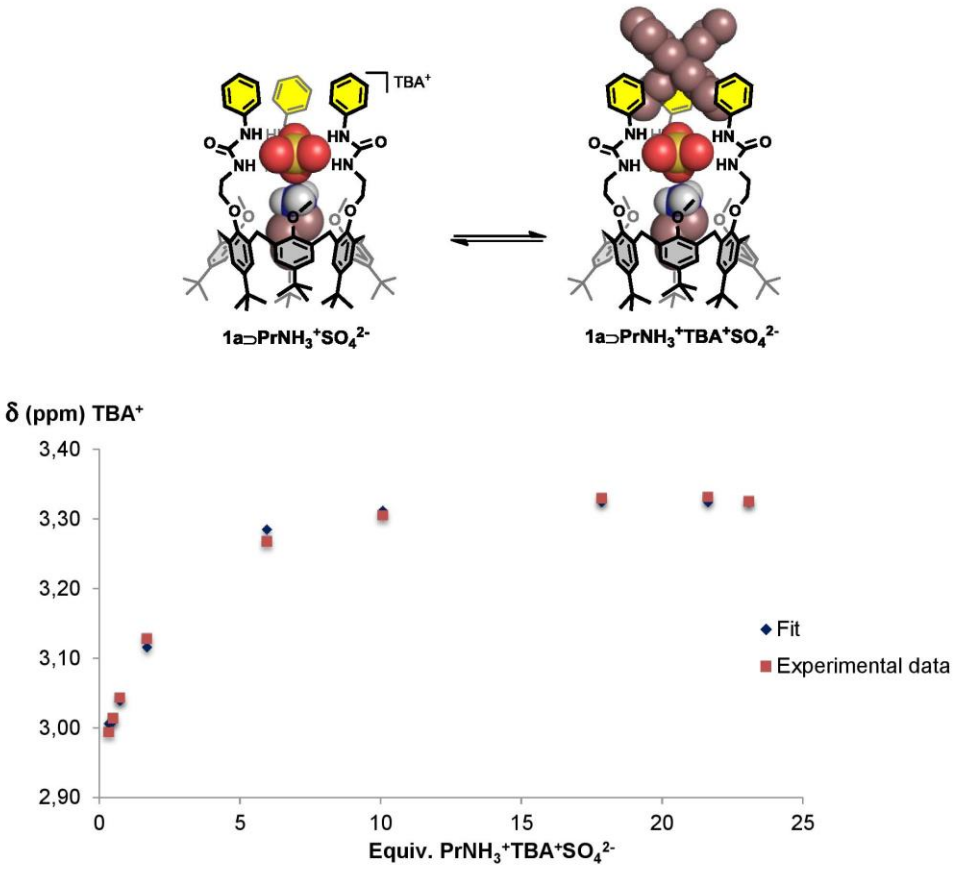

Figure S19. Variation of the chemical shift of the CH_2N^+ (TBA^+) upon the addition of $PrNH_3^+TBA^+SO_4^{2-}$ (0 to 23 equiv.) to **4a** in $CDCl_3$ (600 MHz); $[\mathbf{1a}]_0 = 3.32 \times 10^{-3}$ M. Parametric adjustment performed with a 1:1 binding model.

V. 1D and 2D NMR spectra of **3b**, **4a**, **4b**

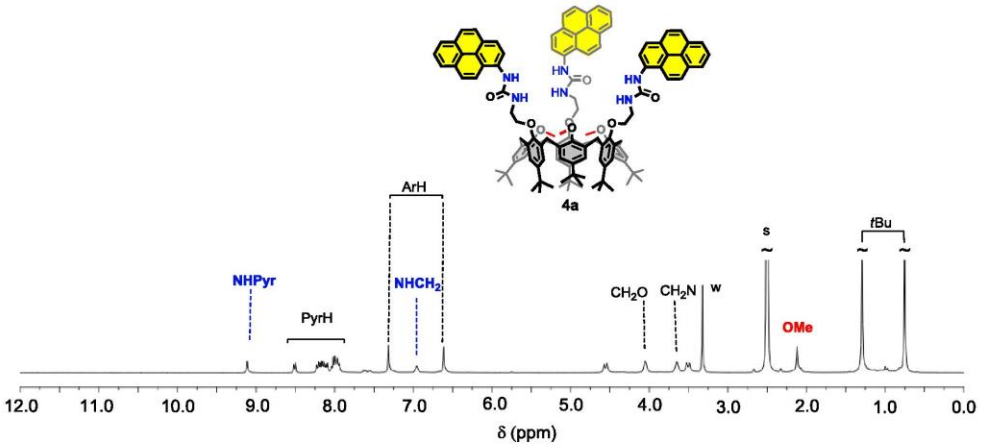

Figure S20. ^{1}H NMR spectrum (400 MHz, DMSO-d6) of compound **4a**. s: residual solvent; w: water.

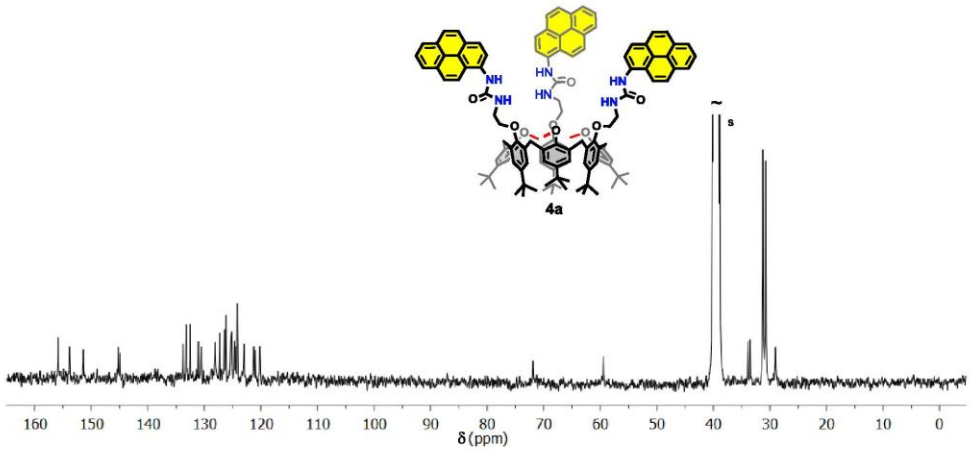

Figure S21. ^{13}C NMR spectrum (100 MHz, DMSO-d6) of compound **4a**. s: residual solvent.

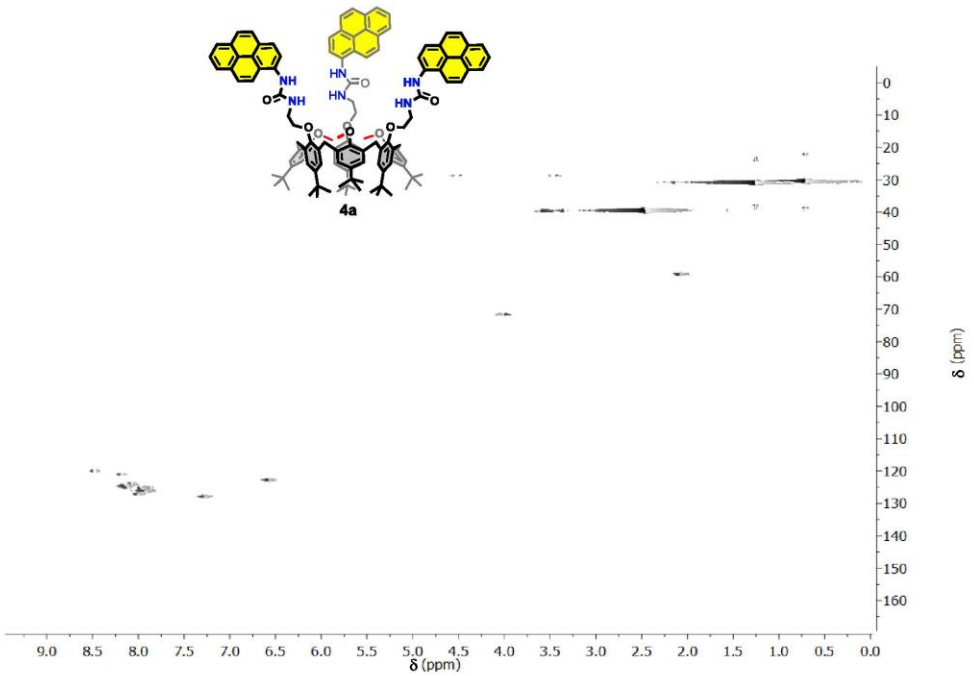

Figure S22. HSQC spectrum (DMSO-d6) of compound **4a**.

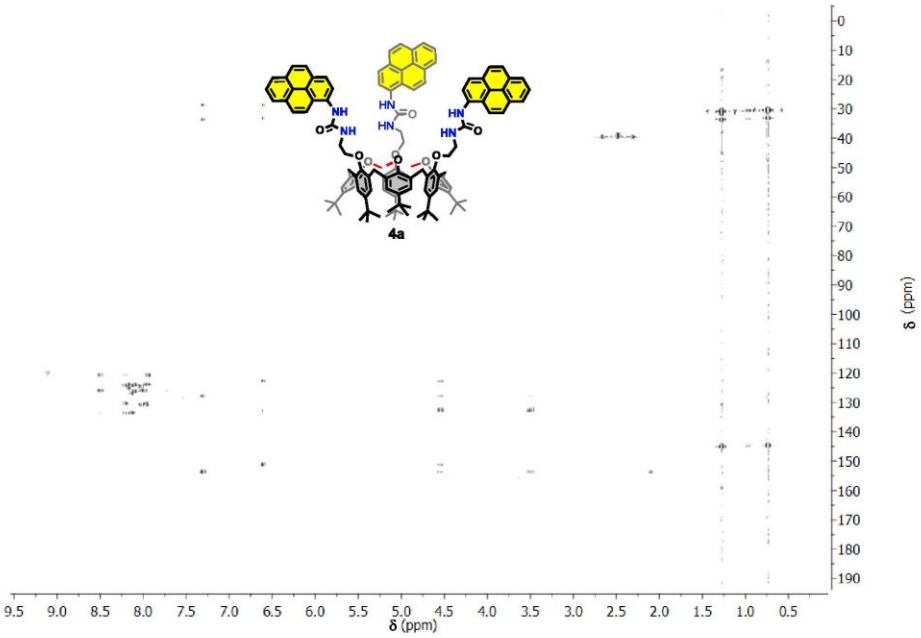

Figure S23. HMBC spectrum (DMSO-d6) of compound **4a**.

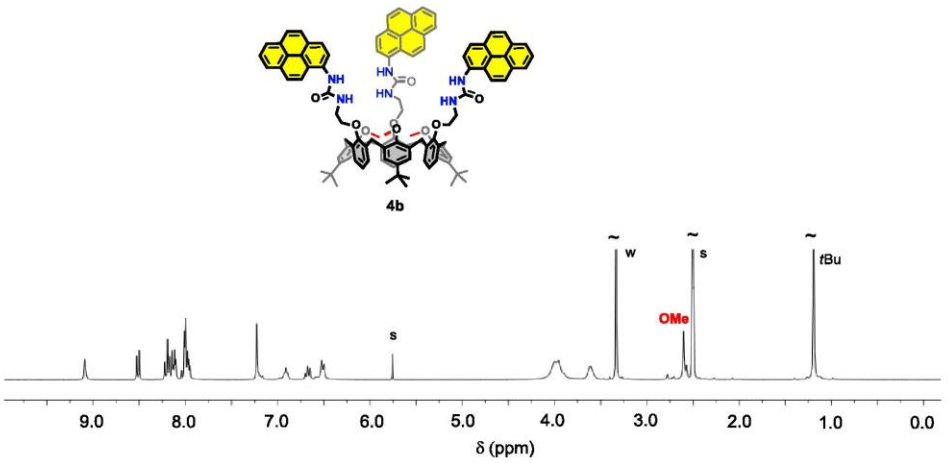

Figure S24. ^{1}H NMR spectrum (300 MHz, DMSO-d6) of compound **4b**. s: residual solvent; w: water.

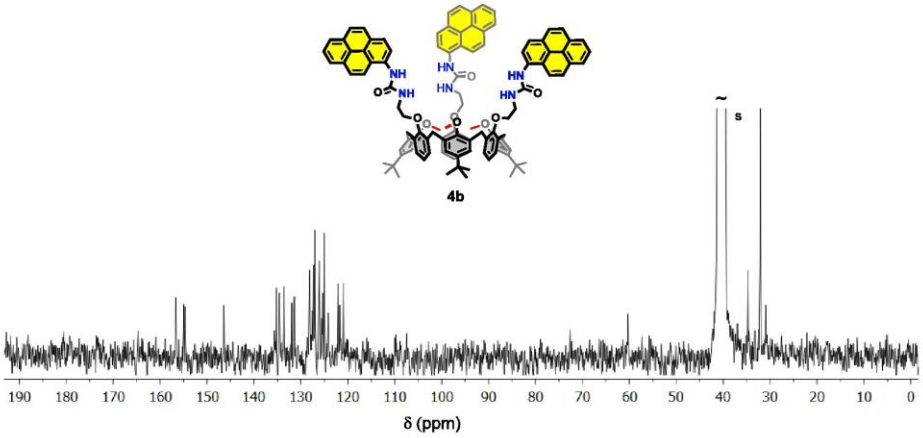

Figure S25. ^{13}C NMR spectrum (75 MHz, DMSO-d6) of compound **4b**. s: residual solvent.

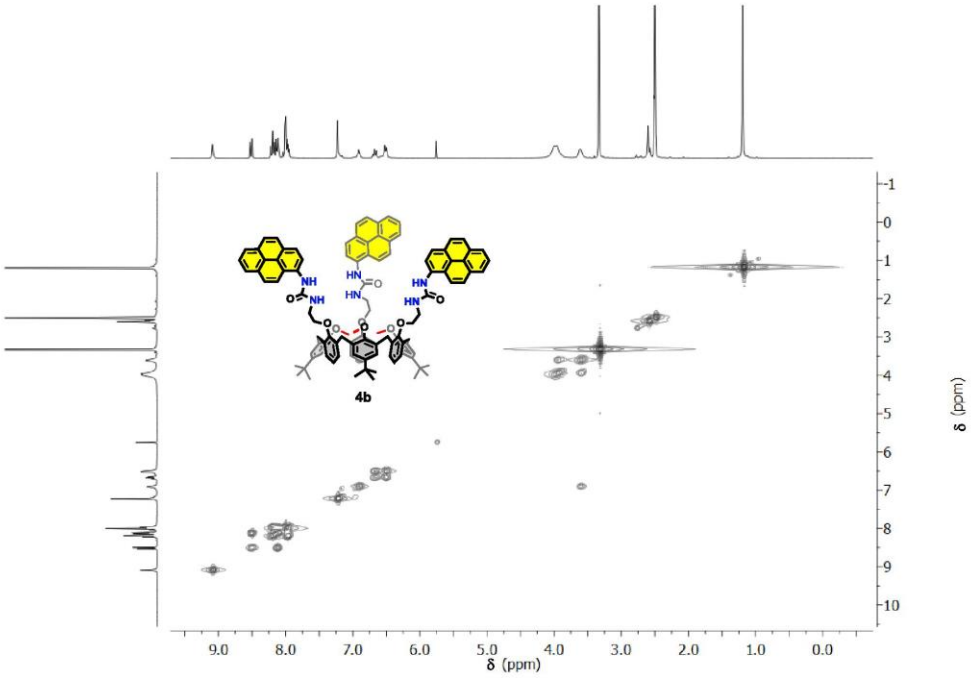

Figure S26. COSY spectrum (300 MHz, DMSO-d6) of compound **4b**.

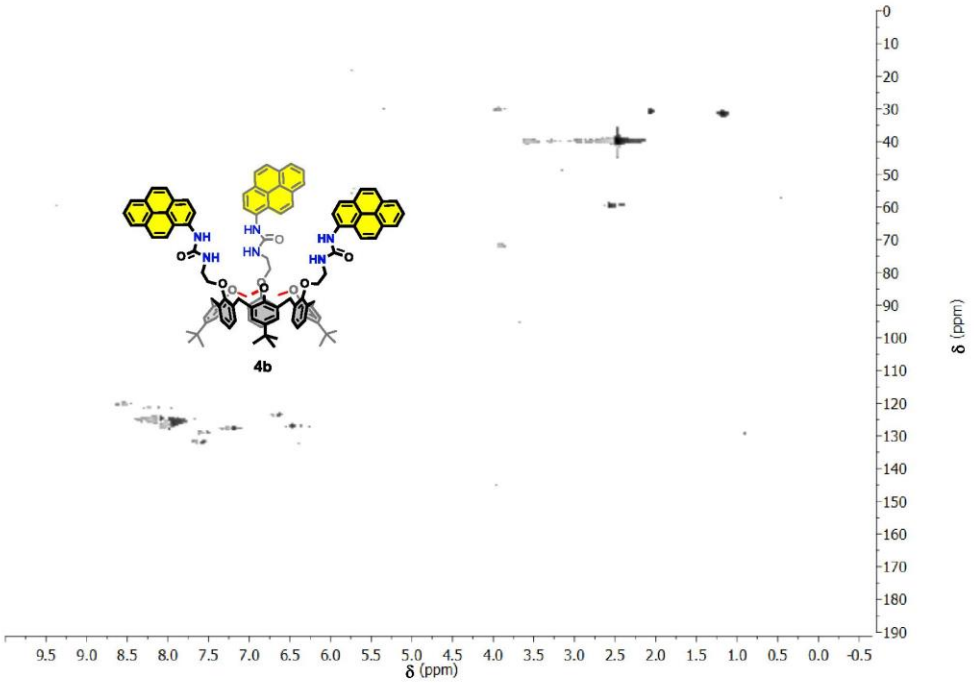

Figure S27. HSQC spectrum (DMSO-d6) of compound **4b**.

SI23

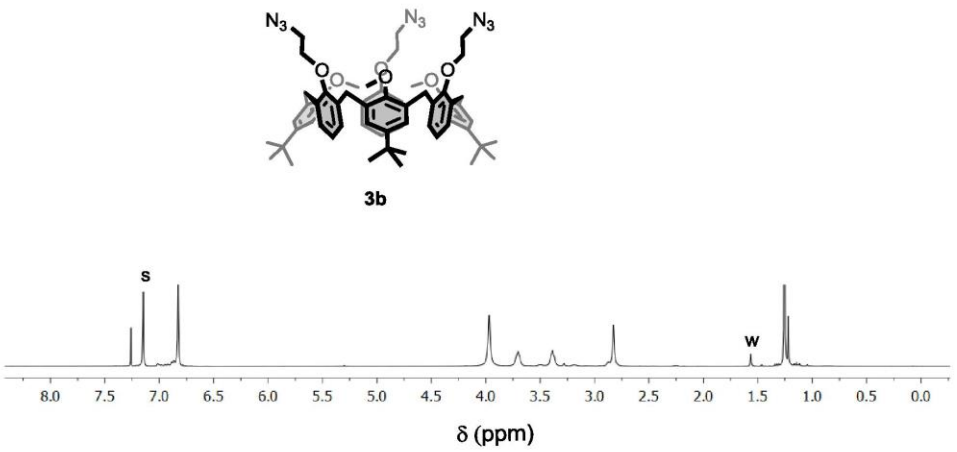

Figure S28. ^{1}H NMR spectrum (300 MHz, $CDCl_3$) of compound **3b**. s: residual solvent; w: water.

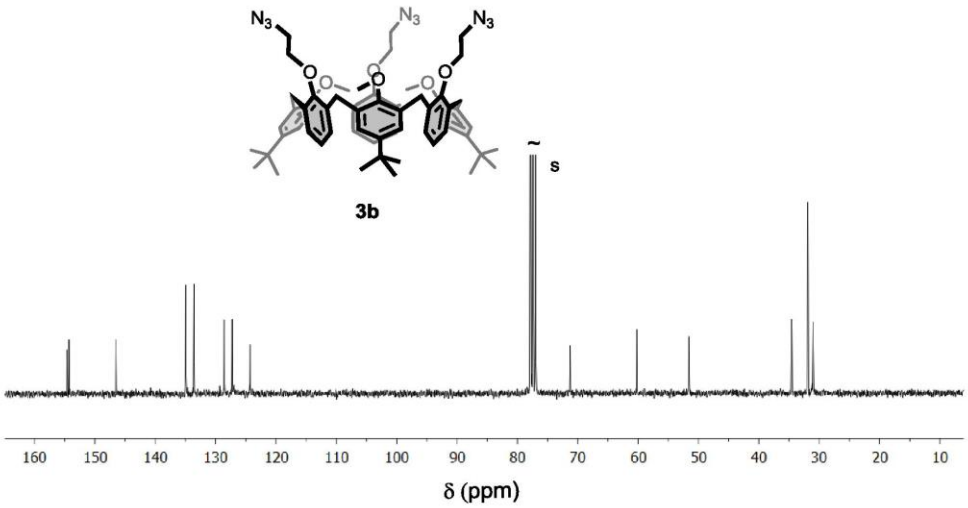

Figure S29. ^{13}C NMR spectrum (75 MHz, $CDCl_3$) of compound **3b**. s: residual solvent.

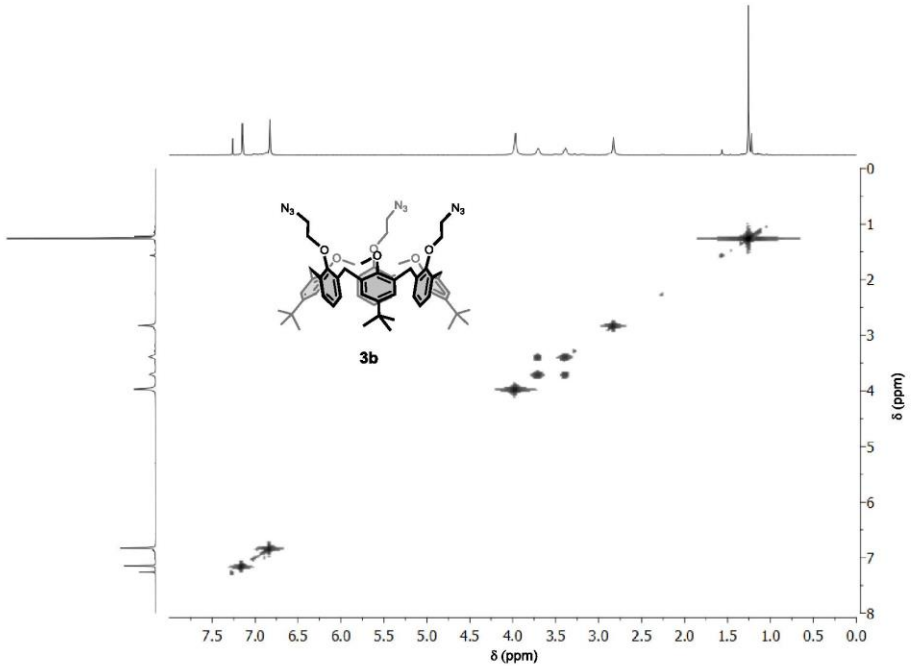

Figure S30. COSY spectrum (300 MHz, $CDCl_3$) of compound **3b**.

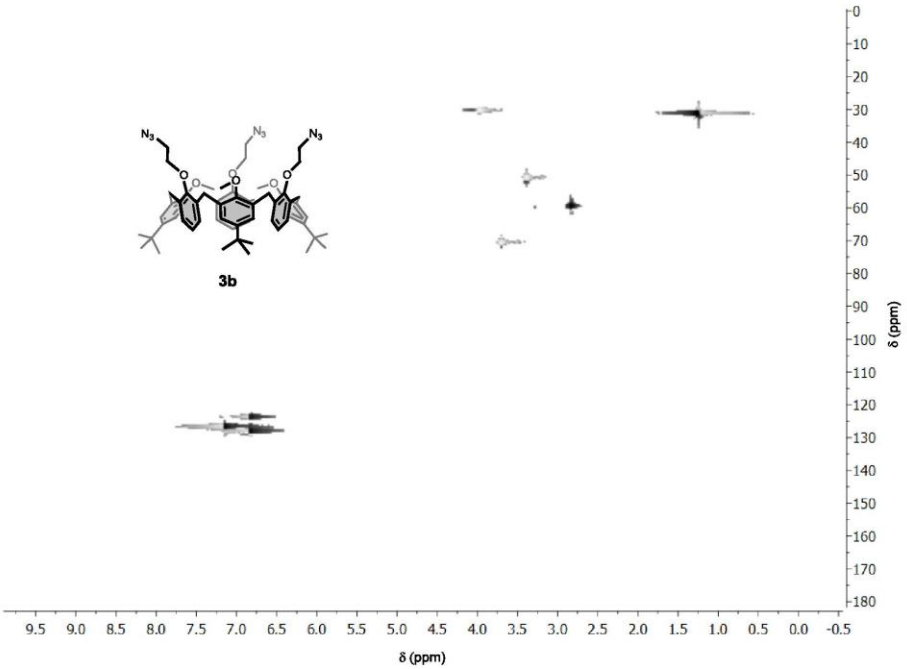

Figure S31. HSQC spectrum ($CDCl_3$) of compound **3b**.

SI25

2.2. COMPLEXATION OF PHOSPHOLIPIDS

2.2.1. CONTEXT OF THE RESEARCH

Considering the results obtained with anions and contact ion-pairs, we wanted to see whether receptor **14a** could be exploited for the sensing of zwitterionic phospholipids. Phospholipids are major components in cell membranes and are very important for the functioning of living systems.[3] They are composed of a hydrophobic tail and a hydrophilic head linked by a glycerol unit. The hydrophilic head is composed in the case of phosphatidylcholines (PCs) and phosphatidylethanolamines (PEs) of a phosphate group and a choline or ethanolamine moiety (Figure 2-3).

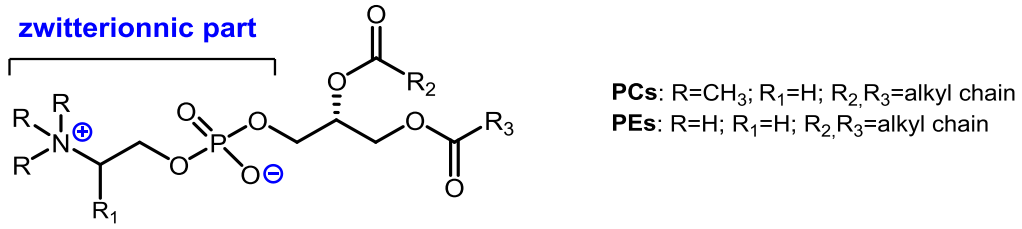

Figure 2-3. Structures of some phospholipids.

In biological systems PCs and PEs are the most abundant phospholipids and are the major components of lipid bilayers. Natural protein receptors recognize and bind PCs and PEs with a high selectivity via specific interactions with their zwitterionic head. Typically, the phosphate group of the phospholipid is coordinated to a metal center[4] or interacts with a positively charged Arg or Lys residue through ionic and H-bonding interactions,[5] while the ammonium group interacts with a polyaromatic binding pocket through cation-π interactions.[6] A possible biomimetic approach for the selective sensing of phospholipids could consist in the use of heteroditopic receptors that associate a polar recognition site to a polyaromatic cavity.[7,8] For example, Rebek and co-workers have developed a Zn salen-based cavitand that efficiently binds

[3] Textbook of biochemistry with clinical correlations, 4th ed.; Devlin, T; M., Ed.; Wiley-Liss: New York, 1997.
[4] Hough, E.; Hansen, L. K.; Birknes, B.; Jynge, K.; Hansen, S.; Hordvik, A.; Little, C; Dodson, E.; Derewenda, Z. *Nature* **1989**, *338*, 357-360.
[5] Clausen, J. D.; Bublitz, M.; Arnou, B.; Montigny, C.; Jaxel, C.; Moller, J. V.; Nissen, P.; Andersen, J. P.; Le Maire, M. *EMBO J.* **2013**, *32*, 3231-3243; Yoder, M. D.; Thomas, L. M.; Tremblay, J. M.; Oliver, R. L.; Yarbrough L. T.; Helmkamp, G. M. Jr. *J. Biol. Chem.* **2001**, *276*, 9246-9252.
[6] Drachmann, N. D.; Olesen, C.; Moller, J. V.; Guo, Z.; Nissen, P.; Bublitz, M. *Febs J.* **2014**, *281*, 4249-4262; Martin, S. F.; Follows, B. C.; Hergenrother, P. J.; Trotter, B. K. *Biochemistry* **2000**, *39*, 3410-3415.
[7] Zelder, F. H.; Salvio, R.; Rebek, J. Jr. *Chem. Commun.* **2006**, 1280–1282.
[8] Cuevas, F; Di Stefano, S.; Oriol Magrans, J.; Prados, P.; Mandolini, L.; De Mendoza, J. *Chem. Eur. J.* **2000**, *6*, 3228-3234.

1,2-dioleoyl-*sn*-glycero-3-phosphocholine (DOPC) reminiscent of the binding motif of the enzyme phospholipase (Figure 2-4).

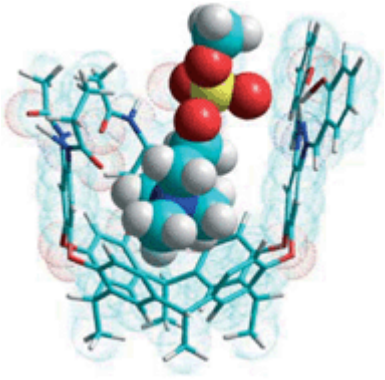

Figure 2-4. A bifunctional Zn-salen cavitand that binds DOPC (figure taken from reference 7).

As presented in the Introduction (section 1.4.2), host **13b** (Figure 2-5) presents interesting properties for phospholipids recognition. It is indeed able to selectively bind PCs over PEs in chloroform with the fatty acid chains of the bound lipids protruding from one of the three macrocycles formed by the thio-urea arms.[9]

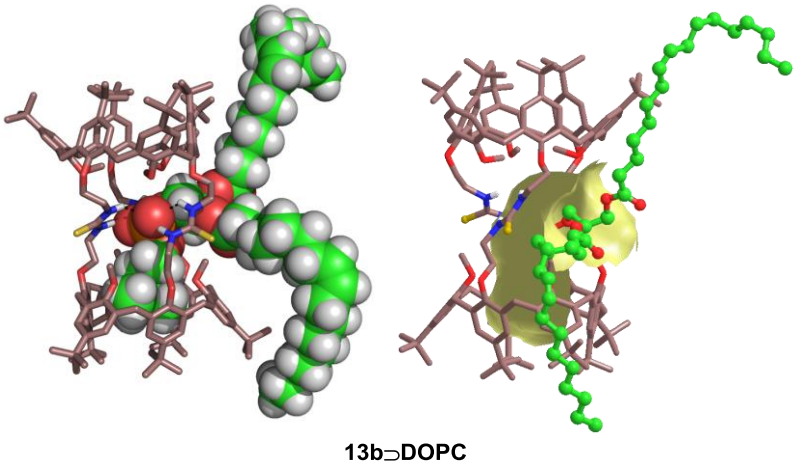

Figure 2-5. Energy minimized structures of **13b⊃DOPC**.[9]

In this thesis, we wished to see if it was possible to give rise to a lipid sensor in terms of detection by fluorescence spectroscopy. We studied the interaction of different phospholipids with host **14a**, using ^{1}H and ^{31}P NMR and fluorescence spectroscopy. Our results have been

[9] Moerkerke, S.; Wouters, J.; Jabin, I. *J. Org. Chem.* **2015**, *80*, 8720-8726.

published in the journal Organic and Biomolecular Chemistry "*A Selective Calix[6]arene-based Fluorescent Chemosensor for Phosphatidylcholine Type Lipids"*(**2016**, asap).

2.2.2. SUMMARY OF PUBLISHED RESULTS:

In the manuscript "*A Selective Calix[6]arene-based Fluorescent Chemosensor for Phosphatidylcholine Type Lipids*" we report on the binding studies of host calix[6]tris-pyrenlyurea **14a** with different phospholipids.

Studies undertaken in $CDCl_3$ by ^1H NMR showed that host **14a** displays a remarkable selectivity for lipids bearing a phosphatidylcholine head (PCs) over those bearing a phosphoethanolamine head (PEs) (Figure 2-3). Indeed, upon addition of a few equivalents of different PCs, the formation of a new C_{3v} species is observed. The metoxy groups are expelled from the cavity (δ_{OMe} > 3.87 ppm) and the receptor NH are shifted downfield, signature of an H-bonding interaction with the phosphate group. Guest exchange is slow on the chemical shift timescale and EXSY experiments enabled us to show that the cationic group of the lipids exhibit a signal at high-field which confirms their inclusion in the cavity. With 1,2-dioleoyl-*sn*-glycero-3-phosphocholine (DOPC) for example, inversion of the signal of the free CH_3N^+ of the lipid (3.27 ppm) gave rise to a signal at 1.54 ppm. The **14a**-PC complexes are thus stabilized by interactions with the zwitterionic head of the guest. No change in the NMR spectra are observed when adding PEs attesting that they are not recognized by **14a**.

Titrations of **14a** with PCs and PEs in $CHCl_3$ were also monitored by emission spectroscopy. Upon addition of the PCs, an increase of the monomer band and a decrease of the excimer band are observed, signature of a complexation at the level of the urea moieties. Depending on the lipid, values ranging from log K ~ 4 to log K ~ 5 were determined for a 1:1 binding model. Not surprisingly, upon addition of PEs no spectral changes were observed.

Titrations by ^{31}P NMR were also undertaken to corroborate these results. Upon addition of host **14a** to a solution of 1-palmitoyl-2-oleyl-*sn*-glycero-3-phosphocholine (POPC) in $CDCl_3$, the signal of bound POPC was clearly detected as the phosphorus signals are in slow exchange on the ^{31}P chemical shift time scale. An affinity log K ~ 4 could also be determined.

Finally, extraction experiments were conducted in order to evaluate the possibility of using host **14a** as a sensor for lipids in an aqueous environment. Remarkably, results showed that **14a**

dissolved in in $CHCl_3$ could be used to quantify, by emission spectroscopy, the amount of DOPC extracted from the aqueous phase.

Organic & Biomolecular Chemistry

PAPER

View Article Online
View Journal

Cite this: DOI: 10.1039/c6ob01880g

A selective calix[6]arene-based fluorescent chemosensor for phosphatidylcholine type lipids†

Emilio Brunetti,[a,b] Steven Moerkerke,[a] Johan Wouters,[c] Kristin Bartik*[b] and Ivan Jabin*[a]

Received 26th August 2016,
Accepted 4th October 2016
DOI: 10.1039/c6ob01880g
www.rsc.org/obc

The development of chemosensors that can selectively detect phosphatidylcholines (PCs) in biological samples is of medical relevance considering the importance of these phospholipids in cell growth and survival. Their selective sensing over phosphatidylethanolamines (PEs) is however a challenging task. We report here on the chemosensing capacities of calix[6]tris-pyrenylurea **1**, which is able to selectively interact with phosphatidylcholine-type lipids in organic media. Host **1** also binds them in a biphasic chloroform/water solution, opening the way to the design of selective chemosensors for these lipids in biological media. The results obtained by NMR, fluorescence spectroscopy and modelling studies show that the selectivity is the result of the high degree of complementarity between the lipids' zwitterionic phosphatidylcholine headgroup and the receptor's H-bonding donor site and hydrophobic pocket. The mode of recognition is reminiscent of natural systems, such as human phosphatidylcholine transfer proteins (PC-TPs), validating the biomimetic approach adopted in our work.

Introduction

Phospholipids are a major class of zwitterionic lipids, present predominantly in cellular membranes.[1] These amphiphilic lipids possess a hydrophobic domain and a hydrophilic head linked together, either by a glycerol unit (glycerophospholipids) or by a sphingosine (sphingolipids) (Fig. 1). Their polar head is composed of a phosphodiester group and typically a nitrogenous moiety such as choline, ethanolamine or serine. Phosphatidylcholines (PCs) and phosphatidylethanolamines (PEs) (Fig. 1) are generally the most abundant membrane phospholipids and the ratio of PCs to PEs in the plasma membrane is, for example, reported as crucial for maintaining cellular growth and survival.[2] The quantification of these lipids in biological samples is thus of medical importance and is classically achieved by gravimetric[3] or colorimetric techniques.[4] Recently, a NMR method for phospholipids quantification has been reported.[5] The selective sensing of PCs over PEs remains however a challenge.

Natural protein receptors recognize and bind PCs and PEs with a high selectivity, thanks to specific interactions with the zwitterionic head. Typically, the phosphate group of the phospholipid is coordinated to a metal center[6] or interacts with a positively charged Arg or Lys residue through ionic and H-bonding interactions,[7] while the ammonium group interacts with a polyaromatic binding pocket through cation-π interactions.[8] A possible biomimetic approach for the selective sensing of phospholipids could consist in the use of heteroditopic receptors that associate a polar recognition site to a polyaromatic cavity.[9]

We have developed calix[6]arene-based systems bearing thiourea or urea moieties, that behave as heteroditopic receptors toward charged or neutral species, such as zwitterions, which could be interesting in the context of phospholipid sensing.[10] Very recently, we have reported that a calix[6]tube possessing two divergent hydrophobic cavities connected *via* three thiourea linkages (Fig. 2, right) is able to selectively bind PCs over PEs in nonpolar solvents.[11] The binding of the phospholipids proceeds through multiple H-bonding interactions between their anionic moiety and the tris-thiourea groups of the host, as well as through π–cationic and CH–π interactions between their cationic $(CH_3)N^+$ group and one of the two polyaromatic calixarene cavities. It is to be noted that the fatty acid chains of the bound lipids do not protrude from the second calixarene cavity but from one of the three macrocycles formed by the (thio)urea arms. Also of interest is our recently developed fluorescent calix[6]tris-urea receptor **1** (Fig. 2, left) that can be used for the sensing of anions and organic ion-pairs, and

[a]*Laboratoire de Chimie Organique, Université libre de Bruxelles (ULB), Avenue F.D. Roosevelt 50, CP160/06, B-1050 Brussels, Belgium. E-mail: ijabin@ulb.ac.be*
[b]*Engineering of Molecular NanoSystems, Ecole polytechnique de Bruxelles, Université libre de Bruxelles (ULB), Avenue F.D. Roosevelt 50, CP165/64, B-1050 Brussels, Belgium. E-mail: kbartik@ulb.ac.be*
[c]*Département de Chimie, Université de Namur (UNamur), Rue de Bruxelles 61, B5-5000 Namur, Belgium*

†Electronic supplementary information (ESI) available: ^{1}H NMR spectra, ^{31}P NMR spectra and fluorescence studies of the complexation properties of **1**. See DOI: 10.1039/c6ob01880g

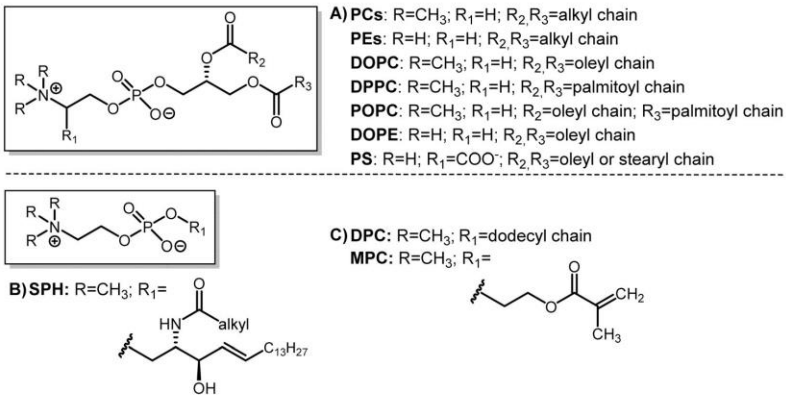

Fig. 1 Structure of (A) various glycerophospholipids, (B) a sphingolipid and (C) non-natural phosphocholines.

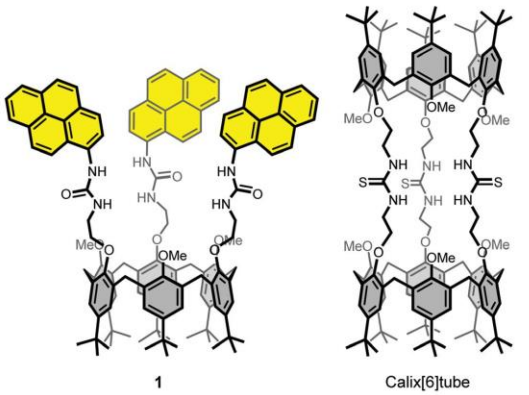

Fig. 2 Structure of calix[6]tris-pyrenylurea **1** (left) and calix[6]tube (right).

for which a cavity-based selectivity, in terms of size and shape of the guests, was observed with ammonium salts.[12] Considering these previous results, we wished to see if receptor **1** could be exploited for the chemosensing of zwitterionic phospholipids and in particular if it could distinguish between PCs and PEs.

Herein, we report on the study by NMR and fluorescence spectroscopy of the interaction of chemosensor **1** with different phospholipids.

Results and discussion

The ability of calix[6]tris-pyrenylurea **1** to bind different phospholipids was investigated in $CDCl_3$ *via* ^{1}H NMR titration experiments. As shown previously, the ^{1}H NMR spectrum of **1** in $CDCl_3$ displays a broad NMR signature due to intramolecular self-association of the urea moieties (Fig. 3a). The quantitative formation of a new species that displays well-defined NMR signals was however observed upon the addition of a few equivalents of either 1,2-dioleoyl-*sn-glycero*-3-phosphocholine (DOPC) (see Fig. 3b for the ^{1}H NMR spectrum of DOPC), 1,2-dipalmitoyl-*sn-glycero*-3-phosphocholine (DPPC), 1-palmitoyl-2-oleoyl-*sn-glycero*-3-phosphocholine (POPC), *N*-acyl-4-sphingenyl-1-O-phosphocholine (SPH), dodecylphosphocholine (DPC) or 2-methacryloxyethyl phosphocholine (MPC) (see Fig. 1 for the structures of the lipids).[13] As a representative example, the ^{1}H spectrum of host **1** in presence of *ca.* 3 equiv. of DOPC is shown in Fig. 3c.

The following common features were observed for all the newly formed host–guest species:

(i) The calixarene adopts a flattened C_{3v} symmetrical cone conformation ($\Delta\delta_{ArH} > 0.62$ ppm and $\Delta\delta_{tBu} > 0.61$ ppm) with the OMe groups expelled from the cavity ($\delta_{OMe} > 3.87$ ppm);

(ii) The presence of strong H-bonding interactions between the urea groups NH_{pyr} and the bound lipid, as evidenced by the significant down-field shift of the NH_{pyr} signal;

(iii) Intra-cavity complexation of the cationic head of the lipid, as clearly evidenced through HSQC and 1D EXSY experiments.[13] For instance, a signal at 1.54 ppm corresponding to the bound Me_3N^+ group is observed upon inversion of the Me_3N^+ signal of free DOPC (selective pulse excitation at 3.27 ppm) (Fig. 4).

These NMR data suggest that host **1** behaves as a heteroditopic receptor capable of binding phosphatidylcholine type lipids through the establishment of specific interactions with their zwitterionic head. In all cases, two sets of signals were apparent over the course of the titration, indicating slow host–guest exchanges on the ^{1}H NMR chemical shift timescale. In the case of **1** ⊃ **DOPC**, all the ^{1}H signals belonging to the free and bound DOPC were assigned by 2D-NMR experiments (COSY, HSQC and ROESY),[13] and the complex-induced shifts (CISs) could be calculated (values given in the inset of Fig. 3). The signals corresponding to the $\alpha(CH_3)_3N^+$ and $\beta(CH_3)_3N^+CH_2$

View Article Online
Organic & Biomolecular Chemistry Paper

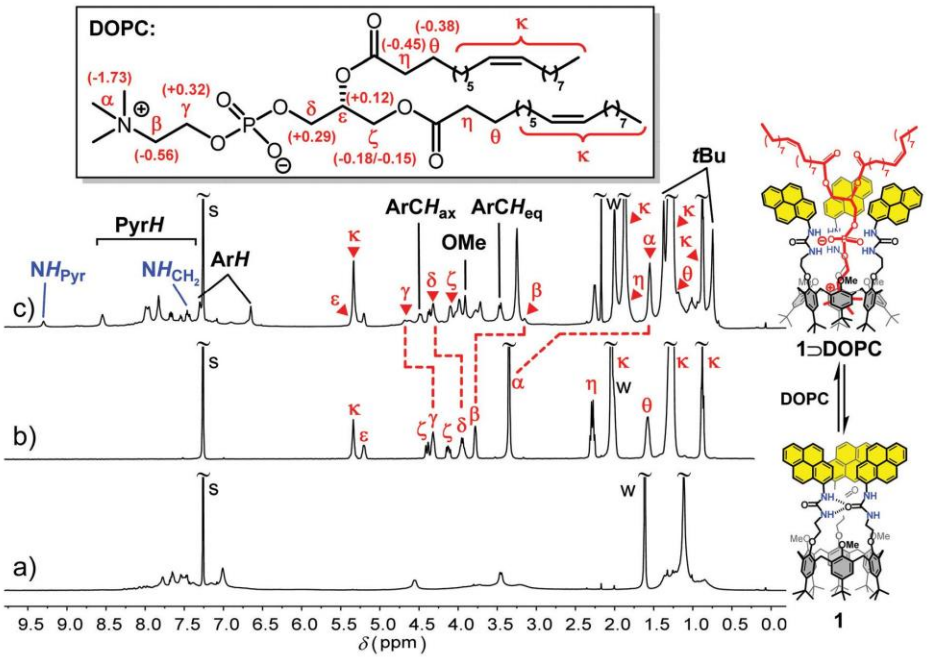

Fig. 3 ^{1}H NMR spectra (600 MHz, 298 K, $CDCl_3$) of: (a) calix[6]tris-pyrenylurea **1**; (b) DOPC; (c) host **1** in presence of *ca.* 3 equiv. of DOPC. Inset: structure of DOPC with the CIS measured at 298 K. CIS defined as $\Delta\delta = \delta$(complexed DOPC) – δ(free DOPC). w: water; s: solvent.

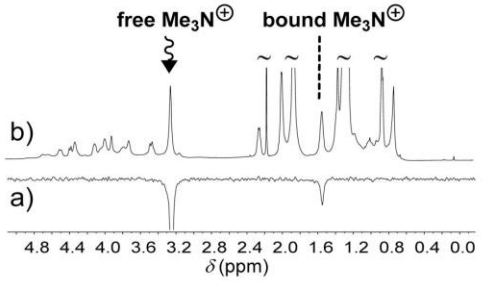

Fig. 4 NMR spectra (600 MHz, 298 K, $CDCl_3$) of host **1** in in the presence of *ca.* 3 equiv. of DOPC: (a) 1D EXSY spectrum (mixing time = 25 ms) after selective excitation of the Me_3N^+ signal at 3.27 ppm; (b) ^{1}H NMR spectrum.

protons display negative CISs, which is coherent with the inclusion of the cationic part of DOPC in the heart of the calixarene cavity. In contrast, the γ, δ and ε protons exhibit positive CIS, in accordance with H-bonding interactions between the H-bond acceptor groups of DOPC (phosphate and esters) and the urea groups of **1**. The negative CIS of the ζ, η and θ protons suggest that they are positioned at the level of the pyrene moieties. All the other protons of DOPC experience negligible CIS, showing that the long oleyl chains protrude from the calixarene-based receptor.

Very interestingly, the ^{1}H spectrum of **1** remained unaffected upon the addition of either 1,2-dioleoyl-*sn-glycero*-3-phosphoethanolamine (DOPE) or 1,2-diacyl-*sn-glycero*-3-phosphoryl-L-serine (PS).[13] This inertness toward PE type lipids implies that the presence of a quaternary ammonium group at the level of the polar head is mandatory for the recognition process, which would be the result of (i) the establishment of CH–π and π–cationic interactions between the Me_3N^+ group and the aromatic walls of the calixarene and (ii) the stronger self-association of PE type lipids in nonpolar solvents.[14]

The binding affinities toward the different PC type lipids in $CDCl_3$ were estimated *via* integration of the Me_3N^+ signal of the free lipid and of the PyrH signals of the host–guest complex. In all cases, the association constants ($\log K_{NMR}$) were too high to be determined accurately by NMR (Table 1).[15] Upon addition of *ca.* 4% of CD_3OD to a solution of host **1** in the presence of 3 equiv. of DOPC in $CDCl_3$, *ca.* 5% of the host–guest complex **1** ⊃ **DOPC** was still detected.[13] In DMSO-d_6, a more competitive solvent, DOPC and DPC were however not recognized.[13]

The binding of POPC by receptor **1** was also investigated in $CDCl_3$ by ^{31}P NMR spectroscopy. The ^{31}P NMR spectrum of POPC exhibits a signal at −0.88 ppm (Fig. 5a). Upon progressive addition of host **1**, the signal corresponding to the bound POPC was clearly detected at −2.18 ppm (Fig. 5b–d). The significant CIS (−1.30 ppm) confirms the formation of H-bonding

Table 1 Affinity of host **1** towards different lipids at 298 K

Complex	Solvent	$\log K_{NMR}$ [a]	$\log K_{FLUO}$ [a]
1 ⊃ **DOPC**	$CDCl_3$	>4	4.8 ± 0.1
1 ⊃ **DPPC**	$CDCl_3$	>4	4.9 ± 0.2
1 ⊃ **POPC**	$CDCl_3$	>4	4.6 ± 0.1
1 ⊃ **SPH**	$CDCl_3$	>4	4.5 ± 0.6
1 ⊃ **DPC**	$CDCl_3$	>4	4.5 ± 0.1
1 ⊃ **MPC**	$CDCl_3$	>4	4.1 ± 0.3
1 ⊃ **DOPE**	$CDCl_3$	nd[b]	nd[b]
1 ⊃ **PS**	$CDCl_3$	nd[b]	nd[b]
1 ⊃ **DOPC**	DMSO-d_6	nd[b]	—
1 ⊃ **DPC**	DMSO-d_6	nd[b]	—

[a] K = [Complex]/([Host] × [Guest]). K_{NMR} and K_{FLUO} refer to binding constants determined by ^{1}H NMR spectroscopy and fluorescence spectroscopy respectively. [b] No binding detected.

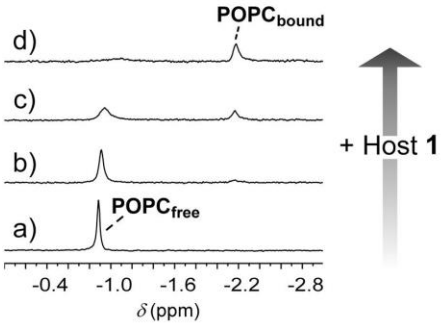

Fig. 5 ^{31}P NMR spectra (400 MHz, 298 K, $CDCl_3$) of: (a) POPC (6.22 mM); (b) after addition of *ca.* 0.1 equiv. of host **1**; (c) after addition of *ca.* 0.3 equiv. of host **1**; (d) after addition of *ca.* 0.6 equiv. of host **1**; triphenylphosphine used as internal reference.

interactions between the phosphate group and the urea moieties. As expected, a high affinity was estimated through integration of the two signals ($\log K_{NMR} > 4$) and no change in the ^{31}P NMR spectrum was observed upon addition of **1** to a DOPE solution.[13]

To gain insight into the recognition process between host **1** and PC type lipids, the geometry of complex **1** ⊃ **DOPC** was optimized by molecular mechanics using the CHARM force field and the Smart Minimizer algorithm (RMS gradient 0.1).[16] The resulting energy minimized structure is in good agreement with the NMR results (Fig. 6). The calixarene displays a flattened conformation with the OMe groups directed toward the outside of the cavity and interactions between host **1** and the zwitterionic head of the lipid are observed. Indeed, the Me_3N^+ group is buried inside the poly-aromatic cavity enabling it to establish π–cationic and CH–π interactions while the convergent urea groups stabilize the edifice through multiple H-bonding interactions. The two oleyl chains of DOPC are located between the three pyrenyl units where they are stabilized through CH–π interactions. From a biomimetic point of view, **1** ⊃ **DOPC** shows strong similarities with the complexes

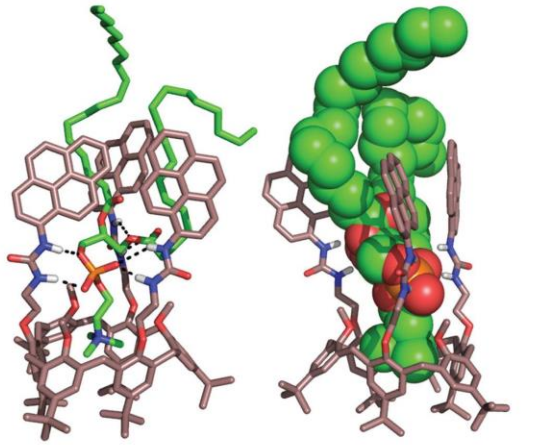

Fig. 6 Energy minimized structure of **1** ⊃ **DOPC**; Hydrogen bonds are indicated by dashed lines. Selected distances (Å): N(host)–O(DOPC): 2.97, 3.00, 3.01, 3.37, 3.38, 3.51; N^+(host)–(π-centroids): 4.24, 4.29, 4.32. With the exception of the NH of the host, all the hydrogen atoms of **1** and of DOPC are omitted for clarity. Two perpendicular orientations of the structure of **1** ⊃ **DOPC** are presented.

formed between PCs and their natural receptors such as the human phosphatidylcholine transfer protein (PC-TP).[17]

The complexation of the different lipids by host **1** was also investigated by fluorescence spectroscopy. No significant changes were observed in the fluorescence spectra of host **1** during the titrations with the PE type lipids (DOPE and PS).[13] With the PC type lipids, an increase of the monomer emission (at 398 and 420 nm) and a decrease of the excimer emission (at 486 nm) were clearly observed over the course of the titrations (see Fig. 7 for DOPC).[13] These spectral changes are the signature of the separation of the self-associated pyrenyl urea groups upon lipid complexation. Association constants ($\log K_{FLUO}$) of the same order of magnitude were determined

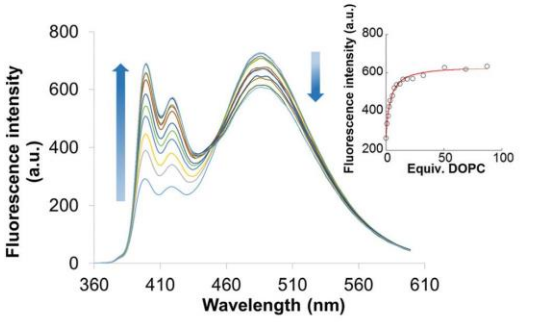

Fig. 7 Emission spectra of **1** upon addition of DOPC (0 to 85 equiv.) in chloroform. $[\mathbf{1}]_0$ = 5.0 μM and λ_{ex} = 345 nm. Inset: variation of fluorescence intensity at 420 nm upon the addition of DOPC. Solid line: fitting to a 1 : 1 binding model.

View Article Online

Organic & Biomolecular Chemistry Paper

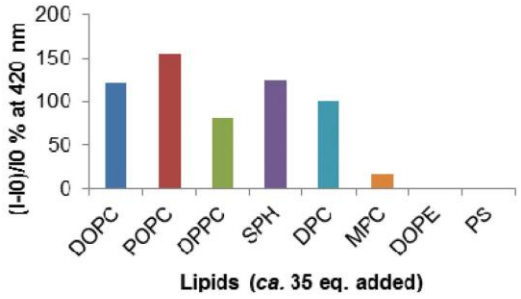

Fig. 8 Fluorescence intensity changes ($(I - I_0)/I_0 \times 100\%$) of **1** (*ca.* 5 μM) in $CHCl_3$ upon the addition of various lipids (λ_{ex} = 345 nm). I_0 is the fluorescence emission intensity at 420 nm for free host **1**, and I is the fluorescence emission intensity after addition of *ca.* 35 equiv. of the lipid.

for all the PC type lipids (Table 1). Such a lack of selectivity shows that the recognition of these lipids is mostly due to specific interactions with their phosphorylcholine polar head. The normalized increase in fluorescence intensity of host **1** at 420 nm in the presence of *ca.* 35 equiv. of the different lipids is shown in Fig. 8. For MPC, a much weaker variation is observed in comparison with all the other PC type lipids. The different behaviour of this lipid may likely originate from the absence of long alkyl chains that could play a role in separating the pyrene moieties. All these results show that host **1** constitutes a selective chemosensor for lipids bearing a phosphorylcholine head.

Preliminary experiments were also undertaken to evaluate the possibility of using host **1** for the chemosensing by fluorescence spectroscopy of PC type lipids in an aqueous environment. Liquid–liquid extraction experiments were undertaken where 20 μL of aqueous solutions of different known DOPC concentrations were added to 2 mL of a micromolar solution of **1** in chloroform.[13] The fluorescence spectra of the chloroform solution recorded after stirring showed the characteristic signature of **1** ⊃ **DOPC**, with the intensity depending on the initial concentration of DOPC in the aqueous solution. The formation of **1** ⊃ **DOPC**, following liquid–liquid extraction experiments, was confirmed by NMR highlighting that the receptor can still efficiently complex DOPC even in a biphasic chloroform/water solution. The affinity of **1** in chloroform for DOPC is not significantly affected by the presence of a large amount of water, and remains larger than 10^4 ($\log K \sim 4.5$). These results are encouraging and suggest that the detection and quantification of PC type lipids in biological media using host **1** could be envisaged.

Conclusion

Calix[6]tris-pyrenylurea **1** behaves as an efficient heteroditopic chemosensor able to strongly interact with lipids in organic media ($\log K > 4$). A high selectivity for phosphatidylcholine type lipids over the closely related phosphatidylethanolamines is observed, highlighting the importance of specific interactions between the receptor and the zwitterionic head of the lipid. This mode of recognition is reminiscent of natural systems such as human phosphatidylcholine transfer proteins (PC-TPs), validating the biomimetic approach adopted in our work, that consists in designing receptors that associate a H-bonding donor site to a hydrophobic pocket in order to achieve a high degree of complementarity with the two ionic groups of zwitterions. Interestingly, liquid–liquid extraction experiments showed that host **1** can still bind phosphatidylcholine type lipids in a biphasic chloroform/water solution, opening the way to the design of selective chemosensors for lipids in biological media.

Experimental section

General experimental methods

DOPC (1,2-dioleoyl-*sn-glycero*-3-phosphocholine), POPC (1-palmitoyl-2-oleoyl-*sn-glycero*-3-phosphocholine), SPH (*N*-acyl-4-sphingenyl-1-O-phosphocholine), MPC (2-methacryloxyethyl phosphocholine), DOPE (1,2-dioleoyl-*sn-glycero*-3-phosphoethanolamine) and PS (1,2-diacyl-*sn-glycero*-3-phosphoryl-L-serine) (all ≥99%) were purchased from Sigma-Aldrich (Missouri, USA). DPC (dodecylphosphocholine) (≥99%) was purchased from Avanti Polar Lipids (Alabama, USA). DPPC (1,2-dipalmitoyl-*sn-glycero*-3-phosphocholine) (≥99%) from Bachem (Bubendorf, Switzeland). Chloroform (both deuterated and non-deuterated) was filtered, prior to use, over a short column of basic alumina to remove traces of HCl/DCl. ^{1}H spectra were recorded at 400 MHz (9.4 T) or 600 MHz (14.1 T). 2D NMR spectra (COSY, HSQC, and ROESY) were recorded to complete signal assignments. 1D EXSY experiments were recorded with an iburp2 pulse sequence. NMR parameters (acquisition time, recycling times, and signal accumulation) were chosen to ensure that quantitative data could be obtained from signal integration in the 1D ^{1}H spectra. Traces of residual solvent were used as an internal chemical shift reference. Chemical shifts were quoted on the δ scale. The NMR and fluorescence spectra were recorded at 298 K unless otherwise stated.

^{1}H NMR titration experiments

All experiments were undertaken following a similar protocol: a known volume (*ca.* 600 μL) of solution of known concentration of host (*ca.* 2 mM) was placed in a NMR tube and the ^{1}H NMR spectrum was recorded. Aliquots (*ca.* 5 μL corresponding to 0.25 equiv. of host) of a stock solution of guest were successively added and a ^{1}H NMR spectrum was recorded after each addition. Aliquots were added until no change was observed for the host signals.

^{31}P NMR titration experiment

A known volume (*ca.* 600 μL) of solution of known concentration of POPC (*ca.* 6 mM) was placed in a NMR tube and the

^{31}P NMR spectrum was recorded. An external capillary tube containing a known concentration of triphenylphosphine was used to provide the reference peak for quantification. Aliquots (*ca.* 5 μL corresponding to 0.25 equiv. of guest) of a stock solution of host **1** were successively added and a ^{31}P NMR spectrum was recorded after each addition.

Fluorescence titration experiments

All experiments were undertaken following a similar protocol: a known volume (*ca.* 2 mL) of solution of known concentration of host (*ca.* 5.0×10^{-6} M) was placed in a cell and the absorbance and emission spectra were recorded. Aliquots (*ca.* 5 μL corresponding to 0.5 equiv. of host) of a stock solution of guest were successively added and a spectrum was recorded after each addition. Aliquots were added until no change was observed in the spectrum. The values obtained for emission were corrected for dilution.

^{1}H NMR characterization of the host–guest complex 1 ⊃ DOPC

^{1}H NMR ($CDCl_3$), 298 K, 600 MHz: δ (ppm) 0.70–0.81 (m, 27H, *t*Bu), 0.87 (m, 6H, DOPC$^{\kappa,in}$), 1.17 (m, 4H, DOPC$^{\theta,in}$), 1.21–1.45 (m, 44H, DOPC$^{\kappa,in}$), 1.35–1.44 (m, 27H, *t*Bu), 1.54 (m, 9H, DOPC$^{\alpha,in}$), 1.80 (m, 4H, DOPC^{n,in}), 2.00 (m, 4H, DOPC$^{\kappa,in}$), 3.15 (m, 2H, DOPC$^{\beta,in}$), 3.46 (m, 6H, $ArCH_2^{eq}$), 3.77 (br s, 6H, CH_2N), 3.90 (m, 9H, OMe), 3.96 (m, 1H, DOPC $^{\zeta,in}$), 4.06 (br s, 6H, CH_2O), 4.21 (m, 1H, DOPC$^{\zeta,in}$), 4.30 (m, 2H, DOPC$^{\delta,in}$), 4.48 (m, 6H, $ArCH_2^{ax}$), 4.66 (m, 2H, DOPC$^{\gamma,in}$), 5.34 (m, 1H, DOPC$^{\varepsilon,in}$), 5.34 (m, 4H, DOPC$^{\kappa,in}$), 6.64 (s, 6H, ArH^{Urea}), 7.30 (s, 6H, ArH^{OMe}), 7.41–8.14 (m, 21H, PyrH), 7.44 (s, 3H, *NH*CH_2). 8.57 (m, 6H, PyrH), 9.31 (s, 3H, *NH*Pyr). The majority of the signals of DOPC^{in} were assigned thanks to the COSY, HSQC and 2D ROESY spectra.

Acknowledgements

E. B acknowledges the Fonds pour la formation à la Recherche dans l'Industrie et dans l'Agriculture (FRIA-FRS, Belgium) for his PhD grant and S. M. the ULB for his PhD grant. The modelling part of this work used resources of the "Plateforme Technologique de Calcul Intensif (PTCI)" (http://www.ptci.unamur.be) located at the University of Namur, Belgium, which is supported by the F.R.S.-FNRS under the convention No. 2.4520.11. The PTCI is member of the "Consortium des Équipements de Calcul Intensif (CÉCI)" (http://www.ceci-hpc.be).

References

1 W. Dowhan, M. Bogdanov and E. Mileykovsaya, in *Biochemistry of Lipids, Lipoproteins and Membranes*, ed. D. E. Vance and J. E. Vance, Elsevier, Amsterdam, 2008, pp. 1–37.
2 (*a*) S. Fu, L. Yang, P. Li, O. Hofmann, L. Dicker, W. Hide, X. Lin, S. M. Watkins, A. R. Ivanov and G. S. Hotamisligil, *Nature*, 2011, **473**, 528–531; (*b*) D. E. Vance, *Biochim. Biophys. Acta*, 2014, **1838**, 1477–1487; (*c*) D. E. Vance, Z. Li and R. L. Jacobs, *J. Biol. Chem.*, 2007, **282**, 33237–33241.
3 J. R. Akins, K. Waldrep and J. T. Bernert Jr., *Clin. Chim. Acta*, 1989, **184**, 219–226.
4 R. K. Raheja, C. Kaur, A. Singh and I. S. Bhatia, *J. Lipid Res.*, 1973, **14**, 695–697.
5 R. Hein, C. B. Uzundal and A. Hennig, *Org. Biomol. Chem.*, 2016, **14**, 2182–2185.
6 (*a*) E. Hough, L. K. Hansen, B. Birknes, K. Jynge, S. Hansen, A. Hordvik, C. Little, E. Dodson and Z. Derewenda, *Nature*, 1989, **338**, 357–360; (*b*) J. R. Byberg, F. S. Jorgensen, S. Hansen and E. Hough, *Proteins*, 1992, **12**, 331–338.
7 (*a*) J. D. Clausen, M. Bublitz, B. Arnou, C. Montigny, C. Jaxel, J. V. Moller, P. Nissen, J. P. Andersen and M. Le Maire, *EMBO J.*, 2013, **32**, 3231–3243; (*b*) X. Qiu, A. Mistry, M. J. Ammirati, B. A. Chrunyk, R. W. Clark, Y. Cong, J. S. Culp, D. E. Danley, T. B. Freeman, K. F. Geoghegan, M. C. Griffor, S. J. Hawrylik, C. M. Hayward, P. Hensley, L. R. Hoth, G. A. Karam, M. E. Lira, D. B. Lloyd, K. M. McGrath, K. J. Stutzman-Engwall, A. K. Subashi, T. A. Subashi, J. F. Thompson, I.-K. Wang, H. Zhao and A. P. Seddon, *Nat. Struct. Mol. Biol.*, 2007, **14**, 106–113; (*c*) M. D. Yoder, L. M. Thomas, J. M. Tremblay, R. L. Oliver, L. T. Yarbrough and G. M. Helmkamp Jr., *J. Biol. Chem.*, 2001, **276**, 9246–9252; (*d*) R. Glockshuber, J. Stadmüller and A. Plückthun, *Biochemistry*, 1991, **30**, 3049–3054.
8 (*a*) N. D. Drachmann, C. Olesen, J. V. Moller, Z. Guo, P. Nissen and M. Bublitz, *FEBS J.*, 2014, **281**, 4249–4262; (*b*) S. F. Martin, B. C. Follows, P. J. Hergenrother and B. K. Trotter, *Biochemistry*, 2000, **39**, 3410–3415.
9 (*a*) F. H. Zelder, R. Salvio and J. Rebek Jr., *Chem. Commun.*, 2006, 1280–1282; (*b*) F. Cuevas, S. Di Stefano, J. Oriol Magrans, P. Prados, L. Mandolini and J. de Mendoza, *Chem. – Eur. J.*, 2000, **6**, 3228–3234; (*c*) J. Oriol Magrans, A. R. Ortiz, M. A. Molins, P. H. P. Lebouille, J. Sánchez-Quesada, P. Prados, M. Pons, F. Gago and J. de Mendoza, *Angew. Chem.*, 1996, **108**, 1816–1819, (*Angew. Chem., Int. Ed. Engl.*, 1996, **35**, 1712–1715).
10 (*a*) D. Cornut, S. Moerkerke, J. Wouters, G. Bruylants and I. Jabin, *Chem. – Asian J.*, 2015, **10**, 440–446; (*b*) M. Ménand and I. Jabin, *Org. Lett.*, 2009, **11**, 673–676; (*c*) D. Cornut, J. Marrot, J. Wouters and I. Jabin, *Org. Biomol. Chem.*, 2011, **9**, 6373–6384; (*d*) S. Moerkerke, S. Le Gac, F. Topić, K. Rissanen and I. Jabin, *Eur. J. Org. Chem.*, 2013, 5315–5322; (*e*) S. Moerkerke, M. Ménand and I. Jabin, *Chem. – Eur. J.*, 2010, **16**, 11712–11719; (*f*) M. Hamon, M. Ménand, S. Le Gac, M. Luhmer, V. Dalla and I. Jabin, *J. Org. Chem.*, 2008, **73**, 7067–7071; (*g*) M. Ménand and I. Jabin, *Chem. – Eur. J.*, 2010, **16**, 2159–2169; (*h*) M. Rebarz, L. Marcélis, M. Menand, D. Cornut, C. Moucheron, I. Jabin and A. Kirsch-De Mesmaeker, *Inorg. Chem.*, 2014, **53**, 2635–2644.
11 S. Moerkerke, J. Wouters and I. Jabin, *J. Org. Chem.*, 2015, **80**, 8720–8726.
12 E. Brunetti, J.-F. Picron, K. Flidrova, G. Bruylants, K. Bartik and I. Jabin, *J. Org. Chem.*, 2014, **79**, 6179–6188.

13 See the ESI.†

14 A. Sen, P. W. Yang, H. H. Mantsch and S.-W. Hui, *Chem. Phys. Lipids*, 1988, **47**, 109–116.

15 It is noteworthy that the signal corresponding to the $(CH_3)_3N^+$ protons of the free lipid shift downfield as the lipid concentration increases. This suggests that the free lipid is in exchange between different environments. This is not simply the signature of a lipid monomer-dimer equilibrium as this signal shifts upfield with lipid concentration in the absence of any host.

16 Structure of host **1**, was built on the basis of previous structures of related calix[6]tube molecules (ref. 10*a* and *c*). Starting conformation for the **1** ⊃ **DOPC** complex has been manually built using Discovery Studio 2016 (BIOVIA, *Dassault Systèmes*). Geometry was further optimized with the same suite of programs using the CHARM force field and the Smart Minimizer algorithm (RMS gradient 0.1).

17 S. L. Roderick, W. W. Chan, D. S. Agate, L. R. Olsen, M. W. Vetting, K. R. Rajashankar and D. E. Cohen, *Nat. Struct. Biol.*, 2002, **9**, 507–511.

Electronic Supplementary Material (ESI) for Organic & Biomolecular Chemistry.

Supporting information

A Selective Calix[6]arene-based Fluorescent Chemosensor for Phosphatidylcholine Type Lipids

Emilio Brunetti, Steven Moerkerke, Johan Wouters, Kristin Bartik* and Ivan Jabin*

List of contents

I. Complexation studies between host **1** and DOPC

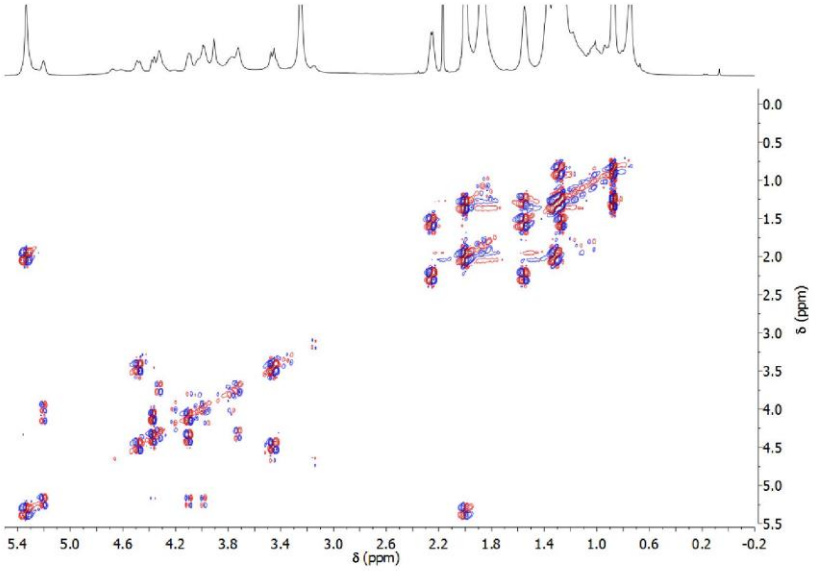

Figure S1. COSY spectrum (600 MHz, 298 K, $CDCl_3$) of compound **1** in the presence of *ca.* 3 equiv. of DOPC.

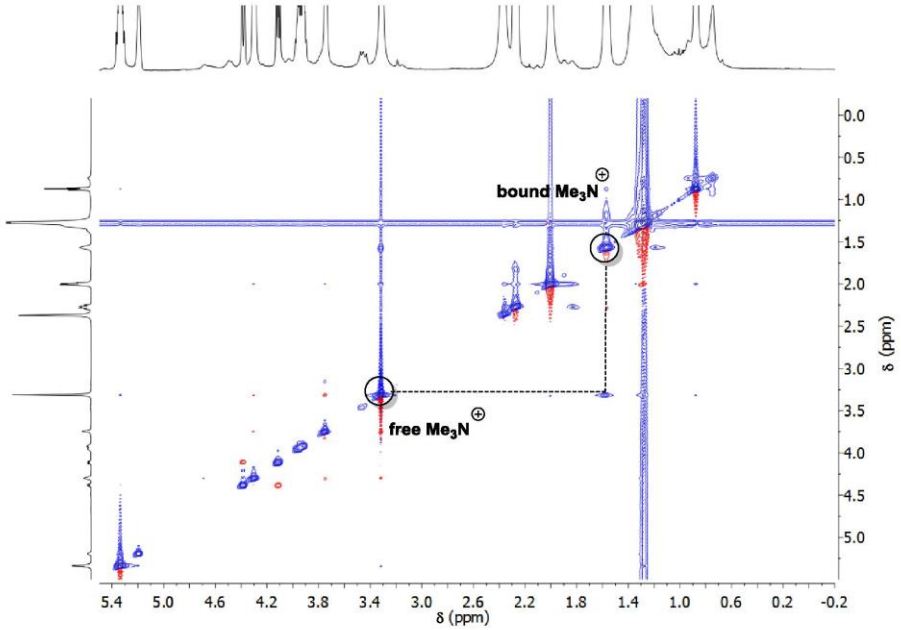

Figure S2. 2D ROESY spectrum (600 MHz, 298 K, $CDCl_3$, mixing time = 300 ms) of compound **1** in the presence of *ca.* 3 equiv. of DOPC.

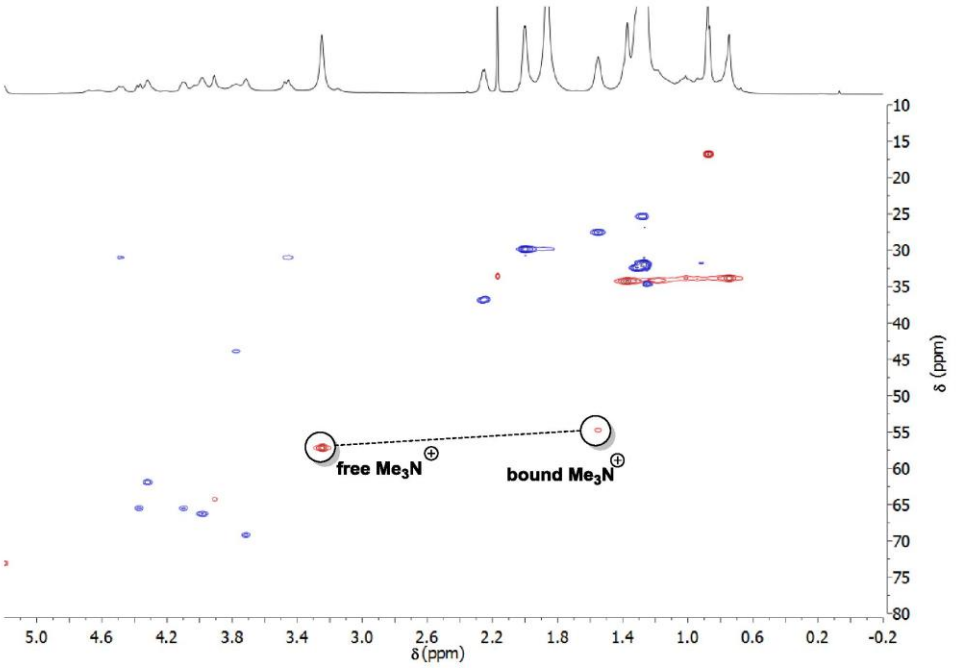

Figure S3. HSQC spectrum (600 MHz, 298 K, $CDCl_3$) of compound **1** in the presence of *ca.* 3 equiv. of DOPC.

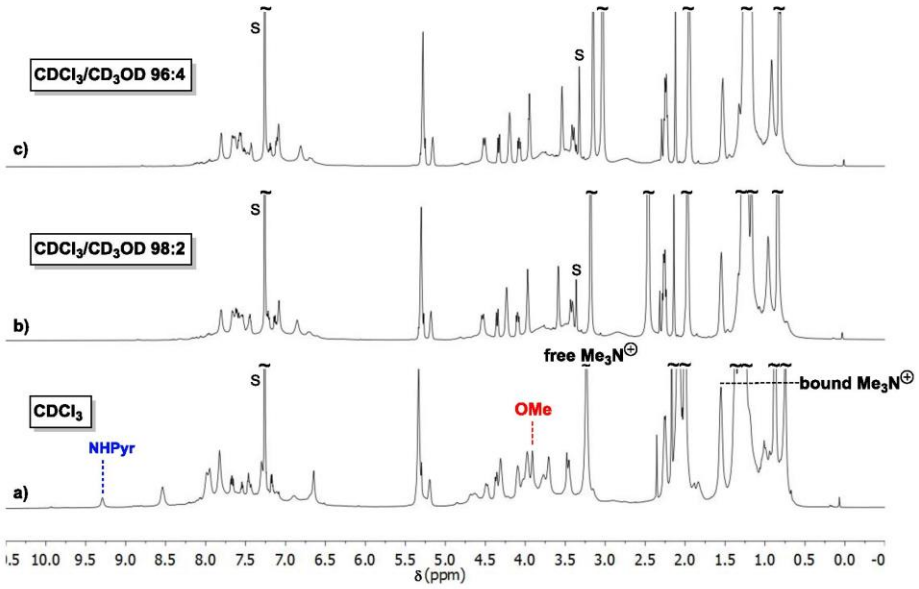

Figure S4. ^{1}H NMR spectra (600MHz, 298 K) of **1** in presence of *ca.* 3 equiv. of DOPC in: a) $CDCl_3$; b) in a mixture $CDCl_3/CD_3OD$ *ca.* 98:2; c) in a mixture $CDCl_3/CD_3OD$ *ca.* 96:4; s: solvent.

3

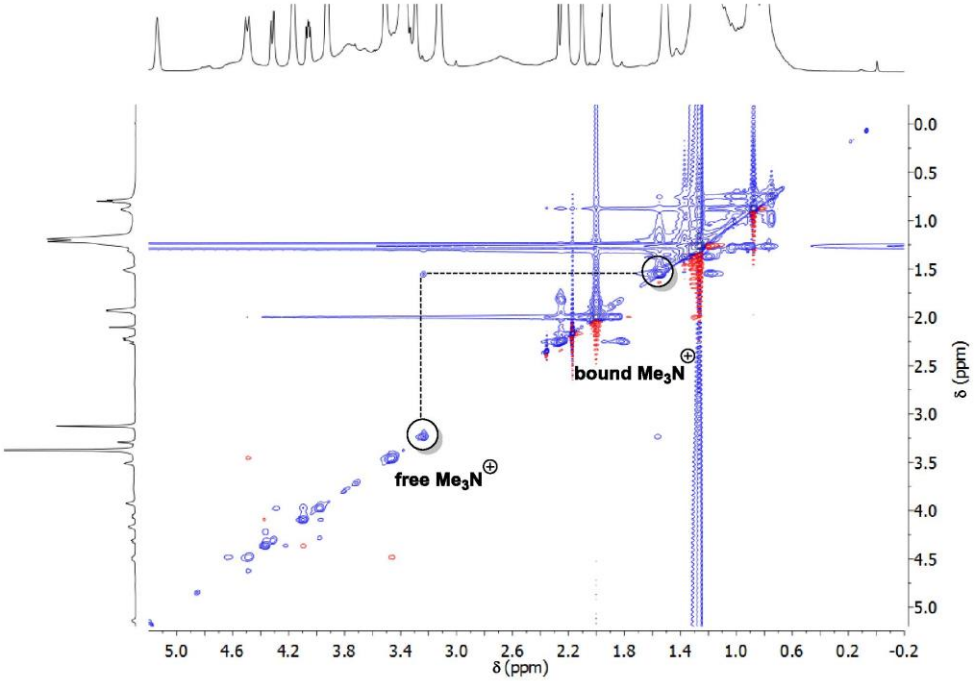

Figure S5. 2D ROESY spectrum (600 MHz, 298 K, $CDCl_3/CD_3OD$ *ca.* 96:4, mixing time = 300 ms) of compound **1** in the presence of *ca.* 3 equiv. of DOPC.

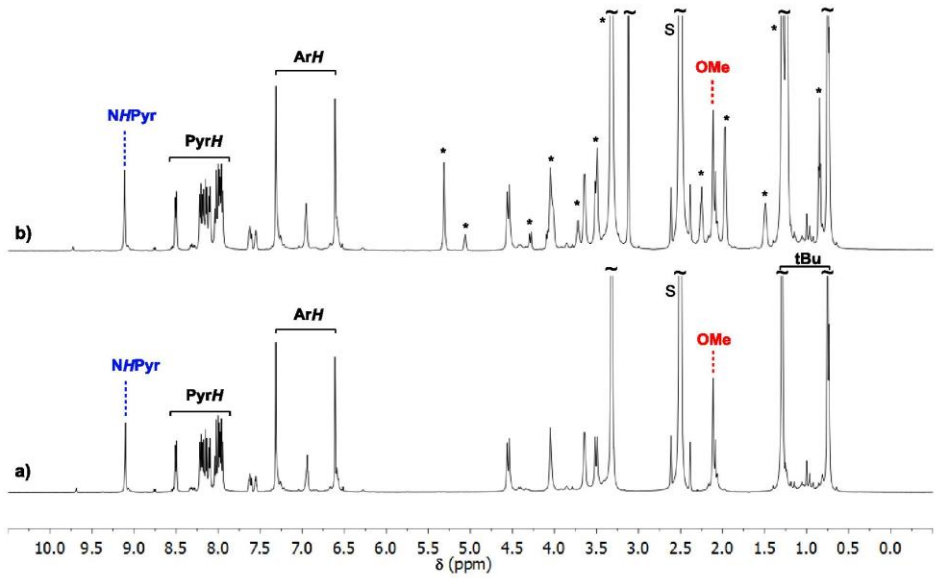

Figure S6. ^{1}H NMR spectra (600MHz, 298 K, DMSO-d_6) of: a) **1**; b) **1** in presence of *ca.* 1 equiv. of DOPC; s: solvent; *: DOPC signals.

II. Complexation studies between host **1** and POPC

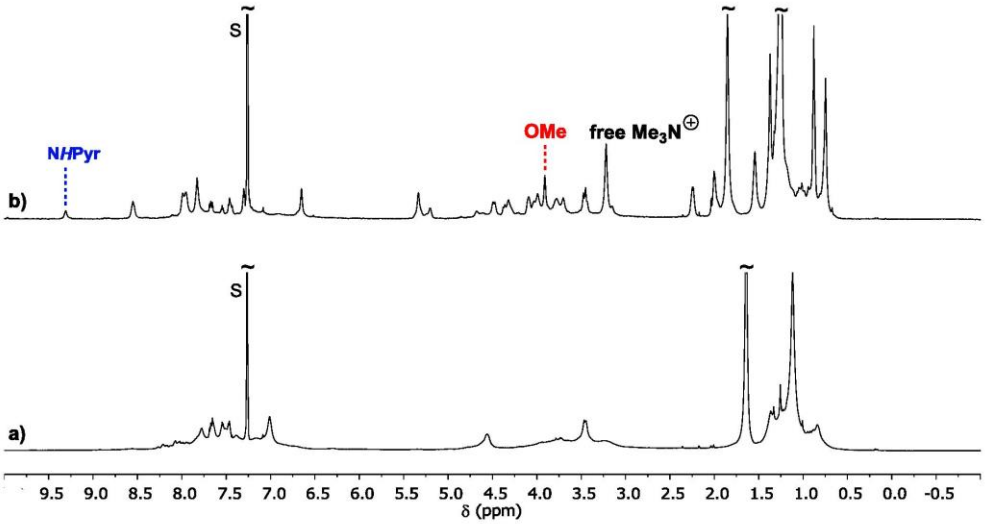

Figure S7. ^{1}H NMR spectra (600MHz, 298 K, $CDCl_3$) of: a) **1**; b) **1** in the presence of *ca.* 2.5 equiv. of POPC; s: solvent.

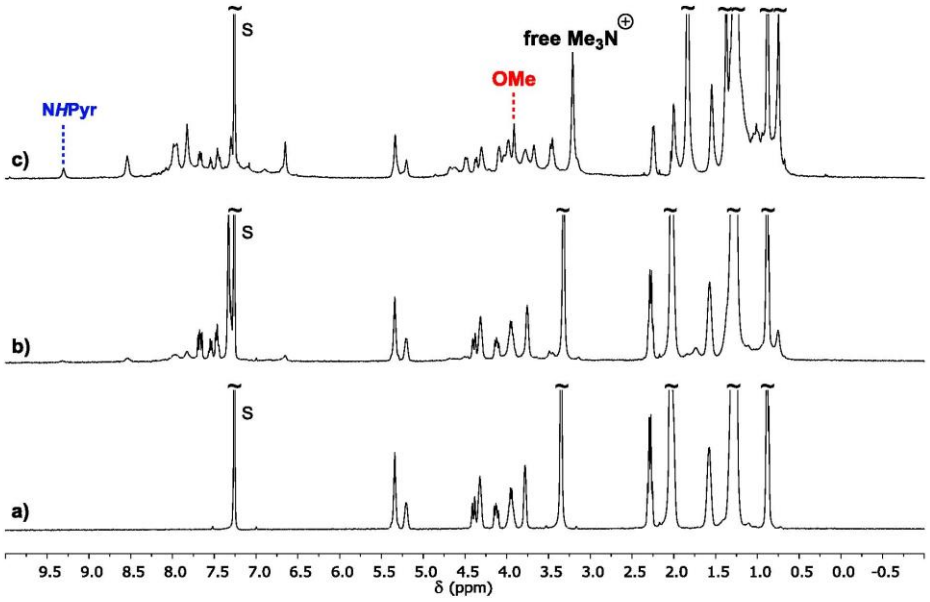

Figure S8. ^{1}H NMR spectra (600MHz, 298 K, $CDCl_3$) of: a) POPC; b) POPC in the presence of *ca.* 0.13 equiv. of **1**; c) POPC in the presence of *ca.* 0.62 equiv. of **1**; s: solvent.

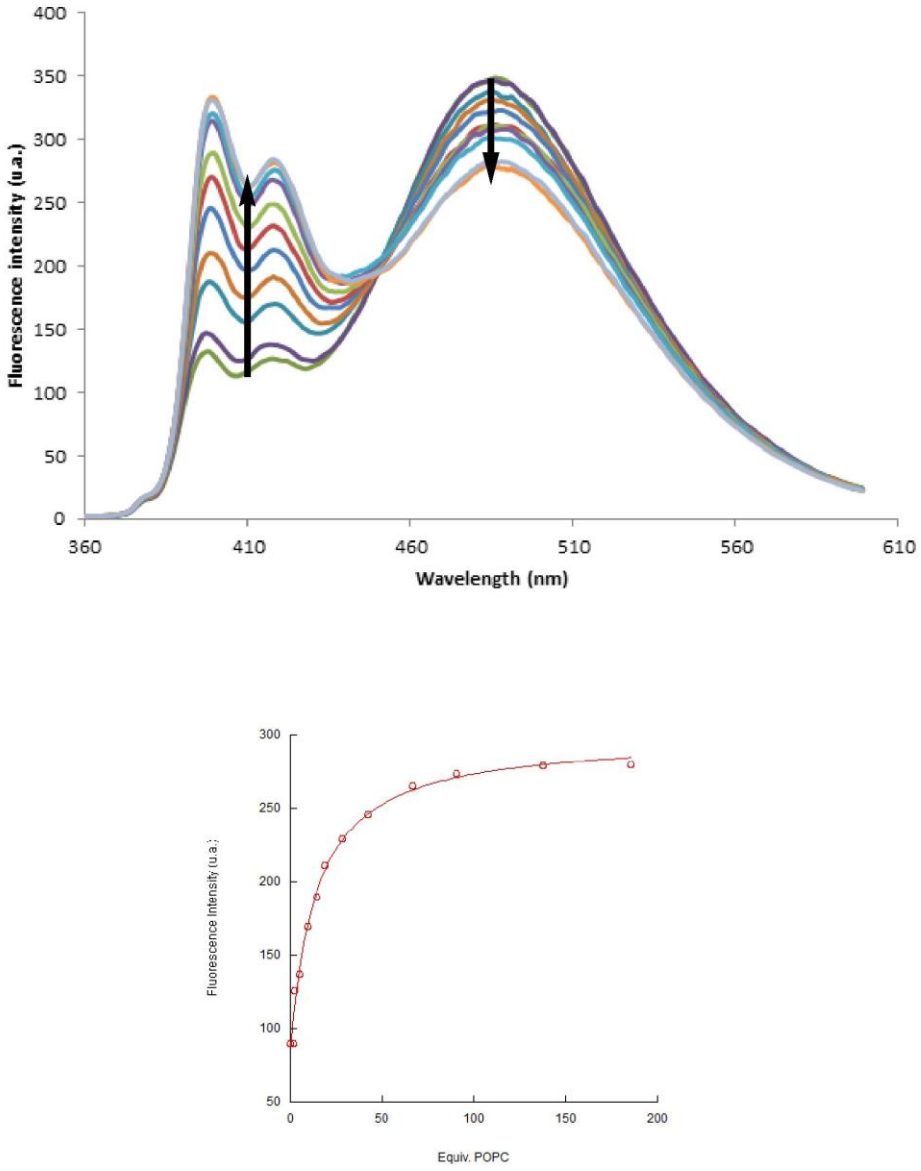

Figure S9. Top: fluorescence spectra of **1** upon the addition of POPC (0 to 185 equiv.) in chloroform. $[\mathbf{1}]_0 = 1.9 \times 10^{-6}$ M. $\lambda_{ex} = 345$ nm. Bottom: variation of fluorescence intensity at 420 nm upon the addition of POPC.

III. Complexation studies between host **1** and DPPC

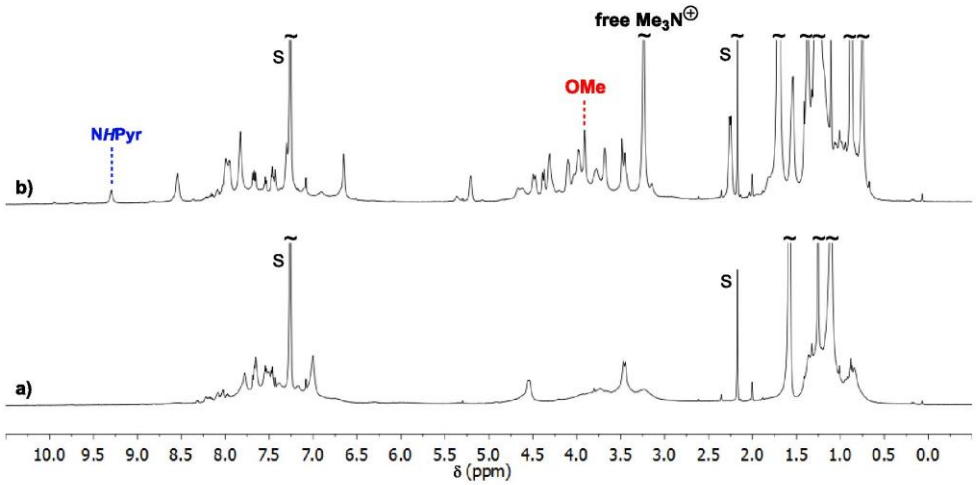

Figure S10. ^{1}H NMR spectra (600MHz, 298 K, $CDCl_3$) of: a) **1**; b) **1** in the presence of *ca.* 3 equiv. of DPPC; s: solvent.

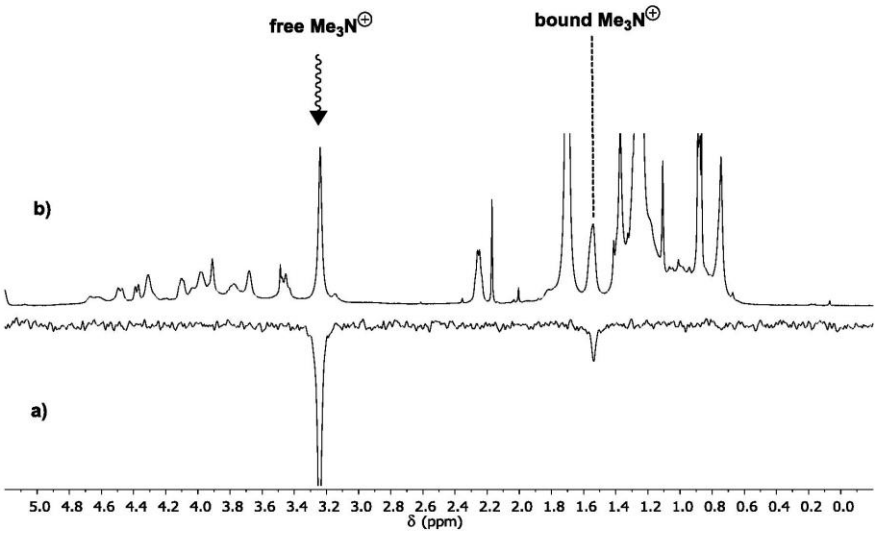

Figure S11. NMR spectra (600MHz, 298 K, $CDCl_3$) of host **1** in in the presence of *ca.* 3 equiv. of DPPC: a) 1D EXSY spectrum (mixing time = 25 ms) after selective excitation of the $^{+}NMe_3$ signal at 3.24 ppm; b) ^{1}H NMR spectrum; ▼: Pulse excitation.

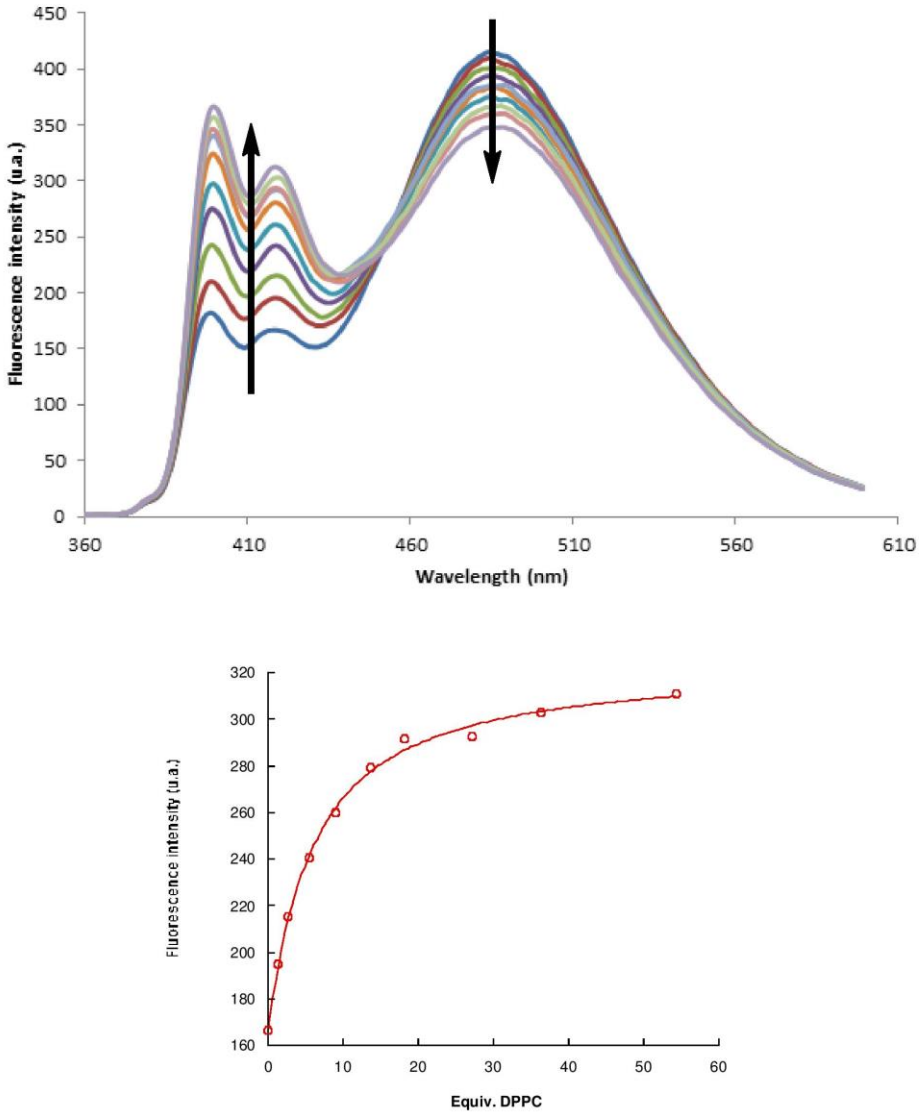

Figure S12. Top: fluorescence spectra of **1** upon the addition of DPPC (0 to 54 equiv.) in chloroform. $[\mathbf{1}]_0 = 2.6 \times 10^{-6}$ M. $\lambda_{ex} = 345$ nm. Bottom: variation of fluorescence intensity at 420 nm upon the addition of DPPC.

8

IV. Complexation studies between host **1** and SPH

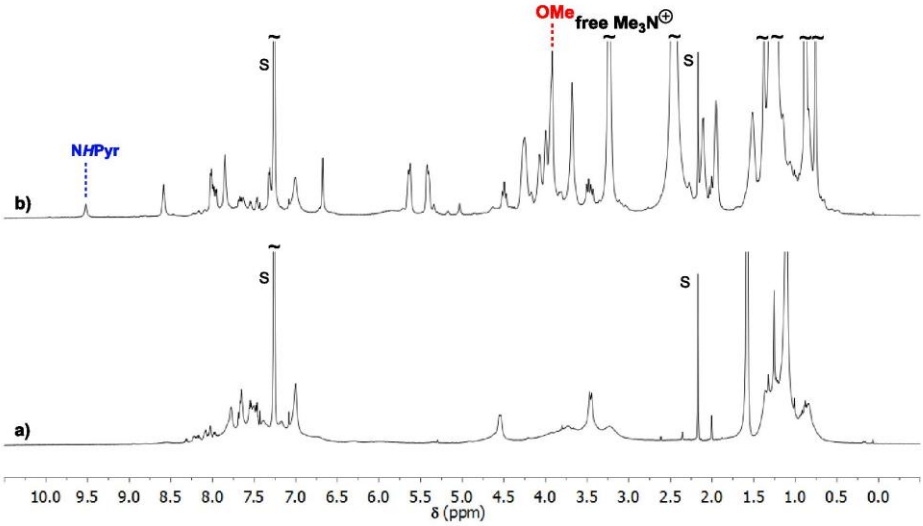

Figure S13. a) ^{1}H NMR spectra (600MHz, 298 K, $CDCl_3$) of: a) **1**; b) **1** in the presence of *ca.* 11 equiv. of SPH; s: solvent.

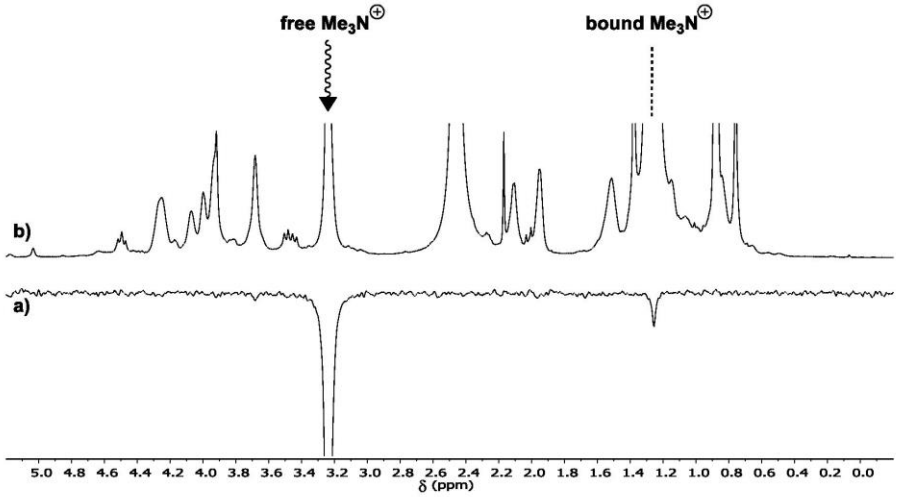

Figure S14. NMR spectra (600MHz, 298 K, $CDCl_3$) of host **1** in the presence of *ca.* 11 equiv. of SPH: a) 1D EXSY spectrum (mixing time = 25 ms) after selective excitation of the $^{+}NMe_3$ signal at 3.32 ppm; b) ^{1}H NMR spectrum; ▼: Pulse excitation.

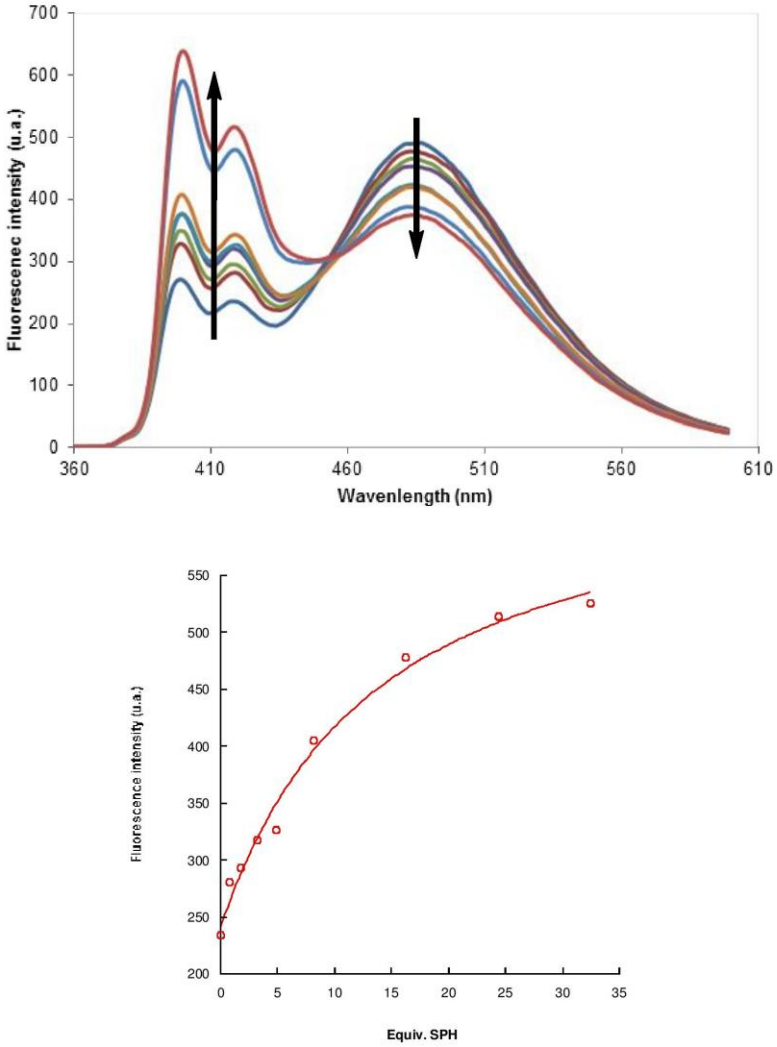

Figure S15. Top: fluorescence spectra of **1** upon the addition of SPH (0 to 32 equiv.) in chloroform. $[\mathbf{1}]_0 = 2.6 \times 10^{-6}$ M. $\lambda_{ex} = 345$ nm. Bottom: variation of fluorescence intensity at 420 nm upon the addition of SPH.

10

V. Complexation studies between host **1** and DPC

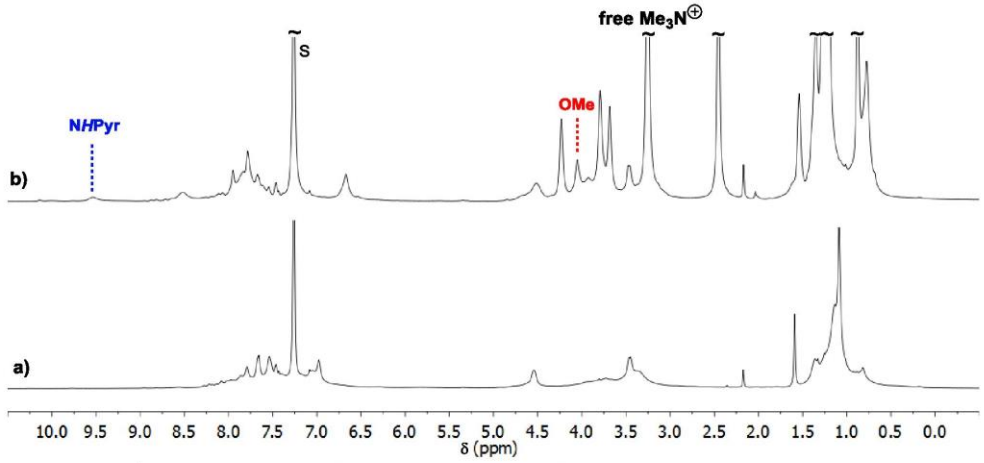

Figure S16. ^{1}H NMR spectra (600MHz, 298 K, $CDCl_3$) of: a) **1**; b) **1** in the presence of *ca.* 6 equiv. of DPC; s: solvent.

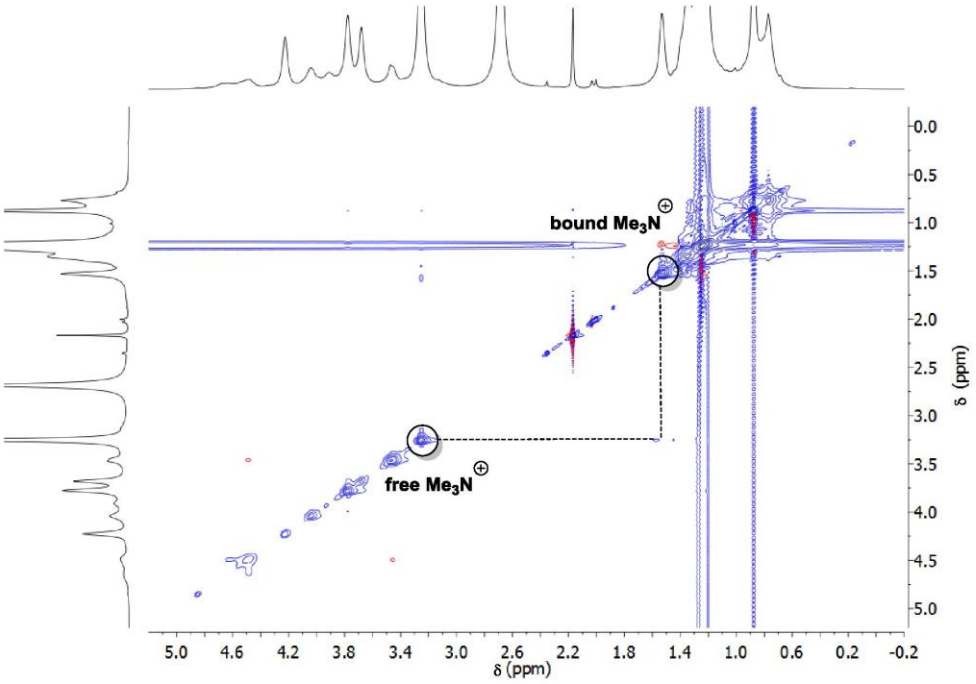

Figure S17. 2D ROESY spectrum (600 MHz, 298 K, $CDCl_3$, mixing time = 300 ms) of host **1** in the presence of *ca.* 6 equiv. of DPC.

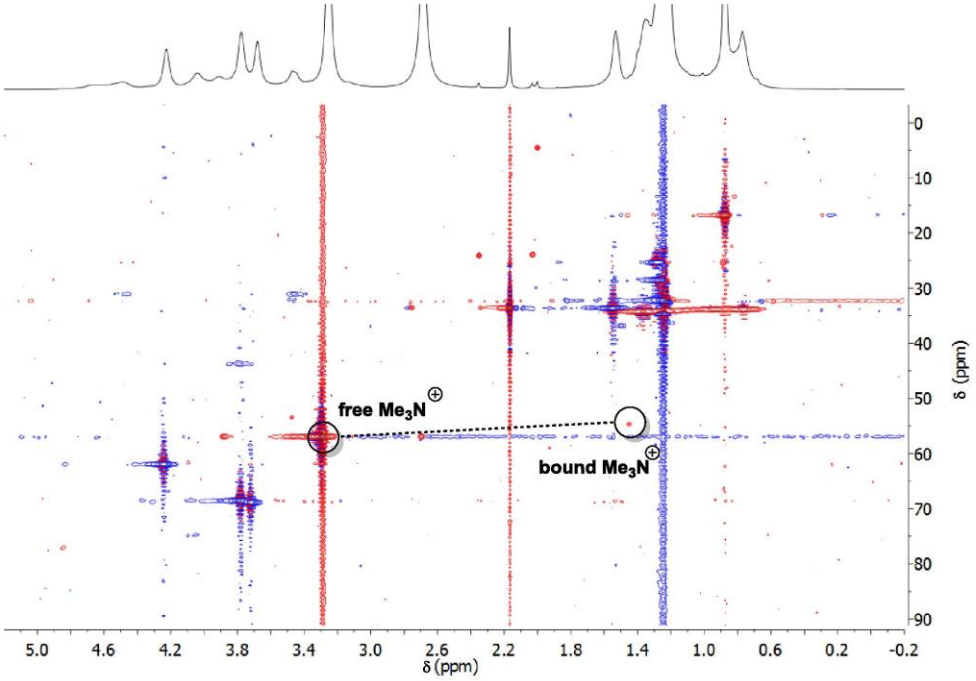

Figure S18. HSQC spectrum (600 MHz, 298 K, $CDCl_3$) of compound **1** in the presence of *ca.* 6 equiv. of DPC.

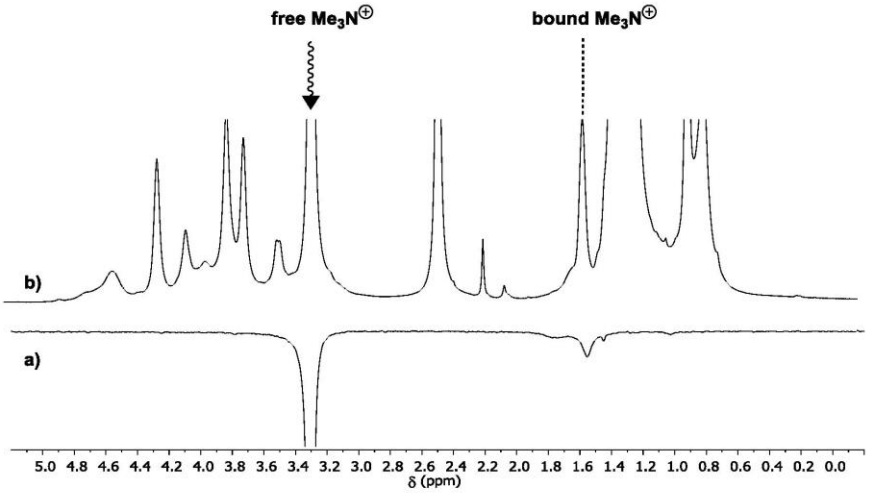

Figure S19 NMR spectra (600MHz, 298 K, $CDCl_3$) of host **1** in the presence of *ca.* 6 equiv. of DPC: a) 1D EXSY spectrum (mixing time = 25 ms) after selective excitation of the $^{+}NMe_3$ signal at 3.26 ppm; b) ^{1}H NMR spectrum; ▼: Pulse excitation.

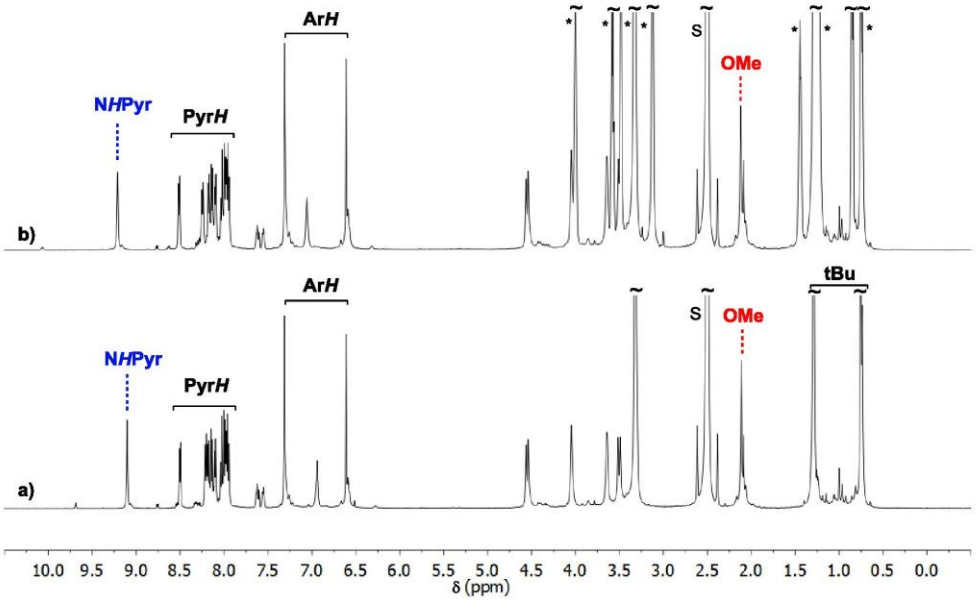

Figure S20. ^{1}H NMR spectra (600MHz, 298 K, DMSO-d_6) of: a) **1**; b) **1** in presence of *ca.*7 equiv. of DPC; s: solvent; *: DPC signals.

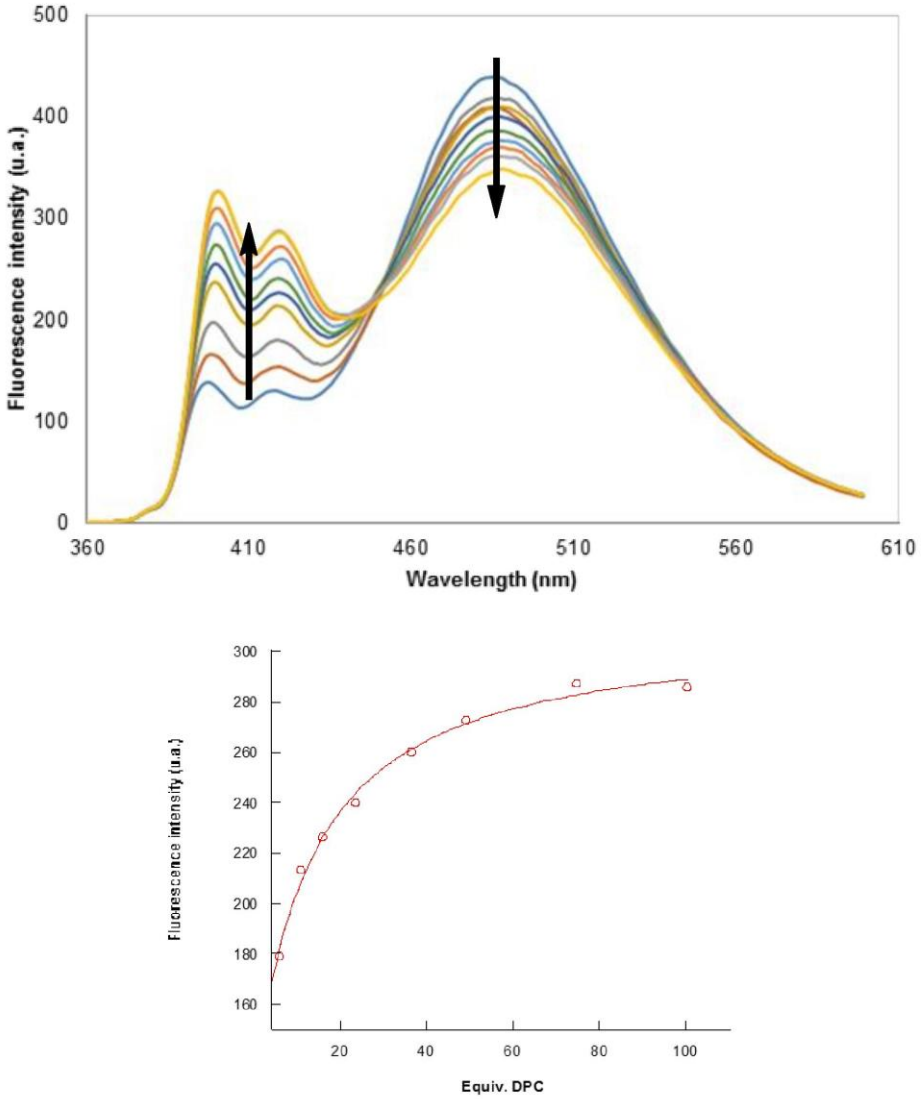

Figure S21. Top: fluorescence spectra of **1** upon the addition of DPC (0 to 100 equiv.) in chloroform. $[\mathbf{1}]_0 = 2.2 \times 10^{-6}$ M. $\lambda_{ex} = 345$ nm. Bottom: variation of fluorescence intensity at 420 nm upon the addition of DPC.

VI. Complexation studies between host **1** and MPC

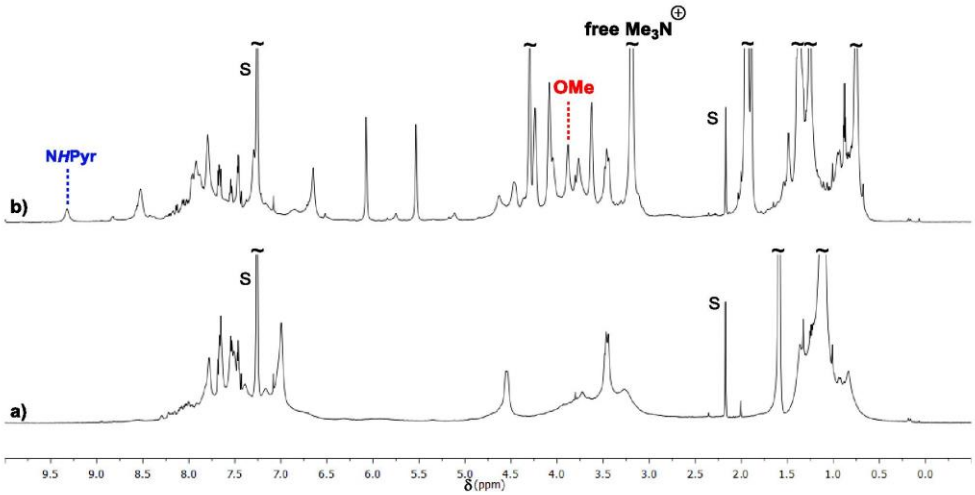

Figure S22. ^{1}H NMR spectra (600MHz, 298 K, $CDCl_3$) of: a) **1**; b) **1** in the presence of *ca.* 4.5 equiv. of MPC; s: solvent.

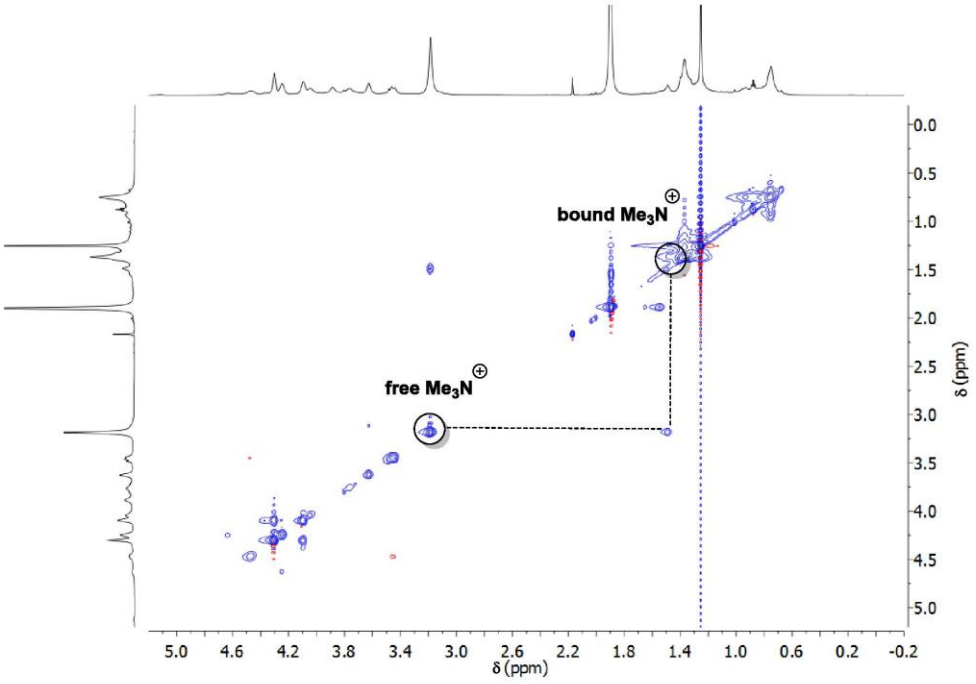

Figure S23. 2D ROESY spectrum (600 MHz, 298 K, $CDCl_3$, mixing time = 300 ms) of compound **1** in the presence of *ca.* 4.5 equiv. of MPC.

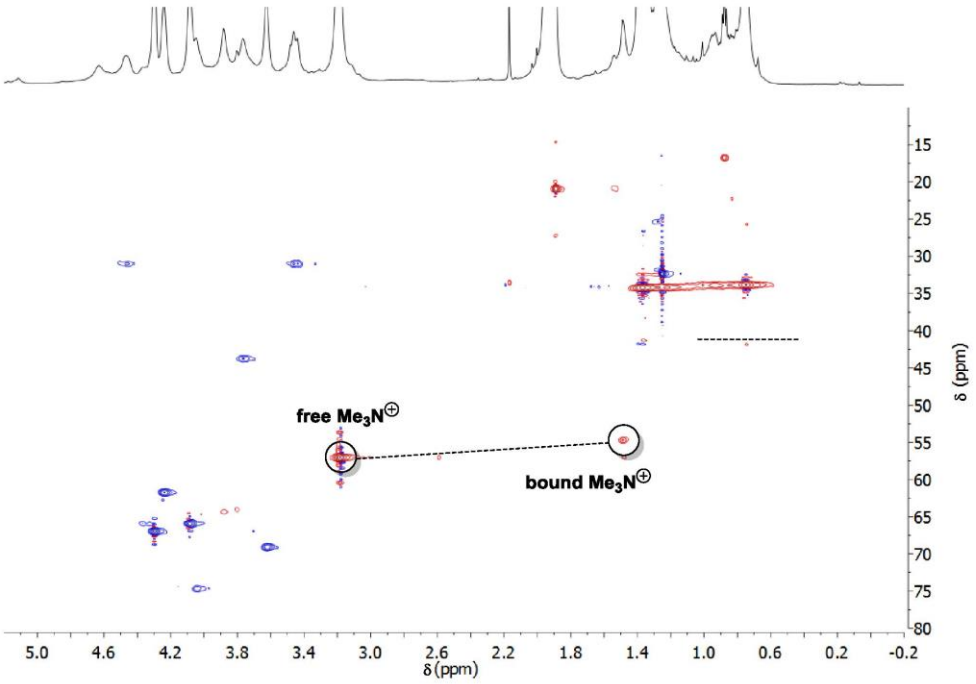

Figure S24. HSQC spectrum (600 MHz, 298 K, $CDCl_3$) of compound **1** in the presence of *ca.* 4.5 equiv. of MPC.

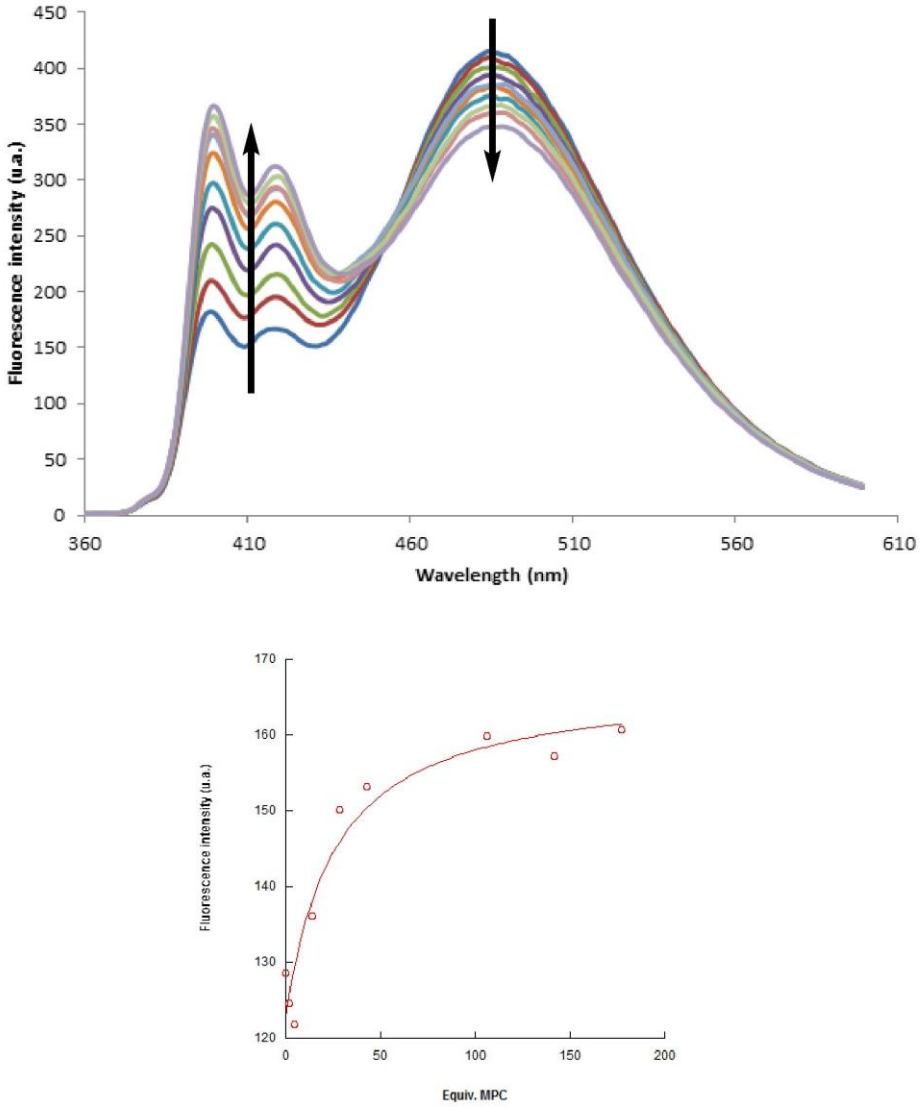

Figure S25. Top: fluorescence spectra of **1** upon the addition of MPC (0 to 71 equiv.) in chloroform. $[\mathbf{1}]_0 = 2.9 \times 10^{-6}$ M. $\lambda_{ex} = 345$ nm. Bottom: variation of fluorescence intensity at 420 nm upon the addition of MPC.

17

VII. Complexation studies between host **1** and DOPE

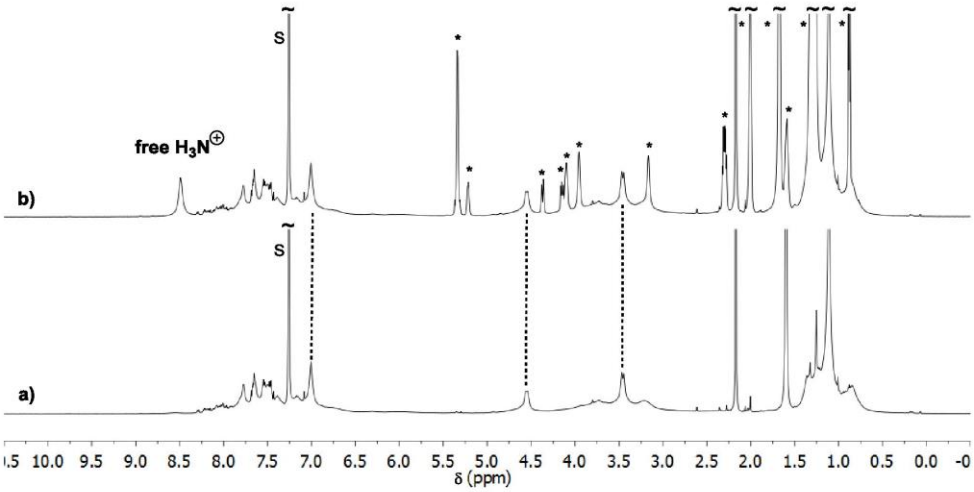

Figure S26. ^{1}H NMR spectra (600MHz, 298 K, $CDCl_3$) of: a) **1**; b) **1** in the presence of *ca.* 3 equiv. of DOPE; s: solvent; *: DOPE signals.

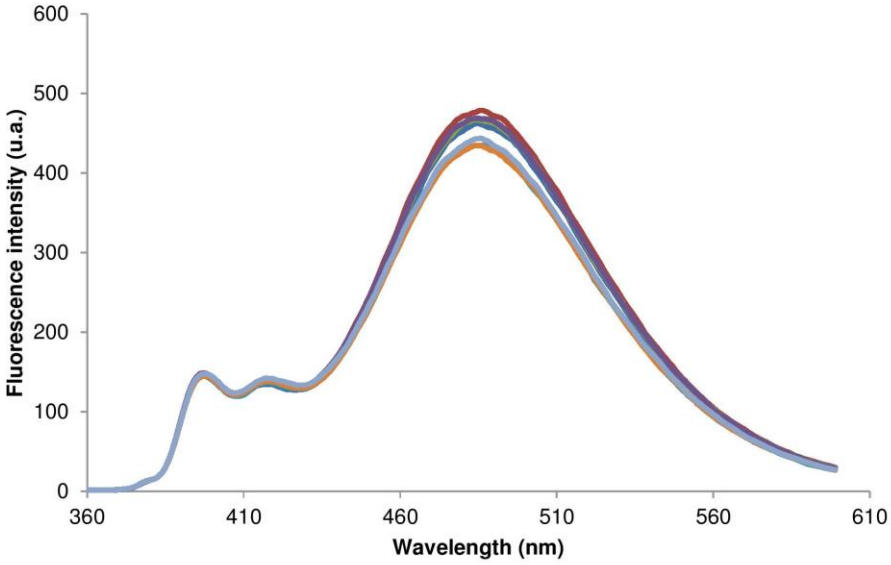

Figure S27. Fluorescence spectra of **1** upon the addition of DOPE (0 to 140 equiv.) in chloroform. $[\mathbf{1}]_0 = 2.5 \times 10^{-6}$ M. $\lambda_{ex} = 345$ nm.

VIII. ^{31}P NMR measurements

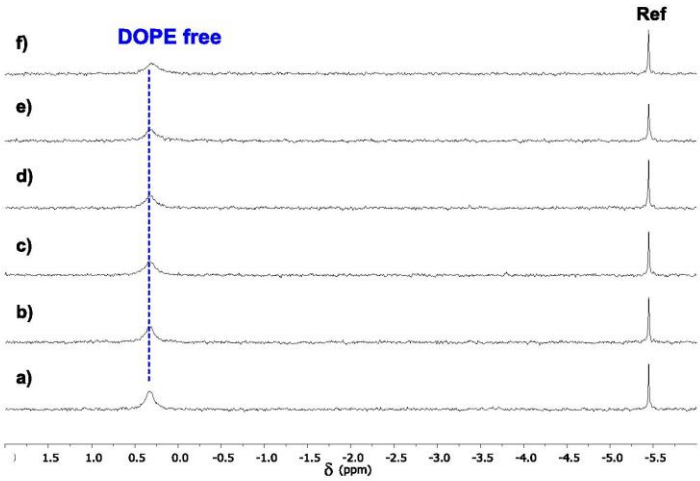

Figure S28. ^{31}P NMR spectra (400MHz, 298 K, $CDCl_3$) of: a) a solution of DOPE (*ca.* 2.9 mM); b) to f) a solution of DOPE (*ca.* 2.9 mM) after addition of host **1** up to 0.6 equiv.

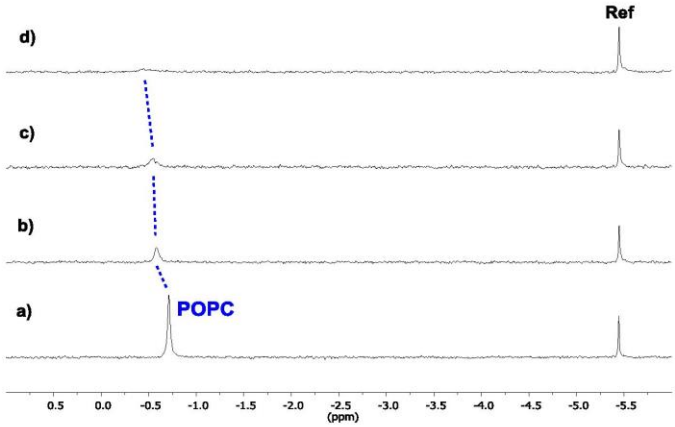

Figure S29. ^{31}P NMR spectra (400MHz, 298 K, $CDCl_3$) of: a) a solution of POPC (*ca.* 4.3 mM); b) to d) a solution of POPC (*ca.* 4.3 mM) diluted up to a concentration of 0.7 mM.

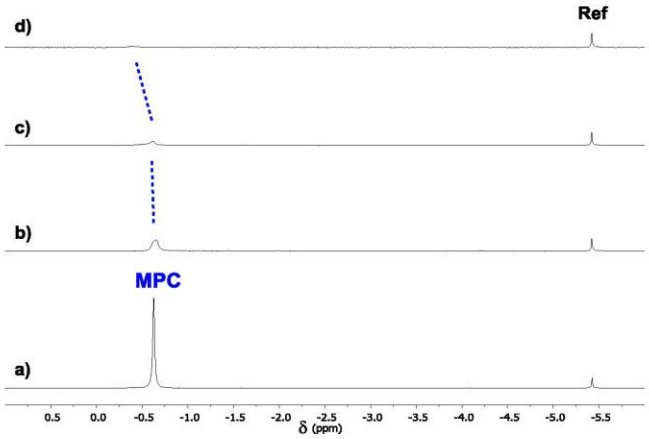

Figure S30. ^{31}P NMR spectra (400MHz, 298 K, $CDCl_3$) of: a) a solution of MPC (*ca.* 16 mM); b) to d) a solution of MPC (*ca.* 16 mM) diluted up to a concentration of 0.3 mM.

IX. Extraction experiments

1. Two liquid-liquid extraction experiments were conducted preparing two different 20µL water solutions of 2 known DOPC concentration. After adding these solutions to a solution of **1** in chloroform, the resulting fluorescence intensity was monitored.

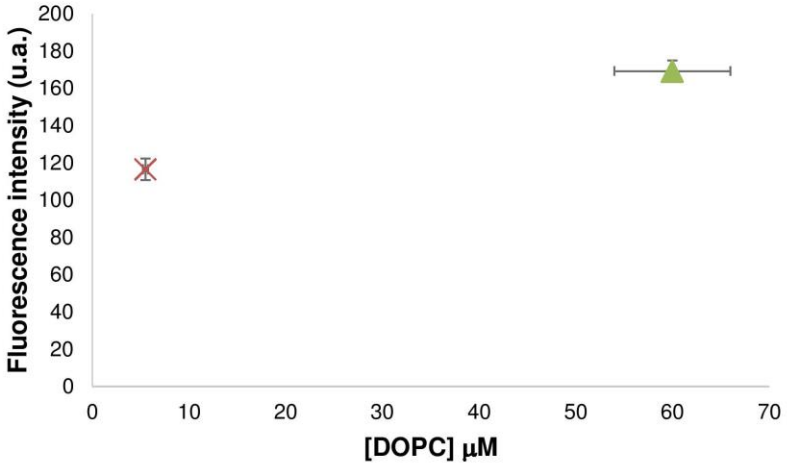

Figure S31. Red cross: fluorescence intensity of a solution of **1⊃DOPC** upon addition of a solution of DOPC in water (*ca.* 5.5 µM) to a solution of **1** (*ca.* 2 µM in 2 mL) in $CHCl_3$. Green triangle: fluorescence intensity of a solution of **1⊃DOPC** upon addition of a solution of DOPC in water (*ca.* 60 µM) to a solution of **1** (*ca.* 2 µM in 2 mL) in $CHCl_3$. λ_{ex} = 345 nm. Errors estimated of ± 10% for the equivalents of DOPC and ± 5 % for the fluorescence intensity.

2. NMR experiments

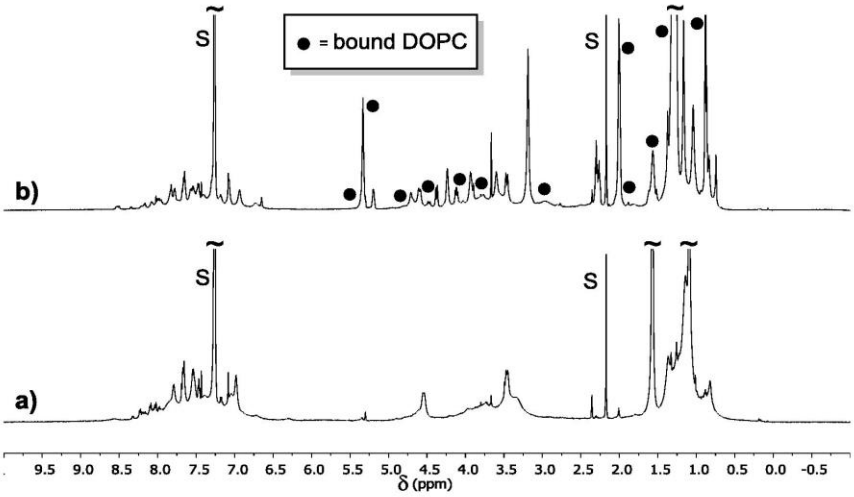

Figure S32. ^{1}H NMR spectrum (600MHz, 298 K, $CDCl_3$) of: a) 1.1 mM solution of **1** in $CDCl_3$ (600 µL); b) after addition of 100 µL of a 12 mM solution of DOPC in D_2O after mixing; s: solvent.

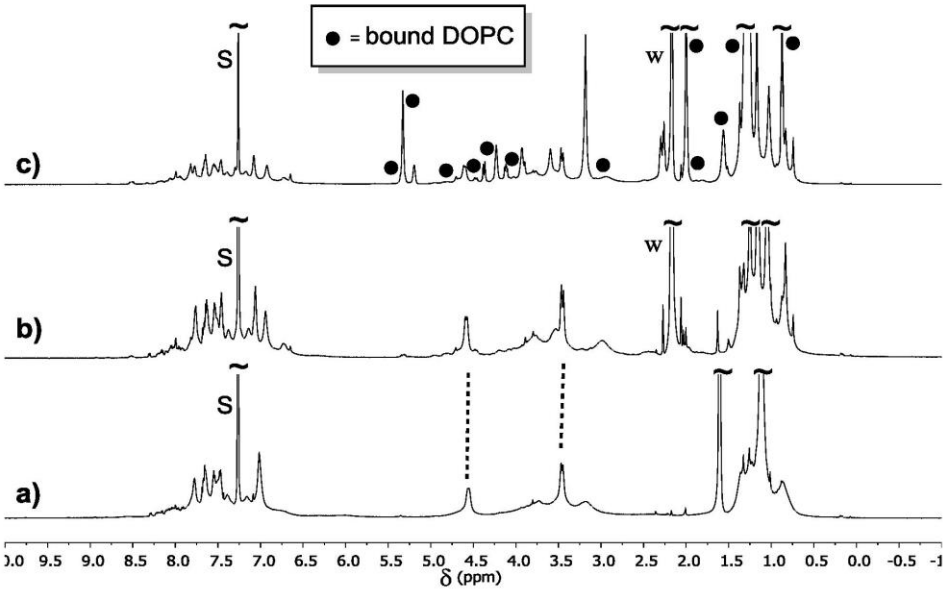

Figure S33. ^{1}H NMR spectra (600MHz, 298 K, $CDCl_3$) of: a) **1**; b) **1** after addition of a solution of DOPC liposomes prepared D_2O; c) **1** after addition of a solution of DOPC liposomes prepared D_2O and after heating and stirring for 16h at 50°C; s: solvent; w: water.

3. Fluorescence titration

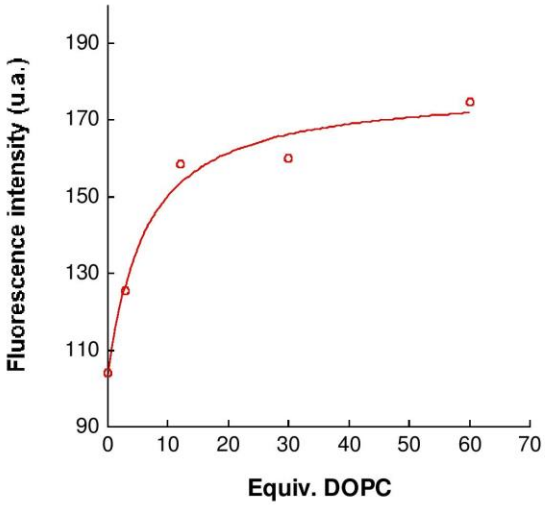

Figure S34. Variation of fluorescence intensity at 397 nm upon the addition of DOPC in chloroform to a 1.9×10^{-6} M solution of **1** in 2 mL chloroform in the presence of 20 µL of water. Solid line corresponds to 1:1 binding which yields a log $K = 4.5 \pm 0.2$; $\lambda_{ex} = 345$ nm.

2.3. CONCLUSIONS

The results presented in this chapter show that calixarene receptors bearing fluorescent units are very sensitive molecular chemosensors. The fluorescent calix[6]tris-pyrenylurea **14a** and its analog **14b,** which has a more open cavity, are furthermore remarkably selective.

Receptor **14a** exhibits a remarkable selectivity for the sulfate anion in DMSO, enabling its selective sensing by fluorescence spectroscopy. In $CDCl_3$, it is able to efficiently bind ammonium ions only in association with the sulfate anion. This cooperative binding of ammonium sulfate salts was also observed in a more protic environment (1:11 $CD_3OD/CDCl_3$). The binding constants determined by UV−vis absorbance, fluorescence, and NMR titrations were found to be in agreement in all cases. Corroborating conformational changes of the receptor upon binding were observed by fluorescence and NMR spectroscopies. Interestingly, a cavity-based selectivity, in terms of the size and shape of the guest, was observed for both receptors. While **14a** displays a strong affinity for small or linear ammonium salts, **14b** was found to have the ability to recognize the 3,4-O-dimethyldopammonium sulfate salt and not the corresponding serotonin derivative. This work opens interesting perspectives on the elaboration of unique fluorescent cavity-based systems for the selective sensing of anions or biologically relevant ammonium salts such as neurotransmitters.

Receptor **14a** is also an efficient heteroditopic chemosensor able to strongly interact with lipids in organic media (log $K > 4$). A high selectivity for phosphatidylcholine type lipids over the closely related phosphatidylethanolamines was observed, highlighting the importance of specific interactions between the receptor and the zwitterionic head of the lipid. This mode of recognition is reminiscent of natural systems such as human phosphatidylcholine transfer proteins (PC-TPs). This validates the biomimetic approach adopted in our work, that consists in designing receptors that combine a H-bonding donor site to a hydrophobic pocket in order to achieve a high degree of complementarity with the two ionic groups of zwitterions. We also observed, via extraction experiments, that host **14a** can still bind phosphatidylcholine type lipids in a biphasic chloroform/water solution, opening the way to the use of calix[6]arenes as selective chemosensors for lipids in biological media.

CHAPTER 3.
INCORPORATION AND STUDY OF CAVITANDS IN MICELLES

3.1. INTRODUCTION

One of the goals of our work, as mentioned in the introduction, is to evaluate the possibility of transferring molecular receptors, in particular calix[6]arenes, into aqueous media and to study their binding properties in water. The development of molecular receptors, that are able to recognize neutral or charged species with a high affinity and selectivity in water, is indeed an important field of research as many medical and environmental applications can be envisaged.[1]

Most studies with molecular receptors are carried out in organic media as only few synthetic receptors are water-soluble (e.g. cucurbiturils, cyclodextrines). Most synthetic receptors are only soluble in organic media, which is the case of calixarenes. Moreover, water is a highly competitive medium as water molecules, which are good H-bond donors/acceptors, can actively interfere in the recognition process by efficiently solvating the different binding partners. Water is also a solvent with a high dielectric constant and polar interactions are consequently screened. On the other hand, an attractive feature of working in water is that molecular recognition can benefit from the hydrophobic effect.[2]

Two strategies exist for transferring hydrophobic receptors into an aqueous medium. **A first strategy is the grafting of hydrophilic moieties onto the receptor**. The solubilization in water of hydrophobic receptors has been achieved, for example, via the grafting of sulfonates, carboxylates, ammoniums, PEG, sugars or peptides.[3] For calix[4]arenes, we can mention water-soluble calix[4]tetra-sulfonates[4], which are able to recognize small neutral molecules or metallic cations or sugar bearing calix[4]arenes, which are able to recognize specific proteins.[5] Reinaud's group has shown that a water-soluble calix[6]tris-imidazole bearing three Me_3N^+ cationic moieties on the large rim can complex Zn^{2+} at the level of the imidazole groups and hydrophobic amines in the calixarene cavity in a cooperative way at pH ~ 7 (Figure 3-1).[6]

[1] Lehn, J.-M. *La chimie supramoléculaire concepts et perspectives*; **1997**.
[2] Chandler, D. *Nature* **2002**, *417*, 491; Biedermann, F.; Nau, W. M.; Schneider, H.-J. *Angew. Chem. Int. Ed.* **2014**, 53, 11158-11171.
[3] Oshovsky G. V.; Reinhoudt D. N.; Verboom W. *Angew Chem Int Ed Engl.* **2007**, *46*, 2366-93.
[4] Morel, J. P.; Morel-Desrosiers, N. *Org. Biomol. Chem.* **2006**, *4*, 462–465.
[5] Baldini, L.; Sansone, F.; Scaravelli, F.; Massera, C.; Casnati, A.; Ungaro, R. *Tetrahedron Lett.* **2009**, *50*, 3450–3453.
[6] Bistri, O.; Colasson, B.; Reinaud, O. *Chem. Sci.* **2012**, *3*, 811-818.

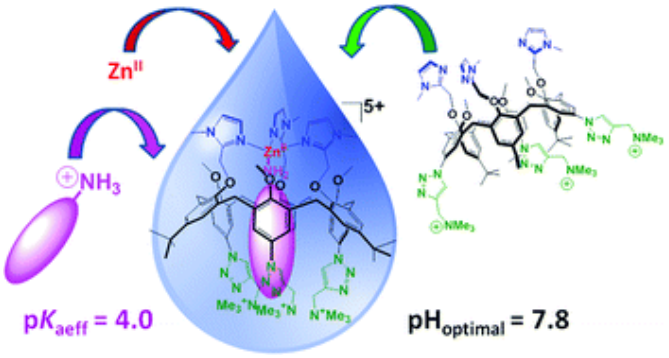

Figure 3-1. The hydrosoluble zinc calix[6]arene-based receptor and its recognition properties in water (figure taken from reference 6).

The Reinaud's group has also shown that similar systems can complex Cu^{+} and Cu^{2+} in water.[7] Water soluble calix[6]tren derivatives, obtained via grafting of cationic moieties or PEG chains, have recently been synthesized and their complexing properties in water explored.[8] A copper calix[6]tren with grafted cationic moieties was observed to be stable on a large pH range showing similar host-guest properties to its analogue soluble in organic solvents, recognizing guests, such as nitriles, amines and alcohols.

An alternative solution that can be considered in order to transfer hydrophobic molecular receptors into water is the use of micelles. Micelles are aggregates of amphiphilic molecules (surfactants) composed of a hydrophilic head and a hydrophobic tail that self-assemble when placed in an aqueous environment in order to limit their contact with water (Figure 3-2).

[7] Brugnara, A.; Topić, F.; Rissanen, K.; De la Lande, A.; Colasson, B.; Reinaud, O. *Chem. Sci.* **2014**, *5*, 3897-3904.

[8] Inthasot, A. **2016**. PhD thesis: Nouveaux récepteurs cavitaires dérivés de calix[6]arènes: fonctionnalisation sélective, chimie de coordination et reconnaissance moléculaire dans l'eau. Laboratoire de Chimie Organique, Université libre de Bruxelles and Laboratoire de Chimie Biochimie Pharmacologie et Toxicologie, Université Paris Descartes.

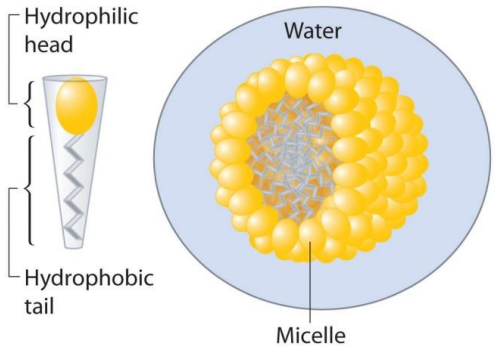

Figure 3-2. Schematic representation of a micelle.

The transfer of hydrophobic compounds into an aqueous medium, via their incorporation into micelles, is a widely used strategy for various applications. For example, in decontamination processes, chelating agents incorporated into micelles are used for the extraction of heavy metals from water.[9] Micelles are also used for drug solubilization and in catalysis where the proximity of the different reactants and high concentration in the small micelles volume can have a very beneficial effect of reaction rate.[10,11] Lipophilic molecules can be solubilized in the core of the micelle and thus transferred into an aqueous environment without the need of any tedious synthetic step (Figure 3-3).

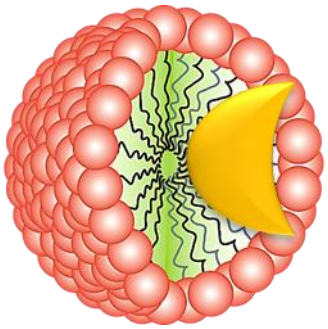

Figure 3-3. Schematic representation of lipophilic receptor incorporated into a micelle.

Different types of micelles exist depending on the nature of the surfactant: ionic bearing either a positive or negative charge at the level of their head group, zwitterionic or non-ionic.[10] Examples of these surfactants are presented in Figure 3-4: a cationic surfactant cetyltrimethylammonium bromide (CTABr) composed of an aliphatic chain, a quaternary ammonium polar head and bromide as counter-ion; an anionic surfactant, sodium

[9] Stalikas, C. D. *Trends Anal. Chem.* **2002**, *21*, 343–355; Hébrant, M.. *Coord. Chem. Rev.* **2009**, *253*, 2186–2192.; Xiao, F.; Wang, Y.; Shen, X.; Perera, J. M.; Stevens, G. W. *Colloids Surf.* A **2015**,482, 109–114.
[10] Rosen, M. J. John Wiley & Sons, Inc.; Hoboken, **2004**.
[11] Mancin, F.; Scrimin, P.; Tecilla, P.; Tonellato, U. *Coord. Chem. Rev.* **2009**, *253*, 2150–2165.

dodecylsulfate (SDS), composed of an aliphatic chain with a sulfate group as polar head with sodium as a counter-ion; non-ionic surfactant, Triton X-100, composed of an aromatic hydrocarbon tail and a polyethylene oxide polar head and finally a zwitterionic surfactant dodecylphosphocholine (DPC), composed of an aliphatic chain and a phosphocholine head.

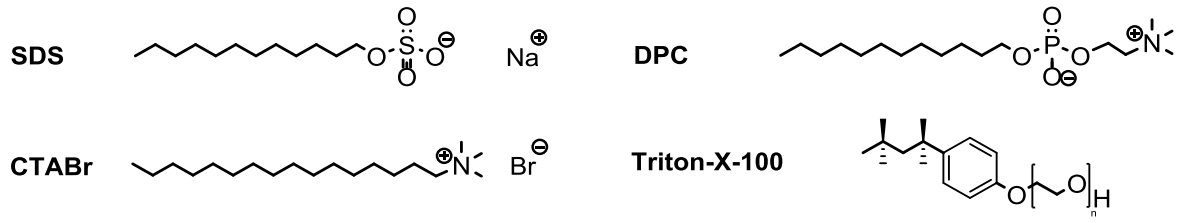

Figure 3-4. Structures of different types of surfactants.

DPC was the surfactant used in this thesis. It is characterized by an aggregation number of 56 (the number of surfactant monomers composing one micelle) at 20 mM and 298 K and a critical micellar concentration (cmc) of 1.1 mM (the surfactant concentration above which micelles can be formed).[10]

3.2. EXAMPLES OF MICELLAR INCORPORATION OF MOLECULAR RECEPTORS

Rebek and co-workers have reported on a resorcinarene-based cavitand, insoluble in water that once incorporated into DPC micelles adopts a bowl conformation, which offers the possibility of recognizing small neutral molecules such as cycloalkanes or adamantanes.[12] They have also observed that the conformational reorganization, after incorporation into DPC micelles, of a water-soluble resorcinare-based cavitand increases significantly its binding capacity toward different guests (Figure 3-5).[12]

[12] Javor, S.; Rebek, J. Jr. *J. Am. Soc. Chem*. **2011**, *133*, 17473-17478.

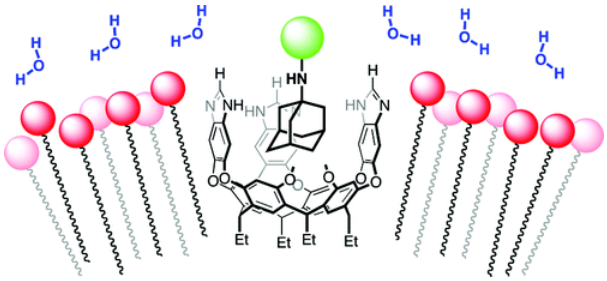

Figure 3-5. Resorcinarene-based cavitand for recognition of small molecules (figure taken from reference 12).

This receptor is able to simultaneously bind the head of the DPC surfactant and other guests, such as adamantane or quinuclidinium derivatives. The determined binding constants are higher in the micellar media than in water showing the power of micelles as protecting environment for recognition. Another example of the effectiveness of micellar incorporation is given by the study of the uranyl-salophen-based receptors in cationic micelles (CTABr and CTACl).[13,14]

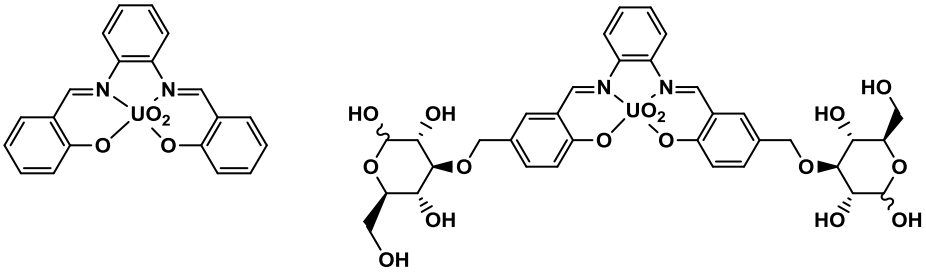

Figure 3-6. Structures of two uranylsalophenes.

Indeed, with the collaboration of Prof. Dalla Cort from the University La Sapienza in Rome, the EMNS laboratory has reported that this hydrophobic receptor is capable to efficiently and selectively recognize fluoride, once incorporated in the micellar media. Remarkably, the micellar system exhibits an affinity for fluoride (log K ~ 4), which is two orders of magnitude higher than the one observed with the water-soluble version of the receptor with grafted sugar moieties (Figure 3-6). These results highlight once again the important role played by the micellar environment in the recognition process.

To our knowledge, there are only very few examples reported in the literature which concern the binding capacities of calixarene-based systems incorporated into micelles. Calix[4]arene-

[13] Cametti, M.; Dalla Cort, A.; Bartik, K. *Chemphyschem* **2008**, *9*, 2168–2171; Cort, A. D.; Forte, G.; Schiaffino, L. *J. Org. Chem.* **2011**, *76*, 7569–7572.
[14] Keymeulen, F.; De Bernardin, P.; Giannicchi, I.; Galantini, L.; Bartik, K.; Dalla Cort, A. *Org. Biomol. Chem.* **2015**, *13*, 2437-2443.

crown ethers dissolved in dodecyl sulfate micellar solutions have been reported to be able to complex cesium or potassium in a selective way.[15] A few years ago, Hu and co-workers prepared a Cu^{2+}-selective self-assembled fluorescent calix[4]arene-based chemosensor by solubilizing the receptor and a fluorescent reporter, perylene, in Triton X-100 micelles. Upon the binding of Cu^{2+}, the fluorescence emission of perylene was quenched. The authors also showed that Cu^{2+} ions can be detected selectively and quantitatively in the presence of other metal ions at concentration in the sub-micromolar range.[16] It has also been reported that calix[6]arenes bearing long aliphatic chains on their small rim can self-assemble via a co-micellization with the cationic surfactant dodecyltrimethylammonium bromide.[17] No binding studies have however been undertaken with these systems.

3.3. AIM OF THE WORK

In this thesis, we focused our attention on the micellar incorporation in DPC micelles of a calix[6]tren zinc complex (**6.Zn^{2+}**), which has already been described in the introduction of this thesis. We also had the opportunity to look at the micellar incorporation of receptors which are related to calixarenes: a homooxacalix[3]arene tris-acid (**15**) and a resorcin[4]arene-based zinc complex (**16.Zn^{2+}**).

The binding properties of calix[6]tren **6** in organic media have been detailed in the introduction. It is able to complex Zn^{2+} at the level of the *tren* cap, leaving a single coordination site accessible for a neutral guest that is incorporated inside the calix[6]arene cavity.[18,19] **6.Zn^{2+}** proved to be remarkably selective regarding the recognition of neutral molecules in organic solvents.

Considering the results in organic media, we wished to evaluate the binding properties of complex **6.Zn^{2+}** in an aqueous medium. In order to transfer this hydrophobic metal complex into water, we incorporated it into DPC micelles. This system was extensively studied using ^{1}H NMR and our results have been published in the journal Organic and Biomolecular Chemistry: "*Primary Amine Recognition in Water by a Calix[6]aza-cryptand Incorporated in*

[15] Capuzzi, G; Fratini, E.; Pini, F.; Baglioni, P.; Casnati, A.; Teixera, J. *Langmuir* **2000,** *16*, 188-194
[16] Hu, X.-J.; Li, C.-M.; Song, X.-Y.; Li, C.-M..; Li, Y.-S. *Inorg. Chem. Commun.* **2011**, *14*, 1632–1635.
[17] Basilio, N.; García-Río, L. *Chem. Eur. J.* **2009**, *15*, 9315–9319.
[18] Darbost, U.; Rager, M.-N.; Petit, S.; Jabin, I.; Reinaud, O. *J. Am. Chem. Soc.* **2005**, *127*, 8517–8525.
[19] Izzet, G.; Douziech, B.; Prangé, T.; Tomas, A.; Jabin, I.; Le Mest, Y.; Reinaud, O. *Proc. Natl. Acad. Sci. U. S. A.* **2005**, *102*, 6831–6836.

Dodecylphosphocholine Micelles" (**2015**, *13*, 2931-2938). The results are summarized in the section 3.4 of this chapter.

The homooxacalix[3]arene derivative has not yet been studied for its binding properties despite its already known synthesis. On the other hand, the resorcin[4]arene derivative has already been the object of studies in the laboratory of Prof. Reinaud. This two receptors were incorporated into DPC micelles and their binding properties evaluated. The results reported in section 3.5 have not yet been the object of a publication.

3.4. SUMMARY OF PUBLISHED RESULTS

"Primary Amine Recognition in Water by a Calix[6]aza-cryptand Incorporated in Dodecylphosphocholine Micelles"

In the paper "*Primary Amine Recognition in Water by a Calix[6]aza-cryptand Incorporated in Dodecylphosphocholine Micelles*"[20] published in the journal Organic and Biomolecular Chemistry, we report on the incorporation of a calix[6]tren zinc complex, **6.Zn^{2+}**, into DPC micelles and on its binding properties towards neutral molecules.[18]

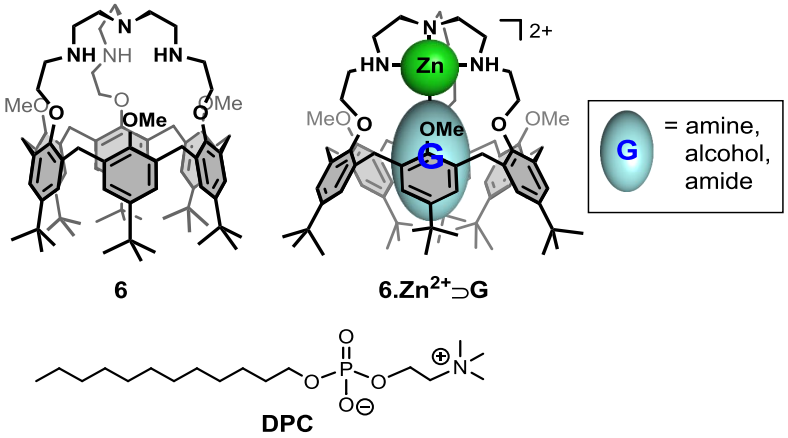

Figure 3-7. Structure of **6**, **6.Zn^{2+}** with a guest in the cavity and structure of DPC.

6.Zn^{2+} was successfully incorporated into DPC micelles by simple mixing it with the surfactant (20 mM) in D_2O at neutral pH (~7.6). Concentrations up to 0.5 mM of **6.Zn^{2+}** were obtained. The NMR spectrum of the complex incorporated into DPC micelles was very similar to the one observed for the complex in chloroform. The downfield shift of the OMe signal (δ >3.9 ppm) suggests that these groups have been expelled from the cavity and probably replaced by water molecules. The Ar*H* and *t*Bu protons appear as two very distinct sets of signals highlighting that the complex adopts a flattened cone conformation. DOSY experiments, confirmed the incorporation into the micelles as the receptor and the surfactant molecules exhibit the same diffusion coefficients.

The binding properties of **6.Zn^{2+}** incorporated in the DPC micelles was compared to those previously reported for the receptor in chloroform. We observed that **6.Zn^{2+}** incorporated in DPC recognizes propylamine ($PrNH_2$), as evidenced by the presence of high field signals for the propyl chain in the ^{1}H NMR spectrum of the system. An apparent affinity constant of 5000

[20] Brunetti, E.; Inthasot, A.; Keymeulen, F.; Reinaud, O.; Jabin, I.; Bartik, K. *Org. Biomol. Chem.* **2015**, *13*, 2931-2938.

M^{-1} at pH~8 was determined. The host-guest complex **6.Zn^{2+}⊃PrNH$_2$** was observed to be stable in the pH range 3–11 which is interesting as **6.Zn^{2+}** incorporated in the micelles is only stable in the pH range 6–9. It was also observed that ethylamine ($EtNH_2$) and heptylamine ($HeptylNH_2$) are recognized with $K_{EtNH2} > K_{PrNH2} > K_{HeptylNH2}$. The fact that the $HeptylNH_2$ chain protrudes outside the cavity forcing the calix[6]arene to adopt an energetically less favorable straight conformation certainly explains the lower affinity for this guest. The relative affinity for $HeptylNH_2$ vs. $PrNH_2$ observed in the micellar environment compared to $CDCl_3$ (0.5 vs. 0.00025) highlights the importance of the hydrophobic effect in the recognition process. No inclusion of alcohols or amino-alcohols was observed.

The calix[6]tren ligand **6** was also successfully incorporated in the DPC micelles but only at low pH (~3), showing that the system needs to be positively charged in order to be incorporated into the micelle. It seems that a favorable interaction with the buried negatively charged part of the zwitterionic surfactant favors incorporation. Analysis of the ^{1}H NMR spectrum highlights that the OMe groups are pointing inside the cavity (δ ~2.4 ppm) and that consequently the cavity is deprived of any guest.

The binding of the neutral guest 2-imidazolidininone (Imi) by protonated ligand was confirmed by the presence of high-field signals for bound Imi (δ ~0.22 ppm for the methylene groups) and by the fact that the OMe signal is shifted downfield attesting that the groups have been expelled from the cavity following guest inclusion. A pH driven shift with **6.Zn^{2+}** in the presence of both $PrNH_2$ and Imi was also observed: at high pH, the complexation of the amine by **6.Zn^{2+}** is observed while at low pH the inclusion of Imi by the protonated ligand is observed.

Organic & Biomolecular Chemistry

PAPER

View Article Online
View Journal | View Issue

Cite this: *Org. Biomol. Chem.*, 2015, **13**, 2931

Primary amine recognition in water by a calix[6]aza-cryptand incorporated in dodecylphosphocholine micelles†

Emilio Brunetti,[a,b] Alex Inthasot,[a,c] Flore Keymeulen,[b] Olivia Reinaud,[d] Ivan Jabin*[a] and Kristin Bartik*[b]

Received 27th November 2014,
Accepted 6th January 2015

DOI: 10.1039/c4ob02495h

www.rsc.org/obc

Water is a unique solvent and the design of selective artificial hosts that can efficiently work in an aqueous medium is a challenging task. It is known that the calix[6]tren zinc complex can recognize neutral guests in organic solvents. This complex was incorporated into dodecylphosphocholine micelles (DPC) and studied by NMR. The incorporated complex is able to extract selectively primary amines from the aqueous environment driven by an important hydrophobic effect which also affects the selectivity of the complex for these amines. This work shows how the incorporation of organo-soluble receptors in micelles can be an elegant and very efficient strategy to obtain water compatible nanosized supramolecular recognition devices which can be prepared *via* a straightforward self-assembly process.

Introduction

The design of artificial receptors that can selectively bind, with a high affinity, charged or neutral species is one of the major objectives of supramolecular chemistry.[1] Indeed, such receptors have potential applications in the sensing of chemical species in the fields of biological and environmental analysis.[2] The development of such receptors is nevertheless challenging because water is a very competitive solvent.[3] Exploiting the hydrophobic effect which can drive apolar guests into apolar cavities is an interesting strategy. In this context, many examples of neutral guest complexation have been reported with water-soluble cavitands having a hydrophobic inner space such as cyclodextrins[4] and cucurbiturils.[5] These macrocycles however remain difficult to modify selectively[6] which limits the design of sophisticated receptors. In the case of the other families of cavitands such as calixarenes, fastidious syntheses are often required in order to make them water-soluble.

Micelles are extensively used in a wide variety of industrial and recovery processes to incorporate lipophilic compounds[7] and are thus a possible solution to overcome the solubility problem of organic receptors in water. This strategy is interesting, as no synthesis needs to be undertaken in order to introduce hydrophilic groups on the receptor. A few examples of receptors and sensors incorporated in micelles have been reported in the literature[8] and in some cases their binding properties have been investigated and shown to be enhanced by the micellar environment. Rebek and co-workers have, for instance, observed that a conformational reorganization of a resorcinarene cavitand incorporated into dodecylphosphocholine (DPC) micelles increases significantly its binding capacity towards different guests.[9] It has also been reported that uranyl-salophen receptors incorporated into cetyltrimethylammonium bromide (CTABr) micelles have an affinity for fluoride which is two order of magnitude larger than the affinity of the related water-soluble receptor.[10,11]

Calix[6]arenes are a well-known class of concave macrocyclic compounds presenting a cavity well adapted for the inclusion of organic guests and which can be selectively modified.[12,13] Depending on their functionalization, they have revealed to be efficient receptors for a variety of neutral or charged species. In this context, different generations of biomimetic receptors based on calix[6]arene ligands bearing nitrogenous coordinating arms on the narrow rim have been developed.[14] In particular,

[a]*Laboratoire de Chimie Organique, Université libre de Bruxelles (ULB), Avenue F.D. Roosevelt 50, CP160/06, B-1050 Brussels, Belgium. E-mail: ijabin@ulb.ac.be; Fax: (+32) 2 650 2799; Tel: (+32) 2 650 3537*
[b]*Engineering of Molecular NanoSystems, Ecole polytechnique de Bruxelles, Université libre de Bruxelles (ULB), Avenue F.D. Roosevelt 50, CP165/64, B-1050 Brussels, Belgium. E-mail: kbartik@ulb.ac.be; Fax: (+32) 2 650 3606; Tel: (+32) 2 650 2063*
[c]*Laboratoire de Résonance Magnétique Nucléaire Haute Résolution, Université Libre de Bruxelles (ULB), Avenue F.D. Roosevelt 50, CP160/08, B-1050 Brussels, Belgium*
[d]*Laboratoire de Chimie et de Biochimie Pharmacologiques et Toxicologiques (CNRS UMR 8601), Université Paris Descartes, 45 rue des Saints-Pères, 75006 Paris, France*

†Electronic supplementary information (ESI) available: 2D DOSY experiment of $\mathbf{1{\cdot}Zn^{2+}}$ incorporated in DPC. NMR PRE experiment with $\mathbf{1{\cdot}Zn^{2+}}$ in DPC. ^{1}H NMR spectrum of $\mathbf{1{\cdot}nH^{+}}$ in DPC. Determination of the *pseudo* pK_a for $PrNH_2$ with $\mathbf{1{\cdot}Zn^{2+}}$ in DPC. ^{1}H NMR spectra of $\mathbf{1{\cdot}Zn^{2+}}$ in the absence and presence of $EtNH_2$ in DPC-*d38*. ^{1}H NMR spectra of $\mathbf{1{\cdot}Zn^{2+}}$ in the absence and presence of $HeptylNH_2$ in DPC. Experimental conditions for titrations of $\mathbf{1{\cdot}Zn^{2+}}$ with amines, alcohols and aminoalcohols in DPC. See DOI: 10.1039/c4ob02495h

View Article Online
Paper Organic & Biomolecular Chemistry

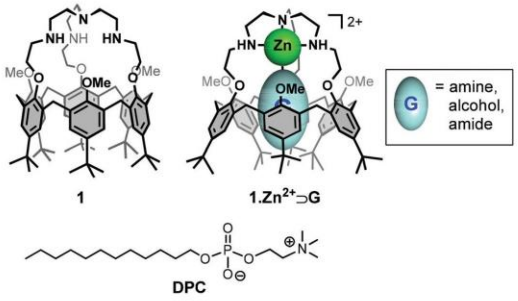

Fig. 1 Structures of ligand **1**, complex **1**·Zn^{2+} ⊃ G and DPC surfactant.

the calix[6]tren receptor **1**,[15] belonging to the third generation has been shown to display unique and versatile binding properties, notably toward metal ions and neutral guests (Fig. 1).[16] Indeed, the tren cap offers a strong binding site for a metal ion (*e.g.* Zn^{2+}, Cu^{n+}). Once coordinated, the metal ion presents a single coordination site accessible for an exogenous neutral guest, which is fully controlled by the hydrophobic funnel. Hence, complex **1**·Zn^{2+} (Fig. 1) can bind with a high selectivity various neutral organic molecules (*e.g.* amines, alcohols, amides, *etc.*) inside the calix[6]arene core in different organic solvents.[17]

With the aim of developing selective molecular receptors that exhibit high affinity for specific guests in water, we were interested in evaluating the binding properties of complex **1**·Zn^{2+} in an aqueous medium. In order to transfer this lipophilic metal complex into water, we thus envisioned its incorporation into micelles. Herein, we report the incorporation of calix[6]tren **1** and of its corresponding metal complex **1**·Zn^{2+} into DPC micelles (Fig. 1). Characterization of the calix[6]arene/micelle systems and evaluation of the binding properties of the incorporated receptors were achieved by NMR spectroscopy.

Results and discussion

Incorporation of complex 1·Zn^{2+} and ligand 1 into DPC micelles. The receptor **1**·Zn^{2+} was successfully incorporated into DPC micelles by simple mixing of the receptor and the surfactant (20 mM) in D_2O at neutral pH (~7.6) and concentrations of up to 0.5 mM of **1**·Zn^{2+} could be obtained.[18] The ^{1}H NMR spectrum of the incorporated receptor **1**·Zn^{2+} in DPC-*d38* micelles shows a NMR pattern which is very similar to the one recorded in $CDCl_3$ (Fig. 2a *vs.* 2b). No significant changes were observed in the ^{1}H NMR spectrum between 283 K and 330 K. As shown previously, the complexity of the NMR profile arises from the heterochirality of the three nitrogen stereocenters which leads to a nonsymmetrical C_1 calixtren-Zn complex.[17] Similarly to **1**·Zn^{2+} in $CDCl_3$, the downfield shift of the OMe signals of the incorporated complex (δ_{OMe} > 3.9 ppm in $CDCl_3$ and in D_2O)[19] suggests that these groups have been expelled

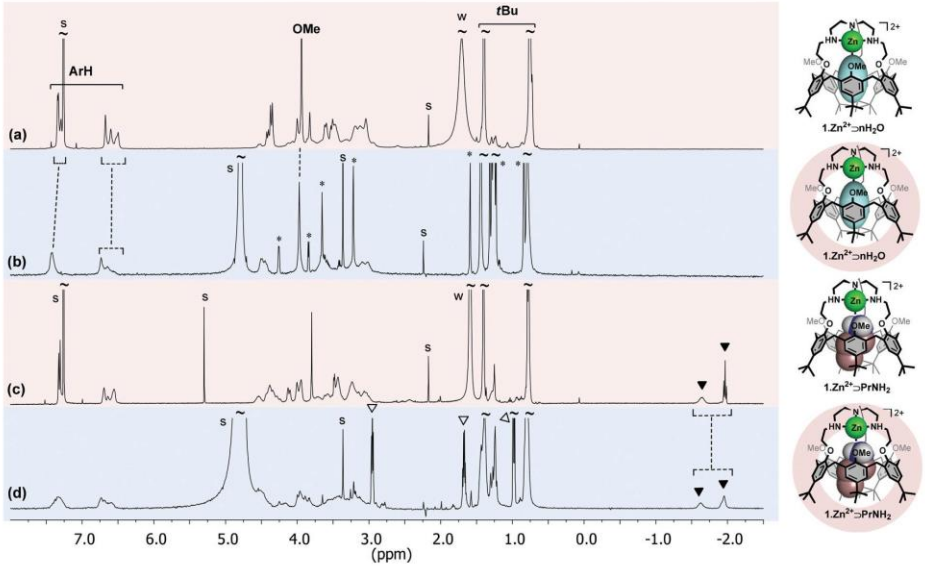

Fig. 2 ^{1}H NMR spectra (298 K) of (a) **1**·Zn^{2+} in $CDCl_3$ (600 MHz); (b) **1**·Zn^{2+} in DPC-*d38* (20 mM in D_2O at pH ~7.6, 600 MHz); (c) **1**·Zn^{2+} in $CDCl_3$ after the addition of ~1 equiv. of $PrNH_2$ (400 MHz); (d) **1**·Zn^{2+} in DPC-*d38* (20 mM in D_2O at pH ~8.6) after the addition of 5 equiv. of $PrNH_2$ (600 MHz). ▼: $PrNH_2$ in; ▽: $PrNH_2$ out; *: residual DPC; s: solvent; w: water.

View Article Online
Organic & Biomolecular Chemistry Paper

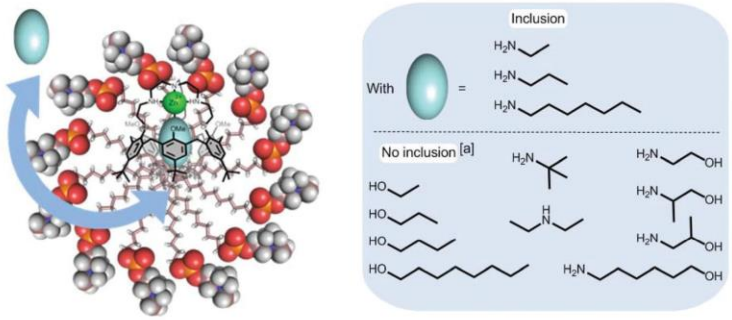

Fig. 3 Summary, using a schematic representation, of the host–guest properties of the receptor **1·Zn²⁺** incorporated in DPC micelles. [a]: see ESI† for experimental conditions.[21]

from the cavity by a coordinated solvent water molecule.[20] Two very distinct sets of signals can be observed for the *t*Bu as well as for the Ar*H* protons, indicating that the calixarene adopts a major flattened cone conformation. The incorporation of **1·Zn²⁺** inside the DPC micelles was unambiguously confirmed by DOSY NMR experiments as both receptor and micelle exhibit the same diffusion coefficient, corresponding to a hydrodynamic radius of ~2 nm.[21] Moreover, knowing that the micellar aggregation number is around 50,[22] it is reasonable to estimate that there is 1 molecule of complex **1·Zn²⁺** per micelle.

In order to gain information about the position of **1·Zn²⁺** in the micelle, paramagnetic relaxation enhancement (PRE) experiments were undertaken.[23] It is indeed possible to obtain reliable information on the localization of receptors in micelles by comparing the PRE data obtained for the receptor protons with those for the surfactant protons.[10] When plotting the relaxation rate enhancement as a function of paramagnetic species concentration, a linear relationship was obtained and the slope, known as the relaxivity, was extracted. The normalized relaxivities for the aromatic and *t*Bu protons of **1·Zn²⁺** have values similar to those of the tail of the surfactant but very different from those of the hydrophilic part.[21] It was thus possible to conclude that the calixarene positions itself in the hydrophobic core. Interestingly, the spectrum of **1·Zn²⁺** in DPC micelles was not significantly modified by the addition of DCl or NaOD in the pH range from 6 to 9, highlighting the stability of the system in this pH window.[24]

The calix[6]tren ligand **1** was also successfully incorporated into DPC micelles, by simple mixing in D_2O of the receptor and the surfactant, as attested by the NMR spectrum.[21] It was however necessary to lower the pH to ~3, showing that the ligand must be protonated at the level of its basic tren cap (**1·*n*H⁺**) in order to be incorporated.[25] This result suggests that the favourable electrostatic interaction of the positively charged **1·*n*H⁺** and **1·Zn²⁺** with the phosphate group of the zwitterionic surfactant is a driving force for their incorporation (Fig. 3). It is noteworthy to mention that the OMe groups of the incorporated receptor **1·*n*H⁺** are pointing inside the cavity (δ_{OMe} = 2.41 ppm), clearly highlighting the absence of a guest molecule inside the cavity. The efficient incorporation of **1·*n*H⁺** and **1·Zn²⁺** into DPC micelles encouraged us to undertake host–guest complexation studies with these systems.

Guest complexation by 1·Zn²⁺ in DPC micelles

Propylamine ($PrNH_2$) is known to display a high affinity for **1·Zn²⁺** in $CDCl_3$.[17] A titration with $PrNH_2$ of the receptor in DPC micelles was monitored by ^1H NMR spectroscopy. As the DPC solution was not buffered, the addition of the amine increased the pH somewhat during the titration (from 7.6 to 8.6). The following observations can be made from the spectrum recorded with the addition of 5 equiv. of $PrNH_2$ (pH = 8.6) (Fig. 2d):

(i) High-field signals for the protons of the alkyl chain of $PrNH_2$ (*i.e.* −1.62 and −1.95 ppm) attest of its inclusion inside the cavity and thus of the formation of the complex **1·Zn²⁺ ⊃ PrNH₂**. These chemical shifts are similar to those obtained with the same system in $CDCl_3$ suggesting a similar positioning of the guest in the cavity (Fig. 2c *vs.* 2d). The exchange process is slow on the NMR chemical shift timescale.

(ii) There are only small changes in the chemical shifts of the aromatic and *t*Bu calixarene protons, which shows that the conformation of the receptor essentially does not change upon inclusion of a small amine such as propylamine. The receptor maintains a flattened cone conformation clearly evidenced by the large difference between the resonances of the *t*Bu or Ar*H* protons pointing inside and pointing outside the cavity ($\Delta\delta_{tBu}$ ~ 0.65 ppm and $\Delta\delta_{ArH}$ ~ 0.67 ppm).

These NMR data show that the host–guest properties of **1·Zn²⁺** toward amines are maintained in the micellar environment (Fig. 3). An apparent binding constant for propylamine (K_{app}) of ~5×10^3 M^{-1} for a 1 : 1 binding was determined by signal integration at pH ~ 8.[26] At pH ~10, this constant was estimated to be >10^4 M^{-1}. The complex **1·Zn²⁺ ⊃ PrNH₂** was observed on a larger pH window (pH from ~3 to ~11) in the micelle than complex **1·Zn²⁺** devoid of organic guest coordinated to the Zn atom (*vide supra*). From these data, a *pseudo* pK_a of ~4.3 for complexed propylamine could be esti-

mated.[21] This value can be compared to the pK_a value of free propylamine of 10.6. This remarkable result shows the extraordinary stabilization of the amine due to its complexation to the metal cation inside the calixarene cavity. This pK_a shift is comparable to the one estimated for heptylamine with a related water-soluble Zn-calixarene receptor bearing imidazole moieties.[27] It is interesting to point out that this related receptor does not complex $PrNH_2$ in water, which highlights the role played by the micellar environment on the complexation properties of the calix[6]tren-based system.

Complex **1·Zn^{2+}** in DPC micelles also binds ethylamine ($EtNH_2$) and heptylamine ($HeptylNH_2$) as evidenced by the presence of high field signals for their alkyl chain protons in the ^{1}H NMR spectra.[21] The affinity constants for these amines relative to $PrNH_2$ were evaluated by competition experiments (Table 1)[28] and the following sequence of affinities was observed at pH ~ 11.1 (±0.1): $EtNH_2$ > $PrNH_2$ > $HeptylNH_2$. They are all of the same order of magnitude, with, however, a significant advantage to the smallest amine, in spite of its lower lipophilicity. This may be explained by a better fit of the guest considering the volume of the calix[6]arene cone as defined by the *t*Bu substituents at the large rim. Indeed, with other related *p*-*t*Bu-substituted calix[6]arene-based metal complexes studied in chloroform, it has been shown that 3- and 4-atom length guests that are fully encapsulated in the cavity (as shown here by the high-field shifted ^{1}H-NMR signals), display the highest affinities. In contrast, the alkyl chain of the larger amino guest has to protrude outside the cavity and, in order to avoid a steric clash with the *t*Bu groups, the calix[6]-arene skeleton is forced to adopt an energetically less favourable straight conformation.[29] Finally, it is interesting to note that the relative affinity for $HeptylNH_2$ (*vs.* $PrNH_2$) in the micellar solution is spectacularly much higher than the one measured in $CDCl_3$ (*i.e.* 0.5 *vs.* 0.00025). Such a difference may well reflect the benefit of the hydrophobic effect for lipophilic amine binding in water.

Very interestingly, the binding of $tBuNH_2$ as well as the secondary amine $(Et)_2NH$ was not observed (from pH ~ 8 to pH ~ 11) despite the fact that these amines are less hydrophilic than $EtNH_2$ or $PrNH_2$. This result shows that steric hindrance at the level of amino group is a major factor of selectivity and thus highlights the cavity-based selectivity ensured by the incorporated receptor. The complexation of other families of guests such as alcohols (ethanol, propanol, butanol, octanol) and aminoalcohols (ethanolamine, (±)-1-amino-2-propanol, (±)-2-amino-1-propanol, 6-amino-1-hexanol) was also studied. Again, no sign of inclusion was evidenced for any of these guests (Fig. 3). The fact that octanol, which should like heptylamine benefit from the hydrophobic effect, is not complexed by the calixarene suggests that the amino group plays a key role for complexation. It has indeed been shown that the affinity of **1·Zn^{2+}** for ethanol in $CDCl_3$ is four orders of magnitude lower than for propylamine ($K_{EtOH/PrNH_2}$ ~2.5×10^{-4}).[17] In order to understand why the aminoalcohols, and in particular the small ethanolamine, are not recognized by **1·Zn^{2+}** incorporated into DPC micelles, the affinity for ethanolamine was measured in $CDCl_3$. The relative affinity compared to $PrNH_2$ was determined to be close to 1 ($K_{PrNH_2/Ethanolamine}$ ~0.8, see Table 1). Such a discrepancy between the results obtained in water/micelle conditions and in an organic solvent is also assignable to the hydrophobic effect that obviously plays a major role in the host–guest recognition processes and in the observed selectivities. In this context, it is worth pointing out that DOSY experiments undertaken with DPC solutions showed that $PrNH_2$ does not incorporate into the DPC micelles but that $HeptylNH_2$ co-micellizes. The diffusion coefficient of $PrNH_2$ in the presence of DPC micelles is indeed identical to the diffusion coefficient of the amine in D_2O and this is not the case for $HeptylNH_2$ which clearly partitions itself between the aqueous and micellar environments. This difference can be rationalized in terms of the hydrophobicity of the amines which are more hydrophobic with increasing chain length.

Table 1 Affinities, relative to $PrNH_2$ (pK_a = 10.58), of various guests G for host **1·Zn^{2+}**

	Relative affinities[a]	
G (pK_a)[b]	DPC (20 mM in D_2O)	$CDCl_3$
$EtNH_2$ (10.67)	1.3 (pH ~ 11.1)	—
$HeptylNH_2$ (10.65)	0.5 (pH ~ 11.2)	~0.00025
$HO(CH_2)_2NH_2$ (9.50)	n.d.[c] (pH ~ 9.4)	0.8

[a] Defined as $[G_{in}]/[PrNH_{2in}] \times [PrNH_{2Free}]/[G_{Free}]$ and measured at 298 K. The subscript "in" stands for "included". Errors estimated ±20%. [b] For the pK_a values, see ref. 30. [c] Not detected with up to 50 equiv. of $HO(CH_2)_2NH_2$.

Guest complexation by 1·*n*H$^+$ into DPC micelles

We have previously shown that calix[6]arene-based receptors bearing either a polyammonium,[31] polyamido[32] or polyureido cap[33] can bind with a high affinity the neutral guest 2-imidazolidinone (Imi) in their cavity. As shown on the XRD structure of one of these host–guest systems,[34] the high affinity for Imi stems from a complementary DAAD-ADDA quadruple H-bonding array between the urea guest and the calixarene host. Imi is also recognized by the protonated calixtren derivative **1·*n*H$^+$** in $CDCl_3$ and, to date, behaves as the best "key" for this receptor.[35] The binding of this neutral guest was thus evaluated in the micellar environment by NMR spectroscopy. It was observed that Imi (~230 equiv.) is not recognized by **1·Zn^{2+}** incorporated in DPC micelles (from pH ~8 to ~11). However, **1·*n*H$^+$** incorporated in DPC micelles at low pH complexes Imi under a slow exchange regime on the NMR chemical shift timescale. A singlet at 0.22 ppm is observed for the two methylene groups of the included Imi and an impressive downfield shift of the signal corresponding to the OMe groups ($\Delta\delta_{OMe}$ = 1.35 ppm) attests to the ejection of these groups from the cavity upon guest inclusion. A large excess of Imi (40 equiv.), which is very soluble in water, was however required to observe the binding. Unfortunately, the addition of Imi also leads to a pH increase and ultimately to a partial

View Article Online
Organic & Biomolecular Chemistry Paper

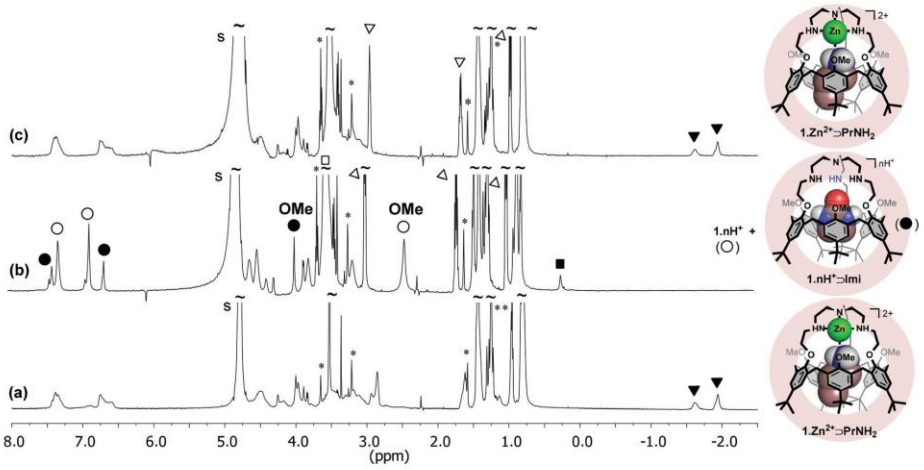

Fig. 4 ^{1}H NMR spectra (600 MHz, 298 K, DPC-*d38* 20 mM in D_2O) of (a) complex **1·Zn^{2+}** in the presence of ~4.5 equiv. of $PrNH_2$ and ~4 equiv. of Imi (pH = 10.5); (b) after the subsequent addition of DCl and ~106 equiv. of Imi (pH = 3.1); (c) after the subsequent addition of NaOD (pH = 8.8). ▼: $PrNH_2$ in; ▽: $PrNH_2$ out; ■: Imi in; □: Imi out; ●: **1·*n*H$^+$** ⊃ **Imi**; ○: **1·*n*H$^+$**; s: solvent.

deprotonation of receptor **1**. As a result, quantitative formation of the complex **1·*n*H$^+$** ⊃ **Imi** was difficult to achieve. From signal integration, the binding constant is estimated to be lower than 10 M^{-1} at pH = 5.3.

Reversible interconversion of host–guest adducts **1·Zn^{2+}** ⊃ **PrNH$_2$** and **1·*n*H$^+$** ⊃ **Imi**

In $CDCl_3$, the quantitative acid–base induced interconversion of complexes **1·Zn^{2+}** ⊃ **EtOH** and **1·*n*H$^+$** ⊃ **EtOH** was previously reported.[17] In order to see if such a supramolecular switching process can be transposed into water and triggered by a pH change, the inter-conversion of the **1·Zn^{2+}** ⊃ **PrNH$_2$** and **1·*n*H$^+$** ⊃ **Imi** host–guest adducts incorporated into DPC micelles was tested (Fig. 4). First, $PrNH_2$ (4.5 equiv.) and Imi (4 equiv.) were added to a solution of **1·Zn^{2+}** in DPC micelles and the resulting NMR spectrum (pH = 10.5) clearly showed the exclusive formation of **1·Zn^{2+}** ⊃ **PrNH$_2$** (Fig. 4a). Fig. 4b shows the spectrum of the same solution at pH 3.1 after the addition of DCl and a large excess of Imi (~106 equiv.) It evidences the disappearance of complex **1·Zn^{2+}** ⊃ **PrNH$_2$** and the formation of **1·*n*H$^+$** ⊃ **Imi** together with some free protonated receptor **1·*n*H$^+$**. The subsequent addition of NaOD (to reach pH = 8.8) restored very easily the initial NMR profile corresponding to **1·Zn^{2+}** ⊃ **PrNH$_2$** (Fig. 4c). This experiment highlights that the host–guest properties of receptor **1** can be nicely tuned and controlled by the pH.

Conclusion

In summary, we have shown that a calix[6]azacryptand (**1**) can be incorporated into DPC micelles either as a Zn^{2+} complex in the [6–9] pH window or as a polyammonium at low pH. The **1·Zn^{2+}** complex, incorporated into DPC micelles, is able to host selectively small or long linear primary amines with high affinity constants. This corresponds to one of the rare examples of systems capable of recognising primary amines in water media.[36] Interestingly, the host–guest complex **1·Zn^{2+}** ⊃ **PrNH$_2$** was detected in the micelles in an even larger pH window (3–11) than was the **1·Zn^{2+}** host itself, which shows that the presence of the amine strengthens the complex even at very low pH where the free amine is fully protonated in water. Moreover, we observed a quite remarkable *pseudo* pK_a shift of propylamine recognised by **1·Zn^{2+}** in DPC micelles (from 10.6 to 4.3). This impressive stabilisation of the basic form of propylamine is the result of its coordination to Zn^{2+} but also the environment provided by the calixarene cavity and the micelle which protects the system from the water. The **1·Zn^{2+}** complex preferentially binds small amines and this size selectivity stands in strong contrast with the previously reported water-soluble calixarene-based Zn^{2+} complex for which hydrophobic amine binding could be detected, but not with small hydrophilic ones.[27] With free receptor **1**, no amine binding was detected even at low pH. However, an entrapped urea guest (*i.e.* Imi) could be observed, though only at a high concentration. Interestingly, a pH driven guest switch was evidenced with **1·Zn^{2+}** in the presence of both an amine and Imi: at high pH, the Zn^{2+} complex binds the amine, at low pH the amino arms are protonated, which leads to the decoordination of the metal ion and the embedment of Imi. All in all, these results validate the very simple strategy that consists of incorporating an organo-soluble receptor in micelles to obtain water compatible nanosized supramolecular recognition devices. Efforts are now being directed towards the design of calixarene-based sensing systems incorporated in micelles.

View Article Online
Paper Organic & Biomolecular Chemistry

Experimental section

Chemicals

DPC and DPC-*d38* were purchased from Avanti Lipids and used with no further purification. D_2O and $CDCl_3$ were purchased from VWR BDH PROLABO. Compounds **1** and **1·Zn^{2+}** were synthesized according to the literature.[15,16]

General procedures

^{1}H NMR spectra were recorded on a 600 MHz, 400 MHz or a 300 MHz spectrometer. For the 1D ^{1}H spectra, parameters (acquisition time, recycling times, and signal accumulation) were chosen so as to ensure that quantitative data could be obtained from signal integration. Traces of residual solvents were used as internal chemical shift references. Chemical shifts are quoted on the δ scale. The NMR spectra were recorded at 298 K unless otherwise stated.

NMR solutions preparation

All solutions for NMR studies were prepared following a similar protocol: **1·Zn^{2+}** (~4 mg) and DPC (~35 mg, deuterated or not depending on the experiments) were added to 5 mL of D_2O in order to have, respectively, concentrations of ~0.5 mM and ~20 mM. Solutions were stirred until a clear solution was obtained.

^{1}H NMR characterization of various complexes 1·Zn^{2+} ⊃ *n*H_2O

^{1}H NMR (DPC 20 mM in D_2O, 298 K, 600 MHz): δ (ppm) 0.79 (bs, 27H, *t*Bu), 1.44 (bs, 27H, *t*Bu), 3.97 (bs, 9H, OMe), 2.87–4.61 (m, 24H, $ArCH_2^{eq}/ArCH_2^{ax}/CH_2N/CH_2O$), 6.49–6.81 (m, 6H, ArH^{OMe}), 7.40 (bs, 6H, ArH^{cap}). **1·Zn^{2+} ⊃ PrNH$_2$**: ^{1}H NMR (DPC 20 mM in D_2O, 298 K, 600 MHz): * δ (ppm) −1.95 (bs, 3H, $CH_3^{PrNH_2,in}$), −1.63 (bs, 2H, $CH_2^{PrNH_2,in}$), 0.74–0.87 (m, 27H, *t*Bu), 1.36–1.57 (m, 27H, *t*Bu), 2.99–4.68 (m, 33H, $ArCH_2^{eq}/ArCH_2^{ax}/CH_2N/CH_2O$/OMe), 6.49–6.99 (m, 6H, ArH^{OMe}), 7.22–7.51 (m, 6H, ArH^{cap}). * The chemical shift of the CH_2N of $PrNH_2$ (in) was not observed due to overlapped signals.

Determination of the apparent affinity of PrNH$_2$ toward complex 1·Zn^{2+} through ^{1}H NMR titration in DPC (20 mM in D_2O)

Different aliquots of a solution of amine ($PrNH_2$) were progressively added to 500 μL of a DPC solution (20 mM in D_2O) containing the complex **1·Zn^{2+}**. Non-deuterated DPC was used and the integration of the $CH_{2\beta}$ and $CH_{2\gamma}$ signals were used as internal reference to determine the concentration of **1·Zn^{2+}**. The integrations of the free guests and of the included guests were used to calculate the apparent affinity defined as $[PrNH_{2in}]/(1 - [PrNH_{2in}]\,[PrNH_{2Free}][\mathbf{1{\cdot}Zn^{2+}}])$ (errors estimated ±20%).

Determination of the relative affinities of heptyl- and ethylamine compared to propylamine through ^{1}H NMR competitive binding studies in DPC (20 mM in D_2O)

At room temperature, ~7 equivalents of heptylamine ($HeptylNH_2$) or ~3 equivalents of ethylamine ($EthylNH_2$) were added to 500 μL of a DPC solution (20 mM in D_2O) containing the complex **1·Zn^{2+}**. Propylamine ($PrNH_2$) was then added (~5 equivalent). The ^{1}H NMR spectrum showed the guest resonances of both complexes **1·Zn^{2+} ⊃ PrNH$_2$** and **1·Zn^{2+} ⊃ HeptylNH$_2$** or **1·Zn^{2+} ⊃ EthylNH$_2$** and signals corresponding to the free amines. The integrations of the signals corresponding to the free guests and included guests were used to calculate relative affinity defined as $[G_{in}]/[PrNH_{2in}] \times [PrNH_{2Free}]/[G_{Free}]$ (errors estimated ±20%).

Determination of the relative affinity of ethylamine compared to propylamine in $CDCl_3$ *via* ^{1}H NMR competitive binding studies

At room temperature, ~30 equivalents of propylamine ($PrNH_2$) and ~15 equivalents of ethylamine ($EthylNH_2$) were added in 500 μL of a $CDCl_3$ solution of complex **1·Zn^{2+}**. A ^{1}H NMR spectrum showed the guest resonances of both complexes **1·Zn^{2+} ⊃ PrNH$_2$** and **1·Zn^{2+} ⊃ EthylNH$_2$** and signals corresponding to the free amines. The integrations of the signals corresponding to free guests and the included guests were used to calculate relative affinity defined as $[EtNH_{2in}]/[PrNH_{2in}] \times [PrNH_{2Free}]/[EtNH_{2Free}]$ (errors estimated ±20%).

Determination of the relative affinity of heptylamine compared to DMF in $CDCl_3$ *via* ^{1}H NMR competitive binding studies

At room temperature, ~40 equivalents of dimethylformamide (DMF) and ~100 equivalents of heptylamine ($HeptylNH_2$) were added in 500 μL of a $CDCl_3$ solution of complex **1·Zn^{2+}**. A ^{1}H NMR spectrum showed the guest resonances of both complexes **1·Zn^{2+} ⊃ DMF** and **1·Zn^{2+} ⊃ HeptylNH$_2$** and the signals corresponding to free DMF and $HeptylNH_2$. The integrations of the signals corresponding to the free and included guests were used to calculate relative affinity defined as $[DMF_{in}]/[HeptylNH_{2in}] \times [HeptylNH_{2Free}]/[DMF_{Free}]$ (errors estimated ±20%). In order to obtain the value corresponding to $K_{PrNH_2/HeptylNH_2}$, we used the value for $K_{PrNH_2/DMF}$ from ref. 17 (1610).

Reversible interconversion of host–guest adducts 1·Zn^{2+} ⊃ PrNH$_2$ and 1·nH$^+$ ⊃ Imi

$PrNH_2$ (4.5 equiv.) and Imi (4 equiv.) were added to a ~0.5 mM solution of **1·Zn^{2+}** in DPC-*d38* micelles (pH ~10.5). In a second stage, DCl and a large excess of Imi (~106 equiv.) were added to the system (pH ~3.1). In the final stage, NaOD was added to reach pH = 8.8.

DOSY experimental parameters

15 values for the magnitude of the gradient pulses (ranging from 2 G cm^{-1} to 50 G cm^{-1}), diffusion delay 50 ms, time-length of the gradient 5 ms, acquisition time 2 s, relaxation delay 7 s, 32 transients.

PRE experimental parameters

For the PRE experiments, aliquots of 5 µl of a 5 mM solution of $K_3[Cr(CN)_6]$ in D_2O were added to the 600 µl solution under study. T1 measurements were undertaken using the classical inversion recovery (180 – τ – 90 – acquisition) sequence, with 15 points and the delay varying between 0 and 7 s. For each signal monitored, the increase in the longitudinal relaxation rate induced by the paramagnetic species ($\Delta 1/T_1$; the difference between the longitudinal relaxation rate measured in the presence and in the absence of the paramagnetic species) was plotted as a function of the concentration of paramagnetic species. A linear regression was undertaken with the experimental data points from which the relaxivity value was derived (slope of the line).

Acknowledgements

E. B., A. I. and F. K. have a PhD grant from the Fonds pour la formation à la Recherche dans l'Industrie et dans l'Agriculture (FRIA-FRS, Belgium). This research was supported by the Fonds de la recherche scientifique (FNRS; FRFC 2.4.617.10.F project), the Agence Nationale de la Recherche (ANR10-BLAN-714 Cavity-zyme(Cu) project), and undertaken within the framework of the COST Action CM1005 "Supramolecular Chemistry in Water".

Notes and references

1 (*a*) J.-M. Lehn, in *Supramolecular Chemistry*, Wiley-VCH, Weinheim, 1995; (*b*) J. W. Steed, D. R. Turner and K. J. Wallace, in *Core Concepts in Supramolecular Chemistry and Nanochemistry*, Wiley-VCH, Chippenam, 2007; (*c*) J. Hartley, T. D. James and C. J. Ward, *J. Chem. Soc., Perkin Trans. 1*, 2000, 3155–3184.

2 B. Valeur and J. C. Brochon, *New Trends in Fluorescence Spectroscopy: Applications to Chemical and Life Sciences*, Springer, Berlin, 2001.

3 G. V. Oshovsky, D. N. Reinhoudt and W. Verboom, *Angew. Chem., Int. Ed.*, 2007, **46**, 2366–2393.

4 J. Szejtli, *Chem. Rev.*, 1998, **98**, 1743–1753.

5 J. Lagona, P. Mukhopadhyay, S. Chakrabarti and L. Isaacs, *Angew. Chem., Int. Ed.*, 2005, **44**, 4844–4870.

6 P. Sinaÿ and M. Sollogoub, *Chem. Commun.*, 2006, 1112–1114.

7 (*a*) W. Chu and C. Y. Kwan, *Chemosphere*, 2003, **53**, 9–15; (*b*) C. e O. Rangel-Yagui, A. Pessoa and L. C. Tavares, *J. Pharm. Pharm. Sci.*, 2005, **8**, 147–163; (*c*) M. Ding, J. Li, H. Tan and Q. Fu, *Soft Matter*, 2012, **8**, 5414–5428.

8 (*a*) N. Basilio, M. Martín-Pastor and L. García-Río, *Langmuir*, 2012, **28**, 6561–6568; (*b*) S. Uchiyama, K. Iwai and A. P. de Silva, *Angew. Chem., Int. Ed.*, 2008, **47**, 4667–4669; (*c*) F. Su, R. Alam, Q. Mei, Y. Tian, C. Youngbull and R. H. Johnson, *PLoS One*, 2012, **7**, 1–7; (*d*) Y. J. Kim, M. T. Lek and M. P. Schramm, *Chem. Commun.*, 2011, **47**, 9636–9638; (*e*) T. Riis-Johannessen and K. Severin, *Chem. – Eur. J.*, 2010, **16**, 8291–8295.

9 S. Javor and J. Rebek, *J. Am. Chem. Soc.*, 2011, **133**, 17473–17478.

10 (*a*) F. Keymeulen, P. De Bernardin, A. Dalla Cort and K. Bartik, *J. Phys. Chem. B*, 2013, **117**, 11654–11659; (*b*) M. Cametti, A. Dalla Cort and K. Bartik, *ChemPhysChem*, 2008, **9**, 2168–2171.

11 A. Dalla Cort, G. Forte and L. Schiaffino, *J. Org. Chem.*, 2011, **76**, 7569–7572.

12 D. Coquière, S. Le Gac, U. Darbost, O. Sénèque, I. Jabin and O. Reinaud, *Org. Biomol. Chem.*, 2009, **7**, 2485–2500.

13 C. D. Gutsche, in Calixarenes: An introduction, *Monographs in Supramolecular Chemistry*, ed. J. F. Stoddart, The Royal Society of Chemistry, Cambridge, 2nd edn, 2008.

14 (*a*) J.-N. Rebilly and O. Reinaud, *Supramol. Chem.*, 2014, **26**, 454–479; (*b*) J.-N. Rebilly, B. Colasson, O. Bistri, D. Over and O. Reinaud, *J. Chem. Soc. Rev.*, 2015, **44**, 467–489.

15 I. Jabin and O. Reinaud, *J. Org. Chem.*, 2003, **68**, 3416–3419.

16 (*a*) G. Izzet, J. Zeitouny, H. Akdas-Killig, Y. Frapart, S. Ménage, B. Douziech, I. Jabin, Y. Le Mest and O. Reinaud, *J. Am. Chem. Soc.*, 2008, **130**, 9514–9523; (*b*) G. Izzet, B. Douziech, T. Prangé, A. Tomas, I. Jabin, Y. Le Mest and O. Reinaud, *Proc. Natl. Acad. Sci. U. S. A.*, 2005, **102**, 6831–6836; (*c*) U. Darbost, X. Zeng, M.-N. Rager, M. Giorgi, I. Jabin and O. Reinaud, *Eur. J. Inorg. Chem.*, 2004, 4371–4374.

17 U. Darbost, M.-N. Rager, S. Petit, I. Jabin and O. Reinaud, *J. Am. Chem. Soc.*, 2005, **127**, 8517–8525.

18 This value is far above the critical micellar concentration (cmc = 1.1 mM). See: R. Stafford, T. Fanni and E. Dennis, *Biochemistry*, 1989, **28**, 5113–5120.

19 The assignment of the OMe signal was confirmed by a NMR HSQC experiment.

20 Similarly to related complexes, the presence of a second water guest, H-bonded to the coordinated one, is likely. See: O. Sénèque, M.-N. Rager, M. Giorgi and O. Reinaud, *J. Am. Chem. Soc.*, 2001, **123**, 8442–8443.

21 See the ESI.†

22 T. Lazaridis, B. Mallik and Y. Chen, *J. Phys. Chem. B*, 2005, **109**, 15098–15106.

23 R. B. Lauffer, *Chem. Rev.*, 1987, **87**, 901–927.

24 Note that all pH values have been measured in D_2O solutions.

25 Note that studies undertaken with the tren ligand in water have shown that, at pH ~ 3, the ligand is protonated at least three times. See: J. W. Canary, J. Xu, J. M. Castagnetto, D. Rentzeperis and L. A. Marky, *J. Am. Chem. Soc.*, 1995, **117**, 11545–11547.

26 As the DPC solution was not buffered, it is therefore difficult to discuss this binding constant quantitatively.

27 O. Bistri, B. Colasson and O. Reinaud, *Chem. Sci.*, 2012, **3**, 811–818.

28 All measurements were conducted in pure water, *i.e.* in absence of buffer in order to avoid any interaction with the complex and micelles that could alter the results.

29 (*a*) O. Sénèque, M.-N. Rager, M. Giorgi and O. Reinaud, *J. Am. Chem. Soc.*, 2000, **122**, 6183–6189; (*b*) E. Brunetti, J.-F. Picron, K. Flidrova, G. Bruylants, K. Bartik and I. Jabin, *J. Org. Chem.*, 2014, **79**, 6179–6188.

30 H. C. Brown, D. H. McDaniel and O. Häfliger, in *Determination of Organic Structures by Physical Methods*, ed. E. A. Braude and F. C. Nachod, Academic Press, New York, 1955.

31 E. Garrier, S. Le Gac and I. Jabin, *Tetrahedron: Asymmetry*, 2005, **16**, 3767–3771.

32 A. Lascaux, S. Le Gac, J. Wouters, M. Luhmer and I. Jabin, *Org. Biomol. Chem.*, 2010, **8**, 4607–4616.

33 (*a*) M. Ménand and I. Jabin, *Chem. – Eur. J.*, 2010, **16**, 2159–2169; (*b*) D. Cornut, J. Marrot, J. Wouters and I. Jabin, *Org. Biomol. Chem.*, 2011, **9**, 6373–6384.

34 S. Le Gac, J. Marrot, O. Reinaud and I. Jabin, *Angew. Chem., Int. Ed.*, 2006, **45**, 3123–3126.

35 S. Le Gac, I. Jabin and O. Reinaud, in *Bioinspiration and Biomimicry in Chemistry*, ed. G. Swiegers, Wiley-VCH, 2012, ch. 12.

36 (*a*) J. Kumpf and U. H. F. Bunz, *Chem. – Eur. J.*, 2012, **18**, 8921–8924; (*b*) G. Gattuso, A. Notti, S. Pappalardo, M. F. Parisi and I. Pisagatti, *Supramol. Chem.*, 2014, **26**, 597–600; (*c*) T. Mizutani, K. Wada and S. Kitagawa, *J. Org. Chem.*, 2000, **65**, 6097–6106; (*d*) E. K. Feuster and T. E. Glass, *J. Am. Chem. Soc.*, 2003, **125**, 16174–16175.

Electronic Supplementary Material (ESI) for Organic & Biomolecular Chemistry.

Supporting information

Primary Amine Recognition in Water by a Calix[6]aza-cryptand Incorporated in Dodecylphosphocholine Micelles

Emilio Brunetti, Alex Inthasot, Flore Keymeulen, Olivia Reinaud, Ivan Jabin and Kristin Bartik**

SI1. 2D DOSY experiment (298K, 600MHz, D_2O) with **1.Zn**$^{2+}$ in DPC

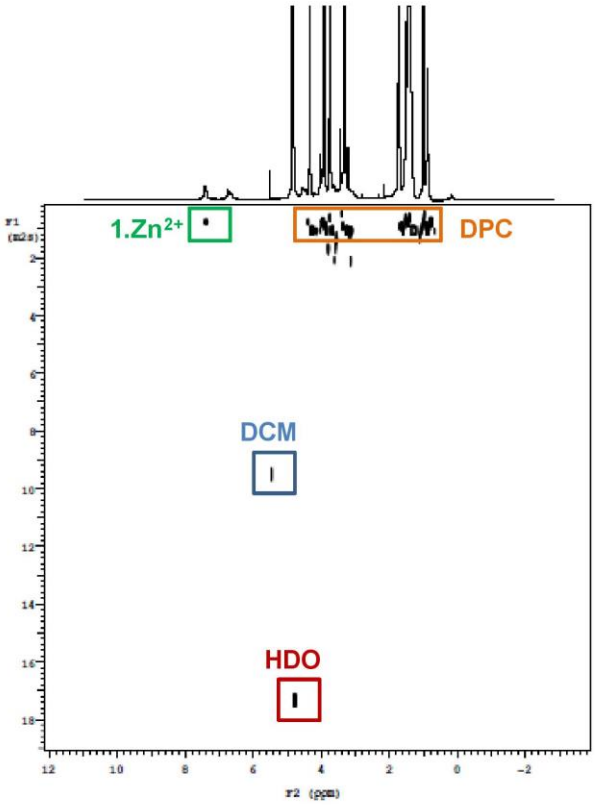

The x- and y- axis represent the regular ^1H chemical shift and the diffusion coefficient, respectively. DCM: residual dichloromethane; HDO: solvent signal chosen as reference for diffusion coefficient determination (D = 19.02x10^{-10} m^2/s at 298 K).

2

SI2. PRE NMR experiments (298K, 600MHz, D_2O) with **1.Zn^{2+}** in DPC

Normalized relaxivity (measured relaxivity divided by relaxivity of αCH_2 protons of the surfactant; φ; $mM^{-1}s^{-1;}$ error < 15%): values for the nuclei of DPC (20 mM) and for the nuclei of the incorporated complex **1.Zn^{2+}** (0.5 mM).

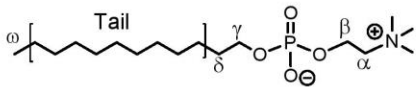

DPC

1.Zn^{2+}⊃nH_2O

$^{+}N(CH_3)_3$	α	β	γ	δ	Tail	ω	ArH^{cap}	$ArH2^{OMe}$	tBu^{OMe}
0.89	1	0.51	0.29	0.18	0.08	0.06	0.18	0.14	0.05

3

SI3. ^{1}H NMR (298K, 300MHz, D_2O) spectrum of **1.nH**$^+$ in DPC

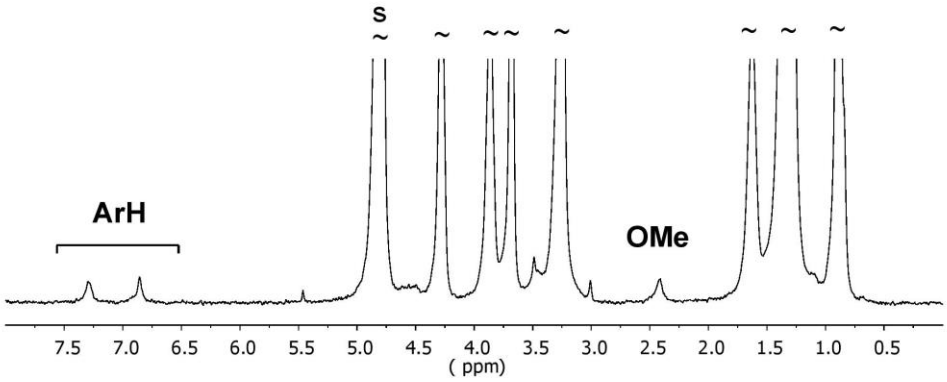

^{1}H NMR spectrum (300 MHz, 298 K) of **1.nH**$^+$ in DPC (20 mM in D_2O at pH ~3.1); s: solvent.

SI4. Determination of the *pseudo* pKa shift for $PrNH_2$

The formation constant K and K'_{pH} are defined according to the following equilibrium:

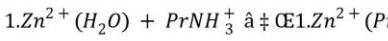

$$1.Zn^{2+}(H_2O) + PrNH_3^+ \hat{a}\ddagger \text{Œ} 1.Zn^{2+}(PrNH_2) + H_3O^+$$

$$K = \frac{\left[1.Zn^{2+}(PrNH_2)\right]\left[H_3O^+\right]}{\left[1.Zn^{2+}(H_2O)\right]\left[PrNH_3^+\right]}$$

$$K'_{pH} = \frac{\left[1.Zn^{2+}(PrNH_2)\right]}{\left[1.Zn^{2+}(H_2O)\right]\left[PrNH_3^+\right]}$$

From analysis and signal integration in the ^{1}H NMR spectra (see experimental section of article for details). K was found to be ~ $5x10^{-5}$ at pH ~8 and K'_{pH} ~5000 M^{-1}. From these data, we can estimate a *pseudo* pK_a (-log$K$) of ~4.3.

SI5. ^{1}H NMR (298K, 600MHz, D_2O) spectra of **1.Zn^{2+}** in the absence and presence of $EtNH_2$ in DPC-*d38*

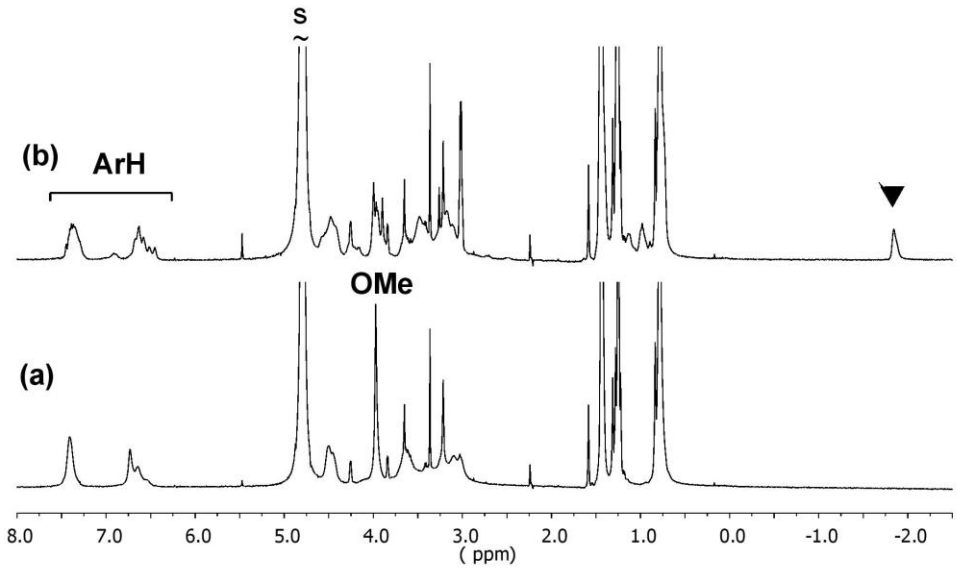

^{1}H NMR spectra (600 MHz, 298 K) of (a) **1.Zn^{2+}** in DPC-*d38* (20 mM in D_2O at pH ~7.6); (b) **1.Zn^{2+}** in DPC-*d38* (20 mM in D_2O) after the addition of ~3 equiv. of $EtNH_2$. ▼: $EtNH_2$ in; s: solvent.

6

SI6. ^{1}H NMR (298K, 600MHz, D_2O) spectra of **1.Zn^{2+}** in the absence and presence of HeptylNH$_2$ in DPC micelles.

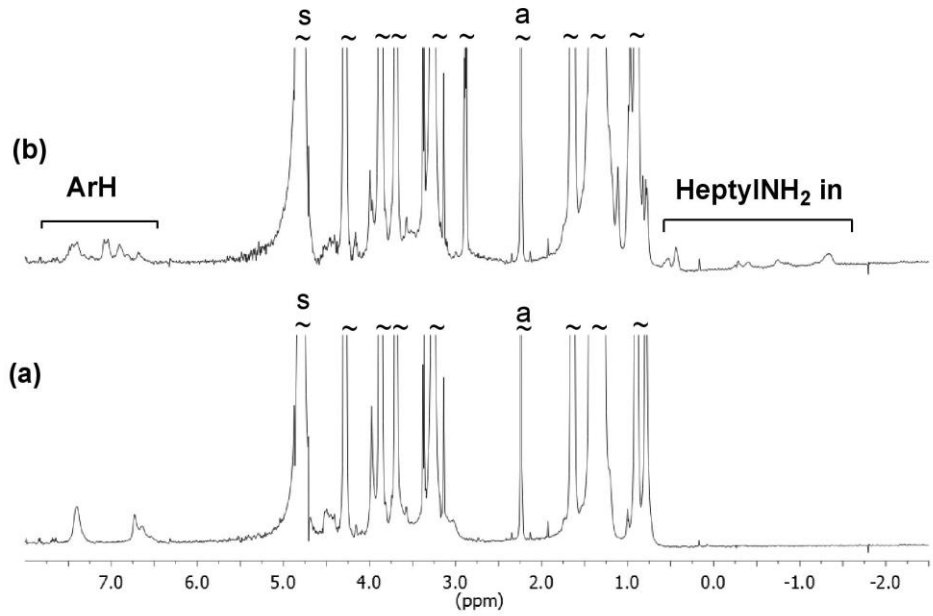

^{1}H NMR spectra (600 MHz, 298 K) of (a) **1.Zn^{2+}** in DPC (20 mM in D_2O at pH ~7.6); (b) **1.Zn^{2+}** in DPC (20 mM in D_2O) after the addition of ~7 equiv. of HeptylNH$_2$. s: solvent; a: acetone.

SI7. Experimental conditions for titrations of **1.Zn^{2+}** with amines, alcohols and aminoalcohols in DPC

The potential binding of different **guests** was monitored via ^{1}H NMR titration experiments at room temperature with ~0.5 mM solutions of **1.Zn^{2+}** in DPC (20 mM in D_2O). Progressive additions of the investigated potential guest, until the final concentration indicated below, were undertaken (pH monitored are also indicated). No signals for included guest were observed in the ^{1}H NMR spectra for the following molecules:

(i) *t*BuNH$_2$ up to 6 mM (pH ~7.8, ~10.4 and 11);
(ii) (Et)$_2$NH up to 15 mM (pH ~7.8 and 11). This amine added after the experiment undertaken in (i);
(iii) ethanol up to 365 mM (pH ~7.6);
(iv) propanol up to 340 mM (pH ~7.6);
(v) butanol up to 18 mM (pH ~7.6). This alcohol added after the experiment undertaken in (iv);
(vi) octanol up to 50 mM (pH ~7.6);
(vii) ethanolamine up to 25 mM (pH ~7.6);
(viii) (±)-1-amino-2-propanol up to 3.5 mM (pH ~6.0 and pH ~10.4);
(xi) (±)-2-amino-1-propanol up to 3.7 mM (pH ~5.5 and pH ~10.5);
(x) 6-amino-1-hexanol up to 10 mM (no pH value available);

3.5. MICELLAR INCORPORATION OF OTHER SYSTEMS

3.5.1. INCORPORATION OF A HOMOXACALIX[3]ARENE INTO DPC MICELLES

Homooxacalixarenes are closely related to calixarenes: the phenolic units are linked by CH_2OCH_2 groups instead of by methylene bridges.[21,22,23] The most studied member of this class of compounds is the hexahomotrioxacalix[3]arene shown in Figure 3-8.[24]

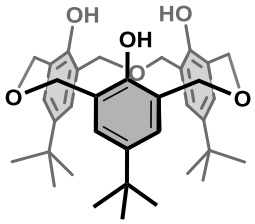

Figure 3-8. Structure of the *p-tert*-butyl-hexahomotrioxacalix[3]arene.

We synthesized, in collaboration with Sara Zahim (Jabin's laboratory), the homooxacalix[3]tris-acid **15** shown in Figure 3-9, using a protocol described in the literature.[25]

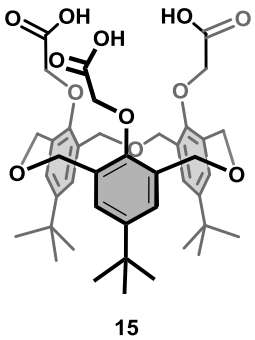

15

Figure 3-9. Structure of host **15**.

Previous results with a tris-acid calix[6]arene in chloroform have shown that ammonium ions can be bound in *endo* and *exo* and that the driving force is the favorable electrostatic interaction between the ammonium head and the carboxylate groups of the receptor. Upon titration with

[21] Vicens, J.; Asfari, Z.; Harrowfield, J., Calixarenes 50th Anniversary: Commemorative Issue; Eds.; Kluwer Academic Publishers: Dordrecht, **1995**.
[22] Gutsche, C. D.; Dhawan, B.; No, K. H.; Muthukrishnan, R. *J. Am. Chem. Soc.* **1981**, *103*, 3782.
[23] Zerr, P.; Mussrabi, M.; Vicens, J. *Tetrahedron Lett.* **1991**, *32*, 1879.
[24] Kang, J.; Cheong, N.-Y. *Bull. Korean Chem. Soc.* **2002**, *23*, 995-997.
[25] Hampton, P. D.; Bencze, Z.; Tong, W.; Daitch, C. E. *J. Org. Chem.* **1994**, *59*, 4838-4843; Takeshita, M.; Inokuchi, F.; Shinkai, S. *Tetrahedron Lett.* **1995**, *36*, 3341–3344; Ni, X. -L.; Rahman, S.; Zeng, X.; Hughes, D. L.; Redshaw, C.; Yamato, T. *Org. Biomol. Chem.* **2011**, *9*, 6535-6

$PrNH_2$, deprotonation of the carboxylic groups was observed and after three equivalent all the carboxylic groups were deprotonated; one $PrNH_3^+$ was complexed inside the cavity (*endo*) and two others in *exo* (Figure 3-10).[26]

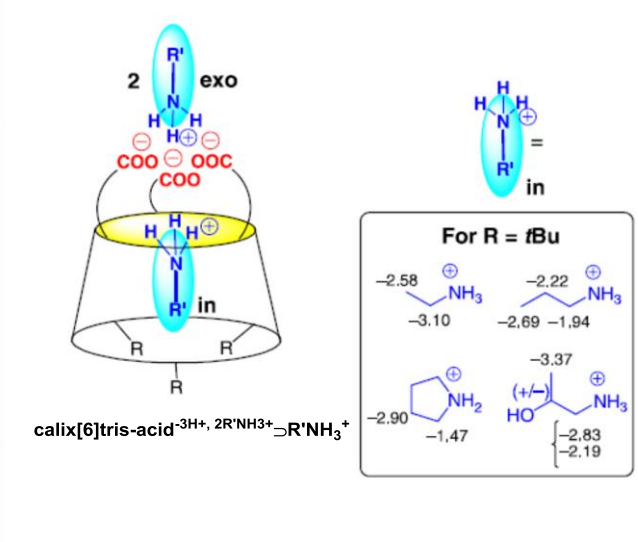

Figure 3-10. *Endo*-complexation of ammoniums ions by the tri-deprotonated calix[6]tris-acid in $CDCl_3$ and NMR complexation induced shifts of various ammonium guests (figure taken from reference 27).

15 was successfully incorporated into DPC micelles by simple mixing of the receptor and the surfactant (20 mM) in D_2O (pH ~8.6). Concentrations of up to 0.3 mM were obtained. The incorporation of **15** inside the DPC micelles was confirmed by DOSY NMR experiments as both receptor and surfactant exhibit the same diffusion coefficient.[27] As the system is incorporated in the micellar core, it is possible that it is only partly deprotonated which we will call $\mathbf{15}^{-n\mathbf{H}^+}$. A titration of the system would be needed to determine the exact pKa of the three carboxylic groups. The ^{1}H NMR spectrum of $\mathbf{15}^{-n\mathbf{H}^+}$ incorporated in DPC micelles shows a pattern very similar to the one recorded in $CDCl_3$ (Figure 3-11a-b). A single set of signals is observed for the *t*Bu as well as for the Ar*H* protons, indicating that the host adopts a C_{3v} symmetry both in $CDCl_3$ and in DPC micelles.

[26] Le Gac, S.; Giorgi, M.; Jabin, I. *Supramolecular Chemistry* **2007**, *19*, 185–197.
[27] The DOSY spectrum is presented in Appendix 2 (7.2).

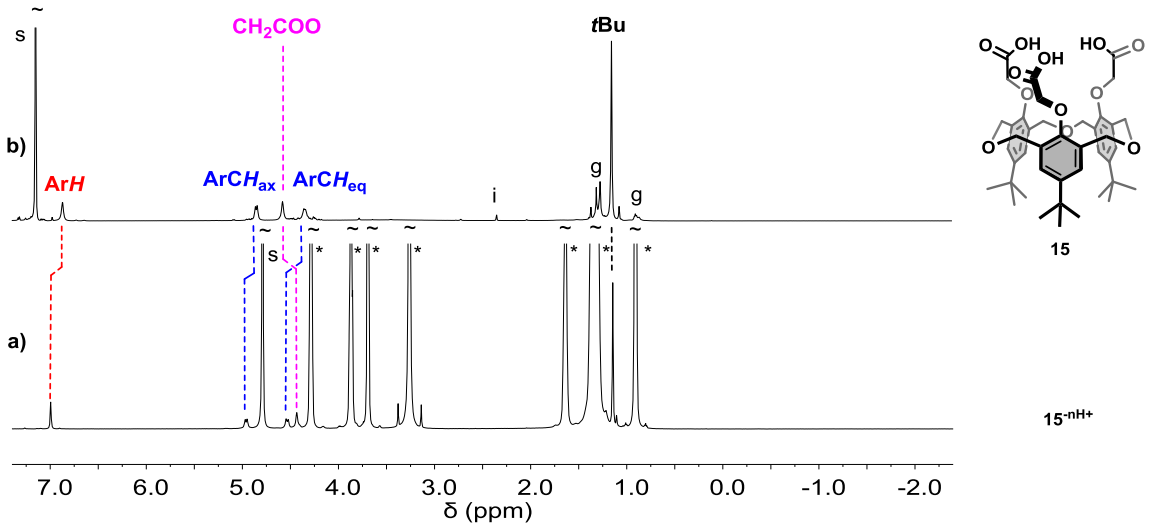

Figure 3-11. ^{1}H NMR spectra (298 K, 600 MHz) of: a) **15**$^{-nH+}$ in DPC (20 mM in D_2O at pH ~8.6); b) **15** in $CDCl_3$ (2.74 mM); *: DPC signals; s: solvent; g: grease; i: impurities.

The binding properties of **15**$^{-nH+}$ incorporated in DPC micelles, and more particularly the affinity of the system for ammonium ions, were investigated by NMR. The spectra recorded after the addition of *tert*-butylamine (*t*BuNH$_2$) to the system are shown in Figure 3-12.

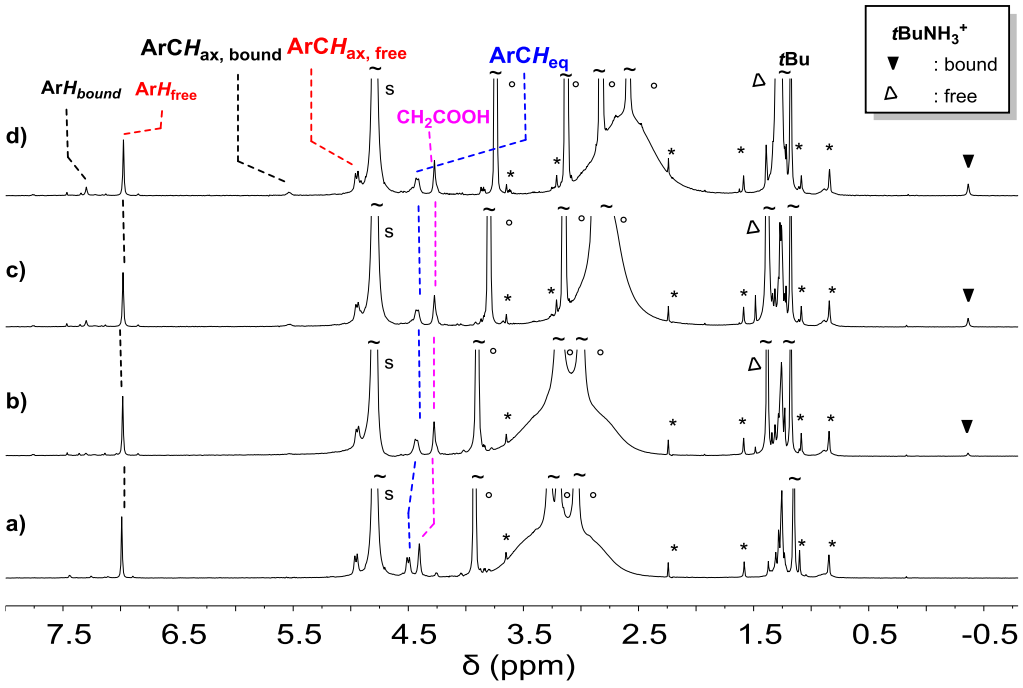

Figure 3-12. ^{1}H NMR spectra (298 K, 20 mM DPC-d_{38} in D_2O, 600 MHz, 11 mM HEPES) of **15**$^{-nH+}$: a) in the absence of *t*BuNH$_2$; b) in the presence of ~4.5 equiv. of *t*BuNH$_2$; c) in the presence of ~23 equiv. of *t*BuNH$_2$; c) in the presence of ~80 equiv. of *t*BuNH$_2$ at pH ~10.2; s: solvent; g: grease; *: residual traces of non-deuterated DPC; °: HEPES.

The poor buffering conditions meant that the pH of the solution increased from 4.8 to 10.2 upon addition of ~80 equiv. of the amine.[28] The high-field signals for the protons of the alkyl chain of *t*BuNH$_3^+$ (-0.37 ppm) in the ^{1}H NMR spectra (Figure 3-12), attest of its inclusion inside the cavity and thus of the formation of the complex **15**$^{-3H+}$⊃***t*BuNH$_3^+$**.[29] The inclusion of the guest was confirmed by a 1D EXSY experiment (Figure 3-13).

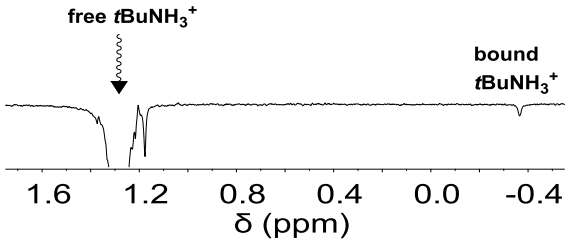

Figure 3-13. 1D EXSY spectrum in DPC-d$_{38}$ (20 mM in D$_2$O at pH ~10.2, 600 MHz) 11 mM HEPES after selective excitation (mixing time = 200 ms) of the CH$_3$ signal at 1.28 ppm host **15**$^{-nH+}$ in the presence of ~80 equiv. of *t*BuNH$_2$; ▼: Pulse excitation.

Upon addition of 0 to 11 equiv. of the guest, the signal of the host CH$_2$ protons next to the carboxylic/carboxylate groups shifts significantly to higher field (from 4.41 to 4.27 ppm) and then no longer shift, indicating complete deprotonation of the acid groups. Certain signals of the host are in fast exchange on the chemical shift timescale and essentially do not shift during the titration: ArC*H*$_{eq}$ ($\Delta\delta$ ~0.01 ppm and $\Delta\delta$ ~0.08 ppm); *t*Bu groups ($\Delta\delta$ ~0.03 ppm). This suggests that the conformation of the receptor does not change much upon guest inclusion. In contrast, the Ar*H* protons and the ArC*H*$_{ax}$ of the host appear in slow exchange ($\Delta\delta_{ArHfree-ArHbound}$ ~0.3 ppm and $\Delta\delta_{ArCHax}$ ~0.59 ppm). By integrating these signals, we were able to determine an apparent affinity constant (K_{app}) of ~13 M^{-1} for *t*BuNH$_3^+$ for a 1:1 binding at pH ~10.2. The affinity constant was determined based on the following equilibrium:

$$\mathbf{15^{-3H+} + \textit{t}BuNH_3^+ \rightleftharpoons 15^{-3H+} \supset \textit{t}BuNH_3^+}$$

However, even after the addition of 80 equivalent of guest the cavity was not completely filled. The included ammonium guest is certainly stabilized by a favorable electrostatic interaction with the carboxylates. The charge balance could be maintained, as for the calixarene system

[28] The pKA of *t*BuNH$_2$ is of ~10.7 at 298 K. In the bulk, under these experimental conditions, the amine appears under the ammonium form.
[29] Under these conditions, it is likely to suppose that system **15** is totally deprotonated.

studied in $CDCl_3$,[26] by other *t*BuNH_3^+ which are in *exo*, or perhaps by ammonium groups of DPC or guest interacting with the carboxylate moieties.

The recognition of other ammoniums was also studied (Figure 3-14): D/L *sec*-Butylammonium (*sec*-ButylNH_3^+), 1-adamantylammonium (AdamNH_3^+)[30] and heptylammonium (HeptylNH_3^+). The titration for AdamNH_3^+ is shown in Figure 3-15.

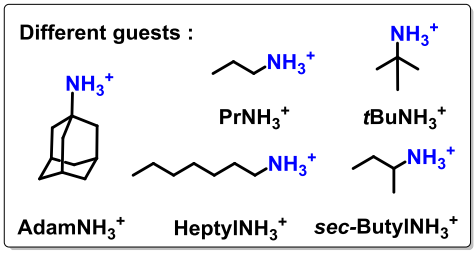

Figure 3-14. Guests studied with host **15**.

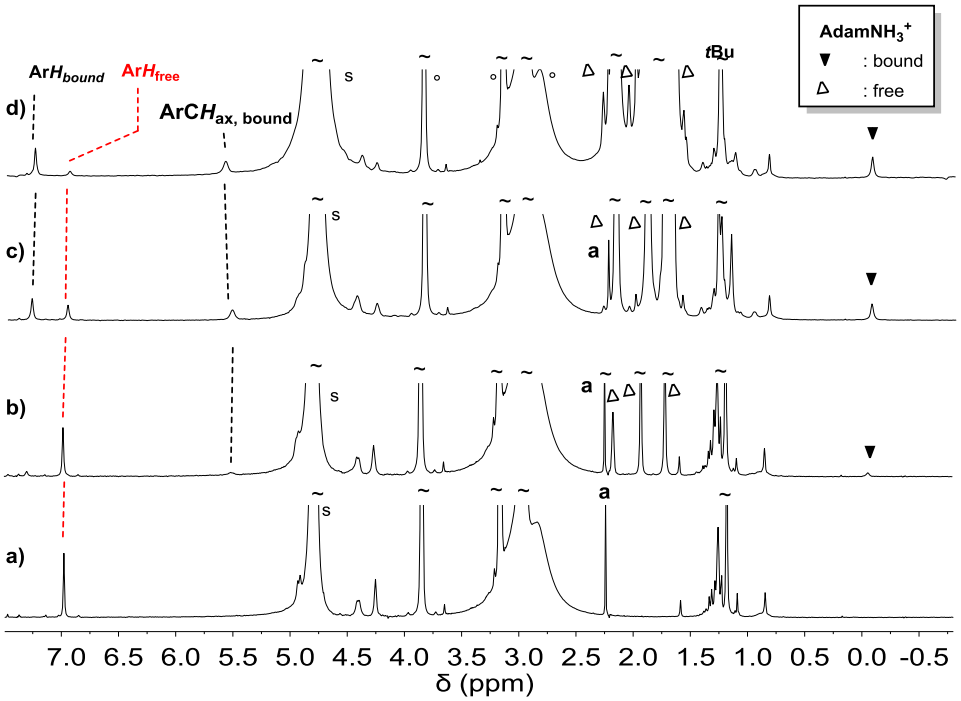

Figure 3-15. ^{1}H NMR spectra (298 K, 20 mM DPC-d_{38} in D_2O, 600 MHz, 11 mM HEPES) at pH ~7.3 of **15**$^{-nH+}$: a) in the absence of Adam$NH_3^+Cl^-$; b) in the presence of ~2 equiv. of Adam$NH_3^+Cl^-$; c) in the presence of 48 equiv. of Adam$NH_3^+Cl^-$; d) in the presence of ~290 equiv. of Adam$NH_3^+Cl^-$; s: solvent; g: grease; singlets are residual traces of non-deuterated DPC; °: HEPES; a: acetone.

[30] The titration was performed by adding the chlorine salt of adamantylamine (Adam$NH_3^+Cl^-$). This explains why in this case the pH did not shift upon addition of the guest.

The NMR spectra of **15**$^{-3H+}$⊃**AdamNH$_3^+$**, **15**$^{-3H+}$⊃***sec*-**ButylNH$_3^+$** and **15**$^{-3H+}$⊃**HeptylNH$_3^+$** exhibit very similar patterns as **15**$^{-3H+}$⊃***t*-**BuNH$_3^+$** (Figure 3-16a-b).[29] Guest inclusion was in each case evidenced by the presence of high field signals in the ^{1}H NMR spectra. The apparent binding constants (K_{app}) for AdamNH$_3^+$ (~80 M^{-1} at pH ~7.3) and for *sec*-ButylNH$_3^+$ (~18 M^{-1} at pH ~11.3) could be determined by integration.[31]

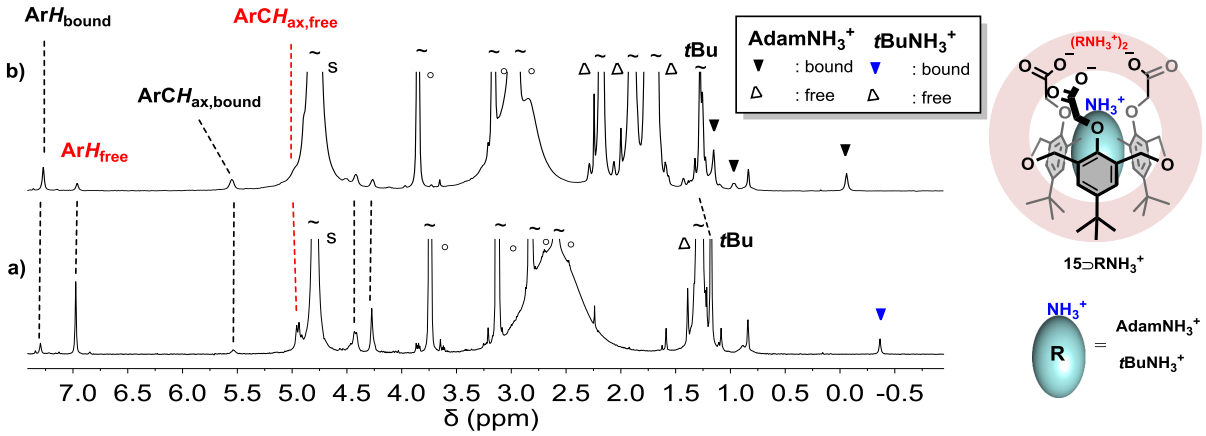

Figure 3-16. ^{1}H NMR spectra (298 K, 20 mM DPC-d$_{38}$ in D$_2$O, 600 MHz, 11 mM HEPES) of **15**$^{-nH+}$ in the presence of: a) 80 equiv. of *t*BuNH$_2$ at pH ~10.2; b) 48 equiv. of AdamNH$_3^+$Cl$^-$ at pH ~7.3; s: solvent; g: grease; singlets are residual traces of non-deuterated DPC; °: HEPES.

In the case of heptylammonium, bound signal overlap made integration difficult. The addition of ~83 equiv. of PrNH$_2$ to the solution containing **15**$^{-3H+}$⊃***sec*-ButylNH$_3^+$** (at pH ~11.3) did not lead to the inclusion of PrNH$_3^+$. The complex **15**$^{-nH+}$⊃***sec*-ButylNH$_3^+$** was observed in the pH range 2-12, i.e. at pH values where the carboxylate groups are expected to be protonated and at pH vales where one expects the ammonium to be in it amine form.[32]

For comparison purposes, the ability of system **15** to complex ammonium ions was also evaluated in deuterated chloroform. Propylamine (PrNH$_2$), D/L *sec*-Butylamine (*sec*-ButylNH$_2$), *t*Buamine (*t*BuNH$_2$) and heptylamine (HeptylNH$_2$) are all recognized in their ammonium form in CDCl$_3$ as evidenced by the presence of high field signals for their alkyl chain protons in the ^{1}H NMR spectra. The signal for the CH$_2$COO protons of the host shifts to higher field during the titration (from 4.95 to 4.82 ppm and then remains constant), indicating that the host undergoes a complete deprotonation. The absolute affinities were not evaluated for the different guests but, after addition of ~3 equivalents of each guest, the cavities were

[31] The binding constant were determined following the same equilibrium presented above for *t*BuNH$_2$. The signals used to determine the binding constant were the Ar*H*$_{free}$ and Ar*H*$_{bound}$ and free guest.
[32] For the other host-guest complex we did not study the stability over pH.

almost completely filled. The affinity constant for D/L *sec*-ButylNH_2 relative to PrNH_2 was however evaluated by a competition experiment: $K_{PrNH2/sec\text{-}ButylNH2}$ ~0.3. The fact that the two affinity constants are of the same order of magnitude in $CDCl_3$, while in water (at pH ~11.3) the affinity for *sec*-ButylNH_3^+ seems to be considerably higher than for PrNH_3^+, is certainly assignable to the hydrophobic effect as PrNH_2 is much more hydrophilic than D/L *sec*-ButylNH_2.

3.5.2. INCORPORATION OF A RESORCIN[4]ARENE DERIVATIVE INTO DPC MICELLES

Resorcinarenes are cavitands composed of 4 to 6 resorcinol units. They are structurally very close to calixarenes and are obtained by the condensation of a resorcinol and an aldehyde.[33] They are bowl shaped and can be functionalized at the level of their wide rim in order to build a structure able to bind a metal or recognize an organic molecule (Figure 3-17).

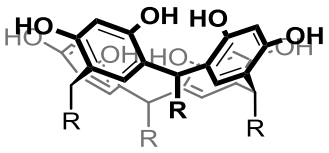

Figure 3-17. Structure of a resorcin[4]arene.

We looked into the possible micellar incorporation of the resorcinarene-based host **16** developed by Dr. Parrot during its PhD thesis in the Reinaud's group (Figure 3-18).[34] This resorcinarene is functionalised by 4 methylimidazole moieties and can bind a zinc cation at the level of the imidazole nitrogens and, simultaneously, a small molecule in its cavity.

[33] Von Bayer, A. *Ber*. **1872**, *5*, 1094; Baekeland, L. H. US patent 942, **1908**, 699.
[34] Parrot, A. **2015**. PhD thesis: Systèmes supramoléculaires biomimétiques : les complexes bols, synthèse, propriétés et réactivité. Laboratoire de Chimie Biochimie Pharmacologie et Toxicologie, Université Paris Descartes.

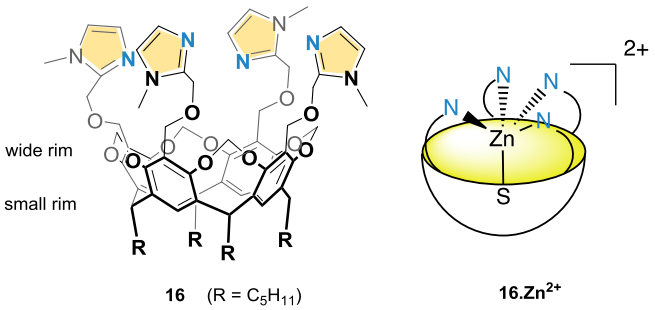

Figure 3-18. Structure of **16** and schematic representation of **16.Zn^{2+}** where S is a solvent molecule (figures taken from Parrot's thesis).

Dr. Parrot observed that **16.Zn^{2+}** exhibits a high binding affinity for the acetate anion in acetonitrile.[34] He also developed a hydro-soluble derivative **W16**, by grafting cationic moieties on the small rim of **16**, and its corresponding zinc complex **W16.Zn^{2+}** (Figure 3-19). A similar system with three imidazole arms and its hydro-soluble equivalent (**Rim$_3$** and **WRim$_3$**) have also been developed and studied in Reinaud's group (Figure 3-19).[35,36,37] The zinc complex **WRim$_3$.Zn^{2+}** was observed to be stable in the pD range 6.5-9.5.

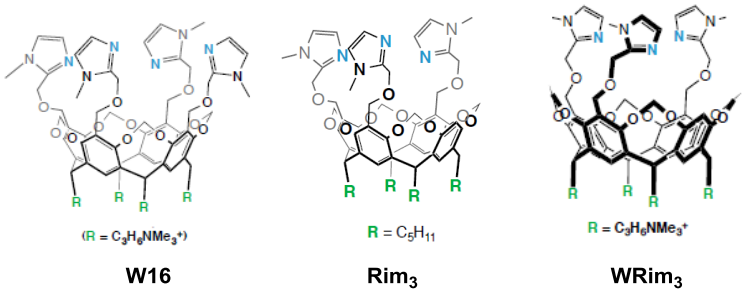

Figure 3-19. Structure of **W16**, **Rim$_3$** and **WRim$_3$** (figures taken from Parrot's thesis).

We successfully incorporated ligand **16** into DPC micelles by simple mixing it with the surfactant (20 mM) in D_2O at neutral pH. The incorporation of **16** was confirmed by DOSY NMR. Concentrations up to ~0.7 mM were obtained. The ^{1}H NMR spectra of incorporated **16** (Figure 3-20) is similar to the one observed for **W16** in water.[34] It was observed with **W16** that its imidazole signals shift with pH, due to changes in the protonation state of the host, and the highest pKa of the system was estimated to be in the 5.2 to 7.6 range at 300 K.

[35] Višnjevac, A.; Gout, J.; Ingert, N.; Bistri, O.; Reinaud, O. *Org. Lett.* **2010**, *12*, 2044–2047 ; Gout, J. ; Višnjevac, A.; Rat, S.; Parrot, A.; Hessani, A.; Bistri, O.; Le Poul, N.; Le Mest, Y.; Reinaud, O. *Inorg. Chem.* **2014**, *53*, 6224–6234.
[36] Gout, J.; Rat, S.; Bistri, O.; Reinaud, O. *Eur. J. Inorg. Chem.* **2014**, *53*, 2819–2828.
[37] Rat, S; Gout, J.; Bistri, O.; Reinaud, O. *Org Biomol Chem.* **2015**, *13*, 3194-3197.

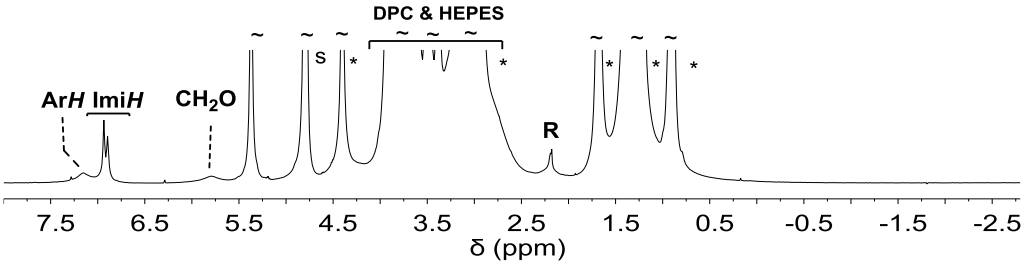

Figure 3-20. ^{1}H NMR spectrum (298 K) of **16** (0.68 mM) in DPC (20 mM in D_2O HEPES 50 mM at pH ~6.7, 600 MHz); s: solvent; R= alkyl chain of **16**; *: DPC signals.

16.Zn^{2+} was also successfully incorporated into DPC micelles by simple mixing it with the surfactant (20 mM) in D_2O at neutral pH. Concentrations up to ~0.5 mM were obtained. (Figure 3-21a).

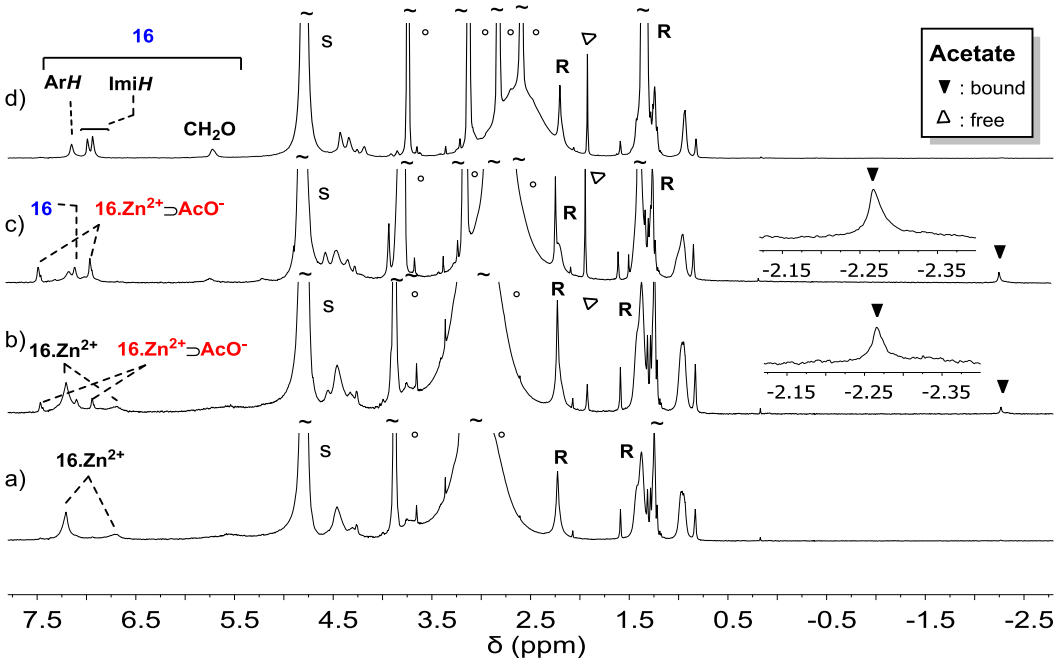

Figure 3-21. ^{1}H NMR spectra (298 K, 600MHz, 20 mM DPC-d_{38} in D_2O, HEPES 10mM) of **16.Zn^{2+}** (0.49 mM): a) at pH ~7.3; b) after the addition of 0.4 equiv. of sodium acetate; c) after the addition of 1.6 equiv. of sodium acetate; d) after the addition of 3 equiv. of sodium acetate; pH~9.9; s: solvent; singlets are residual traces of non-deuterated DPC; R= alkyl chain of **16**; °: HEPES signals.

The titration of the system with sodium acetate was monitored by ^{1}H NMR spectroscopy (Figure 3-21b-d). The pH of the solution increased during the titration due to the lack of buffering capacity.[38] The analysis of the ^{1}H spectra however clearly shows that acetate has been

[38] The solution in this case was prepared by adding ~ 3 mL of NaOD (~ 1M) to a solution of **16.Zn^{2+}** (pH ~6.3, 10 mM HEPES) and 20 mM DPC-d_{38} in D_2O; The pH increased to ~7.3.

included but also that demetalation occurs.[39] Indeed, after addition of ~3 equiv. of acetate, the pH is ~9.9 and only the signals characteristic of the neutral ligand **16** in DPC micelles are observed (Figure 3-21d).

When performing the same titration under more acidic and controlled conditions (pH ~6.3, 10 mM HEPES)[40], two clear overlapping signals are observed for included acetate (Figure 3-22, see expansions): a sharp signal (δ= -2.27 ppm) and a broader one (δ ~-2.32 ppm).

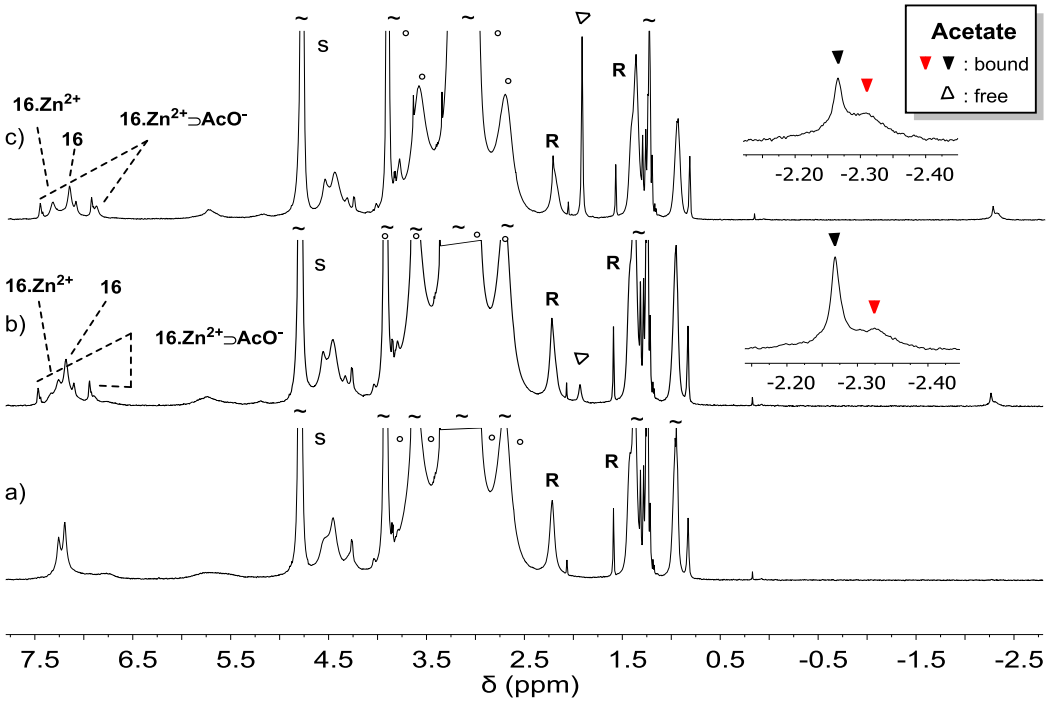

Figure 3-22. ^{1}H NMR spectra (298 K, 600MHz) of **16.Zn^{2+}** (0.49 mM in 20 mM DPC-d_{38} in D_2O, HEPES 10mM, pH ~6.3): a) in the absence of sodium acetate; b) in the presence of 0.5 equiv. of sodium acetate; c) in the presence of 2.8 equiv. of sodium acetate; s: solvent; singlets are residual traces of non-deuterated DPC; R= alkyl chain of **16**; °: HEPES signals.

At this pH (~6.3) it is possible that we are in the presence of two different inclusion complexes **16.Zn^{2+}⊃CH$_3$COO$^-$**, **16H$^+$.Zn^{2+}⊃CH$_3$COO$^-$** but also some free protonated ligand **16H$^+$**.[39]

Protonation would occur at the level of one of the imidazole, which would then no longer be able to coordinate to the metal cation. A solvent molecule would then be coordinated to the

[39] It is important to point that the assignments shown in the figure did not derive from NMR characterization but were made by comparison with the results obtained with **16.Zn^{2+}** in acetonitrile and **W.16.Zn^{2+}** described in Parrot's thesis.
[40] In this case no NaOD was added and the pH did not shift during the titration.

metal in *exo* to complete the coordination sphere of the metal. Due to the presence of multiple species, it was unfortunately not possible to determine affinity constants.

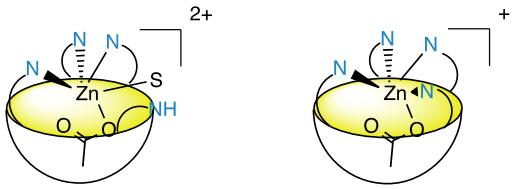

Figure 3-23. Schematic representation of **16H$^+$.Zn^{2+}⊃CH$_3$COO$^-$** (left) and **16.Zn^{2+}⊃CH$_3$COO$^-$** (right) (figures taken from Parrot's thesis).

The presence of two inclusion complexes was also observed and rationalized by Dr. Parrot when working in CD_3CN: when titrating **16.Zn^{2+}⊃CH$_3$COO$^-$** with water, he observed the formation of a second inclusion complex and its proportion was related to the concentration of water in the organic solution.[34]

Spectra of **16.Zn^{2+}** incorporated in DPC micelles with ~3 equivalents of acetate were recorded at 278, 298 and 323 K at pH ~6.3 (Figure 3-24). Very surprisingly, we observed that at low temperature the species giving rise to the broad high field signal for included acetate in the NMR spectrum is favored while at high temperature it is the species giving rise to the sharp signal which is favored.[41] We know from the literature that the pKa of imidazole varies from ~7.4 at 278 K to ~6.6 at 323 K (~ 1mM).[42] It is therefore possible that, at high temperature, the 4-imidazole zinc complex **16.Zn^{2+}⊃CH$_3$COO$^-$** would therefore be favored whereas at lower temperatures the protonated zinc complex **16.H$^+$Zn$^+$⊃CH$_3$COO$^-$** would be favored.[39]

[41] Complex Induced Shifts determined for the sharp included signal of acetate: 4.14 ppm at 323 K and 4.18 ppm at 298 K.
[42] Hochachka, P. W.; Somero, G. N; Biochemical Adaptation **1984** Princeton Legacy Library.

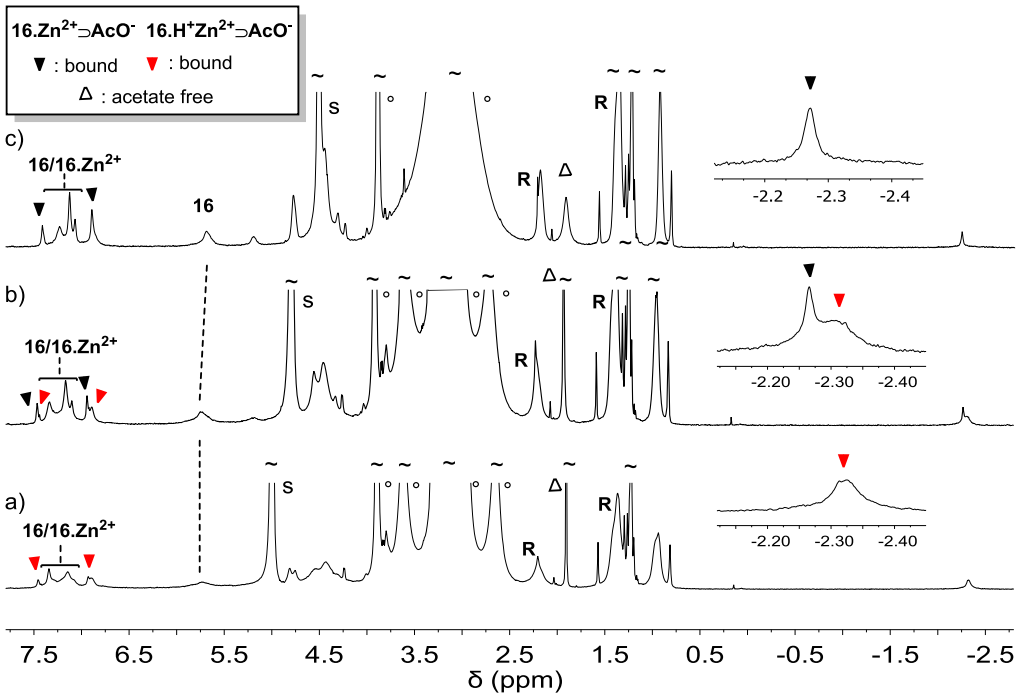

Figure 3-24. ^{1}H NMR spectra (600MHz) of **16.Zn^{2+}** (0.49 mM) at pH ~6.3 with 3 equiv. of sodium acetate in a 20 mM DPC-d_{38} in D_2O HEPES 10mM solution at: a) 278 K; b) 298 K; c) 323 K; s: solvent; singlets are residual traces of non-deuterated DPC; R= alkyl chain of **16**; °: HEPES signals.

At pH ~6.3 and 323 K, where we are in the presence of only one host-guest species, an apparent binding constant for acetate of log *K* ~2.9 could be determined by signal integration for the following equilibrium:

$$\mathbf{16.Zn^{2+} + CH_3COO^- \rightleftharpoons 16.Zn^{2+} \supset CH_3COO^-}$$

This value is relatively large for the complexation of a hydrophilic anion like acetate in water and is very close to the one reported for the water-soluble system **WRim$_3$**: log *K* ~2.8 (pD ~7.4).[37] The ability of this complex to coordinate acetate in aqueous media is quite remarkable. Indeed, whereas many receptors for acetate have been described in the literature, most only work in organic solvents. Those reported to bind acetate in water are uncommon and the corresponding binding constants are relatively moderate.[43]

When adding 6 equiv. of acetate to **16.Zn^{2+}** incorporated in DPC micelles at pH ~8, a mixture of **16.Zn^{2+}⊃CH$_3$COO$^-$** and of free ligand **16** is observed (Figure 3-25a). Integration of the included acetate signal shows that only ~50 % of acetate is included. When zinc perchlorate was added to the solution (1.6 equiv.), the signals characteristic of the free ligand disappear (for

[43] Gale, P. A.; Busschaert, N.; Haynes, C. J. E.; Karagiannidis, L. E.; Kirby, I. L. *Chem. Soc. Rev.* **2014**, *43*, 205.

example the CH_2O at 5.69 ppm) and only the signature of **16.Zn^{2+}⊃CH$_3$COO$^-$** is observed with in this case 100 % of acetate inclusion (Figure 3-25b).[39] The addition of zinc perchlorate shifts the equilibrium between **16** and **16.Zn^{2+}** towards the metal complex, and the amount of guest that can be included increases.

The binding constant for acetate at pH~8 was determined from signal integration and a value slightly higher than at pH 6.3 was determined (log *K* ~3.3 at 323 K). This is also in accordance with the results obtained by Reinaud and co-workers with **WRim$_3$** where a bell curved dependence as a function of pH was observed for the formation of the system **WRim$_3$-Zn-acetate** (detectable in a pD range 5.5-10.5). The optimal pD was determined to be around 7.4.[37]

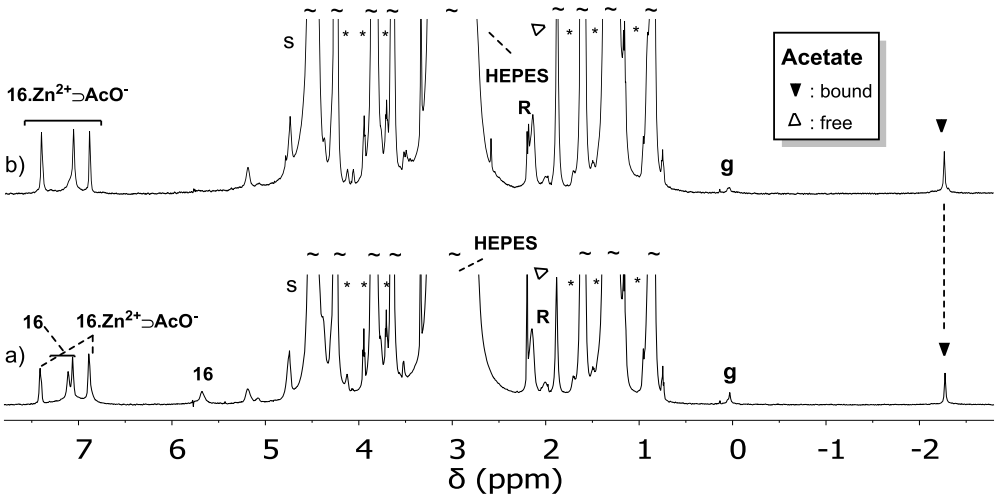

Figure 3-25. ^{1}H NMR spectra (600MHz, 323K) of **16.Zn^{2+}** (0.57 mM) at pH ~7.9 with in a 20 mM DPC in D_2O HEPES 40mM solution with: a) 6 equiv. of sodium acetate; b) 6 equiv. of sodium acetate after the addition of 1.6 equiv. of zinc perchlorate; ; s: solvent; *: DPC; R= alkyl chain of **16**; g: grease.

16.Zn^{2+} incorporated in DPC micelles was also titrated with acetylacetone at pH ~7.3 and guest inclusion was evidenced by the changes in the NMR spectra and in particular the presence of high field signals (Figure 3-27a-d).[39] The coordination of the enolate form of the guest (acetylacetonate: **C$_5$H$_7$O$_2^-$**), at the level of the metal, has been highlighted by Dr. Parrot with this system in CD_3CN. Acetylacetonate is complexed with one acetyl group in *endo*-position and the other in *exo*-position.[34]

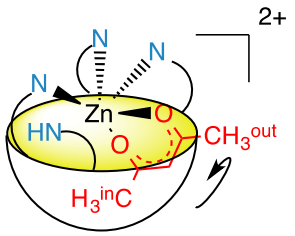

Figure 3-26. Schematic representation of **16H$^+$.Zn^{2+}⊃ C$_5$H$_7$O$_2^-$** (figure taken from Parrot's thesis).

The bidentate coordination of **C$_5$H$_7$O$_2^-$** to the metal cation and the simultaneous protonation of one of the imidazoles means that we can only be in the presence of **16H$^+$.Zn^{2+}⊃ C$_5$H$_7$O$_2^-$**.

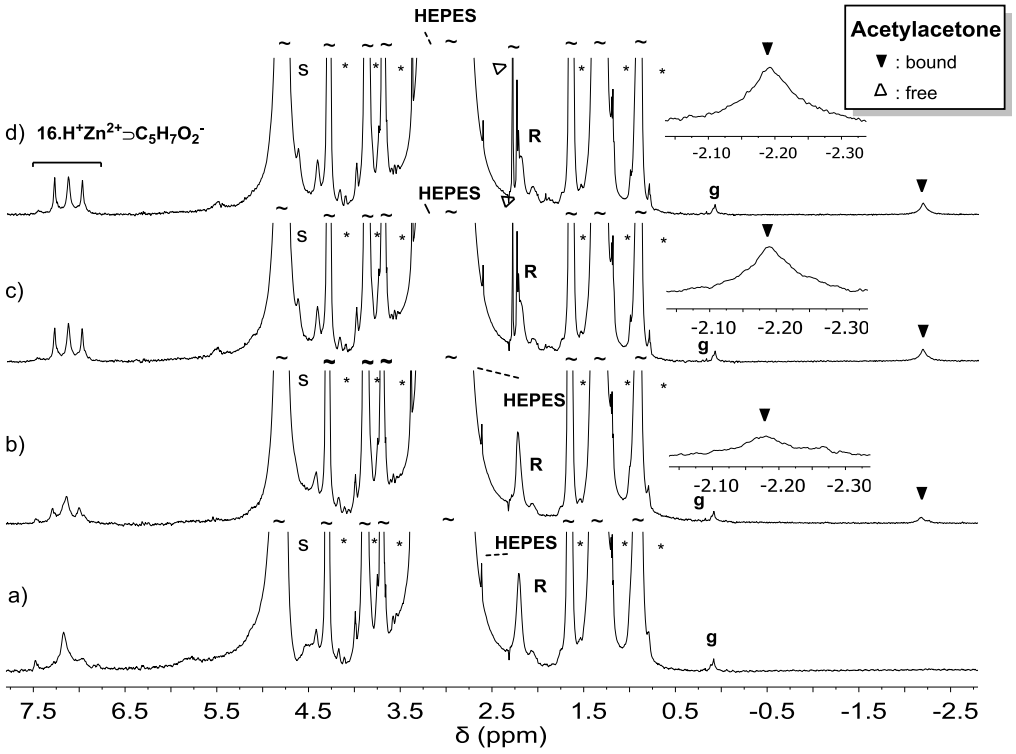

Figure 3-27. ^{1}H NMR spectra (298 K, 600MHz, 20 mM DPC in D_2O, HEPES 40mM) of: a) **16.Zn^{2+}** (0.57 mM) at pH ~7.3; b) **16.Zn^{2+}** after the addition of 0.4 equiv. of acetylacetone; c) **16.Zn^{2+}** after the addition of 1.3 equiv. of acetylacetone; d) **16.Zn^{2+}**after the addition of 1.8 equiv. of acetylacetone at pH~7.3; ; s: solvent; *: DPC; R= alkyl chain of **16**; g: grease.

The quantitative formation of the inclusion complex **16H$^+$.Zn^{2+}⊃C$_5$H$_7$O$_2^-$** is observed and an affinity of log K > 5 at pH~7.3 could be determined. The signal of included **C$_5$H$_7$O$_2^-$** is broad at 298 K but neither the increase nor the decrease of the temperature sharpened the signal.

3.6. CONCLUSIONS

In this chapter we investigated the strategy of transferring molecular receptors into water via micellar incorporation. This approach is indeed a very elegant solution to overcome the solubility problem of organic receptors. We studied hydrophobic receptors, which are only soluble in organic solvents.

We have shown that a calix[6]azacryptand based receptor (host **6**) can be incorporated into DPC micelles either as a Zn^{2+} complex in the 6–9 pH window or as a its multi-protonated form at low pH. The zinc complex maintains its host-guest properties already observed in organic solvent and is able to complex small or long linear primary amines inside the calixarene cavity. The inclusion complex **6.Zn^{2+}⊃PrNH$_2$** was observed even at very low pH where the free amine is fully protonated in water. This shows that the environment provided by the calixarene cavity and the micelle stabilizes $PrNH_2$ in its basic form. The fact that incorporated **6.Zn^{2+}** binds small amines and longer amines with a similar affinity stands in strong contrast with the results obtained with a water-soluble calix[6]tris-imidazole zinc complex where the binding of long hydrophobic amines was observed but not the binding of small hydrophilic ones. It also stands in contrast with the results obtained in $CDCl_3$ where smaller amines are much better recognized than the longer chain ones. This shows that the hydrophobic effect plays a key role in driving guests from water into the calixarene cavity incorporated in DPC micelles.

We also successfully used the micellar incorporation strategy with a homooxacalix[3]tris-acid derivative, **15**, and a resorcin[4]arene zinc complex bearing four methylimidazole moieties, **16.Zn^{+}**. We were able to show that **15** incorporated into DPC micelles can bind different ammoniums, albeit with low affinity. Regarding **16.Zn^{2+}** incorporated in DPC micelles, we observed that it can recognize small organic molecules such as acetate and acetylacetonate.

Our results highlight that the use of micelles to transfer lipophilic receptors into an aqueous environment is a valuable method and, furthermore, that NMR spectroscopy is a very powerful technique to study the incorporation and the binding properties of micellar based supramolecular receptors.

Chapter 4.
Funnel complexes: study of exchange dynamics

4.1. INTRODUCTION

As presented in the general introduction, calix[6]tris-imidazole zinc (Figure 4-1) can be considered as a model for the active site of metallo-enzymes. In order to contribute to a better understanding of this system, we wanted to investigate the mechanism of guest exchange which has to date not yet been elucidated.

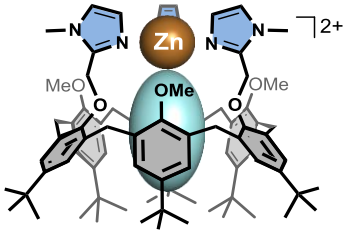

Figure 4-1. Schematic representation of calix[6]tris-imidazole zinc with included guest **1.Zn^{2+}⊃G**.

More often, when looking at host-guest recognition processes, a dissociative mechanism is considered: the guest can leave the host without the need to be replaced by another guest (Figure 4-2).

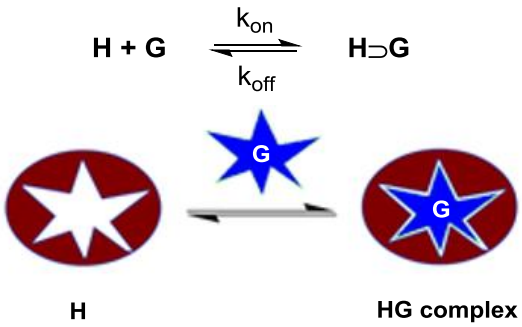

Figure 4-2. Schematic representation of a Host-Guest equilibrium.

The change in the concentration of the host-guest complex can be expressed as a function of k_{out}, the first order dissociation rate constant and k_{in}, the second order association rate constant:

$$\frac{d[HG]}{dt} = -k_{out}[H \supset G] + k_{in}[H_{free}][G_{free}]$$

At equilibrium $\frac{d[HG]}{dt} = 0$ and the following equation holds:

$$k_{in}[H_{free}][G_{free}] = k_{out}[H \supset G]$$

A pseudo-first order rate constant can be defined for the association process, $k_{in}' = k_{in}[H_{free}]$. The residence times are defined as follow:

$$\tau_{in} = \frac{1}{k_{out}} \text{ and } \tau_{out} = \frac{1}{k_{in}[H_{free}]}$$

In the case of system **1.Zn^{2+}**, since it is not possible for the zinc cation to be tri-coordinated, the outgoing guest cannot simply vacate cavity before the incoming guest arrives.[1] Due to steric constraints, it is also not possible for the incoming and outgoing guests to be simultaneously included in the cavity. The exchange of the guest can therefore neither be a simple dissociative mechanism nor *endo*-associative mechanism.

The hypothesis that we put forward is that the guest exchange mechanism is an associative mechanism and that the *exo*-coordination of a ligand is required to enable the guest to leave the cavity (Figure 4-3). In this context it is interesting to point out that previous studies have shown, that a dicationic metal calix[6]arene system presents a coordination site inside the calixarene cavity (for an *endo* molecule) but also a second coordination site accessible for an *exo*-molecule outside the cavity.[2]

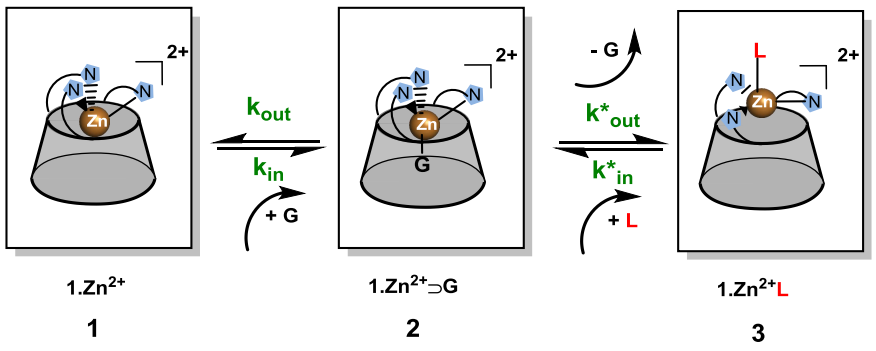

Figure 4-3. Hypothetical mechanism presented for guest departure from the cavity of **1.Zn^{2+}**.

The following equilibria represent the systems shown in Figure 4-3:

Equilibrium 1: $1.Zn^{2+} + G \leftrightharpoons 1.Zn^{2+} \supset G$

[1] Dudev, T.; Lim, C. *J. Am. Chem. Soc.* **2000**, *122*, 11146-11153; Amin, A. E.; Truhlar, D. *J. Chem. Theory Comput.* **2008**, *4*, 75-85.
[2] Sénèque. O. **2002**. PhD thesis: Nouveaux ligands biomimétiques dérivés de calix[6]arenes. Etude de la complexation du zinc et du cuivre et comparaison avec les systèmes naturels protéiques. UF.R. Biomedicale, Université Paris Descartes.

Equilibrium 2: $1.\mathrm{Zn}^{2+} \supset \mathrm{G} + \mathrm{L} \leftrightharpoons 1.\mathrm{Zn}^{2+}\mathrm{L} + \mathrm{G}$

The change in the concentration of the host-guest complex can be expressed as a function of the different rate constants:

$$\frac{d[1.\mathrm{Zn}^{2+} \supset \mathrm{G}]}{dt} = -k_{out}[1.\mathrm{Zn}^{2+} \supset \mathrm{G}] + k_{in}[1.\mathrm{Zn}^{2+}][\mathrm{G}] - k^*_{out}[1.\mathrm{Zn}^{2+} \supset \mathrm{G}][\mathrm{L}] + k^*_{in}[1.\mathrm{Zn}^{2+}\mathrm{L}][\mathrm{G}]$$

At equilibrium, the concentration in host-guest complex does not change and the following equation holds:

$$(k_{out} + k^*_{out}[\mathrm{L}])[1.\mathrm{Zn}^{2+} \supset \mathrm{G}] = (k_{in}[1.\mathrm{Zn}^{2+}] + k^*_{in}[1.\mathrm{Zn}^{2+}\mathrm{L}])[\mathrm{G}]$$

We can see that the $(k_{out} + k^*_{out}[\mathrm{L}])$ characterizes the processes corresponding to the exit of the guest G from the cavity. We can thus write:

$$\tau_{in} = \frac{1}{(k_{out} + k^*_{out}[\mathrm{L}])}$$

$$\frac{1}{\tau_{in}} = k_{tot} = (k_{out} + k^*_{out}[\mathrm{L}])$$

where k_{tot} represents the sum of all first order (or pseudo-first order) rate constants. It is linearly dependent on the concentration of the ligand L that can be *exo*-coordinate to the metal (*a* and *b* are two constants):

$$k_{tot} = a + b * [\mathrm{L}]$$

If a more complete scheme is considered for guest exchange following an associative mechanism, an intermediate step where zinc is penta-coordinated should be considered as shown in Figure 4-4 where all rate constants are indicated. As an empty cavity is not favored the equilibrium between species **A** and **B** is shifted towards species **B** where, the zinc is tetra-coordinated. With the advent of a ligand **L**, a trigonal bipyrimidal geometry is established where the metal cation is penta-coordinated with **G** inside the cavity and **L** outside the cavity (species **C**). The *endo*-coordinated ligand **G** is then able to leave the cavity leaving the metal once again in a tetrahedral geometry but in this case with an *exo*-ligand (species **D**). A new guest molecule

G can be then enter the cavity and the metal will once again be in a trigonal bipyramidal geometry. The de-coordination of the *exo*-ligand **L** will bring the system back to species **B**. The residence time (τ_{in}) of the guest **G** inside the cavity should thus be influenced by the nature and the concentration of **L**.

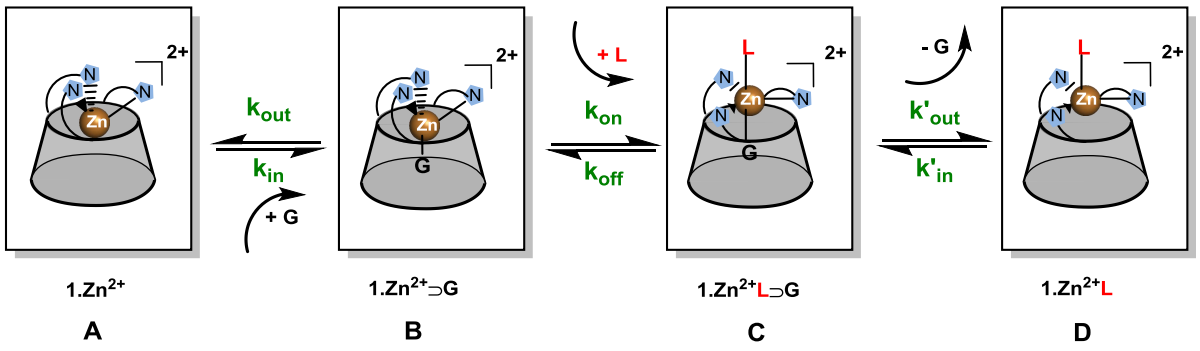

Figure 4-4. Hypothetical mechanism presented for guest exchange for system **1.Zn**$^{2+}$.

The different equilibria shown in Figure 4-4 are:

Equilibrium 1: $1.\mathrm{Zn}^{2+} + \mathrm{G} \leftrightharpoons 1.\mathrm{Zn}^{2+} \supset \mathrm{G}$

Equilibrium 2: $1.\mathrm{Zn}^{2+} \supset \mathrm{G} + \mathrm{L} \leftrightharpoons 1.\mathrm{Zn}^{2+}\mathrm{L} \supset \mathrm{G}$

Equilibrium 3: $1.\mathrm{Zn}^{2+}\mathrm{L} \supset \mathrm{G} \leftrightharpoons 1.\mathrm{Zn}^{2+}\mathrm{L} + \mathrm{G}$

If we consider independently the process corresponding to the guest leaving the cavity of species **B** or **C** we can write:

$$\frac{1}{\tau_{in}^{B}} = k_{out} \quad \text{and} \quad \frac{1}{\tau_{in}^{C}} = k'_{out}$$

The inverse of the mean life-time of G in a cavity would be given by the sum of the inverse of the residence time of the guest in state **B** and the inverse of the residence time of the guest in state **C**. The equilibrium between species **B** and **C** must however be considered as it will influence the proportions of the two species. If we make the hypothesis that the concentrations of species A and D are negligible we can write that the sum of the molar fraction of species B and C is equal to 1:

$$x_B + x_C = 1$$

The inverse of the mean life-time of G in a cavity would then be given by:

$$\frac{1}{\tau_{in}} = \frac{x_B}{\tau_{in}^B} + \frac{x_C}{\tau_{in}^C}$$

$$\frac{1}{\tau_{in}} = k_{out} * x_B + k'_{out} * x_C$$

Considering the equilibrium constant which characterizes equilibrium **B-C**:

$$K = \frac{[1.\mathrm{Zn}^{2+}\mathrm{L} \supset \mathrm{G}]}{[1.\mathrm{Zn}^{2+} \supset \mathrm{G}] * [\mathrm{L}]}$$

we have:

$$K = \frac{x_C}{x_B * [\mathrm{L}]} \quad and \quad x_C = \frac{K[\mathrm{L}]}{1 + K[\mathrm{L}]} \quad and \quad x_B = \frac{1}{1 + K[\mathrm{L}]}$$

we thus have:

$$\frac{1}{\tau_{in}} = k_{out} * (\frac{1}{1 + K[\mathrm{L}]}) + k'_{out}(\frac{K[\mathrm{L}]}{1 + K[\mathrm{L}]})$$

If we make the hypothesis that $x_C \ll x_B$ we have that:

$$\frac{\mathrm{K}[\mathrm{L}]}{1 + \mathrm{K}[\mathrm{L}]} \approx K[\mathrm{L}] \quad \text{and} \quad \frac{1}{1 + K[\mathrm{L}]} \approx 1$$

and we come to the following expression:

$$\frac{1}{\tau_{in}} = k_{out} + k'_{out} * K * [\mathrm{L}]$$

If the equilibrium **B-C** is shifted towards **B,** which will be the case in the absence of an *exo*-ligand, the residence time of G will simply be given by the inverse of k_{out}. Following the mathematical development presented above, k_{tot}, like in the case of the previous simpler model will be linearly dependent on the concentration of the ligand L that can be *exo*-coordinate to the metal, (*a'* and *b'* being constants).

$$k_{tot} = \frac{1}{\tau_{in}} = a' + b' * [\mathrm{L}]$$

To generalize, if different species in solution can *exo*-coordinate and enable the guest to leave the cavity, including the guest G itself, the following more general equation should be considered (where *A* and *B*s are constants):

$$k_{tot} = \sum_{i=1}^{n} \frac{1}{\tau_{\mathrm{in}}\mathrm{G}} \approx A + (B[\mathrm{L}_i] + B_{ii}[\mathrm{L}_{ii}] + .. + B_n[\mathrm{L}_n])$$

Measuring the residence time of a guest as a function the nature and concentration of L in order to validate these equations will be the main goal of this research. In this context, 1D EXchange SpectroscopY (EXSY) NMR experiments will be very valuable as we will be able to have access to kinetic constants, and therefore to residence times.[3,4]

4.2. 1D-EXSY NMR

When considering a simple isomerization equilibrium between A and B, the exchange can be characterized by the kinetic constants k_{AB} and k_{BA}, where k_{AB} represents the jump rate from site A to site B and mutually for k_{BA} (Figure 4-5). The inverse of these kinetic constants, τ_A and τ_B, represent the residence time in sites A and B respectively.

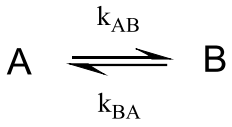

Figure 4-5. Exchange between a site A and a site B.

The chemical environments in site A and site B being different, the nuclei of the system in these two environments will have different resonance frequencies and relaxation times, and we talk about chemical exchange. Different regimes can be considered when comparing the lifetimes to the NMR chemical shift timescale which is the difference between the resonance frequencies in sites A and B: $|\nu_A - \nu_B|$. For the simple A-B equilibrium, the two regimes that can be distinguished are:

- τ_A and $\tau_B >> |\nu_A - \nu_B|^{-1}$: the exchange is slow compared to the NMR chemical shift timescale. Two signals are observed in the spectrum, one for each site;

[3] Claridge, T. **1999.** High-Resolution NMR techniques in organic chemistry, Tetrahedron organic chemistry series Volume 19. Wiley.
[4] Perrin, C. L.; Dwyer, T. J. *Chem. Rev.* **1990**, *90*, 935.

- τ_A and $\tau_B << |\nu_A - \nu_B|^{-1}$: the exchange is fast compared to the NMR chemical shift timescale. A unique averages signal is observed.

Information on the rate constants characterizing the exchange process can be obtained via EXchange SpesctroscopY (EXSY) experiments. EXSY is an incoherent transfer of longitudinal magnetization that allows qualitative observations or quantitative measurements of exchange processes. EXSY measurements can be used to quantify dynamic processes in the 10-5000 ms time window (corresponding to k_{ex} ~0.2-100 s^{-1}) for systems in slow exchange on the NMR chemical shift timescale.[4] Physical process in this time window include slow conformational changes, such as ligand binding or cis-trans isomerization. To obtain quantitative information from EXSY experiments, as a rule of thumb, Equation 4-1 has to be satisfied:

$$\Delta\nu \gg \frac{1}{k_{exchange}} \gg \frac{1}{T_1}$$

Equation 4-1

where $k_{exchange} = k_A + k_B$ in the case of a simple two site exchange; T_1 is the longitudinal relaxation time and $\Delta\nu$ the frequency difference between the signals of the species in exchange. Indeed, exchange must be slow on the chemical shift timescale and relaxation must not be too fast or the signal will not be observed throughout the EXSY experiment.[4]

If we consider the exchange between sites A and B, the exchange can be monitored, via 1D EXSY experiments, by selectively inverting the signal of the species (site A or B) by a 180°-pulse. The pulse sequence used is showed below (Figure 4-6).

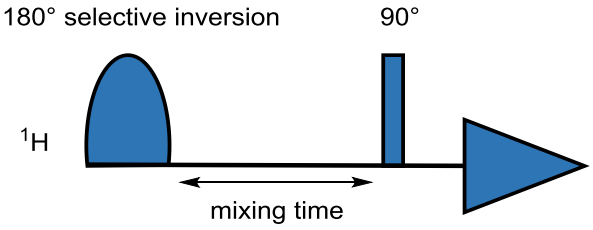

Figure 4-6. General scheme of the 1D EXSY sequence.

Spectra are recorded after different mixing times (τ_m). Exchange between the two sites and relaxation will occur during the mixing time. An example of spectra that would be obtained after selective inversion at site B is shown in Figure 4-7.

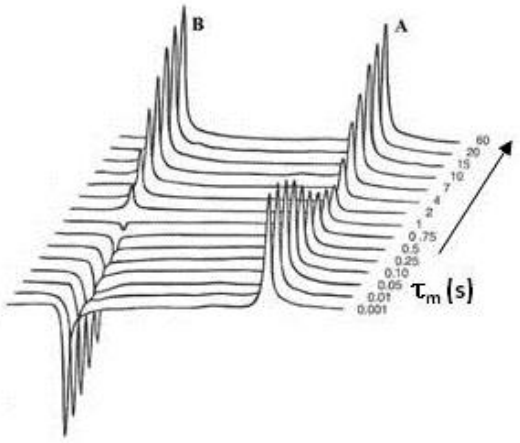

Figure 4-7. Site B is selectively inverted and spectra are recorded for different mixing times.[3]

As it can be observed in Figure 4-7, the signal which was selectively inverted (B) is negative for short mixing times but returns to its initial intensity as the mixing time increases (longitudinal relaxation characterized by T_{1B}). For the signal that corresponds to the species in site A, its intensity is function of the exchange process (k_{BA}) and of its relaxation (T_{1A}). This explains why it initially decreases before returning to its equilibrium intensity for long mixing times. If difference spectra are recorded (difference with the spectrum for the system at equilibrium), the inverted signal returns to zero while the other signal is negative and first increases in absolute intensity before returning to zero.[3]

It is noteworthy that the theory for the determination of the kinetic constants in EXSY measurement presented here is derived from the development made for kinetic NOE measurements.[5] In order to determine the kinetic constants associated with the exchange, signals A and B must be integrated for the different mixing times. The fractional enhancement (f) can be computed:

$$f = \frac{I_\tau - I_0}{I_0}$$

Equation 4-2

where I_τ corresponds to the integration of the signal after a mixing time τ and I_0 corresponds to the integration at equilibrium. When B is selectively inverted, the ratio of the fractional enhancements R_B is defined as:

[5] Hu, H.; Krishnamurthy, K. *Journal of Magnetic Resonance*. **2006**, *182*, 173-177.

$$R_B(\tau) = \frac{f_A(\tau)}{f_B(\tau)}$$

Equation 4-3

In order to obtain the kinetic constant k_{BA}, R_B is determined for different τ. The kinetic constant k_{BA} is the initial slope of the $R_B(\tau)$ curve (Equation 4-4).[6] For k_{AB}, the same procedure is followed by inverting A.

$$k_{BA} \approx \lim_{\tau \to 0} \frac{dR_B(\tau)}{d\tau}$$

Equation 4-4

Many examples have been reported in the literature on the use of EXSY experiments (1D or 2D experiments which we have not described here) to measure of residence time of guests complexed by molecular receptors.[7] For the study of the dynamics of guest complexation in the cavity of calix[6]arenes, we can mention the work on a receptor composed of a calixarenic and a CTV unit reported by Jabin and co-workers (Figure 4-8).[8] 1D EXSY experiments were performed in order to determine the residence time of the guest (imidazolidinone) in the two complexation sites.

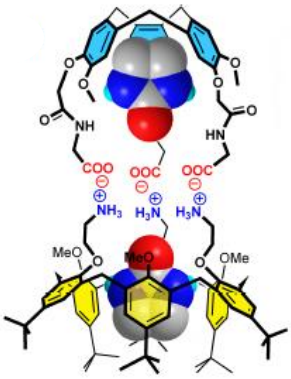

Figure 4-8. Supramolecular assembly of a calixarene and a CTV with 2 imidazolidinone as guest (figure taken from reference 8).

Naruta et al. used 2D EXSY experiments to evaluate kinetic and thermodynamics parameters related to the process of encapsulation of small hydrocarbons (e.g. methane) into a cavitand-

[6] Gerig, J. T. *J. Org. Chem.* **2003**, *68*, 5244-5248.
[7] Pons, M. ; Millet, O. *Progress in Nuclear Magnetic Resonance Spectroscopy*, **2001**, *38*, 267-324.
[8] Le Gac, S.; Luhmer, M.; Reinaud, O.; Jabin, I. *Tetrahedron* **2007**, *63*, 10721-10730.

porphirin.[9] Turro et al. described kinetic and thermodynamic properties of water encapsulation by a [60]fullerene (Figure 4-9) and used 2D EXSY measurements to determine association and dissociation constants as well as the activation energies.[10]

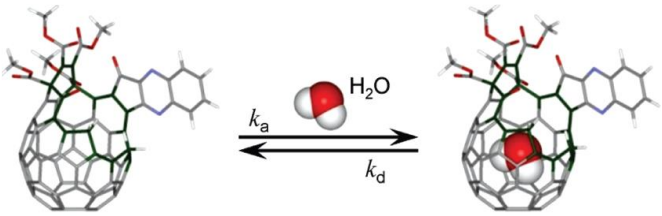

Figure 4-9. Water encapsulation by an open cage [60]fullerene derivative (figure taken from reference 10).

4.3. RESULTS AND DISCUSSION

To verify our hypothesis that we described in the introduction to this chapter i.e. that an *exo*-ligand is needed in order for guest exchange to occur in calixarene-Zn^{2+} based systems where the zinc is only tri-coordinated to the calixarene, we undertook 1D EXSY experiments with three different systems **1.Zn**$^{2+}$, **2.Zn**$^{2+}$ and **6.Zn**$^{2+}$ (Figure 4-10). We looked at the exchange of different guests (dimethylformamide, acetonitrile and ethanol) and focused our work mostly on investigating the role of water in the exchange process (water as the possible *exo*-ligand).

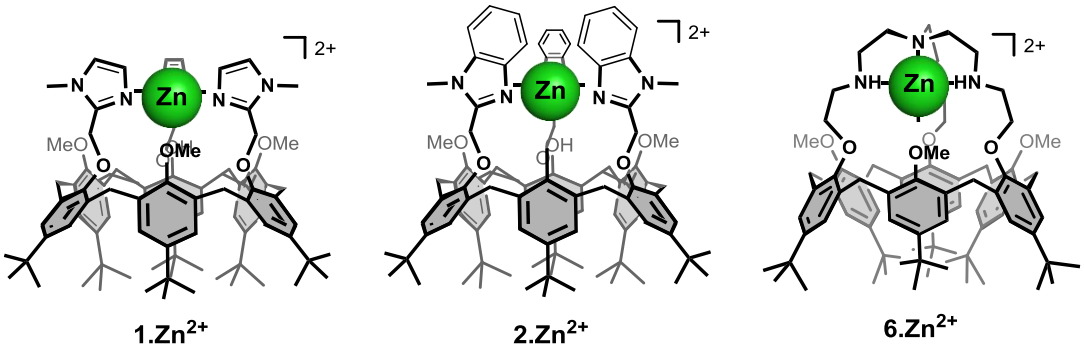

Figure 4-10. Structure of **1.Zn**$^{2+}$, **2.Zn**$^{2+}$ and **6.Zn**$^{2+}$.

4.3.1. EFFECT OF WATER ON GUEST EXCHANGE WITH SYSTEM **1.ZN**$^{2+}$

The NMR spectra of calix[6]tris-imidazole zinc **1.Zn**$^{2+}$ recorded in DCM-d_2 in the presence of a large excess of dimethylformamide (DMF), acetonitrile (CH_3CN) or ethanol (EtOH) are

[9] Nakazawa, J.; Sakae, Y.; Aida, M.; Naruta, Y. *J. Org. Chem.* **2007**, *72*, 9448-9455.
[10] Frunzi, M.; Baldwin, A. M.; Shibata, N.; Iwamatsu, S., Lawler, R. G., Turro, N. J. *J. Phys. Chem* A **2011**, *115*, 735-740.

shown in Figure 4-11.[11] All the cavities are filled with corresponding guest. The three nitrogen arms of the host coordinate the zinc cation and the guest molecule in the cavity completes the tetrahedral coordination sphere of the metal.[12]

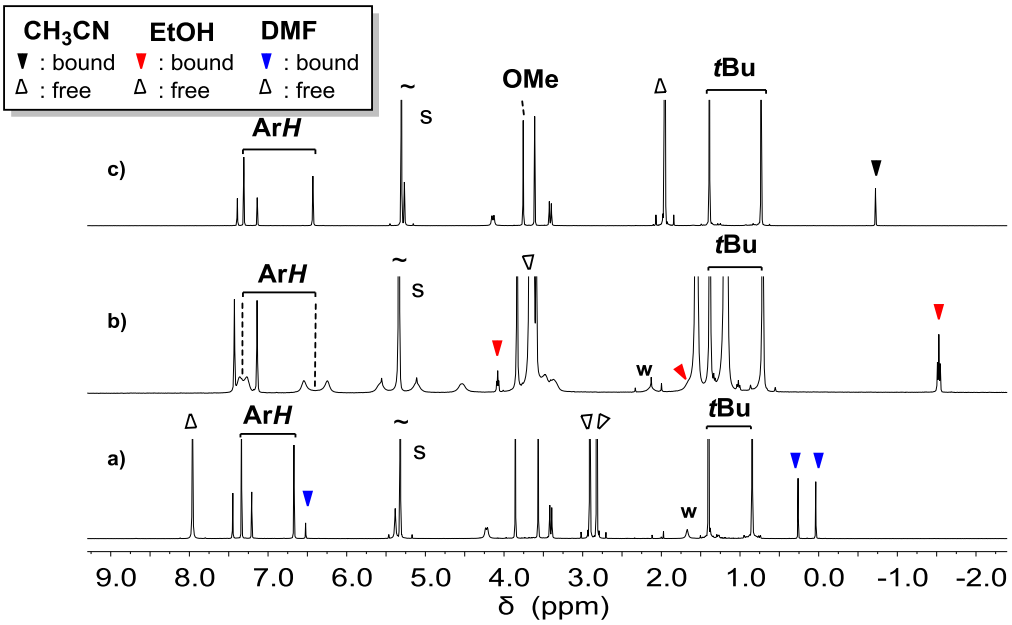

Figure 4-11. ^{1}H NMR spectra (600MHz) of **1.Zn^{2+}** in DCM-d_2 in the presence of a) 32 equiv. of DMF and ~1.5 equiv. of water at 298 K; b) 53 equiv. of EtOH and ~0.3 equiv. of water at 253 K; c) 42 equiv. of CH_3CN and ~0 equiv. of water at 298 K; s: solvent; w: water.

The following common features are observed in the spectra of all three host-guest complexes: all NMR profiles are sharp and characteristic of a flattened C_3 symmetrical cone conformation ($\Delta\delta_{ArH}$ > 0.56 ppm and $\Delta\delta_{tBu}$ > 0.66 ppm); the methoxy protons are shifted downfield confirming that they are expelled from the cavity (δ_{OMe} > 3.55 ppm); upfield signals are present for the guest confirming their inclusion. Guest complexation is in slow exchange on the NMR chemical shift timescale and the intra-cavity complexation of the different guests was clearly evidenced through 1D EXSY experiments. For instance, a signal at 2.92 ppm, corresponding to a CH_3 group of free DMF, is observed upon inversion of the signal at 0.26 ppm corresponding to one of the CH_3 group of bound DMF. The 1D EXSY spectra recorded for different mixing times are shown in Figure 4-12.

[11] The entire ^{1}H NMR characterization of the complexes is presented in the chapter Material and methods.
[12] Sénèque, O.; Rondelez, Y.; Le Clainche, L.; Inisan, C.; Rager, M.-N. ; Giorgi, M.; Reinaud, O. *Eur. J. Inorg. Chem.* **2001**, 2597-2604.

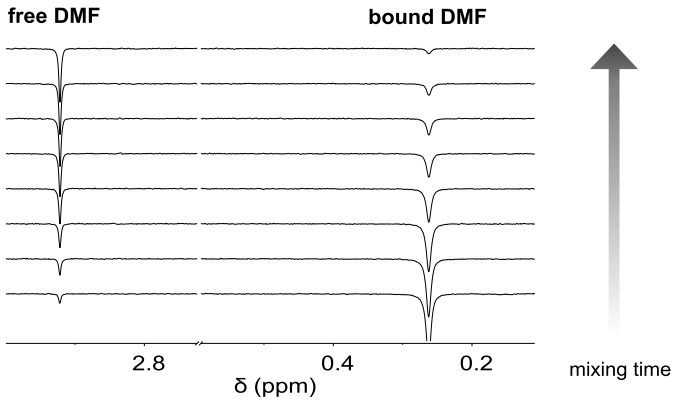

Figure 4-12. 1D EXSY spectra (600MHz, 298 K, DCM-d_2) of **1.Zn^{2+}** in the presence of 32 equiv. of DMF and ~8.3 equiv. of water at different τ_m (25 to 1500 ms) by inverting the signal of low field bound DMF.

1D EXSY experiments were undertaken to monitor the exchange of the three different guests in the presence of different amounts of water. In each case, the signal(s) of the included guest was inverted. There are three signals for included DMF and, when experiments were undertaken with each of these signals, the results were not significantly different. The fractional enhancements "R", as defined in Equation 4-3, are shown in Figure 4-13 as a function of the mixing time for the **1.Zn^{2+}⊃DMF** system and for different water concentrations. The fractional enhancements reported are the average of the values obtained when inverting each of the signals corresponding to the methyl groups of included guest. Upon water addition, only a very small broadening of the signals of the bound guest is observed in the ^{1}H NMR spectra and the signature of the system did not change. Experiments were only recorded for short mixing times where a linear relationship is observed. The slopes of the lines yield k_{tot}.

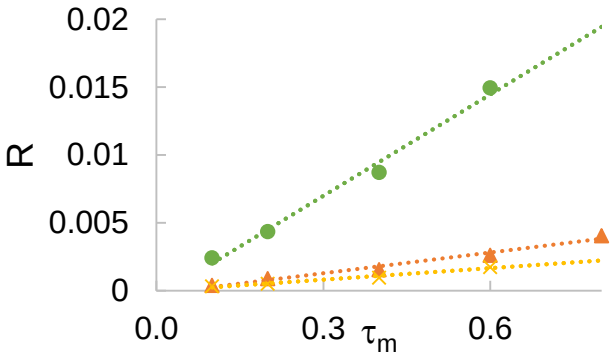

Figure 4-13. Evolution with mixing time τ_m of the fractional enhancement determined for the more downfield CH_3 signal of bound DMF. Data showed for ~6.3 (yellow), ~12.5 (orange) and ~61 (green) equiv. of H_2O and 32 equiv. of DMF.

The evolution of k_{tot} as a function of the number of equivalents of water (relative to **1.Zn^{2+}**) is given in Figure 4-14 for the **1.Zn^{2+}⊃DMF** system.[13] The following can be derived from analysis of the data:

- without water, no guest exchange is observed;
- k_{tot} increases linearly with water concentration for a relatively large window.

This suggests that the model described in the introduction to this chapter could be valid with water as *exo*-ligand, L. As guest exchange does not occur in the absence of water even when there is a large excess of DMF (the experiments were undertaken in the presence of 32 equiv. of DMF) this suggests that DMF does not seem to play the role of *exo*-ligand L.

Entry	Equiv. water	$k_{tot}(s^{-1})$ (298K) DMF
1	1.5	0
2	6.3	0.0026 ± 0.0002
3	8.3	0.0028 ± 0.0002
4	12.5	0.0045 ± 0.0003
5	61.0[14]	0.0226 ± 0.0021

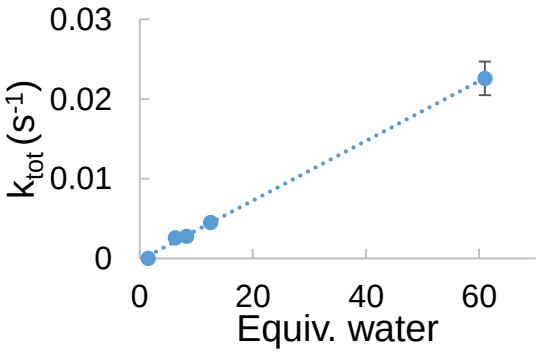

Figure 4-14. Rate constant (k_{tot}), characterizing the exchange of DMF at 298 K, as a function of the number of equivalents of water in the DCM-d_2 solution. The errors for k_{tot} are fitting errors. Error for number of equivalents of water was estimated to be 10 %.

Similar EXSY experiments were undertaken with ethanol as guest. They were undertaken at lower temperature (253 K instead of 278 K in the case of DMF), as at room temperature, the signal of the included guest was too broad to be efficiently inverted during the EXSY experiment.[15] Upon addition of water, a significant broadening of the signals of bound ethanol is observed showing that water significantly modifies the kinetic of the buried guest (cf. expansions for the CH_3 and OH groups in Figure 4-15). The k_{tot} derived from the EXSY experiments undertaken in the presence of different number of equivalents of water are shown in Figure 4-16. As in the case of DMF, a linear dependence of k_{tot} is observed with water concentration.

[13] For the sake of convenience, when k_{tot} is too small to be measured we will give it a value of 0.
[14] In these really wet conditions we observe ~50 % **1.Zn^{2+}⊃DMF** and ~50 % of **1.Zn^{2+}⊃(H$_2$O)$_2$**.
[15] The VT study of **1.Zn^{2+}⊃EtOH** is presented in Appendix 2 (7.2).

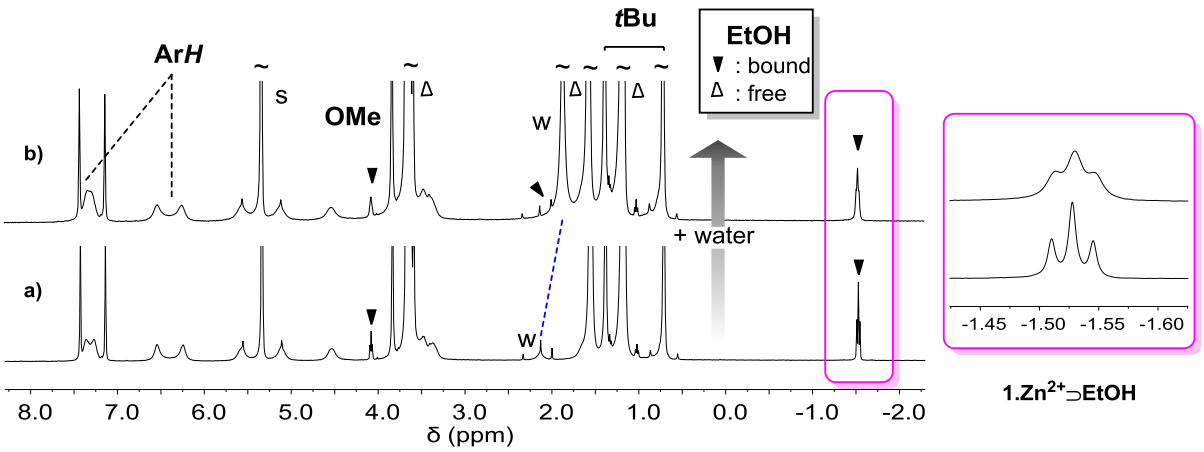

Figure 4-15. ^{1}H NMR spectrum (600MHz, 253 K) of **1.Zn^{2+}** in DCM-d_2 with 53 equiv. of EtOH in the presence of of: a) ~0.3 equiv. of water; b) 9 equiv. of water.

Entry	Equiv. water	k_{tot}(s^{-1}) EtOH (253K)
1	0.3	0.0126 ± 0.0017
2	1	0.0258 ± 0.016
3	2.6	0.0753 ± 0.05
4	9	0.465 ± 0.052

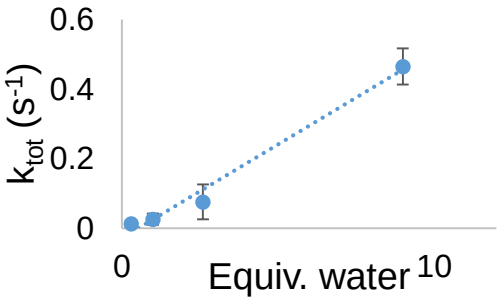

Figure 4-16. Rate constant (k_{tot}), characterizing the exchange of EtOH at 253 K, as a function of the number of equivalents of water in the DCM-d_2 solution. The errors for k_{tot} are fitting errors. Error for number of equivalents of water was estimated to be 10 %.

The results of the EXSY experiments undertaken with acetonitrile as a guest are shown in Figure 4-17. Experiments were run at 298K, like in the case of DMF, as the guest signals were not broad at this temperature, even in the presence of a large excess of water. As in the case of DMF and EtOH a linear dependence of k_{tot} is observed with water concentration.

Entry	Equiv. water	$k_{tot}(s^{-1})$ (298K) CH_3CN
1	0	0
2	0.2	0.0047 ± 0.0003
3	1.4	0.0065 ± 0.0013
4	1.6	0.0108 ± 0.0009

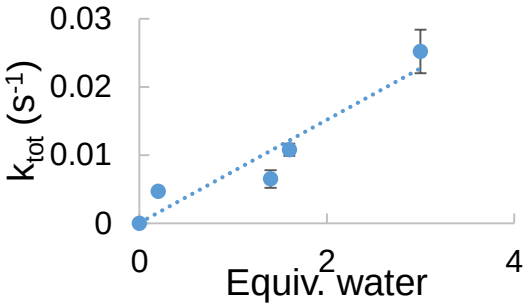

Figure 4-17. Rate constant (k_{tot}), characterizing the exchange of CH_3CN at 298 K, as a function of the number of equivalents of water in the DCM-d_2 solution. The errors for k_{tot} are fitting errors. Error for number of equivalents of water was estimated to be 10 %.

The value of k_{tot} clearly depends on the nature of the guest buried inside the cavity (Figure 4-18). For a same number of equivalents of water, k_{tot} of CH_3CN is significantly larger than for DMF at 298K. The k_{tot} for ethanol is even larger, as at 253 K it is already one order of magnitude larger than the k_{tot} for CH_3CN at 298K.

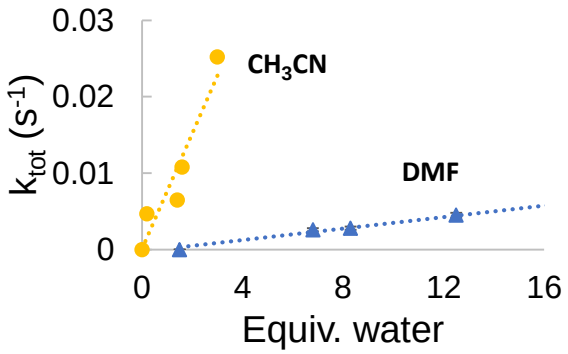

Figure 4-18. Dependence of k_{tot} at 298 K with water concentration in the case of: DMF (blue triangles) and CH_3CN (yellow dots).

The linear dependence observed for the k_{tot} of all three guest of **1.Zn^{2+}**, as a function of the number of equivalents of water in solution, clearly suggests that the model described in the introduction to this chapter could be valid with water as *exo*-ligand, L. All three guest furthermore do not seem to be able to play the role of the *exo*-ligand necessary to allow guest to occur. Indeed, all experiments were undertaken with a large excess of guest and when there is no water present, guest exchange is not observed. A hypothesis that can be put forward at this stage is that EtOH, DMF and CH_3CN are sterically too hindered to be able to interact with the zinc via *exo*-coordination at the level of the imidazole moieties.

The addition of ethanol was monitored to see if it could allow guest exchange. After addition of 75 equivalents of ethanol to a solution of **1.Zn^{2+}⊃DMF** with 1 equiv. of water no exchange

was observed for DMF at this water concentration. Increasing water concentration to 29 equiv. lead to an increase of k_{tot} for DMF ($k_{tot, DMF} \sim 0.004\ s^{-1}$). However, at same water concentration, it seems that the presence of EtOH in solution rather than increasing k_{tot} for DMF it slightly decreases it (Figure 4-19left).

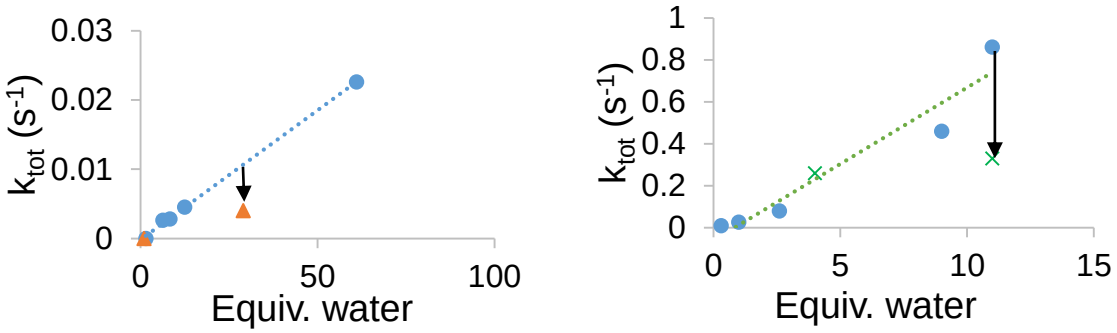

Figure 4-19. Left: dependence of k_{tot} with the number of equivalents of water concentration for DMF before (blue dots) and after (orange triangles) the addition of 75 equiv. of EtOH; Right; dependence of k_{tot} with then number of equivalents of water for EtOH before (blue dots) and after (green cross) the addition of 37 equiv. of EtOH.

The effect of the addition of EtOH was also evaluated in the case of a solution of **1.Zn^{2+}⊃EtOH**. After addition of 37 equiv. of EtOH with 11 equiv. of water present in solution we observed a significant decline of k_{tot} (from 0.86 to 0.33 Figure 4-19 right).

The fact that the residence time ($1/k_{tot}$) increases with ethanol concentration for a given water concentration clearly suggests that ethanol cannot play the role of the *exo*-ligand. Concerning the observation that, for a given water concentration, increasing the ethanol concentration slows down the exchange, it can perhaps be put forward that ethanol solvates the water molecules that they are thus less available to be *exo*-complexed to zinc, slowing down the exchange as a penta-coordinated zinc is crucial in the mechanism of guest exchange. The effect seems to be disappear when the concentration of water is lower (Figure 4-19 right).

Based on our results it seems that in the case of system **1.Zn^{2+}** the expression given in Equation 4-5 can be simplified as follows (where *b* is a constant):

$$k_{tot} = b * [H_2O]$$

Equation 4-5.

4.3.2. STERIC HINDRANCE

In order to investigate if steric hindrance at the level of the zinc coordination could be a key parameter governing the *exo*-coordination of a ligand L at the level of the zinc atom, guest exchange with the calix[6]benzimidazole zinc, **2.Zn^{2+}**, was investigated (structure of **2.Zn^{2+}⊃EtOH** in Figure 4-20). The steric hindrance of the benzimidazole groups could make the *exo*-complexation of water more difficult slowing down guest exchange. This could help us to confirm our hypothesis on the existence of an intermediate penta-coordinated species in the exchange process.

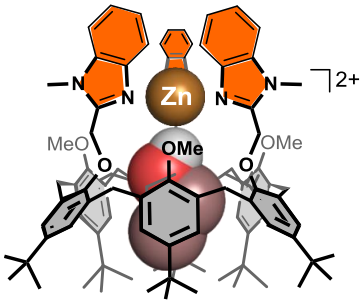

Figure 4-20. Structure of **2.Zn^{2+}⊃EtOH**.

The NMR spectra **2.Zn^{2+}** recorded in DCM-d_2 in the presence of a large excess of acetonitrile (CH_3CN at 298K) or ethanol (EtOH at 253K) are shown in Figure 4-21.[16] Under these experimental conditions all the cavities are filled.

[16] The entire ^{1}H NMR characterization of the complexes is presented in the chapter Material and methods.

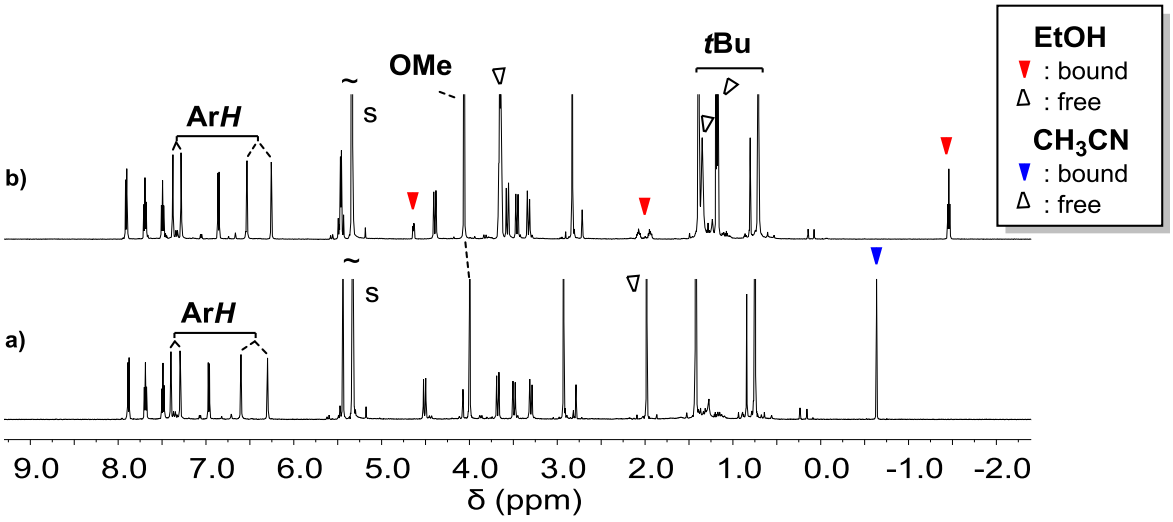

Figure 4-21. ^{1}H NMR spectra (600MHz, DCM-d_2) of **2.Zn^{2+}** in in the presence of: a) 12 equiv. of CH_3CN and ~0 equiv. of water at 298 K; b) 12 equiv. of EtOH and ~0 equiv. of water at 253 K; s: solvent.

As in the case of **1.Zn^{2+}**, each complex can exists as a pair of enantiomers which are in conformational equilibrium. It has however been reported that the helical inversion in system **2.Zn^{2+}** is characterized by a smaller kinetic constant than in **1.Zn^{2+}** and this is probably related to the steric hindrance near the metal center.[12]

Guest exchange is slow on the NMR chemical shift timescale and 1D EXSY experiments were undertaken. As in the case of **1.Zn^{2+}** we monitored the exchange of both guests as a function of water concentration. The k_{tot} determined for ethanol (at 253 K) and acetonitrile (at 298 and 253 K) as a function of the number of equivalents of water (relative to the host concentration) are reported in Figure 4-22 and Figure 4-23 respectively.

Entry	Equiv. water	$k_{tot}(s^{-1})$ (253K) EtOH
1	0	0
2	1.5	0.033 ± 0.007
3	3.0	0.085 ± 0.009
4	6.5	0.183 ± 0.042

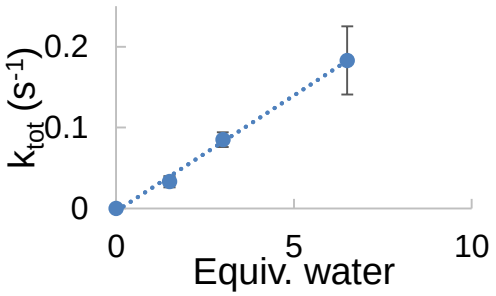

Figure 4-22. Rate constant (k_{tot}), characterizing the exchange of EtOH at 253 K, as a function of the number of equivalents of water in the DCM-d_2 solution. The errors for k_{tot} are fitting errors. Error for number of equivalents of water was estimated to be 10 %.

Entry	equiv. H_2O	$k_{tot}(s^{-1})$ CH_3CN (298K)	$k_{tot}(s^{-1})$ CH_3CN (253K)
1	0	0	0
2	4.3	0.025 ± 0.003	-
3	5.1	0.041 ± 0.003	0.009 ± 0.001
4	7.2	0.061 ± 0.003	-
5	10.5	0.090 ± 0.007	0.030 ± 0.002

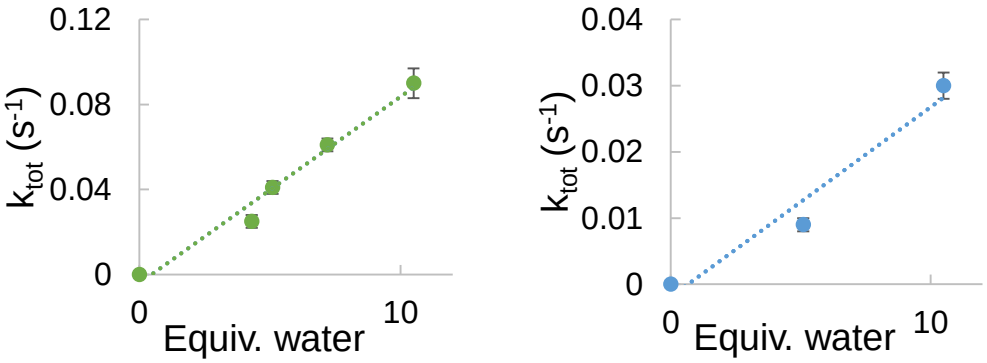

Figure 4-23. Rate constant (k_{tot}), characterizing the exchange of CH_3CN at 298 K (left, green) and 253 K (right, blue), as a function of the number of equivalents of water in the DCM-d_2 solution. The errors for k_{tot} are fitting errors. Error for number of equivalents of water was estimated to be 10 %.

As with **1.Zn^{2+}** a linear dependence of k_{tot} with water concentration is observed and in the absence of any water guest exchange is negligible. The values of k_{tot} for systems **1.Zn^{2+}** and **2.Zn^{2+}** are furthermore of the same order of magnitude for ethanol at 253 K and for acetonitrile at 298 K. The benzimidazole arms consequently do not seem to introduce a significant steric hindrance for the *exo*-coordination of water. When decreasing the temperature from 298K to 253K with the system **2.Zn^{2+}⊃CH$_3$CN**, k_{tot} decreases significantly.

For all the systems that we have look at so far, **1.Zn^{2+}⊃DMF**, **1.Zn^{2+}⊃EtOH**, **1.Zn^{2+}⊃CH$_3$CN**, **2.Zn^{2+}⊃EtOH** and **2.Zn^{2+}⊃CH$_3$CN**, the following common features have been observed:

- the residence time of the guest decreases with increasing equivalents of water, and therefore water concentration;
- under dry conditions, guest residence time is too high to be measured by EXSY experiments;
- the guest itself does not play the role of L.

This leads us to conclude that for systems **1.Zn^{2+}** and **2.Zn^{2+}**, water can play the role of the *exo*-ligand and that the data fits with the theoretical model described in section 4.1 (where α is a constant).

$$\frac{1}{\tau_{in}} = k_{tot} = \alpha * [H_2O]$$

It is interesting to point out that an X-Ray structure of a similar system (a calix[6]tris-ethylimidazole zinc) with acetonitrile inside the cavity has been observed with a H_2O water molecule *exo*-coordinated to the Zn cation.

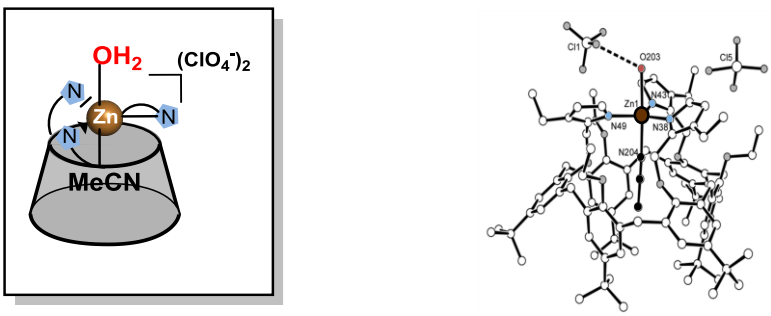

Figure 4-24. Schematic representation of the penta-coordinated complex (left) and XRD structure taken from Sénèque PhD thesis (right) [2].

4.3.3. PENTA-COORDINATED ZINC COMPLEX

The studies described in the previous sections were undertaken with zinc complexes belonging to the N_3 generation of hosts, **1.Zn^{2+}** and **2.Zn^{2+}**. Results seem to corroborate the hypothesis proposed in the introduction for the guest exchange mechanism: an associative mechanism with an intermediate penta-coordinated zinc complex. Water was also identified as a *exo*-ligand which can enables guest exchange to occur.

In the calix[6]tren zinc complex, **6.Zn^{2+}** (Figure 4-25) the metal center is tetra-coordinated in the absence of a guest due to the coordination of the apical nitrogen to the metallic center, and penta-coordinated in the presence of an *endo*-guest. A different guest exchange mechanism could therefore be expected. With **6.Zn^{2+}**, the guest should be able to leave the cavity without the help of an *exo*-ligand; we will then expect a dissociative mechanism instead of an associative mechanism (Figure 4-25).

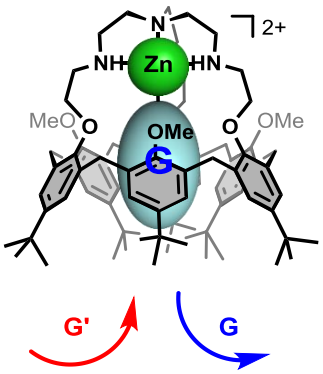

Figure 4-25. Schematic representation of a dissociative mechanism with **6.Zn^{2+}**.

The NMR spectra of calix[6]tren zinc, **6.Zn^{2+}** recorded in DCM-d_2 in the presence of an excess of acetonitrile (DMF, at 298K) or ethanol (EtOH, at 253K)[17] are shown in Figure 4-26.[18] Under these condition all cavities will be filled with a guest and the zinc metal is coordinated to the 4 nitrogens of the tren cap and to the guest molecule. The exchange of the guest is slow on the NMR timescale. Analysis of the spectra show that the calixarene adopts a flattened alternate cone conformation with the three tert-butyl groups belonging to the anisole units directed towards the inside of the cavity. The geometry around the Zn cation is trigonal bipyramidal and the three amino arms wrapping the zinc cation adopt an asymmetric conformation with two

[17] The VT study of **6.Zn^{2+}⊃EtOH** is presented in Appendix 2 (7.2).
[18] The entire ^{1}H NMR characterization of the complexes is presented in the chapter Material and methods.

coordinated arms presenting a relative helical orientation opposite to each other. The ^{1}H NMR signature of the host structure attested to a dissymmetric conformation as three signals are observed for the methoxy groups.[19]

For the sake of comparison with the previous systems, 1D EXSY experiments were carried out at 298 K for DMF and at 253 K for EtOH. A clear broadening of the signals of buried EtOH upon addition of water is observed (cf. Figure 4-27a-b). This broadening is without any doubt signature of a change in the kinetics of the exchange process of the guest inside the cavity.

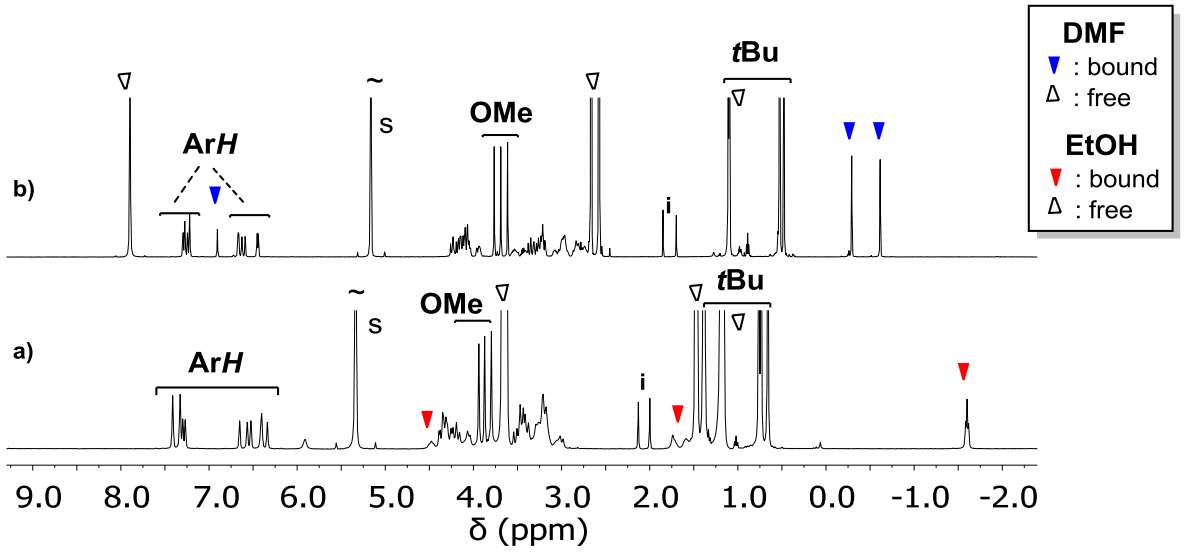

Figure 4-26. ^{1}H NMR spectra (600MHz) of **6.Zn**$^{2+}$ in DCM-d_2 in the presence of: a) 33 equiv. of EtOH and ~0.3 equiv. of water at 253 K; b) 11 equiv. of DMF and ~0.2 equiv. of water at 298 K; s: solvent; i: impurities.

[19] Darbost, U.; Rager, M.-N.; Petit, S.; Jabin, I.; Reinaud, O. *J. Am. Chem. Soc.* **2005**, *127*, 8517-8525.

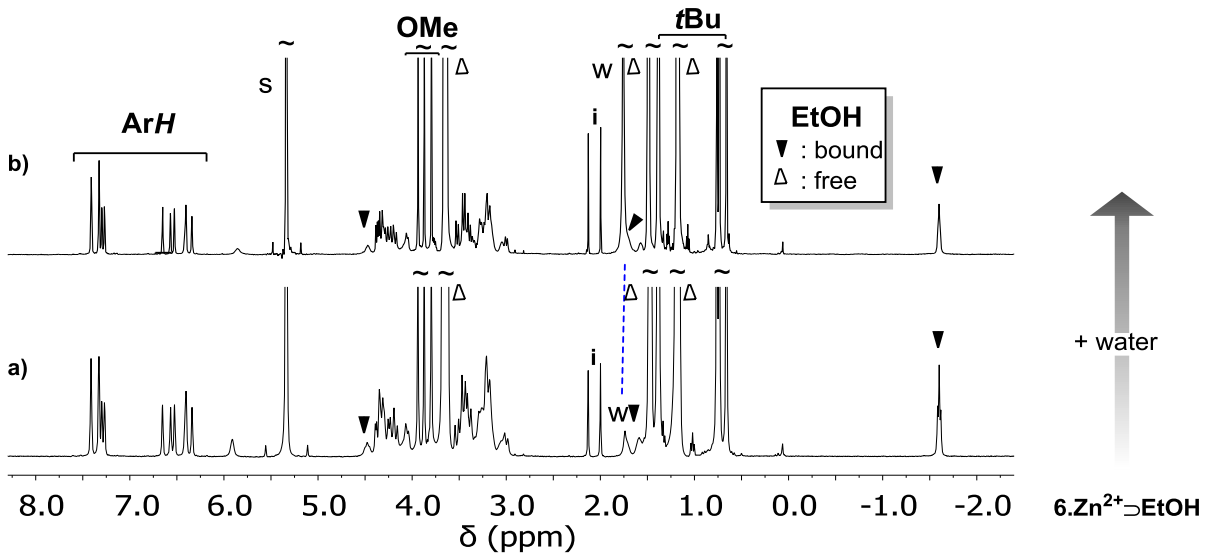

Figure 4-27. ^{1}H NMR spectra (600MHz, 253 K) of **6.Zn^{2+}** in DCM-d_2 in the presence of 33 equiv. of EtOH and: a) ~0.3 equiv. of water; b) 7.0 equiv. of water; s: solvent; i: impurities.

Entry	Equiv. water	k_{tot}(s^{-1}) (253K) EtOH
1	0.3	0.013 ± 0.004
2	0.5	0.028 ± 0.002
3	1.0	0.073 ± 0.006
4	5	1.807 ± 0.374
5	7	2.168 ± 0.629

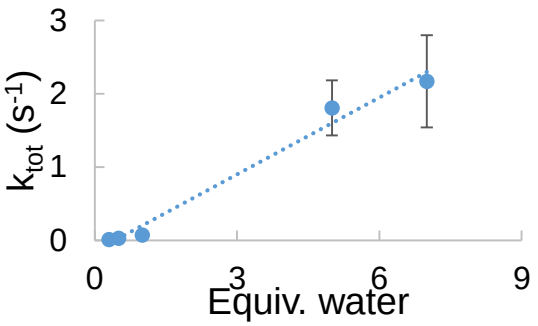

Figure 4-28. Rate constant (k_{tot}), characterizing the exchange of EtOH at 253 K, as a function of the number of equivalents of water in the DCM-d_2 solution. The errors for k_{tot} are fitting errors. Error for number of equivalents of water was estimated to be 10 %.

Entry	Equiv. water	$k_{tot}(s^{-1})$ (298K) DMF
1	0.2	0.019 ± 0.002
2	4.3	0.209 ± 0.014
3	21	1.033 ± 0.108
4	24	1.173 ± 0.125

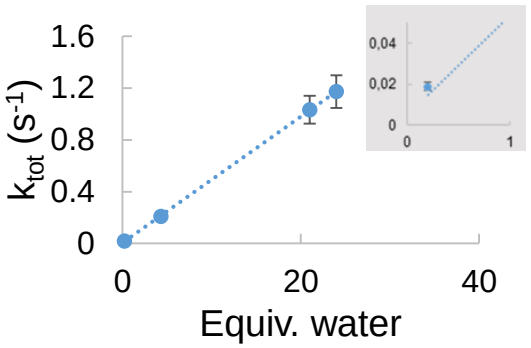

Figure 4-29. Rate constant (k_{tot}), characterizing the exchange of DMF at 298 K, as a function of the number of equivalents of water in the DCM-d_2 solution. The errors for k_{tot} are fitting errors. Error for number of equivalents of water was estimated to be 10 %.

In order to simplify reading, the determined kinetic constants will also be called k_{tot}. The determined k_{tot} from 1D EXSY experiments for ethanol (at 253 K) and acetonitrile (at 298 K), as a function of the number of equivalents of water (relative to the host concentration), are reported in Figure 4-28 and Figure 4-30 respectively. The following observations can be made:

- contrary to what we had expected, guest exchange with **6.Zn**$^{2+}$ is also influenced by the concentration of water in solution;
- the dependence of the kinetic constant seems to be linear with the number of equivalents of water, as observed with systems **1.Zn**$^{2+}$ and **2.Zn**$^{2+}$;
- the exchange rate depends significantly on the guest buried inside the cavity; the values obtained for EtOH and DMF are quite different;
- the kinetic constants are much higher in the case of **6.Zn**$^{2+}$ compared to **1.Zn**$^{2+}$ or **2.Zn**$^{2+}$;
- exchange occurs even in the absence of water (see for example expansion Figure 4-29).

The fact that guest exchange for system **6.Zn**$^{2+}$ is also affected by water concentration suggests, that the exchange could be favored by the coordination of water molecule to the zinc ensuring that the zinc it is at all times at least penta-coordinated. The coordination of the water molecule would take place through the cap and not in the apical position as for **1.Zn**$^{2+}$ and **2.Zn**$^{2+}$ (position occupied by a nitrogen in system **6.Zn**$^{2+}$) (Figure 4-30).

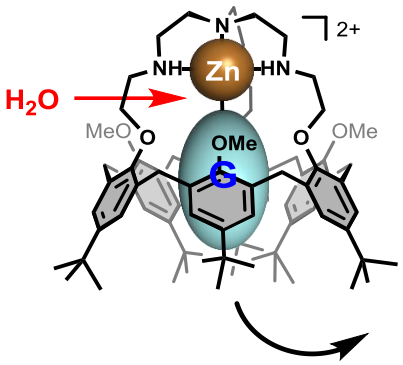

Figure 4-30. Schematic representation of the water access in system **6.Zn**$^{2+}$ with a molecule of DMF buried inside the cavity.

4.3.4. DISCUSSION AND INTERPRETATION

The results presented in the previous section are summarized in Table 4-1 where we present the slopes of the regression lines for k_{tot} vs. the number of equivalents of water.

Table 4-1. Slopes of the regression lines obtained for the dependence of k_{tot} with the equivalents of H_2O. Errors: maximum 10 %.

System	Temp (K)	Slope k_{tot} vs. #H_2O		
		EtOH	DMF	CH_3CN
1.Zn^{2+}	298	-	0.004	0.009
1.Zn^{2+}	253	0.05	-	-
2.Zn^{2+}	298	-	-	0.008
2.Zn^{2+}	253	0.03	-	0.002
6.Zn^{2+}	298	-	0.05	-
6.Zn^{2+}	253	0.35	-	-

It is noteworthy that for systems **1.Zn^{2+}** and **2.Zn^{2+}** the intercept of the regression line is essentially zero. The kinetic constants that we have determined from our 1D EXSY experiments all relate to processes which enable the guest to leave a cavity and its inverse can be considered as the residence time of the guest inside the cavity (τ_{in}). For **1.Zn^{2+}** and **2.Zn^{2+}** in the absence of water the guest would have an infinite τ_{in}. For system **6.Zn^{2+}** at the intercept we have a non-zero values (0.013 s^{-1} for EtOH at 253 K and 0.019 s^{-1} at 298 K for DMF).

Results with EtOH at 253 K (Figure 4-31left) and with DMF at 298 K (Figure 4-31right) show that the dependence of the kinetic constant (k_{tot}) with water concentration increases with the donor character of the calixarene complex: steeper slopes are observed for **6.Zn^{2+}** compared to **1.Zn^{2+}** or **2.Zn^{2+}**. Zinc is a Lewis acid and its donor or acceptor character depends on the different ligands bound to it. It is more acidic when its coordination is higher and water coordination is favored by a poorer metallic center. Upon water coordination, the acidity of the zinc is lowered and the guest is more labile.

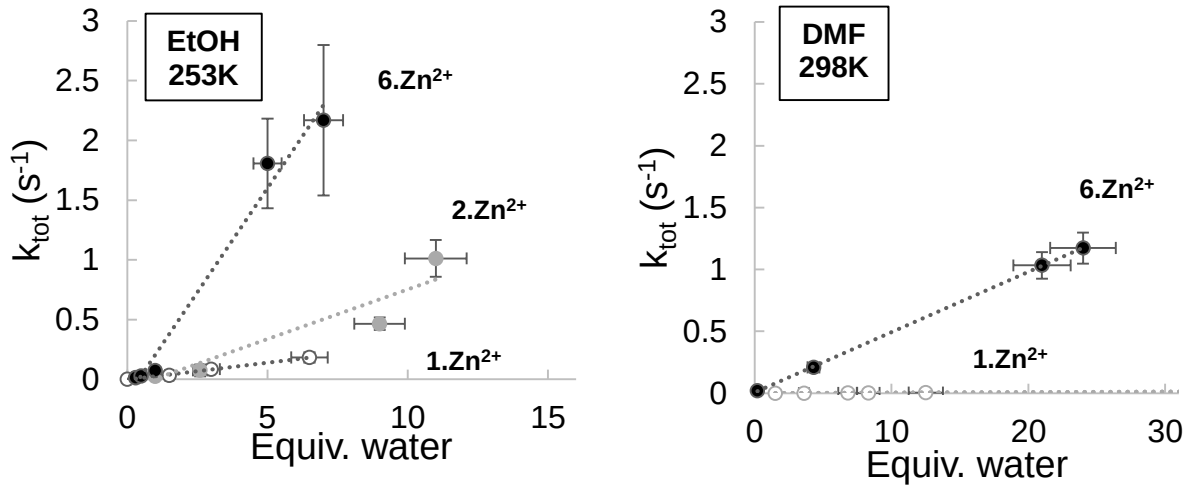

Figure 4-31. Comparison of the dependence of k_{tot} with the equivalents in water in solution in the case of: left) EtOH at 253 K; right) DMF at 298 K.

Our results are in agreement with those reported by Dr. Sénèque in his PhD thesis.[2] Indeed he observed that the degree of acidity of the zinc metal center has an important influence on the exchange kinetics of the guest buried inside the cavity. The introduction of a 4th coordinating group such as phenol or phenate on the calix[6]tris-imidazole **1** increased the kinetics of guest exchange, and thus its lability. The more acidic the zinc, the greater the effect of the coordination of water on its acidity.[2] Our results also show that for each system the kinetics are highly dependent on the nature of the guest. The exchange of ethanol is faster in all cases (cf. Table 4-1). Comparison between EtOH and CH_3CN for **2.Zn^{2+}** is shown in Figure 4-32.

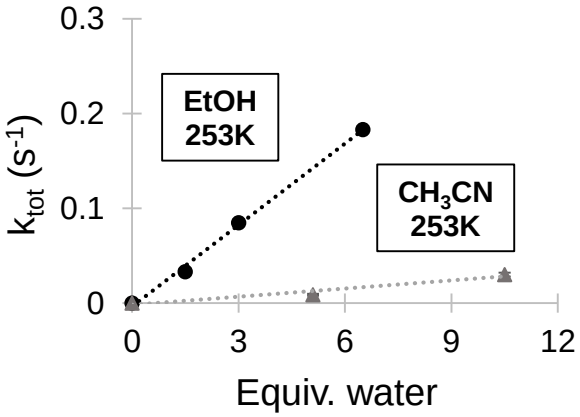

Figure 4-32. Comparison of the dependence of k_{tot} with the number of equivalents of water in solution in the case of **2.Zn^{2+}** for EtOH and CH_3CN at 253 K.

Water coordination to the metal, changes not only its acidity but also its geometry of coordination and the host-guest complex conformation. The change in conformation

destabilizes the guest inside the calixarene cavity. It is possible that the consequence is more important for ethanol than for the other guests as the H-bond interaction between its hydroxyl groups and the oxygens of the small rim, as observed by XRD with systems **1.Zn^{2+}⊃EtOH** and **6.Zn^{2+}⊃EtOH** by Reinaud and Jabin,[2,19] is essential for the stabilization of the host-guest complex. This H-bond interaction could be easily lost following a change in geometry.

In conclusion, water *exo*-coordination which plays a key role in the exchange process, seems to be governed by (i) the accessibility to the metal which depends on the geometry and the conformation of the calixarene and by (ii) the acidity of the metal which depends on its number of coordinating group and the nature of the guest inside the cavity. In order to complete our knowledge of the studied systems we determined by competition experiments the affinities of EtOH and CH_3CN relative to DMF for each system (Table 4-2).

Table 4-2. Affinities of EtOH and CH_3CN relative to DMF determined by ^{1}H NMR in DCM-d_2. Estimated error of ~20 % due to integration of signals of the free and bound guest.

System	Temp. (K)	$K_{EtOH/DMF}$	$K_{CH3CN/DMF}$
1.Zn^{2+}	253	0.06	0.14
2.Zn^{2+}	298	0.7	0.21
6.Zn^{2+}	298	1.6	<0.04

We were however not able to rationalize these results in relation to guest exchange dynamics.

4.4. CONCLUSIONS

The guest exchange mechanism of calix[6]arene zinc complexes had to date not been elucidated. The hypothesis we put forward is that when the zinc cation is tri-coordinated to the calix[6]arene ligand an *exo*-coordination of a molecule is required to allow the *endo*-guest to exchange. Using 1D EXSY experiments we monitored the exchange of different guest from the cavity of the calix[6]tris-imidazole zinc complex **1.Zn^{2+}**. We showed that: (i) the residence time of the guests decreases linearly with increasing equivalents of water; (ii) under dry conditions, guest residence time is too high to be measured by EXSY experiments; (iii) the guest itself does not accelerate the exchange process. This suggest that water plays the role of *exo*-ligand enabling the guest exchange.

In order to investigate if steric hindrance at the level of the zinc coordination could be a key parameter governing the eventual *exo*-coordination of a ligand L at the level of the zinc atom, experiments were undertaken with the calix[6]benzimidazole zinc, **2.Zn^{2+}**. Results with this system are not significantly different than the ones obtained with **1.Zn^{2+}**. The benzimidazole arms consequently do not seem to introduce a significant steric hindrance for the *exo*-coordination of water.

Experiments were also undertaken with a calix[6]tren zinc complex **6.Zn^{2+}** where the zinc cation is tetra-coordinated to the calix[6]tren. Despite the fact that we expected that exchange would not be influenced by the presence of water, we observed also with this system that guest exchange is highly dependent on water concentration in solution. Exchange with this system is however significantly faster than with the other two systems and furthermore also possible in the absence of water.

The fact that guest exchange with system **6.Zn^{2+}** is faster than with systems **1.Zn^{2+}** and **2.Zn^{2+}** can be explained by the higher acidity of the zinc, which makes the guest more labile. We also observed that the exchange of EtOH is always faster that of DMF and CH_3CN for each system. This could be explained by water coordination to the metal inducing a change in the geometry of the system, breaking the hydrogen bond that stabilizes the ethanol-host complex.

CHAPTER 5.
CONCLUSIONS

The study of synthetic molecular receptors is an important facet of supramolecular chemistry as these receptors can find applications in the selective extraction, transport or detection of different species. In this thesis we focused our attention on the study of different types of receptors bearing a cavity capable of accommodating small organic molecules. We looked at the binding properties of two families of calix[6]arenes and also at the complexation properties of some related compounds: a homooxacalix[3]arene and a resorcin[4]arene derivatives.

Our work focused on the following three themes:

(i) **the study of the binding properties of a fluorescent calixarene.**

We conducted NMR and emission binding studies with the fluorescent calix[6]tris-pyrenylureas **14a** and **14b** (Figure 5-1). We could show that both receptors are able to bind ammonium sulfate salts with a cavity-based selectivity. While **14a** displays a strong affinity for small or linear ammoniums, **14b**, which has a more open cavity, was able to recognize an ammonium derivate of the dopamine family in chloroform. We also showed that **14a** is a highly selective chemosensor for the sulfate anion in DMSO and for phosphatidylcholine type lipids in chloroform.

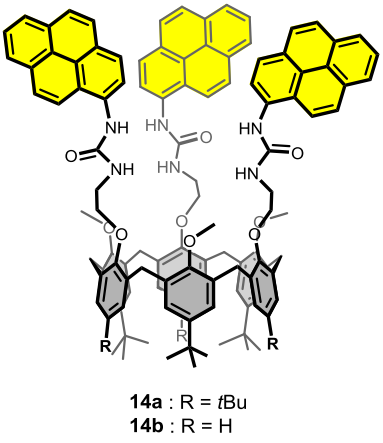

14a : R = *t*Bu
14b : R = H

Figure 5-1. Structure of receptors **14a-b**.

Moreover, our results put in evidence that the strategy of combining a calix[6]arene skeleton to chromophores for the design of multitopic sensitive receptors is a valid and appropriate way to obtain selective chemosensors. Indeed, the complexation observed for these different guests leads to significant changes in the spectrophotometric properties of the host and it is furthermore possible to estimate binding constants. The results were in agreement with those obtained from the NMR studies of the systems.

(ii) **the use of micelles to transfer the hydrophobic molecular receptors into water.**

We studied in micellar media three receptors, which are only soluble in organic solvents. We showed that the calix[6]azacryptand receptor **6** can be incorporated into DPC micelles, either as a Zn^{2+} complex in the 6-9 pH range or as a polyammonium at low pH. We were able to show that **the zinc complex maintains its host-guest properties as observed in organic solvent** and is able to complex small or long linear primary amines inside the calixarene cavity (Figure 5-2). The stability of the ternary complex **6.Zn^{2+}⊃PrNH$_2$** over a large pH range showed that the presence of the amine consolidates the complex even at very low pH where the free amine is fully protonated in water. This highlights that the environment provided by the calixarene cavity and the micelle protects the system from water, stabilizing $PrNH_2$ in its basic form. The results also showed that **the hydrophobic effect plays a key role** in driving guests from water into the calixarene cavity incorporated in DPC micelles.

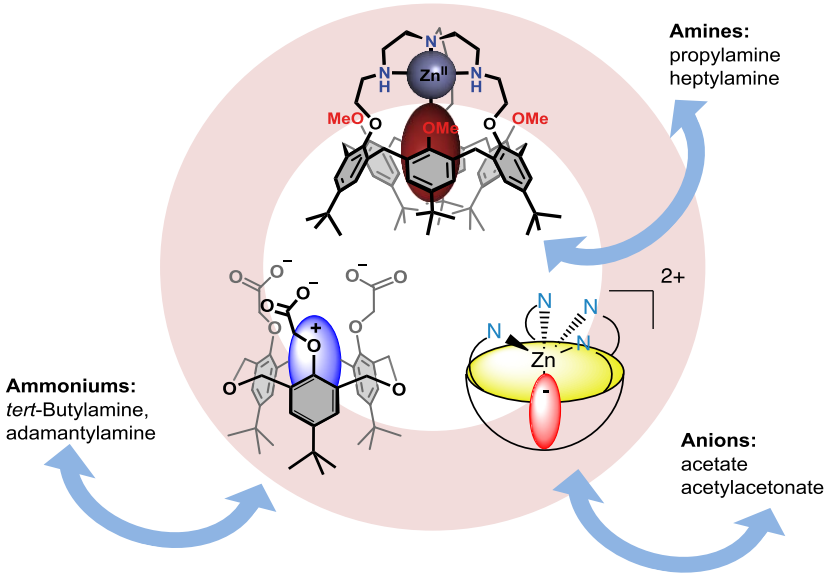

Figure 5-2. Schematic representation of the Host-Guest properties of the studied systems incorporated into DPC micelles.

We also achieved the incorporation into DPC micelles of the homooxacalix[3]tris-acid **15** and of the resorcin[4]arene zinc complex **16.Zn^{2+}**. We demonstrated that **15** incorporated into DPC micelles can bind different ammoniums, albeit with low affinity (Figure 5-2). On the other hand, **16.Zn^{2+}** showed interesting binding properties towards small carboxylates and small diketones (Figure 5-2). Our work shows that the micellar incorporation of hydrophobic receptors is a very elegant solution to overcome the solubility problem of organic receptors in water and that, under these conditions, the receptors maintain binding properties.

(iii) **the elucidation of the guest exchange mechanisms in the cavity of zinc calixarene-based complexes**.

NMR studies were undertaken in order to try and elucidate the mechanism of guest exchange in system **1.Zn^{2+}**. The hypothesis put forward is that an *exo*-coordination of a molecule is required to allow the *endo*-guest to leave the cavity when the zinc cation is tri-coordinated to the calix[6]arene ligand. 1D EXSY experiments were performed in order to determine the residence time of ethanol, acetonitrile and DMF in the calixarene cavity as a function of water concentration. We showed that **the residence time of the guests decreases linearly with increasing equivalents of water**. **Without water in solution, guest residence time is too long** to be evaluated through EXSY experiments. We also observed that **the guest itself does not accelerate the exchange process**. This suggest that **water plays the role of *exo*-ligand enabling guest exchange** (Figure 5-3).

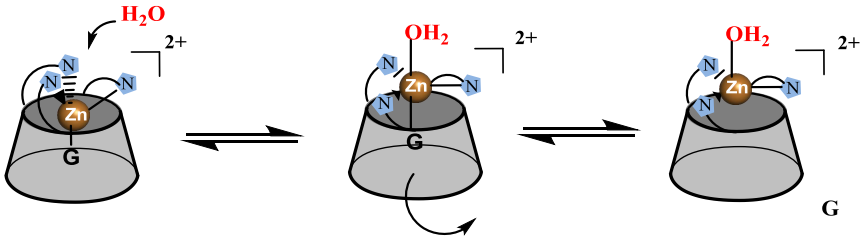

Figure 5-3. Proposed mechanism for guest exchange in system **1.Zn^{2+}** with the coordination of a water molecule.

The study of a similar system with benzimidazole arms, system **2.Zn^{2+}**, showed that steric hindrance at the level of the metal does not hinder in a significant way the exchange process in the presence of water. Experiments were also undertaken with the calix[6]tren zinc complex **6.Zn^{2+}**, where the zinc cation is tetra-coordinated to the calix[6]tren. We expected that the exchange would not be influenced by the presence of water but, on the contrary, we observed that, with this system, guest exchange is also highly dependent on water concentration in solution. Exchange with this system is significantly faster than with the other two systems and also possible in the absence of water. The explanation put forward is that the acidity of the zinc governs in part the exchange rate. We also observed that the exchange of ethanol is always faster than the other studied guests with each system which could be explained by the fact that water coordination to the metal induces a change in the geometry of the system, breaking the hydrogen bonds that stabilize the ethanol-host complex.

In conclusion, the results reported in this thesis clearly show that rightly functionalized calix[6]arene can be remarkable selective and versatile receptors in order to work as efficient chemosensors. The development of molecular receptors combining the benefits of a sensing system with the "water-compatibility" achieved via micellar incorporation would be of particular interest for the detection, for instance, of biologically relevant molecules.

CHAPTER 6.
MATERIALS AND METHODS

The materials and methods and the experimental conditions for the experiments reported in our publications are described in the papers **(***J. Org. Chem.* **2014**, *79*, 6179–6188, *Org. Biomol. Chem.* **2016**. asap and *Org. Biomol. Chem.* **2015**, *13*, 2931-2938).

In this section we only give the experimental conditions for the experiments reported in section 3.5 and in chapter 4. Receptor **15** was synthetized following a protocol described in the literature in collaboration with Sara Zahim of the group of Prof. Jabin. **16** and **16.Zn^{2+}** were synthetized and provided by the group of Prof. Reinaud. **1.Zn^{2+}** and **6.Zn^{2+}** were synthetized and provided by the group of Prof. Jabin. **2.Zn^{2+}** was synthetized and provided by the group of Prof. Reinaud.

CHEMICALS

-DPC ($C_{17}H_{38}NO_4P$), Avanti Polar Lipids >99 %
-DPC-d_{38} ($C_{17}D_{38}NO_4P$), Avanti Polar Lipids 99%
-D_2O (99.9 %), CD_2Cl_2 (99.8 %) and $CDCl_3$ (99.8 %), VWR BDH PROLABO
-$CHCl_3$, Alfa Aesar ≥ 99%
-Tert-Butylamine ($C_4H_{11}N$), Sigma-Aldrich 98%
-D-L *sec*-Butylamine ($C_4H_{11}N$), Sigma-Aldrich 99%
-Adamantylamine hydrochloride ($C_{10}H_{18}NC$), Sigma-Aldrich ≥ 99%
-Propylamine (C_3H_9N), Sigma-Aldrich ≥ 99%
-Sodium deuteroxide solution (NaOD, 40% wt), Sigma-Aldrich 99.5 %
-Acetylacetone ($C_5H_8O_2$), Sigma-Aldrich 99%
-Ethanol (C_2H_5OH) absolute, VWR BDH PROLABO 99.5%
-Acetonitrile (CH_3CN) Extra dry, Acros Organics 99.9 %
-Dimethylformamide (C_3H_7NO), Fisher Chemical ≥ 99.8 %
-Sodium acetate ($C_2H_3NaO_2$), Fluka ≥ 99 %
-Molecular sieve, Fluka
-Hepes ($C_8H_{18}N_2O_4S$) Free acid, Sigma-Aldrich ≥ 99.5 %

GENERAL PROCEDURES FOR ^{1}H SPECTRA

Chloroform (both deuterated and non-deuterated) was filtered, prior to use, over a short column of basic alumina to remove traces of HCl/DCl. ^{1}H NMR spectra were recorded at 400 MHz (9.4 T) or 600 MHz (14.1 T). For the 1D ^{1}H spectra, parameters (acquisition time, recycling times, and signal accumulation) were chosen so as to ensure that quantitative data could be obtained

from signal integration. Traces of residual solvents were used as internal chemical shift references. 2D NMR spectra (COSY, HSQC and ROESY) were recorded to complete signal assignments.

MICELLAR SOLUTIONS PREPARATION

All solutions for NMR studies were prepared following a similar protocol: the host (a few mg) and DPC (~35 mg, deuterated or not depending on the experiments) were added to 5 mL of D_2O in order to have, respectively, concentrations of ~0.5 mM and ~20 mM. Solutions were stirred until a clear solution was obtained.

^{1}H NMR CHARACTERIZATION OF VARIOUS COMPLEXES WITH 15

15^{-nH+}: ^{1}H NMR (DPC 20 mM in D_2O, 298K, 600 MHz): δ(ppm) 1.15 (s, 27H, *t*Bu), 4.43 (bs, J~12.6 Hz, 6H, CH_2O), 4.53 (d, J~12.6 Hz, 6H, $ArCH_2^{eq}$), 4.96 (d, 6H, $ArCH_2^{ax}$), 7.00 (s, 6H, ArH); **15^{-nH+}⊃*t*BuNH$_3^+$:** ^{1}H NMR (DPC-d_{38} 20 mM in D_2O, 298K, 600 MHz): δ(ppm) -0.37 (s, 9H, $tBuNH_3^{+CH3+,in}$), 1.18 (s, 27H, *t*Bu), 4.27 (bs, 6H, CH_2O), 4.42 (d, 6H, $ArCH_2^{eq}$), 5.54 (bs, 6H, $tBuNH_2^{ArCH2ax,in}$), 7.30 (s, 6H, ArH). **15^{-nH+}⊃AdamNH$_3^+$:** ^{1}H NMR (DPC-d_{38} 20 mM in D_2O, 298K, 600 MHz): δ(ppm) -0.07 (s, 6H, $AdamNH_3^{\alpha,in}$), 0.95 (bs, 3H, $AdamNH_3^{\beta,in}$), 1.13 (bs, 6H, $AdamNH_3^{\gamma,in}$), 1.22-1.29 (m, 27H, *t*Bu), 4.26 (bs, 6H, CH_2O), 4.43 (m, 6H, $ArCH_2^{eq}$), 5.55 (bs, 6H, $tBuNH_2^{ArCH2ax,in}$), 7.27 (s, 6H, ArH).

Determination of the apparent affinity of *t*BuNH$_3^+$, *sec*-ButylNH$_3^+$ orAdamNH$_3^+$ toward complex 15 through ^{1}H NMR titration in DPC-d_{38} (20 mM in D_2O). Different aliquots of a solution of guest (*t*BuNH$_2$, *sec*-ButylNH$_2$ or AdamNH$_3$Cl) were progressively added to 500 µL of a DPC-d_{38} solution (20 mM in D_2O) containing **15**. The integrations of the free guests and of the included guests were used to calculate the apparent affinity at a given pH defined as [R-$NH_3^+{}_{bound}$]/(1-[R-$NH_3^+{}_{bound}$][R-$NH_3^+{}_{free}$][**15^{-nH+}**]).(errors estimated ±20%).

Determination of the relative affinity of *sec*-Butylamine compared to propylamine in $CDCl_3$ via ^{1}H NMR competitive binding studies. At room temperature, ~4 equivalents of propylamine ($PrNH_2$) and ~1 equivalent of *sec*-Butylamine (*sec*-ButylNH$_2$) were added in 500 µL of a $CDCl_3$ solution of **15**. A ^{1}H NMR spectrum showed the guest resonances of both complexes **15^{-3H+}⊃PrNH$_3^+$** and **15^{-3H+}⊃*sec*-ButylNH$_3^+$** and signals corresponding to the free amines. The integrations of the signals corresponding to free guests and the included guests

were used to calculate relative affinity defined as $[PrNH_3^+{}_{in}]/[sec\text{-}ButylNH_{2in}]$ x $[secButylNH_{2Free}]/[PrNH_{2Free}]$ (errors estimated ±20%).

Determination of the apparent affinity of CH_3COO^- toward complex $\mathbf{16.Zn^{2+}}$ through ^{1}H NMR titration in DPC (20 mM in D_2O). Different aliquots of a solution of sodium acetate were progressively added to 500 µL of a DPC solution (20 mM in D_2O) containing $\mathbf{16.Zn^{2+}}$. The integrations of the free guests and of the included guests were used to calculate the apparent affinity at a given pH defined as $[CH_3COO^-{}_{bound}]/(1-[CH_3COO^-{}_{bound}][CH_3COO^-{}_{free}][\mathbf{16.Zn^{2+}}])$.(errors estimated ±20%).

Determination of the relative affinity of EtOH compared to DMF in DCM-d_2 via ^{1}H NMR competitive binding studies. A few equivalents of EtOH and a few equivalents of DMF were added in 600 µL of a DCM-d_2 solution of $\mathbf{1.Zn^{2+}}$. A ^{1}H NMR spectrum showed the guest resonances of both complexes $\mathbf{1.Zn^{2+}}\supset\mathbf{EtOH}$ and $\mathbf{1.Zn^{2+}}\supset\mathbf{DMF}$ and signals corresponding to the free guests. The integrations of the signals corresponding to free guests and the included guests were used to calculate relative affinity defined as $[DMF_{in}]/[EtOH_{in}]$ x $[EtOH_{Free}]/[DMF_{Free}]$ (errors estimated ±20%). We thus determine $K_{DMF/EtOH.}$ The same procedure was undertaken for CH_3CN. The relative affinities toward the other complex $\mathbf{2.Zn^{2+}}$ and $\mathbf{6.Zn^{2+}}$ were also determined following the same procedure described above.

General DOSY experimental parameters: 15 values for the magnitude of the gradient pulses (ranging from 2 G/cm to 50 G/cm), diffusion delay 50 ms, time-length of the gradient 5 ms, acquisition time 2 s, relaxation delay 7 s, 64 transients.

GENERAL PROCEDURE for 1D EXSY EXPERIMENTS

Prior to the determination of the kinetic constants in the exchange, it was necessary to determine the relaxation times. The longitudinal relaxation times T_1 were determined using the Inversion-Recovery sequence: the magnetization is inverted through the *application* of a 180° pulse, then the magnetization vector initially aligned with the –z-axis relaxes at a rate determined by T_1. The return to equilibrium was monitored by integrating spectra after a delay τ.

1D EXSY experiments were recorded with iburp2 shaped pulses with selective excitation of the bound guest (150 Hz). Evolution with mixing time τ_m of the normalized integrated intensity

of the signal of bound guest and free guest. The integrated intensities at equilibrium $I_{in}°$ and $I_{out}°$ were measured in a 1D spectrum obtained with identical gain (generally 32 transients with acquisition time and relaxation delay tailored for each different experiment). The mixing time, was increased (generally 8 increments were used 20-160 ms, 100-800 ms or 400-3200 ms depending on each experiment) The rate constants k_{tot} were determined as the initial slope of the signal intensity ratio $I_{out}°/I_{in}°$ measured as a function of mixing time (cf. Figure-4-14 for an example).

^{1}H NMR CHARACTERIZATION OF VARIOUS COMPLEXES WITH **1.Zn^{2+}**, **2.Zn^{2+}** AND **6.Zn^{2+}**

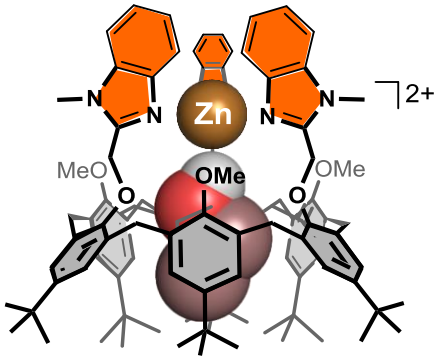

(2.Zn^{2+}⊃EtOH)(ClO$_4$)$_2$

^{1}H NMR (253K, 600 MHz, CD_2Cl_2): δ = -1.46 (t, 3H, EtOH^{CH3} bound); 0.71 (s,27H, *t*Bu$_1$); 1.39 (s, 27H, *t*Bu$_2$); 1.18 (t, 3H, EtOH^{CH3} free); 1.35 (s, 1H, EtOH^{OH} free); δ = 1.90-2.11 (m, 2H, EtOH^{CH2} bound); 2.83 (s, 9H, OCH_3); 3.33 (d, *J* = 15.6 Hz, 3H, Ar-αCH$_{eq}$); 3.46 (d, *J* = 15 Hz, 3H, Ar-αCH$_{eq}$); 3.57 (d, *J* = 15.6 Hz, 3H, Ar-αCH$_{ax}$); 3.65 (m, 2H, EtOH^{CH2} free); 3.99 (s, 9H, NCH_3); 4.39 (d, *J* = 15 Hz, 3H, Ar-αCH$_{ax}$); 4.64 (dd, 1H, EtOH^{OH} bound); 5.46 (s, 6H, Bz-αCH_2); 6.26 (s, 3H, ArH$_1$); 6.53 (s, 3H, ArH$_1$); 6.86 (d, *J* = 8.4 Hz, 3H, BzH); 7.28 (d, *J* = 2.4 Hz, 3H, ArH$_2$); 7.49 (t, *J*= 8.4 Hz, 3H, BzH); 7.38 (d, *J* = 2.4 Hz, 3H, ArH$_2$); 7.69 (t, *J* = 8.4 Hz, 3H, BzH); 7.91 (d, *J* = 8.4 Hz, 3H, BzH).

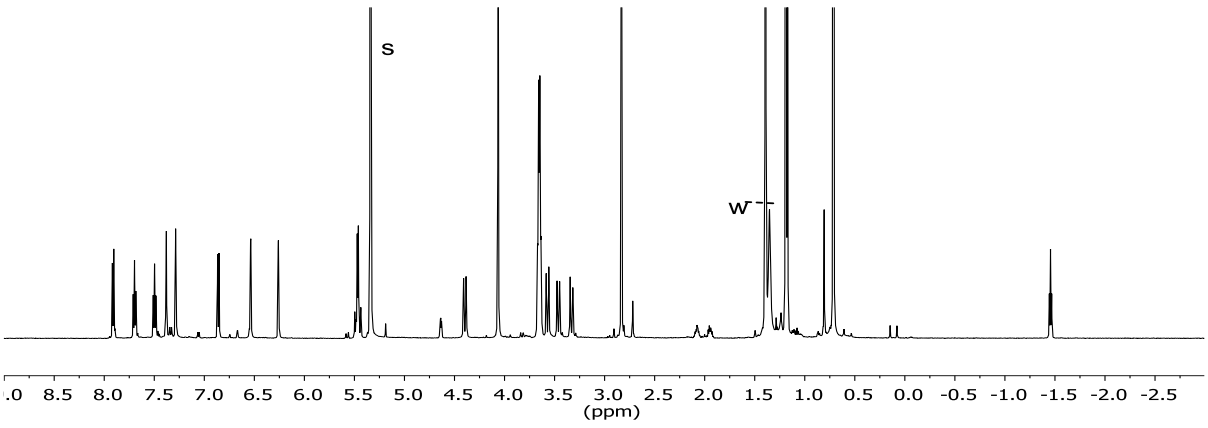

Figure 6-1. ^{1}H NMR spectrum (600MHz, 253 K) of **2.Zn^{2+}** in DCM-d_2 in the presence of ~ 12 equiv. of EtOH.

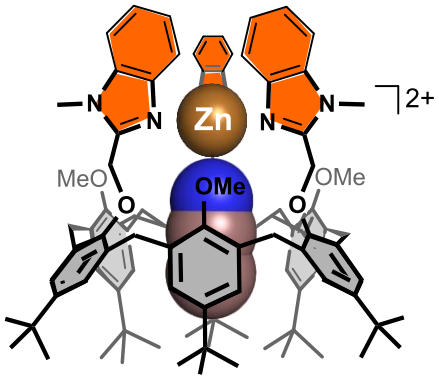

(2.Zn^{2+}⊃CH_3CN)(ClO_4)$_2$

^{1}H NMR (298K, 600 MHz, CD_2Cl_2): δ = -0.66 (s, 3H, CH_3CN bound); 0.73 (s,27H, *t*Bu_1); 1.40 (s, 27H, *t*Bu_2); 1.96 (s, 3H, CH_3CN free); 2.90 (s, 9H, OCH_3); 3.27 (d, *J* = 15.6 Hz, 3H, Ar-αCH_{eq}); 3.46 (d, *J* = 15 Hz, 3H, Ar-αCH_{eq}); 3.61 (d, *J* = 15.6 Hz, 3H, Ar-αCH_{ax}); 3.97 (s, 9H, NCH_3); 4.48 (d, *J* = 15 Hz, 3H, Ar-αCH_{ax}); 5.42 (s, 6H, Bz-αCH_2); 6.27 (s, 3H, ArH_1); 6.58 (s, 3H, ArH_1); 6.94 (d, *J* = 8.4 Hz, 3H, BzH); 7.27 (d, *J* = 2.4 Hz, 3H, ArH_2); 7.47 (t, *J*= 8.4 Hz, 3H, BzH); 7.38 (d, *J* = 2.4 Hz, 3H, ArH_2); 7.67 (t, *J* = 8.4 Hz, 3H, BzH); 7.86 (d, *J* = 8.4 Hz, 3H, BzH).

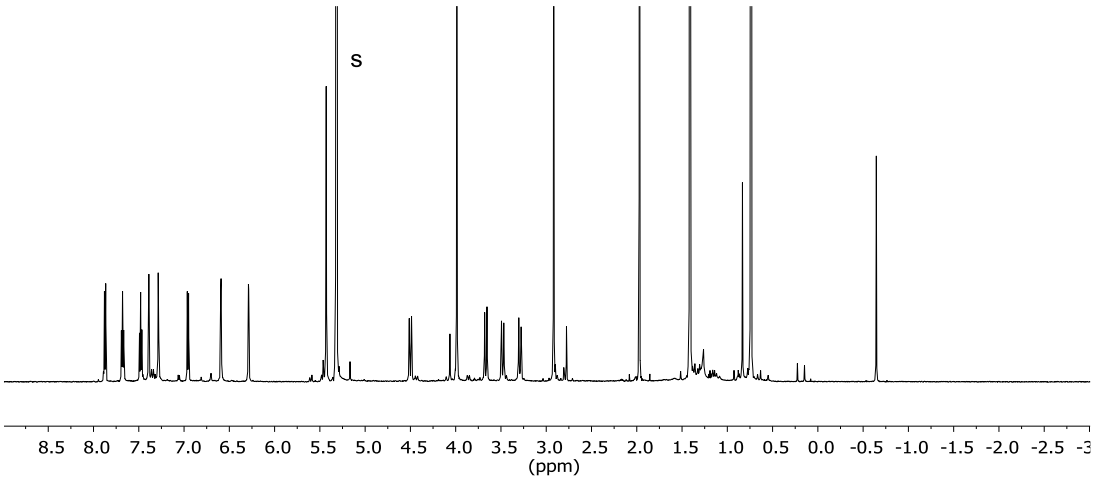

Figure 6-2. ^{1}H NMR spectrum (600MHz, 298 K) of **2.Zn^{2+}** in DCM-d_2 in the presence of ~ 5 equiv. of CH_3CN.

^{1}H NMR (253K, 600 MHz, CD_2Cl_2): δ = -0.71 (s, 3H, CH_3CN bound); 0.71 (s,27H, *t*Bu_1); 1.39 (s, 27H, *t*Bu_2); 2.00 (s, 3H, CH_3CN free); 2.86 (s, 9H, OCH_3); 3.39 (d, *J* = 15.6 Hz, 3H, Ar-αCH_{eq}); 3.46 (d, *J* = 15 Hz, 3H, Ar-αCH_{eq}); 3.62 (d, *J* = 15.6 Hz, 3H, Ar-αCH_{ax}); 3.99 (s, 9H, NCH_3); 4.46 (d, *J* = 15 Hz, 3H, Ar-αCH_{ax}); 5.40 (s, 6H, Bz-αCH_2); 6.24 (s, 3H, ArH_1); 6.56 (s, 3H, ArH_1); 6.96 (d, *J* = 8.4 Hz, 3H, BzH); 7.27 (d, *J* = 2.4 Hz, 3H, ArH_2); 7.47 (t, *J*= 8.4 Hz, 3H, BzH); 7.37 (d, *J* = 2.4 Hz, 3H, ArH_2); 7.67 (t, *J* = 8,4 Hz, 3H, BzH); 7.89 (d, *J* = 8.4 Hz, 3H, BzH).

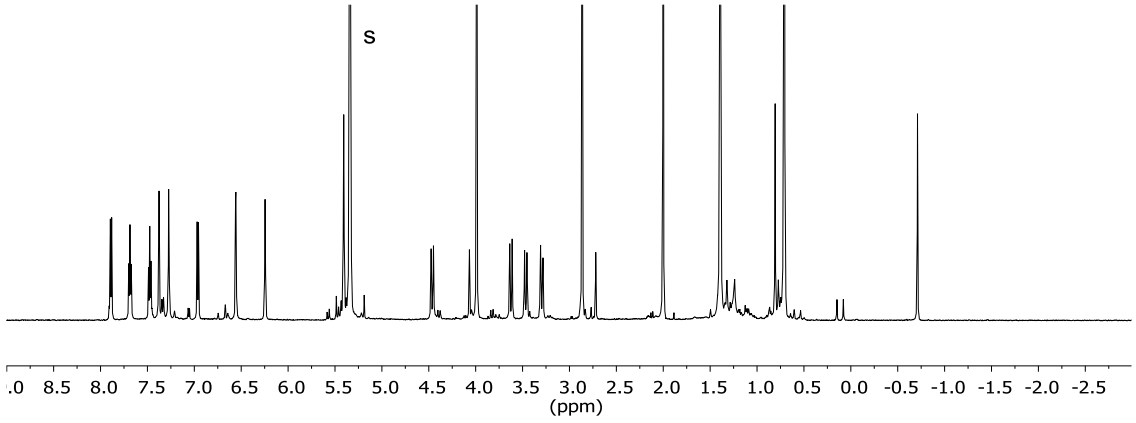

Figure 6-3. ^{1}H NMR spectrum (600MHz, 253 K) of **2.Zn**$^{2+}$ in DCM-d_2 in the presence of ~ 5 equiv. of CH_3CN.

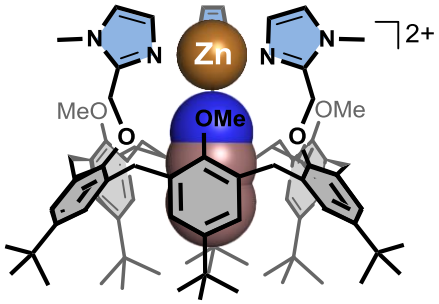

(1.Zn^{2+}⊃CH$_3$CN)(TfO)$_2$

^{1}H NMR (253K, 600 MHz, CD_2Cl_2): δ = -0.72 (s, 3H, CH_3CN bound); 0.73 (s, 27H, *t*Bu$_1$); 1.39 (s, 27H, *t*Bu$_2$); δ = 1.96 (s, 3H, CH_3CN free); 3.41 (d, *J* = 15 Hz, 6H, Ar-αCH$_{eq}$); 3.61 (s, 9H, OCH_3); 3.76 (s, 9H, NCH_3); 4.14 (d, *J* = 15 Hz, 6H, Ar-αCH$_{ax}$); 5.27 (s, 6H, Im-αCH_2); 6.43 (s, 6H, ArH$_1$); 7.14 (d, *J* = 1,5 Hz, 3H, ImH); 7.31 (s, 6H, ArH$_2$); 7.39 (d, *J* = 1,5 Hz, 3H, ImH).

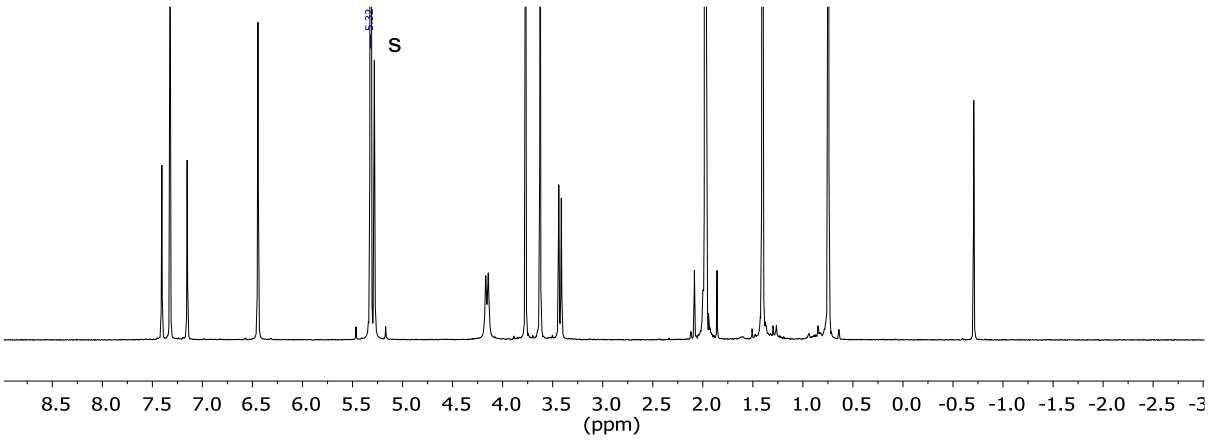

Figure 6-4. ^{1}H NMR spectrum (600MHz, 298 K) of **1.Zn^{2+}** in DCM-d_2 in the presence of ~42 equiv. of CH_3CN.

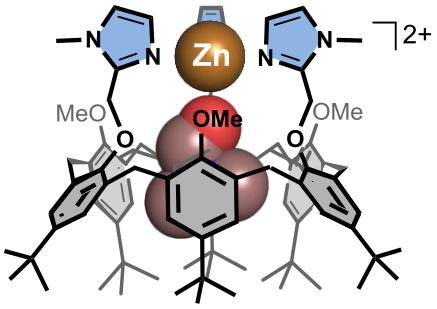

(1.Zn^{2+}⊃DMF)(TfO)$_2$

^{1}H NMR (298K, 600 MHz, CD_2Cl_2); δ = 0.02 (s, 3H, DMF bound); 0.25 (s, 3H, DMF bound); 0.83 (s, 27H, *t*Bu$_1$); 1.39 (s, 27H, *t*Bu$_2$); 2.81 (s, 3H, DMF free); 2.89 (s, 3H, DMF free); 3.39 (d, *J* = 15 Hz, 6H, Ar-αCH$_{eq}$); 3.55 (s, 9H, OCH_3); 3.84 (s, 9H, NCH_3); 4.21 (d, *J* = 15 Hz, 6H, Ar-αCH$_{ax}$); 5.37 (s, 6H, Im-αCH_2); 6.51 (s, 1H, DMF^{COH} bound); 6.66 (s, 6H, ArH_1); 7.19 (d, *J* = 1.5 Hz, 3H, ImH); 7.32 (s, 6H, ArH_2); 7.43 (d, *J* = 1.5 Hz, 3H, ImH); 7.95 (s, 1H, DMF^{COH} free).

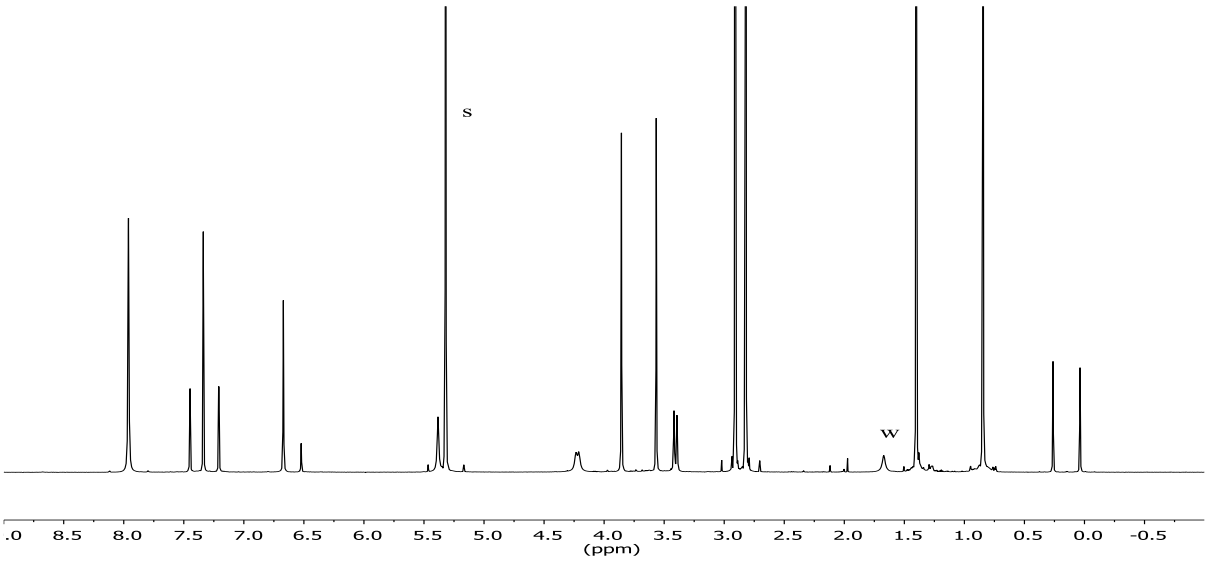

Figure 6-5. ^{1}H NMR spectrum (600MHz, 298 K) of **1.Zn^{2+}** in DCM-d_2 in the presence of 32 equiv. of DMF.

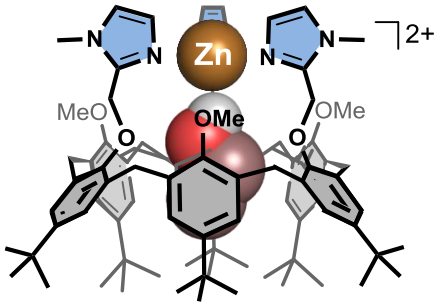

(1.Zn^{2+}⊃EtOH)(TfO)$_2$

^{1}H NMR (253K, 400 MHz, CD_2Cl_2): δ = -1.53 (t, 3H, EtOH^{CH3} bound); 0.71 (s,27H, *t*Bu$_1$); 1.38 (s, 27H, *t*Bu$_2$); 1.18 (t, 3H, EtOH^{CH3} free); 1.55 (s, 1H, EtOH^{OH} free); 1.46-1.76 (m, 2H, EtOH^{CH2} bound); 3.59 (s, 9H, OCH_3); 3.23-3.79 (bs, 6H, Ar-αCH_{eq}); 3.65 (m, 2H, EtOH^{CH2} free); 3.83 (s, 9H, NCH_3); 4.54 (bs, 6H, Ar-αCH_{ax}); 4.08 (t, 1H, EtOH^{OH} bound); 5.12 (bs, 3H, Im-αCH_2); 5.57 (bs, 3H, Im-αCH_2); 6.08-6.72 (s, 6H, ArH_1); 7.14 (s , 3H, ImH); 7.20-7.42 (s, 6H, ArH_2); 7.43 (s, 3H, ImH).

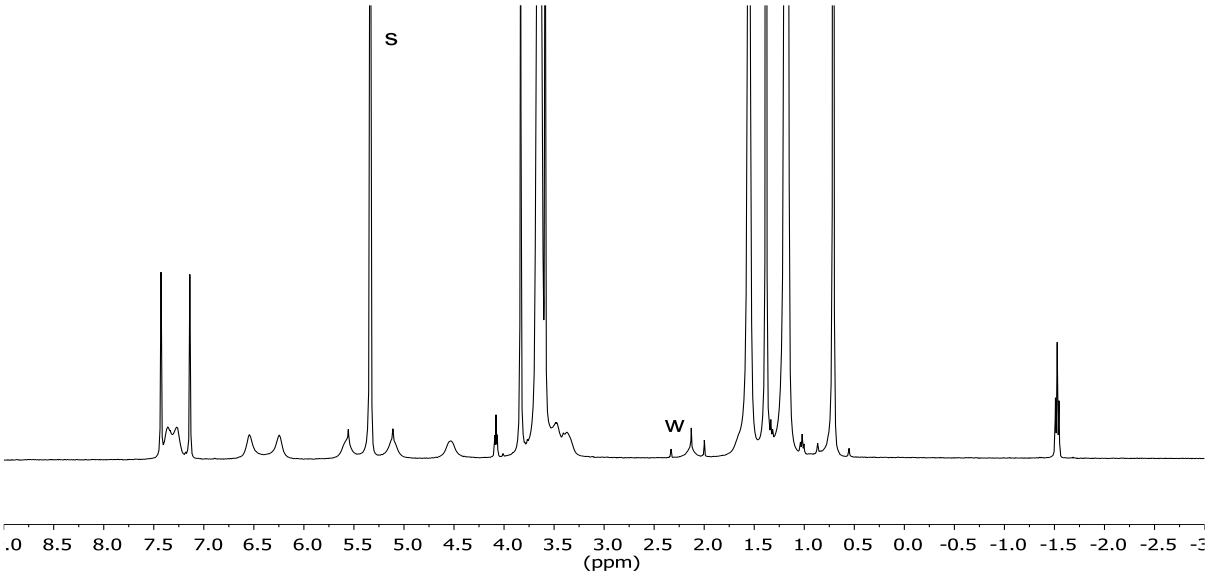

Figure 6-6. ^{1}H NMR spectrum (600MHz, 253 K) of **1.Zn^{2+}** in DCM-d_2 in the presence of 53 equiv. of EtOH.

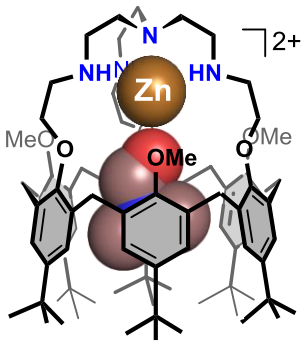

(6.Zn^{2+}⊃DMF)(ClO_4)$_2$

^{1}H NMR (298K, 600 MHz, CD_2Cl_2): δ = -0.28 (s, 3H, DMF bound); 0.04 (s, 3H, DMF bound); 0.78 (s, 9 H, tBu_1); 0.82 (s, 9 H, tBu_1); 0.83 (s, 9 H, tBu_1); 1.38 (bs, 18 H, tBu_2); 1.39 (bs, 9 H, tBu_2); 2.80 (s, 3H, DMF free); 2.89 (s, 3H, DMF free); 2.92-3.93 (m, 24 H, $NHCH_2CH_2N$-$NHCH_2CH_2N$-OCH_2CH_2N-Ar-αCH_{eq}); 3.81 (s, 3 H, OCH_3); 3.88 (s, 3 H, OCH_3); 3.95 (s, 3 H, OCH_3); 4.06-4.49 (m, 12 H, OCH_2CH_2NH-Ar-αCH_{ax}); 6.54 (br. s, 1 H, ArH_1); 6.55 (br. s, 1 H, ArH_1); 6.68 (d, Hz, 1H, ArH_1); 6.72 (d, Hz, 1 H, ArH_1); 6.76 (d, 2H, ArH_1); 6.99 (s, 1H, DMF^{COH} bound); 7.29 (b s 2H, ArH_2); 7.31 (d, J ~ 2 Hz, 1 H, ArH_2); 7.36 (d, J ~ 2 Hz, 1H, ArH_2), 7.34 (m, 2 H, ArH_2); 7.46 (d, 1H, ArH_2); 7.94 (s, 1H, DMF^{COH} free).

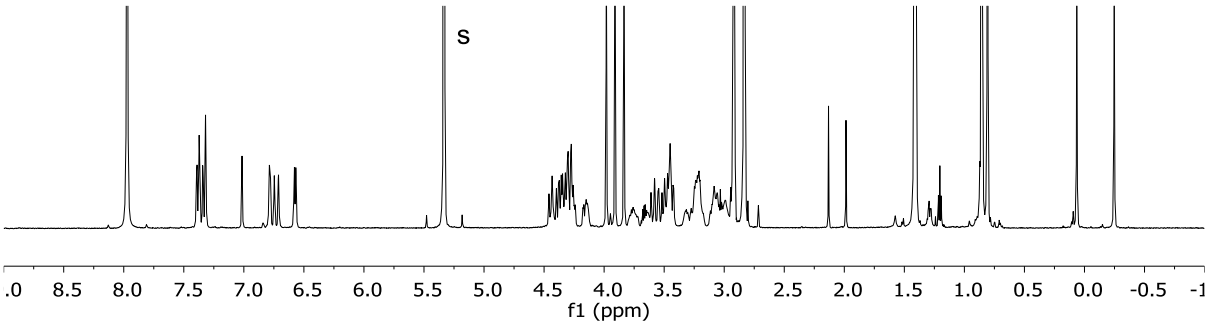

Figure 6-7. ^{1}H NMR spectrum (600MHz, 298 K) of **6.Zn^{2+}** in DCM-d_2 in the presence of 12 equiv. of DMF.

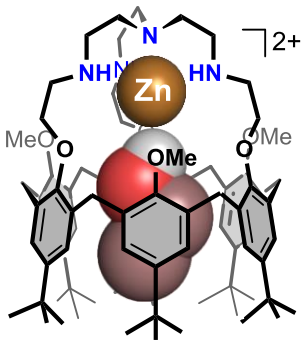

(6.Zn^{2+}⊃EtOH)(ClO_4)$_2$

^{1}H NMR (253K, 600 MHz, CD_2Cl_2): δ = 0.66 (s, 9 H, tBu_1); 0.74 (s, 9 H, tBu_1); 0.76 (s, 9 H, tBu_1); 1.18 (t, 3H, $EtOH^{CH3}$ free); 1.38 (bs, 18 H, tBu_2); 1.39 (bs, 9 H, tBu_2); 1.47 (t, 1H, $EtOH^{OH}$ free); 1.53-1.80 (m, 2H, $EtOH^{CH2}$ bound); 2.92-3.58 (m, 24 H, $NHCH_2CH_2N$-$NHCH_2CH_2N$-OCH_2CH_2N-Ar-αCH_{eq}); 3.65 (m, 2H, $EtOH^{CH2}$ free); 3.80 (s, 3H, OCH_3); 3.87 (s, 3 H, OCH_3); 3.94 (s, 3 H, OCH_3); 3.99-4.43 (m, 12 H, OCH_2CH_2NH-Ar-αCH_{ax}); 4.47 (t, 1H, $EtOH^{OH}$ bound); 6.34 (s, 1H, ArH1); 6.40 (m, 2 H, ArH_1); 6.52 (s,1H, ArH_1); 6.57 (s, , 1 H, ArH_1); 6.65 (s, 1H,ArH_1); 7.27 (s, 1H, ArH_2); 7.30 (s, 1H,ArH_2); 7.33 (bs , 2H, ArH_2); 7.43 (bs, 2H, ArH_2).

Figure 6-8. ^{1}H NMR spectrum (600MHz, 253K) of **1.Zn^{2+}** in DCM-d_2 in the presence of 33 equiv. of EtOH.

CHAPTER 7.
APPENDICES

7.1. 1:1 BINDING MODEL

The 1:1 interaction between a host (H) and a guest (G) forming the complex HG can be described by the following equilibrium, which is characterized by a binding constant (*K*a):

$$H + G \rightleftharpoons HG$$

$$Ka = \frac{[HG]}{[H] * [G]}$$

Concentrations in host and guest can be written as a function of the initial concentrations and of the concentration of complex.

$$[H] = [H]_0 - [HG]$$

$$[G] = [G]_0 - [HG]$$

By replacing these expressions in the equation describing the binding affinity we can write:

$$Ka = \frac{[HG]}{([H]_0 - [HG]) * ([G]_0 - [HG])}$$

The concentration in complex can be isolated[1]:

$$[HG] = \frac{[H]_0 * \left(1 + \frac{[G]_0}{[H]_0} + \frac{1}{Ka * [H]_0}\right)}{2} - \frac{[H]_0 * \sqrt{(1 + \frac{[G]_0}{[H]_0} + \frac{1}{Ka * [H]_0})^2 - 4 * \frac{[G]_0}{[H]_0}}}{2}$$

In order to determine *K*a, a property of the systems which changes during the titration has to be monitored. Binding affinities have been determined using Nuclear Magnetic Resonance, UV-vis absorption spectroscopy or Emission spectroscopy.

[1] For the mathematic development and the determination of binding constants: Hirose, K. *J. Incl. Phenom. Macrocyl. Chem.* **2001**, *39*, 193-209. Thordason, P. *Chem. Soc. Rev.* **2011**, *40*, 1305-1323.

TITRATIONS BY UV-VIS ABSORPTION SPECTROSCOPY

Beer-Lambert law expresses that for a given wavelength (λ), the absorption of a species is function of its concentration:

$$A = \varepsilon * l * C$$

Where A is the absorbance of the solution, l the optical pathway in cm, ε the molar extinction coefficient in $M^{-1}cm^{-1}$ and C the concentration of a species in M^{-1}. In the case of a solution containing n species, the total absorption of the solution can be express as the sum of the absorption of each species:

$$A = A_1 + A_2 + \cdots\cdots + A_n$$

In the case of a titration, we can write when the guest does not absorb:

$$A = [H] * \varepsilon_H * l + [HG] * \varepsilon_{RI} * l$$

where ε_H and ϵ_{HG} are respectively the molar extinction coefficients of the host and the complex formed.

$$A = ([H]_0 - [HG]) * \varepsilon_H * l + [HG] * \epsilon_{HG} * l$$

$$A = [H]_0 * \varepsilon_H * l + (\epsilon_{HG} - \epsilon_H) * [HG] * l$$

Writing that $A_0 = [H]_0 * \epsilon_H * l$ et $\Delta\varepsilon = \epsilon_{HG} - \epsilon_H$, the total absorbance can be rewritten:

$$A = A_0 + \Delta\varepsilon * [HG] * l$$

Finally, by replacing the expression of the complex concentration by the one obtained before, we obtain:

$$A = A_0 + \Delta\varepsilon * l * \frac{[H]_0 * (1 + \frac{[G]_0}{[H]_0} + \frac{1}{Ka * [R]_0})}{2} - \frac{[R]_0 * \sqrt{(1 + \frac{[I]_0}{[R]_0} + \frac{1}{Ka * [R]_0})^2 - 4 * \frac{[I]_0}{[R]_0}}}{2}$$

The values of Ka and $\Delta\varepsilon$ can be determined by parametric adjustment to the experimental by the least-squares method.

TITRATIONS BY EMISSION SPECTROSCOPY

Fluorescence intensity of a species C is given by the equation:

$$F = k_C * [C]$$

Where k_C corresponds to the fluorescence constant, which includes the yield detection of the fluorimeter, the molar extinction coefficient, the fluorescence quantic yield and the intensity of the incident beam.

In the case of a solution containing n fluorescent species, the total fluorescence of the solution can be expresses as the sum of the fluorescence of each species:

$$F = F_1 + F_2 + \cdots\cdots + F_n$$

In our case, during a titration, if we monitor the formation of a complex HG from a host H and a guest G (which does not fluoresce), we can write:

$$F = k_H * [H] + k_{HG} * [HG]$$

We can write:

$$F = (k_{HG} - k_H) * [HG] + k_H * [H]_0$$

By writing that $F_0 = k^0_H[H]_0$, $\Delta k = (k_{HG} - k_H)$ and after assuming that the modification of the fluorescence intensity is only due to the complexation of G by host H ($k_H = k^0_H$), we obtain:

$$F = k_0 + \Delta k * [HG]$$

Finally, replacing the expression of the complex concentration obtained before, we obtain

$$\mathrm{F} = k_0 + \Delta k * \frac{[H]_0 * (1 + \frac{[G]_0}{[H]_0} + \frac{1}{Ka * [R]_0})}{2} - \frac{[R]_0 * \sqrt{(1 + \frac{[I]_0}{[R]_0} + \frac{1}{Ka * [R]_0})^2 - 4 * \frac{[I]_0}{[R]_0}}}{2}$$

The values of *K*a and Δk can be determined by parametric adjustment to the experimental by the least-squares method.

TITRATIONS BY NMR SPECTROSCOPY

During a titration followed by NMR spectroscopy, the complexation equilibrium can be in slow or fast exchange compared to the chemical shift timescale.

In the case of slow exchange, three different sets of signals are observed during the titration (the signals of the free host and guest, and the signals of the formed complex). By simple integration at equilibrium of the different signals, the binding constant can be determined.

In the case of fast exchange, the observed chemical shift is a weighted average of the chemical shift of the free species and the chemical shift of the complex ones. Thus, the binding affinity constant can be determined by parametric adjustment to the experimental given by these equations:

$$\delta = x_H \delta_H + x_{HG} \delta_{HG}$$

Where δ correspond to the observed chemical shift, δ_H to the chemical shift of free host and δ_{HG} to the chemical shift of the formed complex. x_{HG} corresponds to the molar fraction of the complex. Finally, binding constant can be determined through this equation as the molar fraction depends on *K*a.

7.2. ADDITIONAL SPECTRA

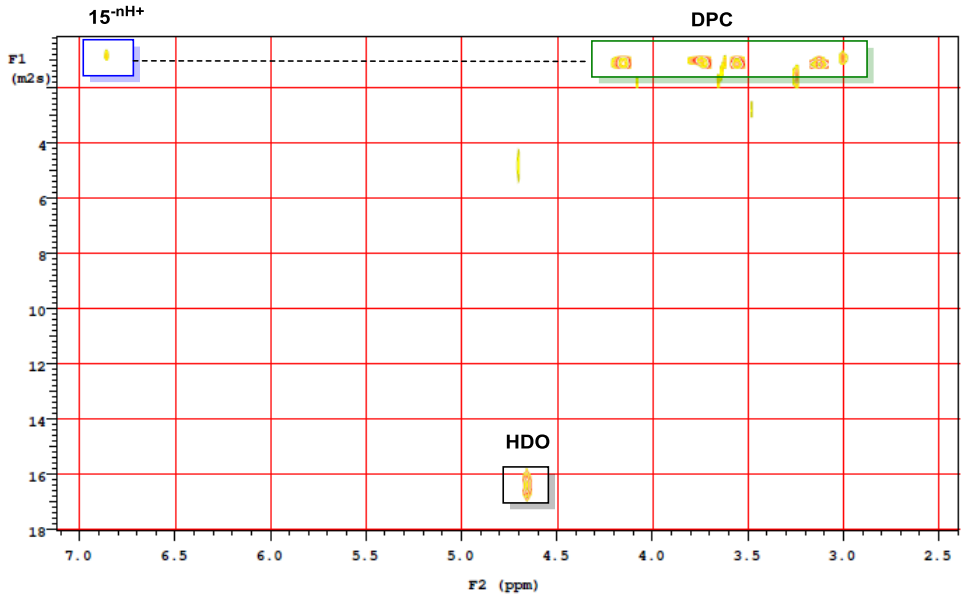

Figure 7-1. DOSY experiment (600 MHz, 298 K, DPC 20 mM) with **15** incorporated into DPC micelles.

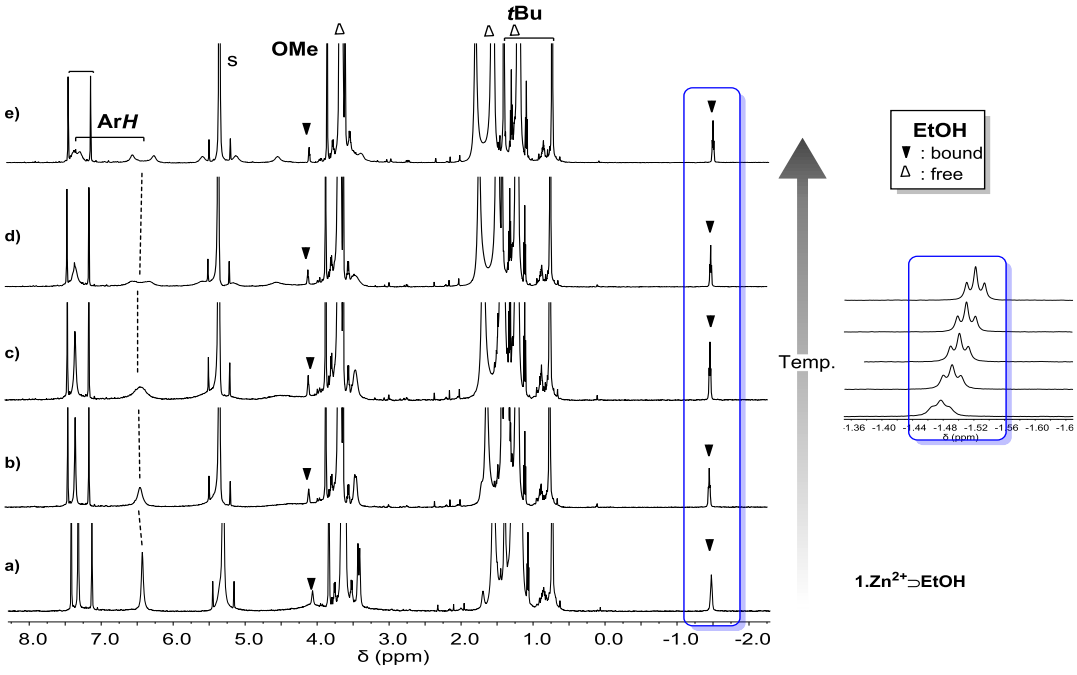

Figure 7-2. ^{1}H NMR spectra (600MHz, DCM-d_2) of **1.Zn^{2+}** in the presence of ~120 equiv. of ethanol and ~8.5 equiv. of water at: a) 298 K; b) 283 K; c) 273 K; d) 263 K a) 253 K.

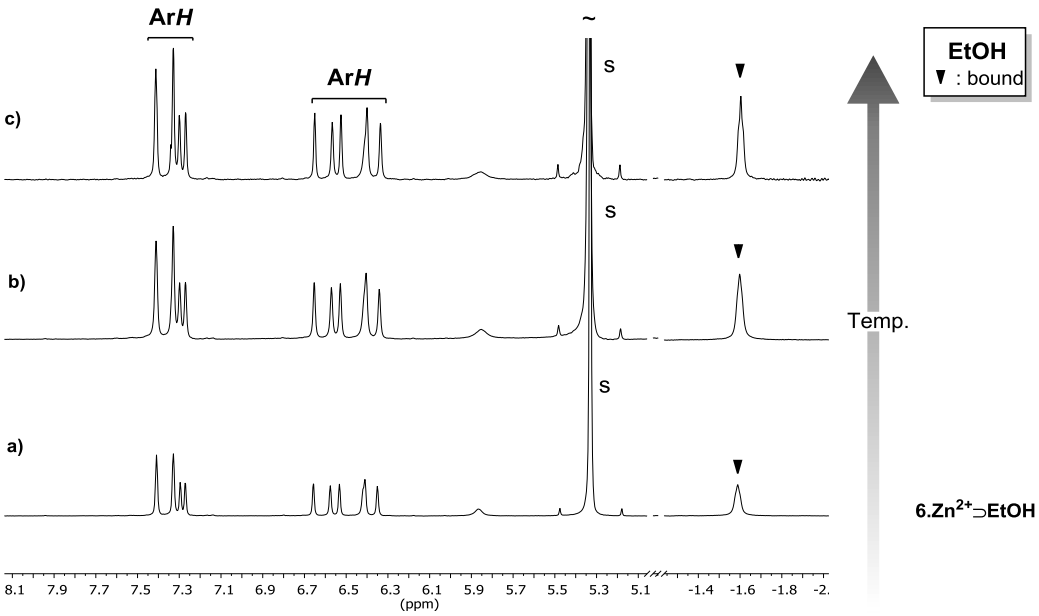

Figure 7-3. ^{1}H NMR spectra (600MHz, DCM-d_2) of **6.Zn^{2+}** in the presence of ~74 equiv. of EtOH and ~7 equiv. of water at: a) 263 K; b) 253 K; c) 248 K.

7.3. COMMUNICATIONS, POSTERS AND PUBLICATIONS

Oral communications

15th edition of the Young Belgian Magnetic Resonance Scientist Symposium (YBMRS 2014), 5-6 December 2016, Spa, Belgium.
"*Mechanism of guest exchange in the cavity of a biomimetic calix[6]arene based receptor: input of 1D EXSY NMR*". E. Brunetti, O. Reinaud, M. Luhmer, I. Jabin and K. Bartik.

Symposium «Supramolecular Chemistry and Materials», 21-22 May 2015, Leuven, Belgium.
"*The power of micelles: amine recognition in water by a calix[6]aza-cryptand*". E. Brunetti, I. Jabin and K. Bartik.

13th edition of the Young Belgian Magnetic Resonance Scientist Symposium (YBMRS 2014), 24-25 November 2014, Spa, Belgium.
"*NMR Study of the Recognition Properties of a Calix[6]aza-cryptand Incorporated in DPC Micelles*". E. Brunetti, I. Jabin and K. Bartik.

5th Training School COST Action CM 1005–Supramolecular Chemistry in Water, 11-14 November 2014, Padova, Italy.
"*Amine Recognition in Water by a Calix[6]aza-cryptand Incorporated in Dodecylphosphocholine Micelles*". E. Brunetti, I. Jabin and K. Bartik.

COST Action CM1005 Meeting "Supramolecular gels and micelles as potential environments for molecular recognition and catalysis in water", 10-11 May 2013, Rome, Italy.
"*Input of EXSY 1D NMR Spectroscopy to understand Guest Exchange mechanism of calix[6]arene Tris-imidazole zinc receptors*". E. Brunetti, A-I. Bidegaray, G. Bruylants, O. Reinaud, I. Jabin and K. Bartik.

COST Action CM1005 Meeting "Biomimetic Calix[6]arene Based Receptors", 21-22 March 2013, Bruxelles, Belgium.
"*Characterization of the affinity of calix[6]tris-ureas for ion pairs and triads*". E. Brunetti, J.-F. Picron, K. Bartik and I. Jabin.

Posters:

11th International Symposium on Macrocyclic and Supramolecular Chemistry (ISMSC 2016), 10-14 July 2016, Seoul, South Korea.
"*Water assistance for guest exchange in the cavity of a biomimetic calix[6]arene based receptor*" E. Brunetti, O. Reinaud, M. Luhmer, I. Jabin and K. Bartik.

13th International Conference on Calixarenes (Calix 2015), 05-09 July 2015, Giardini Naxos, Italy.
"*Neutral Guest Recognition in Water by a Calix[6]aza-cryptand Incorporated in Zwitterionic Micelles*". E. Brunetti, A. Inthasot, F. Keymeulen, O. Reinaud, I. Jabin and K. Bartik.

10th International Symposium on Macrocyclic and Supramolecular Chemistry (ISMSC 2015), 28 June-2 July 2015, Strasbourg, France.
"*Neutral Guest Recognition in Water by a Calix[6]aza-cryptand Incorporated in Zwitterionic Micelles*". E. Brunetti, A. Inthasot, F. Keymeulen, O. Reinaud, I. Jabin and K. Bartik.

Journée de l'Ecole Doctorale Thématique CHIM (EDT CHIM 2014), 05 November 2014, Bruxelles, Belgium.
"*Amine Recognition with a Micelle-Incorporated Calix[6]arene Based Receptor*". E. Brunetti, O. Reinaud, I. Jabin and K. Bartik.
The poster presented won the "*Best Poster Prize*".

European-Winter School on Physical Organic Chemistry "Physical Organic Chemistry of Complex Systems" (WISPOC 2014), 02-07 February 2014, Bressanone, Italy.
"*Biomimetic calix[6]arene based receptor: study of the binding properties and exchange dynamics*". E. Brunetti, G. Bruylants, O. Reinaud, I. Jabin and K. Bartik.
The poster presented won the "*COST Poster Prize*".

12th edition of the Young Belgian Magnetic Resonance Scientist Symposium (YBMRS 2013), 02-03 December 2013, Blanckenberge, Belgium.
"*Input of EXSY 1D NMR spectroscopy to elucidate the guest exchange mechanism in the cavity of a biomimetic calix[6]arene based receptors*". E. Brunetti, G. Bruylants, O. Reinaud, I. Jabin and K. Bartik.

European-Winter School on Physical Organic Chemistry "Supramolecular Chemistry" (WISPOC 2013), 27 Janaury-02 February 2013, Bressanone, Italy.
"*Physicochemical characterization of the affinity of calix[6]arene based receptors for ion pairs and triads*". E. Brunetti, J.-F. Picron, G. Bruylants, K. Bartik and I. Jabin.

11th edition of the Young Belgian Magnetic Resonance Scientist Symposium (YBMRS 2012), 26-27 November 2012, Spa, Belgium.
"*Study of the binding affinity of organic ion pairs by multitopic calixarene-based receptors*". E. Brunetti, J.-F. Picron, G. Bruylants, K. Bartik and I. Jabin.

Publications:

1) "A Selective Calix[6]arene-based Fluorescent Chemosensor for Phosphatidylcholine Type Lipids "Emilio Brunetti, Steven Moerkerke, Johan Wouters, Kristin Bartik and Ivan Jabin *Org. Biomol. Chem.* **2016**, 14, 10201-1027.

2) "Kinetic and Thermodynamic Stabilization of Metal Complexes by Introverted Coordination in a Calix[6]azacryptand" Alex Inthasot, Emilio Brunetti, Manuel Lejeune, Nicolas Ménard, Thierry Prangé, Luca Fusaro, Gilles Bruylants, Olivia Reinaud, Michel Luhmer, Benoit Colasson and Ivan Jabin *Chem. Eur. J.* **2016**, 22, 4855-4862.

3) "Primary Amine Recognition in Water by a Calix[6]aza-cryptand Incorporated in Dodecylphosphocholine Micelles" Emilio Brunetti, Alex Inthasot, Flore Keymeulen, Olivia Reinaud, Ivan Jabin and Kristin Bartik *Org. Biomol. Chem.* **2015**, 13, 2931-2938.

4) "Fluorescent Chemosensors for Anions and Contact Ion Pairs with a Cavity-Based Selectivity" Emilio Brunetti, Jean-François Picron, Karolina Flidrova, Gilles Bruylants, Kristin Bartik, and Ivan Jabin *J. Org. Chem.* **2014**, 79, 6179–6188.

7.4. LIST OF RECEPTORS USED

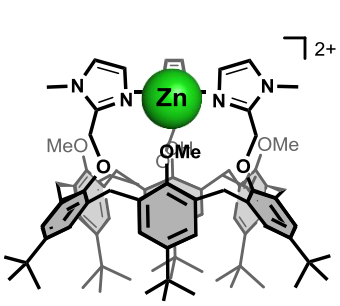

1.Zn^{2+}

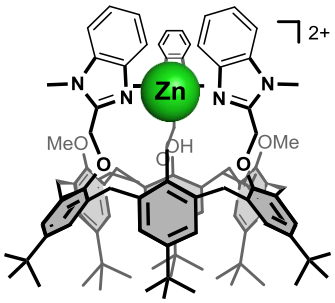

2.Zn^{2+}

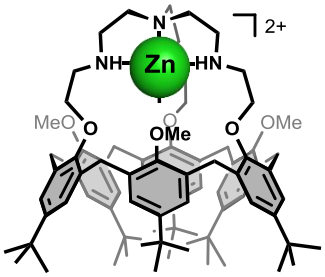

6.Zn^{2+}

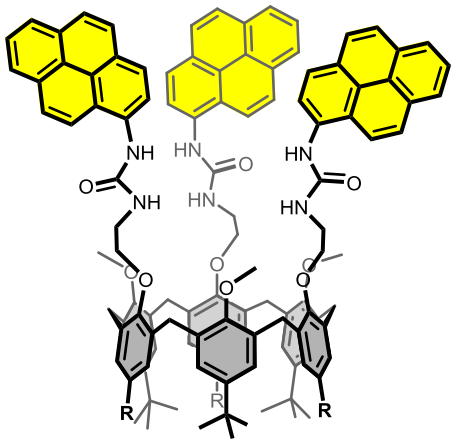

14a : R = *t*Bu
14b : R = H

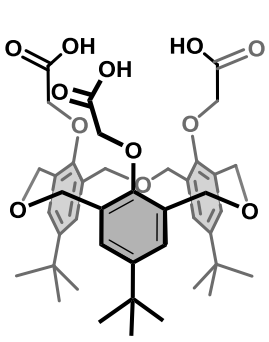

15

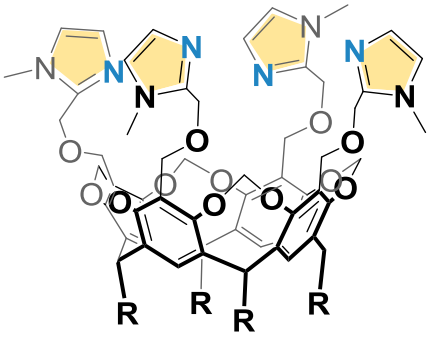

16 (R = C_5H_{11})